

Combined methods for liquid radioactive waste treatment

*Final report of a co-ordinated research project
1997–2001*



INTERNATIONAL ATOMIC ENERGY AGENCY

IAEA

February 2003

The originating Section of this publication in the IAEA was:

Waste Technology Section
International Atomic Energy Agency
Wagramer Strasse 5
P.O. Box 100
A-1400 Vienna, Austria

COMBINED METHODS FOR LIQUID RADIOACTIVE WASTE TREATMENT

IAEA, VIENNA, 2003

IAEA-TECDOC-1336

ISBN 92-0-100903-8

ISSN 1011-4289

© IAEA, 2003

Printed by the IAEA in Austria
February 2003

FOREWORD

The IAEA Co-ordinated Research Project (CRP) on Combined Methods for Liquid Radioactive Waste Treatment was initiated in 1997 to identify, through the exchange of information and the results of experimental work, specific combined methods for liquid radioactive waste treatment and to define their applicability and efficiency for processing of different waste streams. Substantial advantages can be accrued by selecting a combination of two or more processes and their consecutive or simultaneous application for treatment of liquid waste. The multiple or combined process approach may allow resources and materials recovery, provide volume reduction or allow processing of waste in a single equipment unit. Research and development in this field would contribute toward improvement of efficiency, safety and cost of the whole waste management system.

The CRP brought together 14 research teams from 12 countries. The progress in the CRP implementation was discussed at three Research Co-ordination Meetings held in the Republic of Korea (Nuclear Environment Technology Institute, Korean Electric Power Corporation, 18–22 May 1998), in China (China Institute of Atomic Energy 10–14 April 2000) and in Belgium (Nuclear Research Center SCK/CEN 8–19 October 2001). The programme of the CRP was oriented not only on the research, but also on the development and application of different new combined methods for treatment of liquid radioactive waste aimed at increasing the treatment efficiency. Some combined processes developed in the frame of this CRP have been applied at pilot plant scale for treatment of actual radioactive wastes.

The results of four years of investigation and development in the framework of the CRP are summarized in this report, together with individual reports of all institutions that participated in the CRP. The summary report was prepared by the IAEA Secretariat with assistance of consultants from the Czech Republic (J. John), India (P.K. Wattal) and the Russian Federation (V. Tsyplenkov). The IAEA would like to express its thanks to all those who participated in the CRP implementation and preparation of this report.

The IAEA officer responsible for this publication was V.M. Efremkov of the Division of Nuclear Fuel Cycle and Waste Technology.

EDITORIAL NOTE

The use of particular designations of countries or territories does not imply any judgement by the publisher, the IAEA, as to the legal status of such countries or territories, of their authorities and institutions or of the delimitation of their boundaries.

The mention of names of specific companies or products (whether or not indicated as registered) does not imply any intention to infringe proprietary rights, nor should it be construed as an endorsement or recommendation on the part of the IAEA.

CONTENTS

1. SCIENTIFIC BACKGROUND	1
2. OBJECTIVES AND SCOPE OF THE CO-ORDINATED RESEARCH PROJECT	2
3. INSTITUTES PARTICIPATING IN THE CO-ORDINATED RESEARCH PROJECT AND AREAS OF PARTICULAR RESEARCH	2
4. RESULTS OF INVESTIGATIONS AND DISCUSSIONS	4
4.1. Materials with combined properties	4
4.1.1. Sorption-reagent materials	5
4.1.2. Biosorbents and their modifications	5
4.1.3. Titanium dioxide based materials with combined photo-catalytic and ion-exchange properties	6
4.1.4. Modified mesoporous titanium based materials	6
4.2. Combined single stage processes	7
4.2.1. Electrosorption	7
4.2.2. Photocatalytic degradation of organic complexants with sorption of the released metal ions on the TiO ₂ photocatalyst/absorber	8
4.2.3. A multilayer adsorption/ion-exchange column for the treatment of liquid decontamination waste	8
4.3. Combined multi-stage processes	9
4.3.1. Treatment of boric acid waste from PWR operation	9
4.3.2. Treatment of tritiated organic solvent	10
4.3.3. Combined sorption/membrane filtration or sorption/centrifugation for colloid-containing waste streams	11
4.3.4. Combination of sorption and precipitation for treatment of liquid radioactive waste	11
4.3.5. Multi-stage sorption/floculation-ultrafiltration-sorption process for liquid radioactive waste treatment	12
4.3.6. Photocatalytic degradation of organic complexants combined with subsequent treatment of the solution by sorption on optimised absorbers	13
4.3.7. Combined processes for management of organic wastes	14
4.3.8. Development of the combined waste treatment system for NPP operational waste	15
4.3.9. Treatment of aqueous radioactive waste containing uranium, thorium and radium radionuclides by chemical precipitation and laterite soil sorbent	15
5. CONCLUSIONS	16
ANNEX: PAPERS PRESENTED	
Selection of optimal conditions for the removal of radionuclides from waste solutions by a combination of two methods: Sorption and membrane filtration or sorption and centrifugation	21
<i>Yu.P. Davydov, V.M. Efremenkov, D.Yu. Davydov, I.G. Toropov, L.M. Zemskova, V.V. Toropova</i>	
Volume reduction of low level liquid PWR waste treatment of tritiated solvents	31
<i>A. Bruggeman, J. Braet</i>	

Development of combined method for treatment of liquid waste from reconstruction of shallow ground repository	46
<i>I.G. Stefanova, M.D. Mateeva</i>	
Application of inorganic sorbents in combination with ultrafiltration membrane technology for the treatment of low level radioactive liquid waste streams	63
<i>Xiguang Su, Zuxi Zheng, Jun Yao, Zhongmao Gu</i>	
Study of combined processes for the treatment of liquid radioactive waste containing complexing agents.....	74
<i>F. Šebesta, J. John, A. Motl, K. Rosíková</i>	
The volume reduction of liquid radioactive waste by combined treatment methods.....	104
<i>T. Szánya, P. Tilky, B. Kanyár, G. Marton, J. Schunk, J. Vízlay, L. Hanák, Z. Németh</i>	
Combined processes and techniques for processing of organic radioactive waste	121
<i>P.K. Wattal, D.S. Deshingkar, C. Srinivas, D.B. Naik, S. Manohar</i>	
Combined treatment of aqueous radioactive waste containing uranium, thorium and radium radionuclides by chemical precipitation and laterite soil sorbtion.....	137
<i>Syed Hakimi Sakuma, Nik Marzukee, Mohd Khairuddin</i>	
Combined liquid waste treatment processes involving inorganic and organic sorbents, reverse osmosis and micro/ultrafiltration.....	150
<i>Ho-Yeon Yang, Jong-Hyun Ha, Myung-Jae Song</i>	
Elaboration of a combined electrosorption method for treatment of LLRW	168
<i>Yu. Karlin, R. Iliasov, I. Sobolev</i>	
Combined methods for complete decontamination of LRW of low and intermediate level of activity by using chitin containing fiber material «Mycoton» and its modifications	188
<i>V.N. Kosyakov, I.E. Veleshko, N.G. Yakovlev, L.F. Gorovoy</i>	
Sorption-reagent methods in LRW management	205
<i>V.A. Avramenko, A.P. Golikov, V.V. Zheleznov, E.V. Kaplun, N.I. Lysenko, D.V. Marinin, T.A. Sokolnitskaya, K.A. Khokhlov, A.A. Yuhkam</i>	
Sorption-catalytic treatment of liquid radioactive waste based on titanium dioxide sorbents	224
<i>P. Manorik, M. Phedorenko, T. Makovskaya, V. Lytvin, S. Demeshko</i>	
LIST OF PARTICIPANTS	245

1. SCIENTIFIC BACKGROUND

The ever increasing pressure to reduce the release of radioactive and other toxic substances into the environment requires constant improvement/upgrading of processes and technologies for treatment and conditioning of liquid radioactive waste. Treatment of liquid radioactive waste quite often involves the application of several steps such as filtration, precipitation, sorption, ion exchange, evaporation and/or membrane separation to meet the requirements both for the release of decontaminated effluents into the environment and the conditioning of waste concentrates for disposal. New and improved materials and processes are under consideration and development in various countries. Also a judicious combination of the processes and their consecutive or simultaneous applications is being pursued to meet the end objectives of improved decontamination, waste volume reduction, safety and overall cost effectiveness in the treatment, conditioning and disposal of these wastes.

Use of sorbents with other treatment methods such as precipitation or membrane separation, is a logical development of liquid waste treatment. Sorption combined with membrane filtration in a single stage process can provide efficient removal of both dissolved and suspended contaminants even in a colloidal form. This combination has not only the advantage of improved sorption kinetics on account of a very high surface area of the sorbents, but also provides for effective separation of the sorbents from the effluents.

The electrosorption technique, where ions move from the solution to the sorbent under the influence of an electric field, is also emerging as a novel technique utilizing powder and colloidal sorbents. This technique can employ non-standard sorbents, which are otherwise ineffective in traditional sorption on account of their column properties and/or their strength.

Photo-degradation is finding wide acceptance for the destruction of organics in spent decontamination solutions. The oxidative destruction process can be significantly enhanced if certain inorganic materials are present as catalysts. One of the most effective catalysts is titanium dioxide which is also known to be an excellent sorbent for a number of radionuclides. Thus, combined treatment of, for example spent decontamination solutions in the presence of a titanium dioxide catalyst, would provide very effective destruction of the complexing agents with release of radionuclides in a form suitable for sorption by the catalyst/sorbent.

Combination of different sorbents and their application in a single stage process has also been identified as an effective approach for removal of a broad spectrum of radionuclides and other contaminants from radioactive waste. The compatibility and synergistic effects of different sorbents in a multi-layer column may also be quite effective.

Combined methods can also involve a multiple process approach. These could be a judicious combination of several treatment modules combined to result in an overall efficient process. For certain organic liquids, such as solvent extraction waste, contaminated oils, scintillation cocktails, and other miscellaneous organic solvents, multiple processes involving chemical and/or advanced oxidative destruction followed by precipitation could be effective for converting organic materials into inorganic forms compatible with the known immobilization matrices.

These entire multiple or combined processes are attractive for investigation and further application for liquid waste treatment since they could provide for resource saving and materials recovery or allow treatment of liquid radioactive waste in a single unit. Such combined processes are also prospective even for the treatment of industrial and other non-nuclear waste streams.

2. OBJECTIVES AND SCOPE OF THE CO-ORDINATED RESEARCH PROJECT

The objective of the Co-ordinated Research Project (CRP) on Combined Methods for Liquid Radioactive Waste Treatment was to outline areas of potential and prospective combinations of different waste processing steps, techniques and materials for improving the overall efficiency of waste treatment. Through conducting of research, exchange of information and results of this research it was intended to identify specific combined methods for treatment of liquid radioactive waste and to define their applicability and potential efficiency for particular waste stream processing.

Practical experience in the development and operation of pilot and full-scale facilities utilizing combined treatment processes for treatment of liquid radioactive waste was considered to be of particular importance and interest. Therefore for the benefit of all participants of the CRP its programme was oriented not only on the research, but also on the development and application of different new materials and combined methods for treatment of liquid radioactive waste aimed at improving the treatment efficiency. The programme was planned to prove, possibly up to a pilot plant scale, the effectiveness of the combined processes for treatment of real radioactive waste.

The following areas have been identified and are recommended for co-operation and joint efforts.

- (a) Use of inorganic sorbents in combination with other treatment processes;
- (b) Use of sorbent mixtures;
- (c) Combined processes for treatment of solutions containing complexing agents and organics;
- (d) Multiple processes for treatment and immobilization of organic liquid waste.

3. INSTITUTES PARTICIPATING IN THE CO-ORDINATED RESEARCH PROJECT AND AREAS OF PARTICULAR RESEARCH

Thirteen institutions from eleven countries expressed their willingness and interest to participate in the research and development outlined in the frame of this CRP. The extensive research covered a broad scale of treatment techniques including ion exchange, sorption, precipitation, membrane techniques (micro- or ultrafiltration, reverse osmosis), techniques for degradation of organic substances (wet oxidation, alkaline hydrolysis, photo-oxidation), electrochemical methods, combustion, sublimation, studies of catalytic properties, and modelling of the processes. A general study of the radionuclide and macroelement speciation helped to fine-tune the performance of some of these methods. Multiple combinations of these techniques were proposed. The fields of research of the institutes participating in the project were as follows:

***Institute of Radioecological Problems of Belarus Academy of Sciences, Minsk, Belarus,
Chief Scientific Investigator: Yu. Davydov***

Removal of radionuclides from the waste solutions by combination of sorption and membrane filtration or sorption and centrifugation;

- Influence of complexing anions in the waste solution on pseudocolloid formation and hydroxide precipitation;
- General radionuclide speciation.

SCK/CEN, Mol, Belgium, Chief Scientific Investigator: A. Bruggeman

- Combined methods for volatilization of boric acid from evaporator concentrates;
- Combined thermal oxidation/catalytic oxidation/sorption method for the treatment of tritiated organic waste.

Institute for Nuclear Research and Nuclear Energy of the Bulgarian Academy of Sciences, Sofia, Bulgaria, Chief Scientific Investigator: I. Stefanova

- Combined sorption/precipitation method for the treatment of liquid radioactive waste;
- Clinoptilolite sorption properties;
- Separation of detergents from liquid radioactive waste.

China Institute of Atomic Energy, Beijing, China,

Chief Scientific Investigator: Xiguang Su

- Sorption/flocculation/precipitation process combined with ultrafiltration and sorption of radionuclides onto natural sorbents;
- Study of radionuclide separation by flocculant precipitation in the presence of highly selective sorption materials;
- Optimization of operation of ultrafiltration units (washing the clogged membranes);
- Sorption properties of clinoptilolites and their modifications.

Czech Technical University in Prague, Prague, Czech Republic,

Chief Scientific Investigator: F. Sebesta

- Titanium dioxide materials with combined photo-catalytic and sorption properties;
- Combined single-step process for photo-catalytic destruction of organic complexants with sorption of the released metal ions on the TiO₂;
- Two-step combined process for photocatalytic destruction of organic complexants combined with subsequent treatment of the solution by sorption.

University of Veszprém, Veszprem, Hungary, Chief Scientific Investigator: T. Szanya

- Performance of multilayer combined adsorption/ion-exchange columns for the treatment of AP-CITROX and LOMI decontamination waste.

Bhabha Atomic Research Centre, Mumbai, India,

Chief Scientific Investigator: P.K. Wattal

- Combined processes for the treatment of liquid organic waste;
- “Alkaline hydrolysis” method for the destruction of TBP in spent solvents of reprocessing origin;
- Wet oxidation and photo-oxidation processes for mineralization of ion exchange resins and organic complexing agents.

Malaysian Institute for Nuclear Technology Research, Kajang, Malaysia,

Chief Scientific Investigator: S.H. Hakimi

- Development of a method for separation of uranium, thorium and radium from raw aqueous waste stream by chemical precipitation combined with sorption on natural soil (Laterite).

Nuclear Environment Technology Institute, Daejeon, Republic of Korea,

Chief Scientific Investigator: Yo-Yeon Yang

- Method for treatment of low level waste as an alternative to evaporation;
- Fibre filtration, ultrafiltration, reverse osmosis, and selective ion exchange for the treatment of boron-bearing and special laundry waste.

**Scientific and Industrial Association “Radon”, Moscow, Russian Federation,
Chief Scientific Investigator: Yu. Karlin,**

- Development and study of a single stage combined electro-sorption process for liquid waste treatment.

**Russian Nuclear Research Center “Kurchatov Institute”, Moscow, Russian Federation,
Chief Scientific Investigator: V. Kosyakov**

- “Mycoton” based materials with combined sorption and flocculation properties;
- Options for EDTA destruction.

**Institute of Chemistry of Russian Academy of Sciences, Vladivostok, Russian Federation,
Chief Scientific Investigator: V. Avramenko**

- Development of sorption-reagent materials for the treatment of liquid waste of complex chemical composition;
- Development and study of novel sorbents for cesium and cobalt separation.

**L.V. Pisarzhevsky Institute of Physical Chemistry of the Ukrainian Academy of Sciences,
Kiev, Ukraine, Chief Scientific Investigator: P. Manorik**

- Novel inorganic sorbents with combined properties (modified with crown-ethers or other ligands);
- 3d-metal oxide (Cr, Fe, Mn, Mo, V) based catalysts for the application in a combined photocatalytic/sorption process.

4. RESULTS OF INVESTIGATIONS AND DISCUSSIONS

During the implementation of this CRP, it was learned that sufficient potential exists for the treatment of low and intermediate level radioactive waste employing rather novel materials with combined properties or adopting a single stage process which combines multiple treatment techniques. In general, the combined methods for liquid radioactive waste treatment actually studied within the framework of the CRP could be broadly grouped under three categories:

- Application of *materials with combined properties* (e.g. materials that exhibit both photo-catalytic and ion exchange properties);
- Application of different waste treatment principles or techniques in a *single stage process* (e.g. the electro-sorption process that combines migration of ions in an electrical field with their sorption onto a suitable sorbent);
- Development of *combined, multi-stage treatment systems* with sequentially incorporated materials, interrelated techniques and waste treatment steps.
- Most research and development within the CRP fell under the first two categories, and represented a broad new approach to liquid radioactive waste treatment.

Based on the categories defined above, the most significant results, obtained by the CRP participants are summarized below.

4.1. Materials with combined properties

The materials with combined properties have been represented in the CRP by synthesis, testing and application studies of specific materials with multifunctional properties. These materials include:

- The new class of specific sorbents or sorption-reagent materials with very high capacity and selectivity for particular radionuclides (Cs, Sr, Co, etc.);
- The modified chitin-based biosorbents of a fibre structure with specific sorption properties for heavy metals and actinides;
- The titanium dioxide based sorbents with high sorption properties and catalytic activity for photo- and chemical oxidation of organic components in liquid radioactive waste.

The results of corresponding investigations and applications are briefly summarized below.

4.1.1. Sorption-reagent materials

New materials having **sorption/reagent properties** have been developed at the *Institute of Chemistry of the Far East Department of the Russian Academy of Sciences, Vladivostok, Russian Federation*. These materials have the capability to interact with the waste solution components and employ dual features of co-precipitation and sorption. When compared with standard ion exchange resins, the insoluble compounds formed in such interactions were found to increase, by tens or even hundreds times, the sorption selectivity for different radionuclides such as strontium, cobalt, mercury, iron, or manganese. The study revealed that this increase in the selectivity is caused by radionuclide co-precipitation on micro-particles formed inside the pores of the inorganic matrices in addition to acting as a sorbent.

These sorbents sufficiently address the removal/separation of such radionuclides as caesium, strontium and cobalt from liquid waste containing highly complexing agents, where these interact with sulphate-, carbonate-, oxalate-, sulphide-, and permanganate ions for which the conventional selective sorbents, such as zeolites, titanates, silico-titanates, or manganese dioxide were inefficient.

These materials have been tested at the pilot-scale facility for the treatment of nearly 1500 m³ of real decontamination waste of complex compositions at the high flow rate up to 100 BV/h. Another pilot sorption/reagent installation has been successfully tested at the A. A. Bochvar Research Centre VNIINM, Moscow.

In addition, the sorption/reagent technique can be further combined with other radioactive waste treatment methods. It can be also used to treat waste containing radiocolloids. Its application has a promising potential in the field of liquid radioactive waste treatment.

4.1.2. Biosorbents and their modifications

Modification of chitin containing sorbents was studied at *Russian Nuclear Research Center “Kurchatov Institute”* in Moscow. Various naturally occurring biosorbents are widely applied specifically for the sorption of long lived radionuclides. Among them, chitin containing sorbents have been found to be very efficient on account of their abundance and the textural characteristics. These chitin containing sorbents named “Mycoton” have a fibre structure consisting of about 70% of chitin, 25% of R-glucans and 5% of melanin located in the cell walls. The sorbents could be tailor made by attaching selective inorganic ion-exchangers, e.g. ferrocynides for caesium, impregnated KMnO₄ for strontium and even making them ferromagnetic for effective separation by magnetic methods.

Radioactive wastes being stored for a long time quite often have radionuclides in colloidal form e.g. cobalt and plutonium in alkaline waste. Neither ion exchangers nor sorbents are capable of providing the required degree of decontamination for such wastes. These problematic wastes can be treated by novel sorbents having combined *absorptive cum flocculative* properties. Mycoton and its various modifications as sorbents with freshly precipitated water soluble chitozan as a flocculent, have been tested and yielded a very high degree of decontamination. Such an complementary combination of two natural polymeric sorbents not only provides a high degree of decontamination but also, very high volume reduction, since these sorbents are combustible. Both the sorbent and the flocculent could be produced on an industrial scale. It should be noted that a continuous multistage counter current absorptive process with centrifugal mixer-settlers is under development for real industrial application of the proposed technology.

4.1.3. Titanium dioxide based materials with combined photo-catalytic and ion-exchange properties

This study carried out at the *Czech Technical University in Prague* included the development of titanium based materials that exhibit combined properties of photocatalysis and ion exchange. Photo-catalytic and sorption properties of a series of titanium dioxide materials were studied in detail. Photocatalytic degradation of organic complexants used in decontamination solutions including EDTA, oxalic and citric acids are emerging as promising processes for the plant scale adoption. The application of these materials in a combined process comprising the removal of organic substances and the separation of radionuclides on the TiO₂ photo-catalyst/absorber from liquid radioactive waste was also studied.

The photo-catalytic degradation of complexes using titanium dioxide based sorbents was quite efficient. Nearly all the organic complexants such as oxalic and citric acids and EDTA could be effectively degraded. The degradation was more efficient in acidic solutions, and was very slow in neutral and alkaline pH range. TiO₂-M and Degussa P25 samples displayed the highest activity for catalyzing the photodegradation of organic complexants.

The degradation of organic complexes proceeded in a way rather different from the degradation of the pure complexants. EDTA complexes were found to be very photostable. For the citrate and oxalate complexes, acceleration of the degradation in the presence of Fe(III) ions was observed.

Out of the materials tested, the HTO suspension demonstrated the best sorption properties. This material alone can be efficiently used to remove metal cations even from neutral and low-alkaline solutions. Degussa P25 and TiO₂-M materials exhibit similar sorption properties. They are prospective for the removal of metal ions from the alkaline solutions with pH > ~ 9.

4.1.4. Modified mesoporous titanium based materials

Another class of sorbents containing crown-ethers, some tetraazamacrocyclic ligands as chelating groups and titanium, silica and titanium/silica gel as a matrix have been synthesized, characterized and studied in the *L.V. Pysarzhevsky Institute of Physical Chemistry of the National Academy of Sciences of Ukraine*. Development has been towards the synthesis of these materials by means of sol-gel methods and their sorption-catalytic properties have been determined. Some of these sorbents, on account of their mesoporous

properties, can uptake hydrophobic templates such as crown-ethers or macrocyclic ligands with regulated hydrophobization on their surfaces.

These materials have very good sorption ability towards organic impurities and even actinides. Few types of catalysts, containing 3d-metal oxides (Cr, Fe, Mn, Mo, V) or their mixtures and with the combined properties for sorption/catalytic treatment in combination with magnetic separation methods make them especially versatile for the treatment of radioactive liquid wastes containing organic impurities and low concentration of actinides.

4.2. Combined single stage processes

Single stage processes combining two or more treatment techniques, that were developed within the CRP for the treatment of radioactive waste, included electro-sorption, photo-catalytic oxidation combined in one stage with sorption, and application of multi-layer sorption processes. In all these cases, different components or principles of waste treatment are combined in a single treatment unit. A brief description of these processes is presented below.

4.2.1. Electrosorption

A novel method, combining in a single stage process migration of ions under an electrical field with simultaneous sorption of radionuclides on a suitable sorbent, was proposed and tested at the *Scientific and Industrial Association "Radon"*, Sergiev Posad, Russian Federation. Conventional sorbents to be used effectively for treatment of liquid radioactive waste, must be sufficiently strong, have low hydraulic resistance, low adhesion to suspended and colloidal mixtures, and also a well developed surface for fast internal diffusion of ions. These requirements explain the fact why most of the sorbents are granular for use in packed bed columns. Finely divided or colloidal sorbents, e.g. freshly prepared BaSO₄, or sorbents with low mechanical strength cannot be used in current absorption technologies for liquid waste treatment.

Electrosorption is more flexible regarding the properties of the sorbents since this method does not require filtration of the solution through a sorbent layer and does not even need a direct contact between the sorbent and the solution. In this technique, the sorbent is placed between two porous diaphragms, which could be microfiltration or ultrafiltration membranes. The waste solutions are made to contact their outer surfaces and under the influence of the electrical field, the ions migrate and are picked up on the sorbent without the liquid passing through the sorbent. Thus in this arrangement, even finely divided sorbents can be used for the treatment of radioactive waste.

Model experiments were performed for the effective removal of ¹³⁷Cs, ⁹⁰Sr + ⁹⁰Y, and ²³⁸UO₂²⁺ with simulated solutions using different sorbents of varied sizes, ranging from granules to freshly prepared precipitates. The sorbents tested included nickel ferrocyanide, precipitated on the silica gel ("Fenix-A"), natural bentonite clay, chitin-chitosan biosorbents, standard anion and cation exchange resins, freshly prepared barium sulfate precipitate, etc.

The kinetics of the process were shown to depend significantly on the sorbent type and not on the particle size of the sorbent. Very high extraction of uranium ions from the solution was observed. The efficiency of electrosorption can be compared to the batch regime of conventional sorption.

For the practical application of the process, a multi-chamber or labyrinth type device is proposed. In these modules, the degree of extraction can be increased considerably by increasing the number of sorbent compartments, and/or by increasing the density of electrical current. Using the electrosorption technique with ceramic membranes in combination with selective sorbents, certain radioactive waste streams of intermediate or high level could be very effectively treated.

4.2.2. Photocatalytic degradation of organic complexants with sorption of the released metal ions on the TiO₂ photocatalyst/absorber

For the treatment of radioactive waste with organic complexants, such as decontamination solutions, ion exchangers, composite absorbers, etc are usually not effective. The photocatalytic degradation process, using titanium dioxide photocatalyst/absorbers, was studied at the *Czech Technical University in Prague*, Czech Republic. This combined process was tested for the removal of organic complexants and/or separation of radionuclides from spent decontamination solutions. The study was performed with both simulated and real liquid waste from NPPs in the Czech and Slovak Republics. These wastes were acidic spent decontamination solution from the second stage of the AP-CITROX decontamination process and liquid waste from electrochemical decontamination.

The process development was based on the results of the general study of the properties of titanium dioxide photocatalyst/absorbers. The optimum degradation of organics was achieved under the combined action of titanium dioxide photocatalyst and hydrogen peroxide.

From the results obtained, it was inferred that a single-step process, combining photocatalytic degradation of organic complexants with sorption of the released metal ions on the TiO₂ photo-catalyst/absorber, is a possible option for treatment of certain liquid radioactive waste. However, the photo-catalytic degradation is effective in the acidic pH range, only, while the sorption of the radionuclides proceeds only in the alkaline pH range.

Thus, for the process to be effective, the photo-degradation step has to be carried out in acidic solution and it has to be followed by pH adjustment to alkaline range, in order to improve conditions of the radionuclides sorption on the titanium dioxide materials. However, decreasing the activity of the waste below the free discharge limit in such a process would probably be difficult to achieve.

4.2.3. A multilayer adsorption/ion-exchange column for the treatment of liquid decontamination waste

Decontamination of reactor primary circuit equipment (main circulating pumps, steam generators, pipelines, etc.) using AP-CITROX and LOMI processes generates waste that, in addition to the radionuclides, contain sodium hydroxide and potassium permanganate, or citric and oxalic acids. The decontamination solutions (especially the alkaline oxidative one) may also contain several undesired organic compounds (oils, fats, detergents etc.), solid grains and colloid impurities that can carriers of radioactive nuclides. A usual practice for the processing of such a waste at nuclear power plants is evaporation followed by solidification of the evaporator concentrate by cementation, bituminization or vitrification. Presence of organics can limit the overall volume reduction reached during evaporation.

As an alternative to evaporation, studies were carried out by joint efforts of the *Nuclear Power Plant Paks and University of Veszprém*, Hungary, employing a new combined

approach using adsorption with ion exchange in a multilayer column. Active carbon, cation exchange resins in Fe(II) or H⁺ forms, and anion exchange resin in the OH⁻ form were used as adsorbers or ion-exchangers, respectively. In addition to these materials, active carbon impregnated with potassium copper ferrocyanide was tested for treatment of the LOMI waste.

After treatment of nearly 173 L of alkaline oxidative waste in a four layer column at a flow rate of 100–400 mL/min and at the temperature of 95°C, the total decontamination factor for ⁵⁴Mn + ⁶⁰Co + ^{110m}Ag was about 1000. The respective volume reduction factor was nearly 40 with respect to the activated carbon column. For the treatment of the acidic reductive waste, a three-layer column was used. After the treatment of nearly 227 L of the waste at a flow rate of 200 mL/min and temperature of 90°C, the total decontamination factor for ⁵⁴Mn + ⁶⁰Co + ^{110m}Ag was around 900. The respective volume reduction factor was 450 with respect to the cation exchanger column.

From the results of these experiments, it can be concluded that the combination of adsorption and ion-exchange processes in a multilayer column can result in very favourable DF and VRF values for the treatment of spent AP-CITROX solutions. However for the LOMI process waste, EDTA degradation/removal would be required to improve the efficiency of the decontamination. The process has been scaled up and a mobile treatment unit was commissioned and is available for in situ AP-CITROX decontamination waste treatment at Nuclear Power Plant Paks, Hungary.

4.3. Combined multi stage processes

Combined multi-stage processes developed within the CRP dealt with different options for the treatment of liquid radioactive waste with varied nature and composition. The wide representation of such processes and their applications for treatment of real operational waste with complex composition suggests a high potential for their full scale application. In most cases, studies were devoted to improving the efficiency of treatment of “problematic” radioactive waste with complex compositions, which could not be effectively addressed by relatively simple or one-stage processes. In particular, low and intermediate level waste from reprocessing of spent fuel, secondary liquid waste from chemical decontamination processes, organic radioactive sludges and spent ion exchange resins, boric acid containing waste from PWR operation, etc., are candidates for treatment using combined multi stage processes. Combined multi-stage processes with carefully selected process components and sequences allow substantial improvement both with respect to the efficiency of waste treatment and its costs. A brief summary of multi-stage waste treatment processes studied in the frame of the CRP is provided below.

4.3.1. Treatment of boric acid waste from PWR operation

Liquid wastes from a pressurised water reactor PWR primary circuit consists of boric acid solutions. In direct evaporation treatment, the volume reduction is limited by the boron concentration. Therefore, separation of boric acid can considerably reduce the volume of radioactive waste from these reactors. A technically simple and economically viable method for separating boric acid by volatilization during evaporation was developed and tested at SCK•CEN, Mol, Belgium.

In this method, the liquid waste is evaporated in a semicontinuous mode with no reflux, at pH below 8, and at elevated temperature and pressure. After an initial period, all boric acid that comes in with the feed leaves the evaporator in the gaseous phase. The non-volatile

chemical and radiochemical impurities, on the other hand, remain quantitatively in the evaporator. The steam loaded with boric acid can be fed to a column for fractional condensation with partial reflux. Here, the boric acid is concentrated in the re-boiler. This simple all-in-one process splits the incoming wastewater stream into three streams: an active waste concentrate, a concentrated boric acid solution and a highly decontaminated effluent.

This process has been tested in a small pilot set up with actual liquid waste at Nuclear Power Plant Doel, Belgium. The installation performed as theoretically expected, giving a boric acid distribution coefficient of about 0.007 at 180°C. The main results of this demonstration experiment showed that the waste volume reduction factor was more than double the current evaporation practice, 80% of the boron was recovered and high DF obtained. The separation of boric acid from liquid radioactive waste appears advantageous when release of the purified effluents with residual boric acid content is not permitted.

In addition, an option for boric acid separation from the non-alkaline dried concentrates was also developed and tested at SCK•CEN. The boric acid concentrates are brought into contact with superheated steam to volatilise the boric acid. By using superheated steam, one can work at a higher temperature without the necessity of using a high steam pressure, and more boric acid can be volatilised with less steam. The boron-free concentrates leave the contactor for further conditioning, whereas the steam loaded with boric acid can be condensed (once-through) or cooled down to a temperature just above its dew point (closed circuit). The steam can be reused after re-heating it to the working temperature. Good results with simulated evaporator concentrates were obtained. During a first 5-h run with dried simulated concentrate, nearly 14.5 kg of boric acid were separated with an average of 26.1 kg steam per kg boric acid.

4.3.2. Treatment of tritiated organic solvent

A combined method was developed at SCK•CEN for the treatment of tritiated organic solvents. The combined treatment method considered thermal oxidation followed by catalytic oxidation of the organics and subsequent sorption of the produced tritiated water onto molecular sieves. Thermal oxidation allows direct injection of the liquid solvent and its oxidation in relatively compact equipment, whereas the catalytic step assures a very high conversion. Condensation and adsorption on molecular sieves can easily and quantitatively trap the tritiated water.

The heart of the installation is a prototype two-stage combustor with effective means of trapping the produced tritiated water. Solvent is atomised into a heated cavity through an injector with excess oxygen. Oxidation products and excess oxygen are passed over heated platinized alumina. The gases coming from the furnace are free of solvent and contain mainly excess oxygen, carbon dioxide and water vapour. These gases are led through two condensers to remove the bulk of the water present in the gas. The water is collected in a tank. The remaining gas is then led over a molecular sieve bed to remove the residual water.

The cold tests demonstrated destruction efficiency higher than 99.999%, for compositions from 10% methanol in water to 100% methanol. Presence of 13% of chloroform in the methanol did not degrade the destruction efficiency.

4.3.3. Combined sorption/membrane filtration or sorption/centrifugation for colloid-containing waste streams

Optimization of combined sorption / membrane filtration or sorption / centrifugation processes for liquid waste treatment was studied at the *Institute of Radioecological Problems, Belorussian Academy of Sciences*, Minsk. These techniques are effective for waste solutions having activity in the colloidal form. In certain decontamination solutions, a significant part of the activity may be due to the iron and chromium radionuclides present at micro- or macro-concentrations. For micro-concentrations, semi-permeable membranes could remove these colloidal particles only after the formation of pseudocolloids, that starts at a pH of 4–5. In these conditions, nearly 99.9% of the activity could be removed. For the same solutions, only 80% of these radionuclides could be removed by centrifugation.

Further decontamination could be achieved by acidification of the solution down to pH 1.5–2.0, where pseudocolloids are rapidly destroyed and the resulting hydroxocomplexes of Fe(III) and Cr(III) can be removed by sorption due to their high sorption affinity. Thus, a combination of membrane filtration at pH higher than 4.0 followed by acidification and sorption on silica gel provides the necessary decontamination factor of the order of 10^5 .

In the presence of complexing anions in waste solutions, the initiation of pseudocolloid formation is shifted into a range of higher pH. In this case, there are two options for removal of Fe(III) and Cr(III) from the solution. The first one is to carry out the treatment at the higher pH, where the formation of Fe(III) pseudocolloids will proceed (from pH 8.0 onwards). The decontamination factor of about 10^3 can be attained in this case by membrane filtration. Alternatively, partial destruction of the complexing anions by one of the oxidizing methods can bring down their concentration, so the pseudocolloid formation starts at much lower pH range.

In case of Fe(III) and Cr(III) radionuclides present at macro concentration (higher than 10^{-6} mol/L), the formation of pseudocolloids cannot proceed. The ability of these radionuclides to form mono-nuclear, poly-nuclear and other hydroxocomplexes can be used for their removal. It should be noted that the concentration threshold for polymerisation of hydrolysed cations is 10^{-5} – 10^{-6} mol/L and the limiting factor for solution decontamination at the stage of hydroxide precipitation is determined not by the hydroxide solubility from the solubility product point of view, but by the possibility of the polymerisation process to proceed.

Sorption/membrane filtration or sorption/centrifugation are combined treatment methods that can be applied to waste solutions where concentrations of Fe(III) and Cr(III) are very low and at the same time high decontamination factors are required.

4.3.4. Combination of sorption and precipitation for treatment of liquid radioactive waste

This study was performed at the *Institute for Nuclear Research and Nuclear Energy of the Bulgarian Academy of Sciences*, Sofia, for development of a combined method for treatment of liquid radioactive waste at the Novi Han Radioactive Waste Repository.

The method developed consists of combination of two main processes – sorption of radionuclides on a natural inorganic sorbent and precipitation of suspended solids and radionuclides. If necessary, additional separation of surfactants on a modified sorbent is considered. Two waste streams were studied – low saline liquid waste from upgrading of Novi

Han Repository, and higher saline decontamination solution that will be generated in future new facilities. The key target radionuclides were ^{137}Cs , ^{90}Sr and ^{60}Co .

In the sorption step optimisation properties of a series of natural zeolites from North-East Rhodope Mountains in Bulgaria were studied. The materials were compared on the basis of their ion-exchange capacities, distribution coefficients, sorption isotherms and kinetics of ion-exchange in model solutions. Although the distribution coefficients for ^{137}Cs are higher on mordenite than on clinoptilolite, for the rest of the radionuclides, as ^{90}Sr or ^{60}Co that may occur in the real waste, the distribution coefficients are considerably higher on clinoptilolite. Clinoptilolite is also characterised with faster sorption kinetics. For these reasons clinoptilolite from the Beli Plast deposit has been selected as a sorbent for treatment of liquid waste.

A detailed study of the properties of the selected sorbents has shown that clinoptilolite has high sorption capability for many radionuclides, typically present in radioactive wastes — ^{137}Cs , ^{90}Sr , ^{60}Co , $^{110\text{m}}\text{Ag}$, ^{226}Ra , ^{133}Ba . The thermodynamic data has shown that clinoptilolite has high selectivity for Cs, Rb, Ag, Pb, Sr and Ba over Na, Ca and Mg.

The distribution coefficients range from 10^2 to 10^4 ml/g depending on the radionuclide and the composition of the liquid waste. Sorption of the radionuclides of concern (^{137}Cs , ^{90}Sr and ^{60}Co) may be further improved by converting the natural clinoptilolite into sodium form. The sorption kinetics were rather slow, the diffusion coefficients being $8.9 \cdot 10^{-11} \text{ cm}^2 \cdot \text{s}^{-1}$ for ^{137}Cs and $8.2 \cdot 10^{-10} \text{ cm}^2 \cdot \text{s}^{-1}$ for ^{90}Sr for the clinoptilolite in sodium form. Hence, low flow rates are required in column application of the clinoptilolite.

In the precipitation step optimisation part of the study, several precipitation processes were compared. Based on this comparison, mixed hydroxide – calcium phosphate precipitation was selected as a basic precipitation process applicable for precipitation of radionuclides and flocculation of suspended solids. High decontamination factors for ^{60}Co , ^{65}Zn , ^{54}Mn and ^{144}Ce were obtained for both the model low saline and higher saline waste solutions.

In the detergent separation optimisation part of the study, modified *kizelgur* sorbent with specific surface area of $22 \text{ m}^2 \cdot \text{g}^{-1}$ was found to be efficient for the detergents separation, and consequently for increasing the efficiency of other methods in the combined processes.

The developed combined process was tested with the real liquid waste from the research reactor IRT-2000 and the liquid waste from the upgrading of Novi Han repository (both of the low saline, low active waste type). The volume reduction factor of 400 was achieved. The treated effluents fully met the national regulatory criteria for release to the environment – both the radiological standards for drinking water and the environmental protection regulation (gross beta activity below 0.750 Bq/L). As a practical output of this research, a mobile installation for treatment of liquid waste from upgrading of Novi Han Repository was designed and is under construction.

4.3.5. Multi-stage sorption/flocculation–ultrafiltration–sorption process for liquid radioactive wastetreatment

The aim of the study performed at the *China Institute of Atomic Energy (CIAE)*, Beijing, was to evaluate the potential of a three-stage process for treatment of liquid radioactive waste. The process consists of sorption onto various natural or synthetic sorbents

with flocculation/ precipitation as the first stage, followed by ultrafiltration, in the second stage and sorption of radionuclides onto natural sorbents as the last stage. These processes have been considered more efficient and cheaper compared to the existing three-stage process, which includes precipitation, evaporation and ion exchange. The study was performed with both simulated and real liquid waste (pH ~ 7–9; total salt content ~ 5 g/L; hardness ~ 4 mg/L; specific activity $10^3 - 10^4$ Bq/L).

In the sorption/flocculation step, precipitation using conventional flocculants (FeSO_4 , KMnO_4 , or Na_3PO_4) was combined with sorption on the suspended, highly selective sorption materials comprising of natural zeolite, natural manganese ores, cadmium hexacyanoferrate, etc. The results obtained for the zeolites revealed that the DF and K_D values increase with the reduction of their particle size down to ~ 100 mesh. For lower grain sizes these parameters do not depend on the particle size.

For ultrafiltration step, main attention was paid to membrane maintenance. Two approaches to operating the membranes were compared. The *"interval cleaning"* method of operation consisted of backwashing the clogged membrane followed by renewed filtration through the same side of the membrane as in the first cycle. No significant difference among their performance was found. In the *"alternating inlet"* method of operation, the in- and outlets of the filtration unit were exchanged vice versa after backwashing the clogged membrane.

From the results obtained, it could be concluded that for all the natural materials, the sorption kinetics of ^{137}Cs was low. However, conversion of the materials to NH_4^+ , Na^+ , H^+ , Ca^{2+} , or Al^{3+} forms was found to influence significantly the distribution coefficients of ^{137}Cs .

The complete four-step three-stage method developed was tested in a hot experiment with real CIAE radioactive liquid waste stream on 2 l batch scale. For the treatment, pH of samples was adjusted to 7.0–8.0, then 5 g of the ZT-4 zeolite in NH_4^+ form was added (80–160 mesh). After mixing, the flocculant was added. After 24 hours of standing, phase separation was performed by ultrafiltration and the permeate was passed through a zeolite ion-exchange column. The overall decontamination factor for the whole process was nearly $7.5 \cdot 10^4$.

4.3.6. Photocatalytic degradation of organic complexants combined with subsequent treatment of the solution by sorption on optimised absorbers

Potential of a two-step process, combining photocatalytic degradation of organic complexants combined with subsequent treatment of the filtrated solution by sorption on optimised PAN-based composite absorbers, was investigated in detail for the removal of organic complexants and/or separation of radionuclides from spent decontamination solutions. The study was performed at the *Czech Technical University in Prague*, with both simulated and real liquid waste from NPPs in the Czech and Slovak Republics.

A detailed study of options for the separation of radionuclides onto a series of inorganic ion-exchangers, composite absorbers, or cation exchange resins was carried out. Optimisation of the process parameters lead to the conclusion that a two-step process combining photocatalytic degradation of organic complexants and subsequent treatment of the filtered solution by sorption on optimised absorbers offers a prospective option for the treatment of spent decontamination solutions that contain organic complexants. It was found that

separation of the radionuclides released from the organic complexes onto organic resins is preferable to the application of selective inorganic-organic absorbers.

The process was successfully verified on a bench scale with the real waste from electrochemical decontamination of the primary circuit internals in the Jaslovske Bohunice NPP (Slovakia). Attention should be paid to the spent photocatalyst that would represent an additional secondary radioactive waste stream.

4.3.7. Combined processes for management of organic wastes

As is the case with aqueous radioactive waste, organic waste also more often require combination of processes for their treatment. Combined processes for management of organic wastes was developed at *Bhabha Atomic Research Center*, Mumbai, India. Appropriate choice of the processes and their combination have yielded significant reduction not only in the waste volumes but have also reduced the organic content for final disposal/discharge.

For spent solvent of reprocessing origins, *chemical destruction* using 'Alkaline hydrolysis' has not only resulted in the conversion of Tributylephosphate (TBP) into *aqueous soluble* salt of dibutyle phosphate as a reaction products, but also lead to the *recovery and recycle* of the diluent, n-dodecane, practically free of TBP and radioactivity. During alkaline hydrolysis of TBP in n-dodecane, the diluent does not take part in the reaction and separates out as top phase in the product mixture. The products of the reaction get separated out of the dodecane phase rendering it free of TBP. The degradation products of TBP are converted to their respective sodium salts and get into the aqueous phase along with nearly all the radioactivity associated with these degradation products. A very small amount of activity is associated with the diluent degradation products. Runs with the radioactive plant samples having activity in the range of 740–1200 Bq/mL gross alpha and 28,000–37,000 Bq/mL gross beta, gave quantitative recovery of the diluent practically free of activity (residual activity 2–3 Bq/mL for gross alpha and 10–12 Bq/mL for gross beta/gamma). The diluent was free of TBP and of recycleable quality.

Combination of advanced oxidation methods appear to be a prudent choice also for the management of organic waste streams like spent ion exchange resins and organic complexing agents used for decontamination purposes. Organic ion exchange resins in the bead form are highly resilient to mineralization by direct oxidation. For these resins, combination of processes involving catalytic wet oxidation for initial solubilization of these resin into aqueous media, followed by complete mineralization using photo-Fenton reactions are very effective. This combined two-stage process not only results in substantial reduction of the oxidant consumed but also in the reduction of the secondary waste volumes generated. Aqueous media after resins solubilization is amenable to decontamination by conventional methods such as chemical precipitation and the resulting precipitates (sludges) can be immobilised directly into cement. Decontamination using chemical precipitation for the solubilized resins gave high DF values for radionuclides such as ^{137}Cs and ^{60}Co (DF = 60 000, DF = 29 500 respectively).

The organic containing supernatant, lean in radioactivity, can be subjected to photo-Fenton destruction for organics and discharged as low level aqueous radioactive wastes.

4.3.8. Development of the combined waste treatment system for NPP operational waste

In the *Nuclear Environment Technology Institute*, Daejeon, Republic of Korea, a combined process for treatment of liquid radioactive waste generated from nuclear power plants as an alternative to evaporation process has been proposed. Chemicals and impurities contained in liquid radioactive waste cause problems such as corrosion, scaling, and foaming during evaporation. These problems markedly decrease the quality of decontamination, reduce the evaporator life, and increase the maintenance cost. Ion exchange method is regarded as a substitute for the evaporation method. Despite the successful application of the organic ion exchanger with regard to waste volume reduction, their costs and personnel radiation exposure need to be considered.

The combined technology, designed to improve the efficiency of the existing system for liquid waste processing, consisted of fibre filtration (FF), ultrafiltration (UF), reverse osmosis (RO), and selective ion exchange resin (SIES) modules operated sequentially. Fibre filter was employed for effective removal of organics and total suspended solids prior to reverse osmosis. RO unit focused on radionuclide removal and boron permeation. Selective ion exchange beds were employed for the removal of Cs permeated in RO membrane units. Based on the pilot runs with the actual waste, the decontamination factor (DF) of about 5000 was achieved.

The laundry radioactive waste, generated from the washing of the contaminated protection cloths and showers contain large volume of detergents and sometimes, their radioactivity is higher than the limits for free release to the environment. The combined process not only addresses removal of the radionuclides such as cobalt or caesium, but also the destruction of organics in these wastes.

The photo degradation unit had a 3 kW UV lamp (180~400 nm wavelength). With 1000 ppm of H₂O₂ injection, more than 85% of TOC was removed from the laundry wastes. Cobalt and caesium rejection rates were more effective with Polyamide membrane rather than with the Cellulose Acetate (CA) one. However, boron permeation rate was more higher with the CA membrane. The radionuclide rejection rate of UF unit increased with increasing flow rate. The rejection rates of Co, Cs, and surfactants was maximum at a pH of 9, while for boron permeation rate good result were shown at pH 4. In the demonstration test with radioactive waste, the activity of permeate was below the lower limit of detection. Decontamination factor obtained was about 5000 for the radioactive laundry waste having original activity of $8.199 \times 10^{-4} \mu\text{Ci/mL}$.

4.3.9. Treatment of aqueous radioactive waste containing uranium, thorium and radium radionuclides by chemical precipitation and Laterite soil sorbent

Decontamination of aqueous waste stream containing ²³²Th, ²³⁸U and ²²⁶Ra by combined treatment employing chemical precipitation followed by sorption on natural soil (Laterite) were investigated at the *Malaysian Institute for Nuclear Technology Research (MINT)*. High concentration of goethite, pH in the range of 3.79–3.91 and kaolinite clay present in these soils contributed to the adsorption of thorium and uranium on to these soils. Chemical precipitation treatment removed nearly all uranium, thorium and radium from these waste streams at an optimum pH of 9.9 and final polishing through the soil ensured that the effluents are below dischargeable limits. Decontamination Factors (DF) achieved in the treatment process were 391, 234 and 80, for radium, thorium and uranium respectively. At pH

of 9.9, thorium hydroxide ($\text{Th}(\text{OH})_4^0$) species were dominant as precipitate. Radium also precipitated as radium sulphate. Uranium in hexavalent state dominated the solution.

Supernatant from the chemical treatment was adjusted to pH of 4.0 and subjected to sorption by passing these effluents through the soil column. It was observed that the adsorption capacity of the Laterite soil for radium was as high as 0.20 $\mu\text{Ci/g}$. The effluents after the sorption showed concentration of these radionuclides below detection limits. In the pilot scale treatment, the waste quality parameters after this combined treatment fulfilled the requirements set by the national regulatory authority for their release. Role of pH was most important for the effective treatment using this combined process. The effluent radioactivity was less than 37 kBq/L, the authorized release limit set by the national regulatory authority for the release in the nearby river.

5. CONCLUSIONS

The research performed in the frame of the CRP addressed a rather new approach of adopting combined processes for treatment of liquid radioactive waste. This approach covered broad areas both in terms of materials, technologies and processes studied and included a wide spectrum of liquid radioactive waste investigated. The application of materials with combined properties as well as the application of combined processes themselves allows effective treatment of wastes of a complex chemical nature, which are otherwise difficult to treat by traditional or conventional processes and techniques. The areas of investigation included:

- Aqueous waste streams with the various salt contents (from low salt solutions to high salt content evaporator concentrates), aqueous wastes with the various organic components (from liquors containing organic impurities to pure organic solvents of reprocessing origin), radioactive waste with radionuclides in the form of different complexity (colloids, complexes of different compositions, etc.);
- Liquid waste with wide ranges of the target radionuclides, extending from some TENORM radionuclides (uranium, thorium, radium), through complex fission products mixtures (Cs, Sr, Co, etc.) and all the way to alpha bearing liquid waste;
- Development, study and application of different waste treatment methods, materials and their combinations (from conceptual ideas, through validation of particular techniques, to pilot demonstration of the new processes);
- With respect to the direct applicability of the results obtained, the research was extended from more or less academic studies (e.g. the speciation studies) to hot pilot plant demonstrations with hundreds or even thousands of cubic meters of real radioactive waste treated.

Based on the results obtained in the frame of the CRP and their discussion, three main areas related to the application of combined processes for treatment of liquid radioactive waste have been identified:

- Application of materials/sorbents with combined properties,
- Application of single stage processes incorporating multiple treatment techniques.
- Development and application of combined multi-stage treatment processes with interrelated sequential waste treatment steps.

Several materials with combined properties have been identified and characterized in the frame of the CRP. The manufacture of some of these materials has reached the industrial

scale. The examples of such materials could be titanium dioxide and chitin-based biosorbent. These materials have been tested for the treatment of real radioactive waste. The modification of certain sorbents by incorporating particular active groups or ligands have made them highly specific for sorption of radionuclides even in the presence of many interfering salts and organic complexes. Certain materials have been specifically tailored to address the low concentrations of long lived radionuclides generally present in reprocessing waste. In general, the development, synthesis, and characterization of these materials have reached the level of maturity for commercial application.

Combined single stage processes incorporating several techniques or principles are attractive since these can in some cases exploit the versatile properties of novel materials in addition to superimposing the advantages of other treatment techniques. For example, in electrosorption, ultra, nano and even ceramic membranes can be used in conjunction with the novel sorbents. This combined single stage technique can address the treatment of a wide variety of waste having radioactivity even in the colloidal form. Another example of a combined single stage treatment process is photo catalytic destruction of organics and sorption of radionuclides in one single vessel. In this case titanium dioxide used as a catalyst for the destruction of organics in the aqueous waste is also a good sorbent for radionuclides.

Combined multi-stage processes with careful selection of treatment stages and their sequences allow substantial improvement of waste processing systems. Depending on the design objectives such combined processes could substantially improve efficiency and effective implementation of waste treatment with respect to volume reduction, quality of final waste product, requirements for disposal, and general waste management cost. The qualitatively new approach to the problem should be emphasised in this case. When considering or developing combined multi-stage processes for treatment of specific waste stream, right from the early design stages, all the modules that are combined should be considered and evaluated as components of a single system and their interactions and interrelations should be streamlined for optimised performance of the system as a whole.

Detailed information on the results of investigations can be found in the individual reports of the CRP participants which follow this conclusion section.

Annex
PAPERS PRESENTED

SELECTION OF OPTIMAL CONDITIONS FOR THE REMOVAL OF RADIONUCLIDES FROM WASTE SOLUTIONS BY A COMBINATION OF TWO METHODS: SORPTION AND MEMBRANE FILTRATION OR SORPTION AND CENTRIFUGATION

YU.P. DAVYDOV, V.M. EFREMENKOV, D.YU. DAVYDOV, I.G. TOROPOV,
L.M. ZEMSKOVA, V.V. TOROPOVA

Institute of Radioecological Problems, Belorussian Academy of Sciences,
Minsk, Belarus

Abstract. A series of physico-chemical methods have been employed to examine the speciation of Fe and Cr radionuclides in aqueous solution over the pH range 1–12. The results show that Fe(III) and Cr(III) are in the form of pseudocolloids at concentrations less than 10^{-6} mol/L and over the pH ranges 3–12 and 4.5–12 respectively. The effect of complexing ions (oxalate, EDTA, hexametaphosphate) was found to move the beginning of pseudo complex formation to higher pH values and, at a concentration of complexing anion higher than 10^{-3} mol/L, no pseudocolloids were formed over the pH range 1–12. Using the data obtained, it was identified the optimal consideration for maximum removal of a radionuclide by semi-permeable membranes or by centrifugation.

The main scientific direction of our laboratory is the studying of radionuclide forms in solutions in a wide range of pH 1–12. Particularly detailed investigation on the regularities of hydrolysis has been carried out for the following cations – Pu(IV) [1–3], U(IV) [4, 5], U(VI) [6], Zr(IV) [7], Th(IV) [8], Sc(III) [9], Y(III) [10, 11]. Over 40 years of the studies convinced us that the profound knowledge of the state of radionuclides in water solutions can be an effective basis for development of efficient methods for removal of radionuclides from waste solutions.

This particular study is dedicated to the selection of optimal conditions for the removal of radionuclides from liquid radioactive waste by a combination of two methods — sorption and membrane filtration or sorption and centrifugation. Two radionuclides - Fe(III) and Cr(III) have been selected for the experiments.

Previously the following studies on the speciation of Fe(III) and Cr(III) in water solutions have been carried out: investigation of the state of radionuclides at micro concentrations (less than 10^{-6} M) [12, 13]; determination of the cations hydrolysis constants [14, 15]; determination of conditions of their polynuclear hydroxocomplexes formation; investigation of the sorption of mononuclear and polynuclear hydroxocomplexes on KU-2 cation exchange resins and silica gel [16–19]; investigation of the effect of complexing anions on the state of the radionuclides in solution at micro concentration [20]; investigation of the effect of a series of anions on the hydrolysis of the cations with formation of polynuclear hydroxocomplexes in solutions [21]; investigation of the effect of oxidisers and reducers on the hydrolysis of the cations.

The necessary degree of radioactive solution cleaning up depends on the level of its activity concentration. For example, if the initial radionuclide concentration is about 10^{-5} Ci/L ($3.7 \cdot 10^5$ Bq/L) the necessary decontamination factor should be approximately 10^4 since the discharge level is 10^{-9} Ci/L (37 Bq/L). It is not always possible to achieve the decontamination factor of that order of magnitude by applying one method only. Most often a combination of different methods is needed.

Two principally different cases can be distinguished in the treatment of radioactive contaminated solutions depending on the concentration of radionuclides. The first one is when a radionuclide is at micro concentration in solutions. For such solutions, with typical

radionuclides such as Fe(III) and Cr(III), the treatment could be made to form pseudocolloids in the solution at pH above 3–4 (Fig.1,2). These pseudocolloids can be filtered through a semi-permeable membrane and nearly 99.9% of the activity can be removed. Centrifugation method allows only 80% removal of these radionuclides for the same solutions. Further decontamination could be achieved by acidification of the solution down to pH 1.5 – 2.0 where pseudocolloids are rapidly destroyed and sorption activity of Fe(III) as hydroxocomplexes is achieved. The coefficient for their sorption on sorbents like silica gel is about 10^2 . Thus, a combination of two methods viz: membrane filtration at pH higher than 4.0 and, then, acidification and sorption on silica gel provides the necessary decontamination factor of the order of 10^5 .

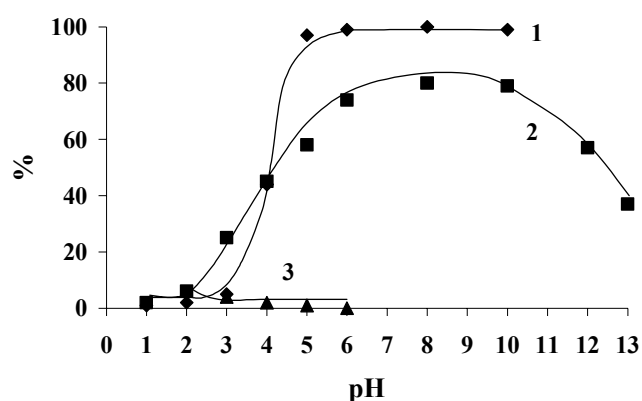


FIG. 1. 1 – ultrafiltration of Fe(III) solution; 2 – adsorption of Fe(III) on the surface of glass; 3 – adsorption of Fe(III) on silica gel from equilibrated solution.

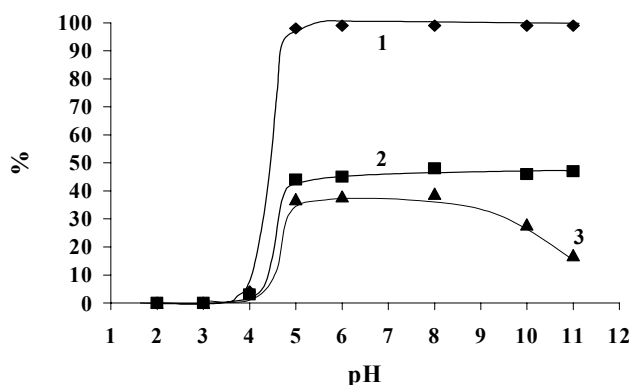


FIG. 2. 1 – dialysis of Cr(III) solution; 2 – centrifugation of Cr(III); 3 – adsorption of Cr(III) on the glass surface. Cr(III) concentration – 10^{-6} M.

The data presented in Fig.1 show that introduction of an absorber (silica gel) in the solution does not result in any additional decontamination of the solution. At the same time, further removal of the radionuclides from the solution can be achieved in a simple way – acidification of the solution down to pH 1.5 – 2.0. Pseudocolloids are rapidly destroyed under these conditions, and sorption activity of Fe(III) hydroxocomplexes could be very high. For example, the coefficient for their sorption on silica gel is about 10^2 . Thus, a combination of two methods – membrane filtration at pH higher than 4.0 and, then, acidification and sorption on silica gel – provides decontamination factor 10^5 .

In the presence of complexing anions in the waste solution, the initiation of pseudocolloids formation shifts in a range of higher pH (Fig. 3, 4). For instance, at the concentration of oxalate-anion in this solution nearly $2.5 \cdot 10^{-1}$ M, the formation of pseudocolloids for Fe(III) does not proceed at all over the entire range of pH.

In that case, there are two options for the removal of Fe(III) and Cr(III) radionuclides from the waste solution. The first one is to carry out the treatment at a higher pH. For example, if the concentration of oxalate-anion in the solution is less than $1 \cdot 10^{-1}$ M, the formation of Fe(III) pseudocolloids will proceed from pH 8.0 onwards, and the decontamination factor of about 10^3 can be attained by membrane filtration. Alternatively, partial destruction of complexing anion by one of the oxidizing methods (ozonation, reagent oxidation etc.) could bring down the concentration of the interfering oxalate anions much lower so as not be interfering. The experimental data obtained (Fig. 3, 4) show that destruction of complexing ligands has not necessarily to be complete. Substantial reduction of their concentration can be enough.

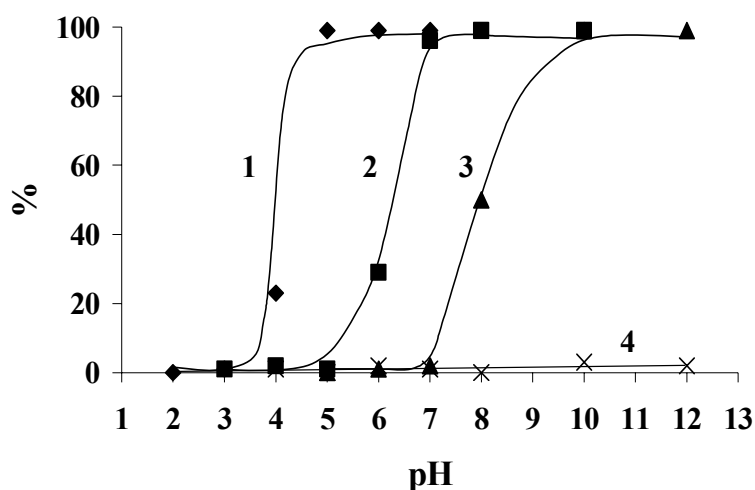


FIG. 3. Retention of Fe(III) by ultrafiltration in the presence of oxalate anion: 1 – 0 M; 2 – 5×10^{-5} M; 3 – 5×10^{-3} M; 4 – 2.5×10^{-1} M.

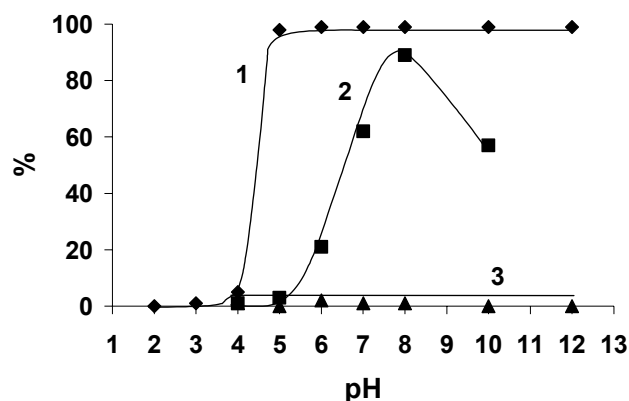


FIG. 4. Retention of Cr(III) by ultrafiltration in the presence of oxalate anion: 1 – 0 M; 2 – 10^{-5} M; 3 – 10^{-3} M.

In case of Fe(III) and Cr(III) radionuclides present in macro concentration levels (higher than 10^{-6} M) e.g in decontamination solution, the formation of pseudocolloids cannot proceed at such high concentration and their form in the solution will be determined by their ability to form mono-nuclear, poly-nuclear and other hydroxy complexes. These complexes could be removed by precipitation in a form of hydroxides followed by dialysis.

The high concentration of the radionuclides assumes that their precipitation in a form of hydroxides could be a possible treatment method. The conditions of Fe(III) and Cr(III) polynuclear hydroxocomplexes formation have been determined in our previous studies [15]. In those studies only the pH and the cation concentration, beginning from which the cation was predominantly (more than 90%) in a form of polynuclear hydroxocomplexes in solution, were determined. However, for the removal of radionuclides from the solution it is important to know exactly the value of their retention by the membrane. In order to achieve this, additional experiments have been carried out. From the data obtained (Tables I–IV) it follows that, in the case of Fe(III), the decontamination factor was about $2 \cdot 10^2$. The same decontamination factor has also been attained by centrifugation at 6000 rpm for the precipitation of Fe(III) radionuclides. Similar values were also obtained in the case of Cr(III) (Table III–IV).

An interesting fact is that for pH higher than 5.0, the retention for Fe(III) radionuclide by dialysis does not change in the pH interval 5.0 – 10.0. Thus, the concentration of iron in the outer compartment of dialyser remains the same at $5 \cdot 10^{-6}$ M. This does not conform very well to the solubility product principles, wherein the product of iron hydrated cation and OH⁻-anion concentrations must remain constant in equilibrium with iron hydroxide at $[\text{Fe}^{3+}] [\text{OH}^-] = 3.8 \cdot 10^{-38}$.

TABLE I. DIALYSIS OF Fe (III) THROUGH A CELLOPHANE MEMBRANE WITH THE PORES OF DIAMETER 2–4 nm. (Concentration of Fe (III) in the initial solution was $1 \cdot 10^{-3}$ Mol/L)

pH of solution	3,0	3,2	3,6	4,0	5,0	7,0	10,0
Concentration of Fe (III) in the outer compartment of dialyser, $\times 10^4$ Mol/L	0,72	0,15	0,05	0,12	0,06	0,05	0,05
	0,68	0,15	0,05	0,10	0,06	0,05	0,05
	0,72	0,10	0,10	0,10	0,06	0,05	0,05
	1	0,52	0,12	0,06	0,05		0,05
	2	0,50	0,14	0,05	0,07		0,045
	1	0,52	0,20	0,05	0,05		0,047
Average value of the concentration	$1,1 \pm 0,4 \times 10^{-4}$	$0,32 \pm 0,1 \times 10^{-4}$	$0,15 \pm 0,05 \times 10^{-4}$	$0,08 \pm 0,02 \times 10^{-4}$	$0,06 \times 10^{-4}$	$0,05 \times 10^{-4}$	$0,05 \times 10^{-4}$
Decontamination factor (D_f)	9	30	66	125	170	200	200
Decontamination factor in the presence of silica gel in the inner compartment of dialyser	5	10	125	200	200	250	250

TABLE II. PRECIPITATION OF Fe (III) BY CENTRIFUGATION (Concentration of Fe (III) in the initial solution was $1 \cdot 10^{-3}$ Mol/L).

pH of solution	3,0	3,2	3,6	4,0	5,0	7,0	10,0
Concentration of Fe(III) in solution after centrifugation, Mol/L	$9 \cdot 10^{-4}$	$7,4 \cdot 10^{-4}$	$4,6 \cdot 10^{-4}$	$2,8 \cdot 10^{-4}$	$0,3 \cdot 10^{-4}$	$0,2 \cdot 10^{-4}$	$0,1 \cdot 10^{-4}$
Decontamination factor (D_f)	1,1	1,5	2,1	3,6	33	50	100
Decontamination factor in the presence of silica gel in the solution	2,0	3,5	10,0	20	15	150	200

TABLE III. DIALYSIS OF Cr (III) THROUGH A CELLOPHANE MEMBRANE WITH THE PORES OF DIAMETER 2–4 nm. (Concentration of Cr (III) in the initial solution was $1 \cdot 10^{-3}$ Mol/L)

pH of solution	5,0	7,0	10,0
Concentration of Cr(III) in the outer compartment of dialyser, Mol/L	$7 \cdot 10^{-4}$ $7 \cdot 10^{-4}$	$5,5 \cdot 10^{-4}$ $3,2 \cdot 10^{-4}$	$4 \cdot 10^{-4}$ $2,4 \cdot 10^{-4}$
Decontamination factor (D_f)	1,4	2,5	3,3
Decontamination factor in the presence of silica-gel	1,4	2,0	30

TABLE IV. PRECIPITATION OF Cr (III) BY CENTRIFUGATION. (Concentration of Cr (III) in the initial solution $1 \cdot 10^{-3}$ Mol/L).

pH of solution	5,0	7,0	10,0
Concentration of Cr(III) in solution after centrifugation, Mol /L	$9 \cdot 10^{-4}$	$3 \cdot 10^{-4}$	$0,5 \cdot 10^{-4}$
Decontamination factor (D_f)	1,1	3,3	20
Decontamination factor in the presence of silica -gel in solution	33	40	45

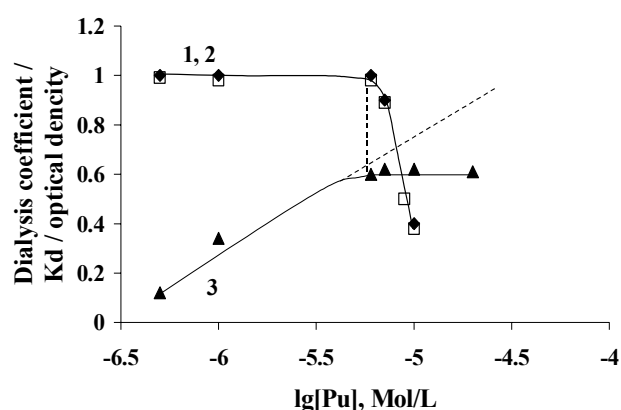


Fig. 5. 1 – Dialysis of Pu(IV); 2 – Sorption of Pu(IV) on cation exchange resin KU-2; 3 – Spectrophotometry of Pu(IV) solutions.

Accordingly, the concentration of Fe^{3+} -cation at pH 5.0 must be $3.8 \cdot 10^{-17}$, and it should decrease with pH increasing. However, the concentration of Fe(III) in the outer compartment of dialyser is a summary value which includes all the soluble hydroxo-forms, apart from polynuclear hydroxocomplexes.

Specific experiments have been carried out to prove that the polynuclear hydroxocomplexes cannot penetrate the cellophane membrane used for dialysis. Thus, in the case of Pu(IV), the conditions (pH and the Pu(IV) concentration) under which plutonium converts from a mononuclear to a polynuclear form have been determined. From the data presented in Fig.5 it could be seen that, from the concentration $2 \cdot 10^{-5}$ M onwards at pH 2.0, Pu(IV) is retained by a semipermeable membrane due to the formation of binuclear hydroxocomplex $\text{Pu}_2(\text{OH})_n^{8-n}$ in the solution. Under the same conditions, the decrease of the plutonium sorption on cation exchange resins and in optical density of Pu(IV) solution were observed. This can be explained by the beginning of polymerization process under the conditions investigated, and as a result decreasing concentration of Pu^{4+} -cation in the solution. Thus, the results obtained by three independent methods confirm that only mononuclear hydroxocomplexes $\text{Pu}(\text{OH})_n^{4-n}$ and hydrated cations $\text{Pu}(\text{H}_2\text{O})_6^{4+}$ can pass the cellophane membrane at dialysis.

So, in the case of iron dialysis, only mononuclear forms can be in the outer compartment of the dialyser. At the same time, the hydrolysis constants available in the literature allow for the correct calculation of the first hydroxocomplex $\text{Fe}(\text{OH})^{2+}$ only. Unfortunately, at present there are no reliable data on the stability constants of such hydroxocomplexes as $\text{Fe}(\text{OH})_2^+$ and $\text{Fe}(\text{OH})_3^0$. In this regard, it seems impossible to calculate the concentration of every mononuclear hydroxocomplex, and hydrated complex in particular, in equilibrium with insoluble particles of iron hydroxide.

In Table V the literature data on polymerisation of some metal ions are summarised.

TABLE V. INITIAL CONDITIONS OF METAL-ION POLYNUCLEAR HYDROXOCOMPLEXES FORMATION IN SOLUTIONS

Metal-ion	Concentration of metal-ion, Mol/l	Form of complex
Pu (IV)	10^{-5}	$\text{Pu}_2(\text{OH})_n$
Fe (III)	10^{-5}	$\text{Fe}_2(\text{OH})_n$
Sc (III)	10^{-3}	$\text{Sc}_2(\text{OH})_2^{4+}$
Cr (III)	10^{-6}	$\text{Cr}_2(\text{OH})_2^{4+}$
Y (III)	10^{-3}	$\text{Y}_2(\text{OH})_2^{4+}$

From these data it can be concluded that the concentration threshold for polymerisation of hydrolysed cations is 10^{-5} – 10^{-6} M. Hence, the limiting capacity of solution decontamination at the stage of hydroxides precipitation is determined not by hydroxide solubility (solubility product principle) but by the possibility of polymerisation process.

Summarising the above, it can be concluded that the decontamination factor $2 \cdot 10^{-2}$ for Fe(III) and Cr(III) at maximum could be obtained by precipitation, and further increase of pH does not lead to a higher degree of radionuclide removal. At the same time, the decontamination factor 10^3 – 10^4 is needed in order to achieve the necessary level of activity concentration 10^{-8} – 10^{-9} Ci/L (37 – 3.7×10^2 Bq/L). From the Tables I and III it could be seen that in the presence of an absorber (silica gel) the decontamination factor for both Fe(III) and Cr(III) increases insignificantly. This means that the forms of the radionuclides remaining in the solution have co-ordination spheres saturated with OH-groups, which cannot be absorbed by silica gel. However, the previous studies showed the hydroxocomplexes of Fe(III) and Cr(III) with lesser quantity of OH-groups in co-ordination sphere of a cation possess an enhanced sorption capacity with respect to silica gel. From the data presented on Fig.6 it could be seen that the sorption coefficient sharply increases with the accumulation of $\text{Fe}(\text{OH})_2^+$ and $\text{Cr}(\text{OH})_2^+$ hydroxocomplexes in the solution. Furthermore, their sorption proceeds in a specific way and is not governed by regularities of ion exchange process. Thus, their sorption on silica gel is not dependent on the concentration of competitive ions. The current study shows that the increase in the concentrations of inactive electrolytes even increase the sorption (for added Na^+ , Ca^{2+} - cations) or have no effect on it (added Al^{3+} -cation) (Fig. 7.). This confirms that the sorption of Fe(III) mononuclear hydroxocomplexes on silica gel is based not on ion exchange. At the same time, the results of radionuclides sorption on cation exchange resins KU-2 show (Fig. 8) show that the growth of the $\text{Me}(\text{OH})^{z-1+}$ hydroxocomplex concentration in the solution results in the decrease of Fe(III) sorption on cation exchange resins. In this case, a standard ion exchange process takes place in the solution, when, with the decrease of cation's charge, its sorption ability decreases.

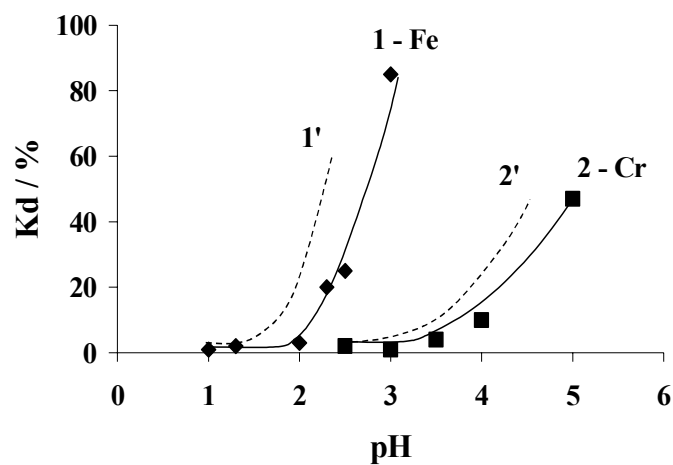


FIG. 6. Sorption of Fe(III) (1) and Cr(III) (2) on silica gel . Percent of the first hydroxocomplex in solution : 1' – Fe(III); 2' – Cr(III).

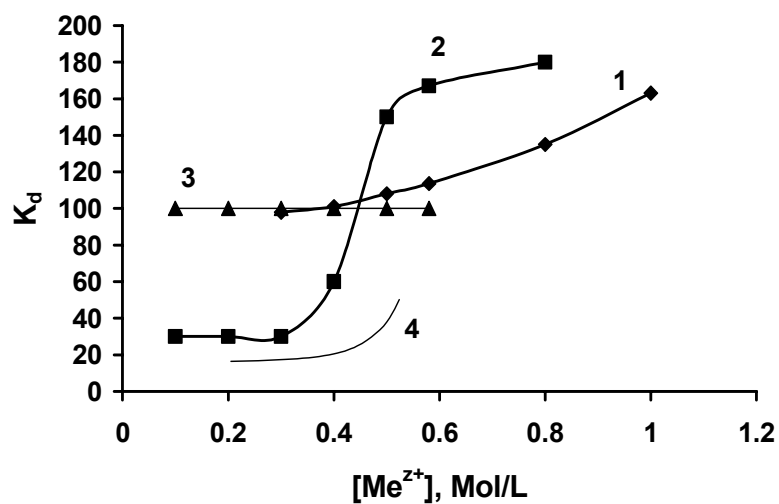


FIG. 7. Dependence of Fe(III) – (1–3) and Cr(III) (4) on silica gel on concentration of inactive electrolyte in solution. pH = 2.7: 1 – Na^+ ; 2 – Ca^{2+} ; 3 – Al^{3+} ; 4 – Na^+ , pH = 4,5.

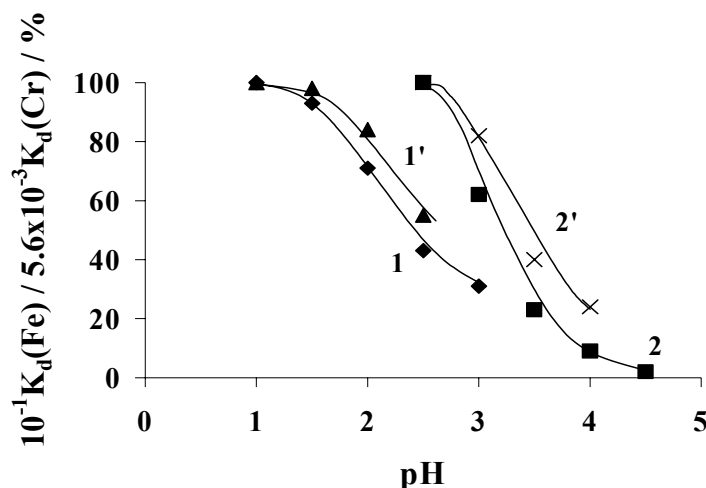


FIG. 8. Sorption of Fe(III) (1) and Cr(III) (2) on cation exchange resin KU-2. Percent of Fe³⁺ (1') and Cr³⁺ (2') cations in solution.

Membrane filtration and sorption or centrifugation and sorption are the combined treatment methods to address the waste solutions where radionuclide concentrations of Fe(III) and Cr(III) are relatively high and at the same time higher decontaminations are to be achieved. In such cases as a first stage, neutralisation of these waste solutions up to pH 5.0 and higher will result in formation of hydroxide sediment, colloidal particles and polynuclear hydroxocomplexes. These can be removed from these waste solution either by membrane filtration or centrifugation, with maximum decontamination factor of $2 \cdot 10^2$ achievable. The radionuclides remaining in the solution after precipitation as hydroxides are in a form that can not be sorbed due to co-ordination saturation of the cations with OH-groups. In order to effectively apply the method of sorption for the removal of these radionuclides, it is necessary to acidify these solutions down to pH 3.0 for Fe(III) and pH 4.0 for Cr(III). These can then be absorbed on sorbents such as silica gel for their effective removal.

REFERENCES

- [1] GREBENCHIKOVA V.I., DAVYDOV Ju.P. Radiochemistry 3, №2, p.155–157 (1961).
- [2] DAVYDOV Ju. P., VJATKIN V.E. SHASHUKOV E.A., Radiochemistry 13, № 3, p. 469–471 (1971).
- [3] DAVYDOV Ju.P. Radiochemistry 14, №4, p. 511–512 (1972).
- [4] DAVYDOV Ju. P., EFREMENKOV V. M.,SKRIPSOVA A.V., Radiochemistry 15, №3, p.452–453 (1973).
- [5] DAVYDOV Ju.P., EFREMENKOV V.M., SKRIPSOVA A.V., Radiochemistry 17,№2,p.160–167 (1975).
- [6] DAVYDOV Ju.P, EFREMENKOV V.M., J. Neorganic Chemistry 28, p. 2316 (1983).
- [7] DAVYDOV Ju.P., EFREMENKOV V.M., ZABRODSKI V.N., VORONIK N.I., J. Radioanal. Chem. 80, №1–2, p.247–253 (1983).
- [8] DAVYDOV Ju.P, TOROPOV I.G., TOROPOVZA V.V. SOSUKEVICH V.M., J. Neorganic Chemistry 41, №1, p.126–130 (1996).
- [9] DAVYDOV Ju.P.,GLAZICHEVA G.I., J. Neorganic Chemistry 25, №6, p.1462–1467 (1980).
- [10] DAVYDOV Ju.P.,VORONIK N.I., J. Neorganic Chemistry 28, №9, p.2240–2244 (1983).
- [11] DAVYDOV Ju.P.,VORONIK N.I, J. Neorganic Chemistry 43, №9, p. 1459 (1998).
- [12] DAVYDOV Ju. P., GRACHOK M.A., BASHIMOVA N.B., Izvestija Acad. of Sciences Belarus,ser. physica-energetic. Science №2, p.49–53 (1974).
- [13] DAVYDOV Ju. P. EFREMENKOV V.M., VORONIK N. I., URUSOVA A.B., Radiochemistry 18, №3, p.341–345 (1976).
- [14] DAVYDOV Ju. P., GRACHOK M.A., Izvestija Acad. of Sciences Belarus, ser. physica-energetic. Science №4, p39–42 (1973).
- [15] DAVYDOV Ju. P., State of radionuclides in solution. Minsk. Science and Technique (1978).
- [16] DAVYDOV Ju. P.,BONDAR Ju.I., J. Neorganic Chemistry 27, №1, p.139–142 (1982).
- [17] DAVYDOV Ju. P.,BONDAR Ju.I., J. Neorganic Chemistry 25,№10 p. 2746–2750 (1980).
- [18] DAVYDOV Ju. P., BONDAR Ju.I., GLAZICHEVA G.I., Radiochemistry 22 №6, p.857–861 (1980).
- [19] DAVYDOV Ju. P.,BONDAR Ju.I., J. Radioanal.Chemistry 51 №2, p.325–335 (1979).
- [20] DAVYDOV Ju.P., EFREMENKOV V.M., URUSOVA A.B., Radiochemistry 25, №1, p.89–92 (1983).
- [21] DAVYDOV Ju.P., TOROPOV I.G., DAVIDOV D.Ju., J. Neorganic Chemistry 44, №7, p.1115–1119 (1999).

VOLUME REDUCTION OF LOW LEVEL LIQUID PWR WASTE TREATMENT OF TRITIATED SOLVENTS

A. BRUGGEMAN, J. BRAET
SCK•CEN, Mol, Belgium

Abstract. In 1989 Belgoprocess, the central radioactive waste processing facility of Belgium, took over the exploitation and personnel of the former Waste department of the Belgian nuclear research centre SCK•CEN. Due to the general minimisation of radioactive waste generation during the last decade, Belgoprocess has now an overcapacity for the treatment of routine waste. One example of such work is reactor waste minimisation study through volatilisation of boric acid. Another example is development of method for processing of tritiated liquid organic waste. The report describes the progress of work on the separation of boric acid and on treatment of tritiated liquid organic waste.

INTRODUCTION

SCK•CEN participated to the IAEA Research Co-ordination Programme "Combined Methods of Liquid Radioactive Waste Treatment" with two projects, "Volume Reduction of Low Level Liquid PWR Waste" and "Treatment of Tritiated Solvents". Liquid wastes from pressurised water reactors (PWRs and VVERs) primarily consist of boric acid solutions. Boric acid is used as a soluble neutron poison to suppress and control the nuclear fission. Although recovery of boric acid from clean effluents is extensively applied in nuclear power plants, much boric acid still ends up in the normally non-recyclable low level liquid waste (LLW), in which it represents the largest constituent besides water. In most cases these wastes are treated by evaporation, which allows high decontamination factors for the discharged distillate. Conditioned and non-conditioned boron-containing evaporator concentrates represent the volumetrically most important fraction of the low level waste at NPPs. Strict measures to minimise the generation of waste at NPPs are introduced because of the escalating costs and provisions for waste treatment, storage and disposal. Substantial reduction of the waste volume and cost is possible by separating boric acid from the radioactivity before, during or after the LLLW evaporation. Separation of boric acid will also result in a waste that is less difficult to process and has a better long term stability [1, 2].

Separation of boric acid from PWR waste can be a very remunerative operation. In Belgium, for example, the costs associated with conditioning, transport and interim storage, and the provisions for future disposal of 1 m³ of evaporator concentrate have now increased to about 25,000 EURO. For each kg of boric acid that can be separated, the concentrate volume can be decreased by 2 dm³. The corresponding decrease of the waste cost amounts then to 50 EURO per kg separated boric acid. This is more than 50 times the price of boric acid that has been separated from ore deposits and purified.

SCK•CEN has been developing processes for the separation of boric acid since more than five years. The key goal of these processes is to achieve higher waste volume reduction factors in a cost effective way, while maintaining low activity discharge limits. An additional goal is to obtain purified boric acid for recycling. Recovery and recycling of boric acid can be necessary for environmental reasons, e.g. when the effluents are discharged in a river that is also a source of drinking water. Volatilisation of boric acid during evaporation is a simple but technically and economically viable method for

separating boric acid and reducing radwaste costs at PWRs [3]. Volatilisation of boric acid after evaporation, i.e. treatment of evaporator concentrates, is being studied as a valuable alternative or complement [4].

The second project concerns the treatment of tritiated solvents. A variety of radioactive waste streams that contain organic materials are in storage and many continue to be generated. More and more countries require that such mixed waste meets minimum treatment standards prior to final disposal. Substantial or complete removal of the organic component of radioactive waste can provide a significant reduction in the volume of radioactive waste and ensure a safer disposal by the elimination of toxic or flammable organic components. Furthermore, the compatibility of the treated waste with secondary conditioning processes (such as cement encapsulation) is likely to be enhanced. In other cases treatment of the mixed waste is followed by an isotopic separation for recovering and recycling the concerned radioisotopes. If also economically it can be justified, recycling appears a preferable solution for this type of waste.

SCK•CEN owns an amount of tritiated liquid organic waste. This waste was generated by the pharmaceutical industry about 20 years ago. In the available documentation it has been described as 95% methanol/water and 5% impurities (petroleum ether, chloroform, and carbon tetrachloride). Small quantities of glycol, formaldehyde and hydrogen could have been formed over the years by radiolysis of the methanol. Analysis of the waste was not possible at SCK•CEN or in Belgium. Sampling alone required a dedicated infrastructure, which was not available at SCK•CEN when this project started. The total volume was 177.5 litres with a specified total tritium activity of about 16.5 TBq (recalculated at 31/10/2000). The waste was divided over 70 2.5-litre glass bottles and one smaller glass bottle. All except two of them were inside 12-litre polyethylene bottles, which were themselves stored in nine 200-litre drums with one or more additional overpacks. Five to eight bottles were stored in each drum.

The Belgian government questioned further storage of the waste at SCK•CEN and forbade massive discharge. NIRAS/ONDRAF asked conversion to tritiated water before conditioning and storage at Belgoprocess. Our objective was thus an appropriate pre-treatment of the waste, with negligible risks for the operators or the environment. Appropriateness meant that we should convert the tritiated organic waste into tritiated water and carbon dioxide. The tritiated water should be free of organic carbon for final conditioning and storage and the carbon dioxide should be fully decontaminated for discharge.

VOLATILISATION OF BORIC ACID DURING EVAPORATION

Distribution coefficient

Boric acid, H_3BO_3 , is a slightly volatile product. It has a certain vapour pressure (equilibrium pressure) which is higher at a higher temperature. But when heated in the absence of water, solid H_3BO_3 decomposes in HBO_2 and water. The easiest way to volatilise boric acid is therefore from boiling aqueous solutions. When boric acid volatilises from aqueous solutions, the experimental distribution coefficient is defined as the ratio of the mole fraction of boric acid in the vapour to the mole fraction of boric acid in the liquid. For practical reasons we use the following approximation:

$$D_{H_3BO_3}(T) = \frac{\text{weight fraction of boric acid in the vapour}}{\text{weight fraction of boric acid in the liquid}}$$

The distribution coefficient D is smaller than one and it increases with increasing temperature. The volatility is due to the undissociated boric acid, H_3BO_3 . The pH affects the boric acid dissociation and thus the apparent value of D . According to D. G. Tskhviraashvili and V.V. Galustashvili [5] the distribution coefficient for boric acid is given by:

$$D = \left(\frac{\rho_s}{\rho_w} \right)^{0.9}, \text{ where } \rho \text{ is the density and the subscripts s and w are steam and water respectively.}$$

Separation process

For the separation of boric acid during evaporation, the process resembles very much the usual evaporation. The LLLW is treated in a semicontinuous evaporator that operates at a constant inventory, at a pH below 8, at elevated temperature and pressure and without reflux. After an initial period all boric acid that comes in with the feed leaves the evaporator in the gaseous phase. The non-volatile chemical and radiochemical impurities, on the other hand, remain quantitatively in the evaporator and the waste volume reduction factor is no longer limited by the boron concentration in the evaporator. The steam loaded with boric acid can be fed to a column for fractional condensation with partial reflux. Here, the boric acid is concentrated in the reboiler [3, 6].

Without the addition of reagents or the production of secondary waste, this simple all-in-one process splits the incoming wastewater stream into three streams:

1. an active waste concentrate containing almost all the radioactive and chemical impurities, together with some boron;
2. a concentrated boric acid solution that can be reused if it is sufficiently pure;
3. an effluent with low boron content and which is highly decontaminated.

Let f be the constant concentration of boric acid in the feed, p in the steam and c in the liquid inventory V (kg) of the evaporator (all expressed as weight fractions) then the evolution of c and of the overall fractional boric acid recovery B as a function of time t (h) can be calculated as follows:

$$c = \frac{f}{D} \left[1 - (1 - D)e^{-D \frac{F}{V} t} \right] \quad \text{and} \quad B = 1 - \frac{c \cdot V}{f \cdot F \cdot t + f \cdot V}$$

Typically, one cycle of the semicontinuous evaporation process has to be stopped as soon as either the concentration of dry residue in the concentrate or the concentration of boric acid in the waste exceeds a pre-set limit, for example either 40 wt.% dry residue or 25 wt.% H_3BO_3 (43000 ppm B). If the H_3BO_3 recovery is still low (e.g. below 80 %) and the H_3BO_3 concentration in the radioactive concentrate is high, then the concentrate can be kept in the evaporator and the feed can change to water containing no H_3BO_3 . Using the same symbols as before, and with $f = 0$ from $t = t_1$, the evolution of c after $t = t_1$ is then

$$\text{given by: } c = c(t_1)e^{-D \frac{F}{V} (t - t_1)}$$

In theory it is possible to completely remove the boron from the radioactive concentrate. In practice a compromise will have to be made between the extra energy input on the one hand and the extra boron recovery on the other hand. It is clear that an extra boron recovery allows a further reduction of the radioactive waste volume.

Experiments

After promising trials using simulated and real PWR waste at SCK•CEN, the process has been tested in a small pilot installation and with realistic liquid waste at the nuclear power plant in Doel, Belgium [6]. Fig. 1 is a schematic representation of the installation.

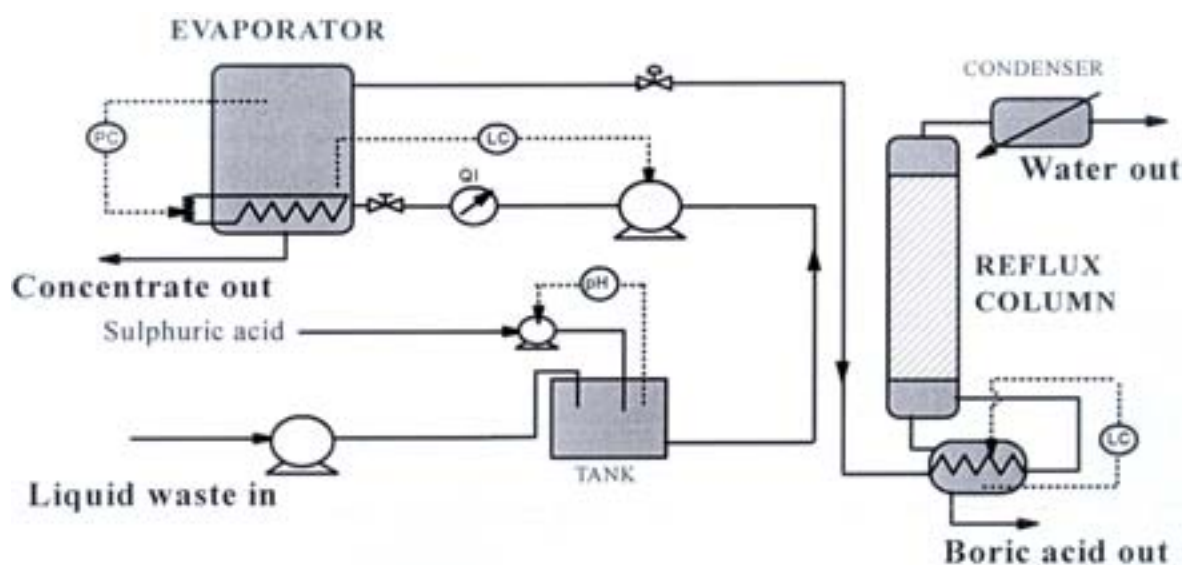


FIG. 1. Schematic representation of an installation for the recovery of boric acid by volatilisation during evaporation (PC: pressure control; LC: level control; pH: pH control; QI: throughput indication).

The operating pressure of the evaporator was 8 bar. During a first phase, we treated the available 11,000 kg LLLW. Evaporation of this waste in a stainless steel steam generator at nearly 180°C produced a boric acid loaded vapour, from which we recovered the boric acid in an atmospheric glass distillation unit. During a shorter second phase, we recycled the distillate from the atmospheric unit and used it as feed for the evaporator, instead of LLLW. At regular times, we sampled and analysed the LLLW feed, the waste concentrate in the evaporator, the boric acid solution in the reboiler of the atmospheric unit and the effluent distillate. Figure 2 shows the evolution of the amount of boron in each stream. The installation performed as theoretically expected for a boric acid distribution coefficient of about 0.007 at 180°C, which is also close to the value expected according to reference [5]. After an initial period, the incoming waste stream could be evaporated without further accumulation of boric acid in the concentrated waste (first phase). Near the end, recycled distillate allowed for a further reduction in the amount of boric acid in the concentrated waste (second phase).

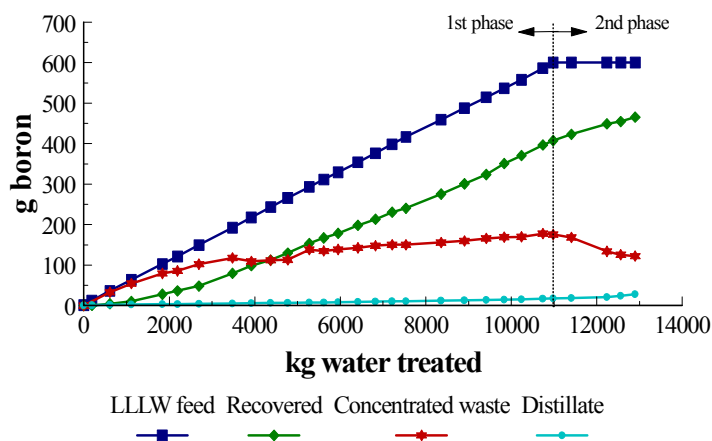


FIG. 2: Separation and recovery of H_3BO_3 during the evaporation of LLLW (first phase), and the further recovery of H_3BO_3 from the evaporator concentrate (second phase).

Economic evaluation

The separation of boric acid from LLLW appears advantageous when release of the LLLW with its boric acid content is not desirable or admitted. The savings will be larger for LLLW containing a relatively high boric acid concentration and a low concentration of other impurities. The savings concern the decrease of the waste volume and the recovered boric acid. The investment and the extra energy determine the extra costs. In most cases the extra energy costs and the savings on boric acid can be neglected. An important investment is needed, but when implemented in a new nuclear power plant, only the added investment cost to a classic evaporation process needs to be considered. Preliminary calculations were carried out for a hypothetical Belgian nuclear power plant, with reasonable values for the concerned parameters, such as 9000 m³ LLLW per year with 175 ppm B and a total dry residue content of 2 kg per m³ [7]. In Fig. 3 the unit cost for

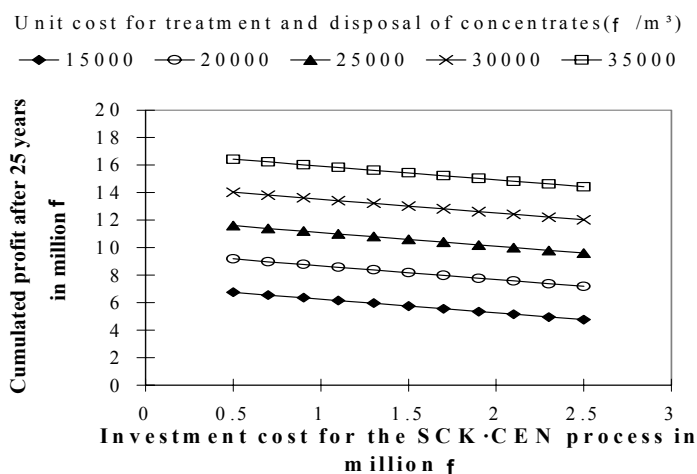


FIG. 3: Expected profit from the separation of boric acid by volatilisation during evaporation.

The main results of this demonstration experiment were:

1. The waste volume reduction factor was more than two times greater than with the current evaporation practice.
2. About 80 % of the boron was recovered as a 3.5 wt.% boric acid solution.
3. A high decontamination factor was obtained (except for tritium) and the effluent was pure enough to be discharged.

for treatment and disposal of evaporator concentrate and the investment cost for the SCK·CEN process are varied over a wide range to calculate the total profit at the end of the expected lifetime of the installation. From Fig. 3 the maximum cost of the installation can be deduced for a certain waste cost when a certain profit is envisaged. Clearly both costs can vary widely, while still making profit.

VOLATILISATION OF BORIC ACID FROM DRIED EVAPORATOR CONCENTRATES

Volatility of solid boric acid

The latest SCK•CEN process for the treatment of evaporator concentrates is based on the volatility of solid boric acid in superheated steam. The volatilisation of solid H_3BO_3 (ortho boric acid) is complicated by its decomposition to the less volatile HBO_2 (meta boric acid). The decomposition temperature depends on the water vapour partial pressure or the dew point of the gaseous phase [8]. The minimal water pressure $p_{\text{H}_2\text{O},\text{min}}$ (Pa) at which boric acid is present as ortho boric acid in the solid phase at a temperature T (K) is given by:

$$\ln p_{\text{H}_2\text{O},\text{min}} = 29.25 - \frac{7310}{T}$$

When the water pressure is higher than the one given by the previous equation then the partial pressure of H_3BO_3 above the ortho boric acid is given by:

$$\ln p_{\text{H}_3\text{BO}_3} = 35.3 - \frac{11800}{T} \Rightarrow \ln \frac{p_{\text{H}_3\text{BO}_3}}{p_{\text{H}_2\text{O}}} = 35.3 - \frac{11800}{T} - \ln p_{\text{H}_2\text{O}}$$

Otherwise, when the water pressure is smaller than $p_{\text{H}_2\text{O},\text{min}}$, only HBO_2 will be stable in the solid phase and the partial pressure of H_3BO_3 above this meta boric acid is given by:

$$\ln p_{\text{H}_3\text{BO}_3} = 6.05 + \ln p_{\text{H}_2\text{O}} - \frac{4490}{T} \Rightarrow \ln \frac{p_{\text{H}_3\text{BO}_3}}{p_{\text{H}_2\text{O}}} = 6.05 - \frac{4490}{T}$$

If (superheated) steam is brought into contact with ortho and/or meta boric acid, H_3BO_3 will volatilise and the steam will be saturated with boric acid. From the previous equations the equilibrium ratio of the H_3BO_3 partial pressure to the H_2O partial pressure of the steam and thus the theoretical steam consumption can be calculated. With this ratio the mole fraction of boric acid in the gaseous phase can be calculated, which gives also the boric acid concentration in the solution after complete condensation of the steam. These data are summarised in Table 1 for steam with a dew point of 100°C ($p_{\text{H}_2\text{O}} = 101325$ Pa).

TABLE I. VOLATILISATION OF SOLID BORIC ACID WITH SUPERHEATED STEAM:

temperature (°C)	$p_{\text{H}_2\text{O},\text{min}}$ (Pa)	$p_{\text{H}_3\text{BO}_3}$ (Pa)	$p_{\text{H}_3\text{BO}_3} / p_{\text{H}_2\text{O}}$	kg steam per kg H_3BO_3	ppm B	wt.% H_3BO_3
100	15667	39	0.0004	748	234	0.13
110	26126	90	0.0009	328	534	0.30
120	42448	197	0.0019	150	1168	0.67
130	67327	415	0.0041	71.1	2460	1.41
140	104427	818	0.0081	36.1	4848	2.77
150	158647	1058	0.0104	27.9	6268	3.58
160	236409	1352	0.0134	21.8	8008	4.58
170	346002	1708	0.0169	17.3	10118	5.79
180	497957	2136	0.0211	13.8	12653	7.23
190	705468	2645	0.0261	11.2	15671	8.96
200	984846	3247	0.0321	9.10	19235	11.0

Separation process and first tests

In the proposed process the non-alkaline, dried concentrates are brought into contact with superheated steam to volatilise the boric acid [4, 9]. By using superheated steam one can work at a higher temperature without the necessity to use an elevated (steam) pressure, and more boric acid can be volatilised with less steam. To approach the theoretical maximum yield, it is important to saturate the superheated steam as much as possible with boric acid and to supply the necessary heat for the volatilisation. Heat and mass transfer rates can be enhanced by a continuous renewal of the phase boundary layers through intensive agitation of the solid waste. The boron free concentrates leave the contactor for further conditioning as waste, whereas the steam loaded with boric acid can be condensed or cooled down to a temperature just above its dew point.

In a once through version of the process, the steam loaded with boric acid is condensed and a boric acid solution is obtained with a concentration that can immediately be derived from $p_{\text{H}_3\text{BO}_3} / p_{\text{H}_2\text{O}}$ at the working temperature and dew point of the steam (Table 1). On the other hand, if the steam is not condensed but cooled down to a temperature slightly above its dew point, e.g. 110°C for a dew point of 100 °C, practically all boric acid can be recovered as a solid material. The boric acid is then not only separated from the less volatile products in the contactor, but also from the more volatile ones in the desublimer. And the steam can be reused after reheating it to the working temperature.

Bench scale tests with boric acid filled containers through which we passed superheated steam confirmed the easy volatilisation of solid boric acid, with less than 15 kg steam needed to volatilise 1 kg boric acid. But the efficiency of the process decreased badly when impurities were added to the boric acid. This was explained by a deterioration of the contact between steam and boric acid, mainly due to a reaction between boric acid and the impurities with the formation of a hard borate layer.

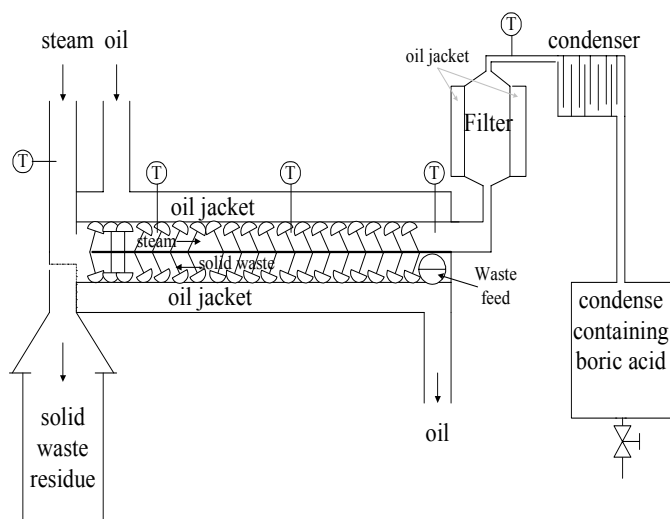


FIG. 4. Experimental set up for the recovery of boric acid from dried evaporator concentrates.

installation is schematically shown in Fig. 4.

During a first 5-h run with dried simulated concentrate, 14.5 kg boric acid were separated with 378.5 kg steam or an average of 26.1 kg steam per kg boric acid [9].

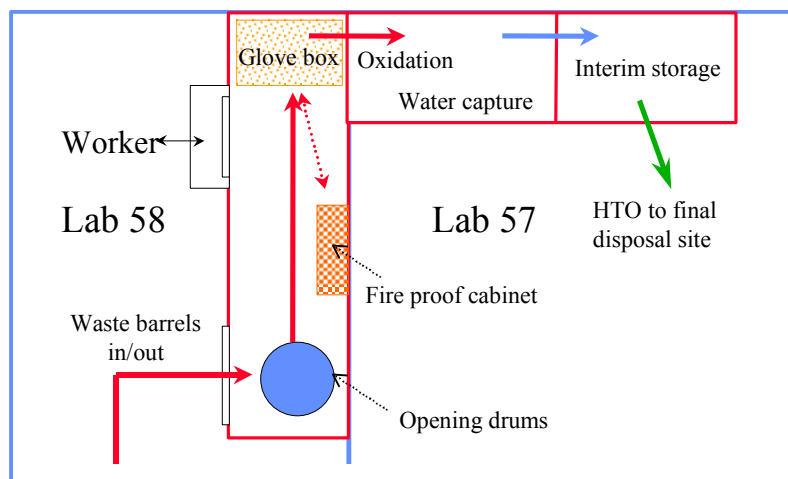
Better results with simulated evaporator concentrates were obtained with a commercially available dryer from Hosokawa Micron. Their Solidaire consists of a mechanical agitator with adjustable paddles, rotating within a cylindrical housing which is jacketed for indirect heating. The Solidaire was successively used for drying the concentrates with hot air and for separating boric acid by volatilisation with superheated steam. The

TREATMENT OF TRITIATED SOLVENTS

Process selection

Since the tritiated solvents stored at SCK•CEN are volatile, highly flammable, toxic and radioactive, extreme precautions had to be taken to open the drums and to treat the waste. The Belgian government restricts tritium discharges in the atmosphere, so the tritiated water had to be recovered from the exhaust stream. To remain under the discharge limits for tritium a very high trapping efficiency was needed. The oxidation itself had to be done in a closed and leak tight system to prevent losses of tritium and to minimise the fire hazard. The conversion of the organic fraction should be high enough and the residual TOC (Total Organic Carbon) in the final waste low enough, according to the limitations to be set by ONDRAF/NIRAS. For the safety of the workers and the protection of the environment the toxicity of methanol and other tritiated compounds, the radiotoxicity of tritiated water and tritiated solvents, and the flammability of methanol and hydrogen had to be carefully dealt with.

For the oxidation of the tritiated liquid organic waste several options exist. Catalytic and thermal oxidation are two well-established technologies for controlling (volatile) organic compounds in the non-nuclear industry. Other options for the destruction are wet oxidation based on chemical, electrochemical, biochemical or photochemical principles. It was our opinion that the wet oxidation techniques were not the most suitable for our problem, because secondary (mixed) waste might be generated, still extra development was needed before they could be used on a (semi) industrial scale or a high conversion of the waste was not assured. On the other hand, catalytic oxidation of volatile organic compounds is known to allow very high conversions. Operated in the gaseous phase, at concentrations under the lower explosion limit and at relatively low temperatures, it is also intrinsically safe. But it requires evaporation of the waste and the use of large gas flows, which result in a large installation and difficulties for a complete product-water recovery. We therefore chose a combination: thermal oxidation followed by catalytic oxidation. Thermal oxidation allows direct injection of the liquid solvent and oxidation of the largest part of it in a relatively compact installation and with no or limited dilution of the radioactivity. External cooling and/or co-injection of (tritiated) water can remove the excess reaction-heat. Catalytic oxidation of the remaining low concentration on solvent vapour ensures a high conversion to water. Condensation and adsorption on molecular sieves can easily and quantitatively trap the tritiated water. On a laboratory scale such a two-stage combustion system had been developed by the R. W. Johnson Pharmaceutical Research Institute, USA and Ontario Hydro Technologies (OHT), Canada [11, 12]. They successfully converted tritiated solvents into tritiated water at about 800 °C. The destruction efficiency was found to be more than 99.999% for a variety of organic substances.



Description of the process and the installation

Treatment of the tritiated solvents at the SCK•CEN laboratories in Mol comprises three phases: unpacking and sampling of the bottles,

actual treatment of their content and interim storage of the product-water. Three large processing cells with bottom and top ventilation are used to separate the different phases of the treatment to minimise the danger. Figure 5 shows an overview of this infrastructure. One cell has been equipped for the opening of the drums, the sampling and the transfer of the liquid into a primary vessel. A second cell houses the oxidation system and its associated water collection system, whereas the last one is used for the temporary storage of the tritiated water. When interventions are needed inside a cell, for example during the opening of the drums and bottles, the worker uses an overpressure suit with separate air supply. Sparks are prevented and explosion, fire and tritium detectors are placed at several places.

For the opening of the drums special care has to be taken because the tritium contamination may have spread over the different barriers, for example due to a damaged bottle. The work is done by two workers using air-supplied suits inside the cell while a third is in standby outside the cell. The secondary overpacks are thus removed inside the cell, but removal of the primary overpacks and opening of the glass bottles is carried out in an inert atmosphere (helium) glove box, which is also present in the same cell. The glove box is necessary to separate the solvents (and possibly the hydrogen) from the surrounding air, because of the flammability, and to protect the workers from the tritiated solvents, because of the radiotoxicity. The gas inventory of the glove box is fed to the processing installation to oxidise solvent vapour present in the helium, and to trap the produced tritiated water, before discharging the off gases to the ventilation. The processing installation can thus be used for either the treatment of the solvent or the treatment of the glove box atmosphere.

The heart of the installation is a prototype two-stage combustion installation, including means for an effective trapping of the produced tritiated water. It has been built by Ontario Power Technologies, OPT. The main construction material was stainless steel. Figure 6 provides a cross-section of the oxidation furnace. A 10-cm diameter seamless Hastelloy 276 tube that is 128 cm long contains the key components of the oxidation system. Solvent is atomised into a heated cavity through an injector using oxygen as the propellant.

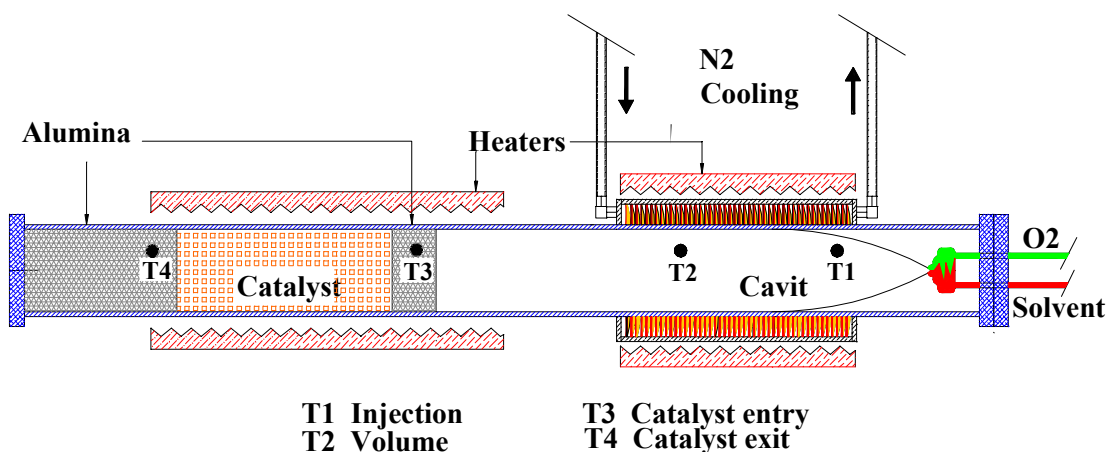


FIG. 6. Cross-section of oxidation furnace.

Oxidation products and excess oxygen are re-mixed in an alumina diffuser zone downstream of the cavity before passing over heated platinized alumina. The furnace is charged with 2.5 kg of 0.5% platinum on alumina catalyst. The catalyst occupies 2.3 litres.

The gases leave the furnace via an alumina packed zone and are separated into condensable and non-condensable streams.

Two sets of heaters are attached to the 6.7-mm thick furnace walls. The furnace temperatures can be adjusted independently to optimise solvent destruction efficiencies in each of the two zones. The wall temperature at the entry port is set between 500 and 850 °C while the catalyst temperature is set between 500 and 750 °C. Four thermocouples have been installed within the furnace to monitor oxidation performance. A nitrogen gas cooling circuit has been installed under the cavity heater to remove heat of combustion when the need arises. The oxidation system can be used to treat gas with a composition ranging from air to pure helium. Either the injected solvent or the glove box atmosphere can be treated in this furnace.

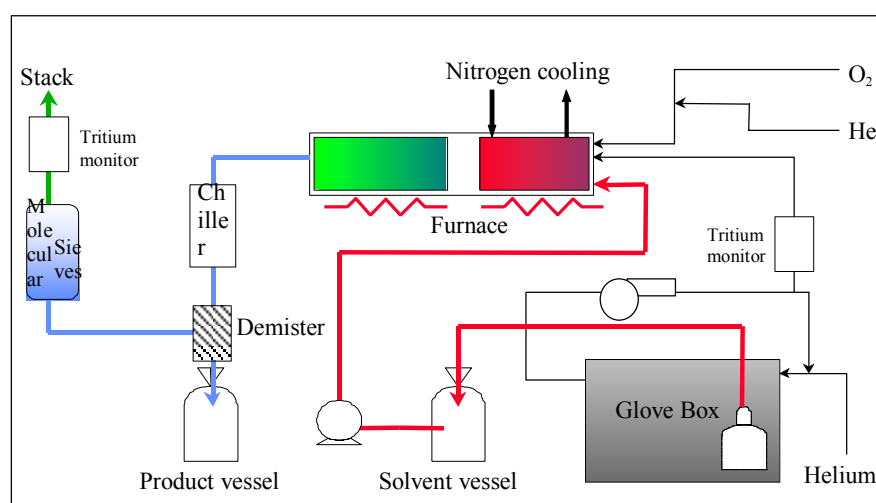
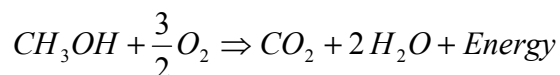


FIG. 7. Simplified scheme of the installation for oxidation.

condensers cooled by separate refrigerated circulators (one at 7°C, the second at 1°C) to remove the bulk of the water present in the gas. The water is collected in a tank. Small water droplets are separated in a cooled demister and added to the product water. The remaining gas is then led over a molecular sieve bed to remove the residual water. Two molecular sieve beds are operated in parallel, giving the possibility to regenerate one bed without interrupting the treatment of the waste. The effective operating lifetime of each molecular sieve bed can be increased without compromising the tritium emission by using a 'polishing' bed in the exhaust line of the absorption system.

According to the available documentation, 95% of the solvent should be either methanol or water. Complete oxidation of methanol is in accordance with the following stoichiometric relation:



In practice however, this exothermic reaction will require excess oxygen for the complete oxidation of the methanol. The heat liberated during the oxidation of the methanol is calculated by means of the HSC software package [13]. At a maximum solvent flow rate of 2.5 L/h and a 100% excess of oxygen, the liberated heat equals 10.8 kW. At a moderate solvent rate of 1 L/h $Q_{heat} = 4.3$ kW. Depending on the amount of water present and/or co-injected, a lower amount of heat is produced. This heat has to be removed from the furnace. Sensible heat removed from the furnace with the product gas is between 3.12

Figure 7 shows a simplified scheme of the treatment installation. The gases coming from the furnace are supposed to be free of solvent and to contain mainly excess oxygen, carbon dioxide and water vapour. The tritium is under the form of HTO. These gases are lead through two

kW and 1.25 kW for the respective flow rates, assuming an exhaust gas temperature of 600°C. Consequently the heat losses in the furnace for a 100% methanol feed must be between 7.68 kW and 3.05 kW, both by natural and forced cooling. The available 12-m³/h nitrogen cooling around the furnace should remove about 2.5 kW, depending on the temperature difference of the in and outgoing nitrogen. In the absence of water in the feed, the maximum workable methanol throughput is limited by the removal of heat from the furnace. Co-injection of water is a straightforward solution but we try to avoid any unnecessary tritium dilution that results in an increase of the to-be-conditioned amount of tritium contaminated water.

For a given tritium release limit and a given throughput, the required minimum efficiency for the overall tritium trapping, including leak tightness, completeness of the oxidation and product-water recovery depends on the specific activity of the treated solvent. Even if we dilute the more active bottles with less active ones in the process vessel, overall efficiencies up to more than 99.9% are required for a throughput of 1 L/h and a 100% excess of oxygen. Neglecting all other losses this means that dew points below – 25°C should be obtained when no water is added. When treating the glove box atmosphere, dew points as low as – 40°C are required.

To demonstrate the feasibility of the process, a series of cold tests were carried out at OPT, Canada. After the installation had been transferred to Mol, Belgium, a fully integrated test at SCK•CEN confirmed the results of the earlier tests as well as the good operation in combination with the glove box.

During the different tests, the following parameters were varied to study their influence on the destruction efficiency:

- Temperature of operation
- Stoichiometric excess of oxygen
- Ratio methanol/water
- Presence of chloroform
- Flow rate of solvent

The conclusions were as follows:

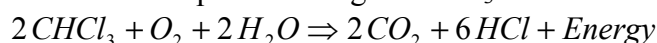
- The wall temperatures (external heating) are preferably set between 750 and 850°C for the cavity region and between 650 and 750°C for the catalyst region. The external nitrogen cooling effectively removes heat. Most of the solvent should be burned in the cavity, and only residual solvent or small concentrations of solvent vapour from the glove box should be oxidised in the catalyst region. The temperature in the catalyst region should not exceed 1000°C.
- A stoichiometric oxygen excess of 50% should be maintained. At lower excess the combustion is not complete.
- The destruction efficiency is always higher than 99.999%, for compositions from 10% methanol in water until 100% methanol. 13% chloroform in the methanol did not degrade the destruction efficiency.
- The processing rate is limited by heat transport considerations rather than by degradation of the destruction efficiency. Processing rates on the order of 21 g/min (1.6 L/h) methanol are easily attainable and higher processing rates appear feasible particularly if the feedstock is diluted with water.

The desire for negligible environmental emission drives the need for efficient product-water recovery. To confirm that the emission targets are attainable, the molecular sieve beds were tested under expected operating conditions by injecting water through the oxidation system and by collecting water during the combustion runs. It was shown that a dew point of -60°C could be obtained and maintained. Adding a polishing bed in series allows to avoid possible problems with too early and thus too frequent regenerations in case of tritium breakthrough at a fraction of the anticipated water loading capacity. Of course the dew point before the molecular sieve beds should be kept as low as possible. Together with our general desire to increase the available cooling capacity and for having a cooling backup, this had been the reason for the addition of a second chiller operating at 1°C instead of 7°C .

First results and adaptation of the installation

Unpacking of the drums and sampling of the content of the 2.5-litre bottles posed no significant problems. All our solvent analyses confirmed that tritium was the only radioisotope present, except for very small amounts of ^{14}C (below 0.01% of the tritium activity). The measured tritium activities for separate bottles corresponded merely qualitatively with those calculated from the available documentation, but the average tritium activity was only 10% higher than expected. The measured pH of the solvent was low, mostly about 1. A few bottles contained some precipitate. About one third of the bottles contained two liquid phases, indicating the presence of other components besides completely miscible methanol and water. At Kinectrics (formerly OPT) the organic content of each phase in each bottle has been measured by gas chromatography. By comparing the corresponding density for the organic content with the measured density, the water content could also be estimated. Apparently many bottles, and especially the bottom phase when there were two phases, contained large amounts of chloroform (CHCl_3) and/or dichloromethane (CH_2Cl_2).

The unexpected presence of major amounts of CHCl_3 and CH_2Cl_2 imposed a complete revision of the process and the installation. Burning of chlorinated hydrocarbons results in the production of hydrogen chloride, HCl , and chlorine, Cl_2 . In the temperature range we are using, $800\text{--}1000^{\circ}\text{C}$, the production of Cl_2 is minimal [14] and the reaction equation for the complete burning of CHCl_3 can be written as:



It is noteworthy that the complete burning of CHCl_3 requires H_2O . This water can be present in the feed, it can be produced in situ by the oxidation of e.g. CH_3OH or it can be co-injected in the furnace. Also, 1 mole CHCl_3 gives rise to the production of 3 mole HCl . For a solvent composition of e.g. 20 wt.% CHCl_3 , 50 wt.% CH_3OH and 30 wt.% H_2O , this results in a HCl concentration of 18 wt.% or 5 M for the condensate at the exit of the furnace. When treating more chlorinated fractions, e.g. bottom phases, even supersaturated HCl solutions can be obtained. Inevitably this leads to corrosion problems, destruction of the molecular sieves and tritium releases because of leaks and/or decreased trapping efficiency.

Mainly downstream of the furnace corrosion problems could be expected. In the furnace HCl gas is formed at high temperature. With dry HCl the dangerous pit corrosion is not very important, even at high temperature. Furthermore the construction material of the thick walled furnace is the more corrosion resistant Hastelloy C276. But in the presence of water, i.e. from the first cooler condenser, very corrosive hydrochloric acid

solutions could be formed [15]. Because of the acidity of the solvent itself, possible corrosion problems upstream of the furnace had also to be taken into account.

To allow the treatment of the chlorinated and acid tritiated liquid waste, the process is amended as follows:

- Depending on the chlorine content and the composition of the to-be-treated phase, methanol and water are co-injected. For calculating the respective flow rates we first calculate the relative amount of water that should be present downstream of the furnace to obtain a HCl concentration of maximum 15 wt.% in the condensate. Above a 15 wt.% HCl solution the HCl vapour pressure is only $5 \cdot 10^{-5}$ bar at 20°C (and lowers at lower temperature). In other words, the cooler condensers extract then nearly all HCl from the gaseous phase and this HCl accumulates in the condensate vessel. We then compute the amount of water that is already present in the feed, the amount that will be formed by the oxidation of this feed and the supplementary amount needed. Afterwards the methanol/water ratio of the required co-injection is estimated to optimise the heat balance. Once the relative flow rates have been fixed, the corresponding relative oxygen flow rate (at least 50 and preferably 100% stoichiometric excess) can be calculated. The exact flow rates are then determined as a function of the maximum available oxygen flow.
- The condensate is neutralised with K_2CO_3 . To prevent possible downstream corrosion and because the tritiated water has anyhow to be neutralised before its transfer to Belgoprocess, the condensate is directly neutralised in the condensate vessel. To avoid unnecessary dilution of the tritium a calculated substoichiometric amount of solid K_2CO_3 is added in advance to the condensate vessel.
- As an ultimate protection for the downstream parts of the installation, an acid trap is placed between the condensate vessel and the molecular sieve beds. This is a fixed bed reactor with three beds of solid K_2CO_3 . Traces of HCl that are still present as gas or aerosols are transformed in KCl, H_2O and CO_2 . Preliminary cold test with relatively HCl concentrations demonstrated the proper functioning of this trap.

The massive presence of chlorinated hydrocarbons, the above described amendments of the process and the acidity of the original waste lead to an adaptation of the installation, which is now being implemented.

- Between the furnace and the condensate vessel, all stainless steel components, including both cooler condensers and all tubing, fittings and valves are replaced by Hastelloy C276 ones.
- The stainless steel condensate vessel is replaced with a glass one, provided with a stirrer, means for adding solid and dissolved K_2CO_3 , automatic pH control, temperature control and a cooling mantle.
- The standard molecular sieves are replaced by more acid resistant ones.
- Potentially exposed stainless steel valves and other components that operate at room temperature or slightly above are replaced by equivalent PTFE ones.
- The stainless steel process feed vessel is replaced by a glass one.
- A peristaltic pump is used for the injection of the waste. Its pump head is replaced by a PTFE-tubing pump head. PTFE is compatible with chloroform, methanol and the low pH. Furthermore this pump head delivers a higher pressure.
- Other components in the solvent feed line are also replaced by more compatible ones.
- Pumps and other means are added for the co-injection of methanol and water.

CONCLUSIONS

SCK•CEN participated to the IAEA Co-ordinated Research Co-ordination Programme "Combined Methods of Liquid Radioactive Waste Treatment" with two projects, "Volume Reduction of Low Level Liquid PWR Waste" and "Treatment of Tritiated Solvents". The first project lead to a process that combines the evaporation of water with the volatilisation of boric acid. Separation of boric acid by volatilisation offers promising perspectives for the operators of PWRs and VVERs who want to decrease the volume of their operational LLLW and the corresponding costs. In a small pilot installation at the Doel NPP, we demonstrated the technical feasibility of separating boric acid during the evaporation of representative LLLW. In comparison with the current evaporation practice for LLLW, the SCK•CEN process achieves much higher waste volume reduction factors while maintaining low activity discharge limits. Preliminary economic evaluations reveal good prospects. For the treatment of evaporator concentrates, we are developing a process to volatilise boric acid from solid waste with the use of superheated steam. This process appeared very promising during laboratory and "cold" pilot tests.

The treatment of mixed waste poses a considerable challenge for the nuclear industry. The second project, "Treatment of Tritiated Solvents", aims at the complete destruction of liquid tritiated organic waste and recovery of the tritium as product-water for further conditioning and disposal, or for possible recycling. It uses a combination of thermal oxidation and catalytic after-oxidation, and a combination of simple condensation with adsorption on molecular sieve beds. By splitting the bulk process from the final "polishing", high efficiencies can be obtained in a relatively small installation. This work is carried out in co-operation with a Canadian firm, which also delivered the original process installation for treating the volatile, highly flammable, toxic and highly radioactive tritiated organic waste that was stored at SCK•CEN. Only after integrating this installation in an appropriate infrastructure we could safely unpack and sample the waste, which was documented as a mixture of tritiated methanol and water. But the consequent analyses revealed large amounts of chlorinated compounds. Although this complication imposed a major revision of the process and the installation, the combination of the cited methods still presents a safe, environmentally acceptable and relatively economical solution for treating this type of waste.

REFERENCES

- [1] S. Santraille et al., *Radioactive Waste Management and Disposal*, L. Cecille Ed., Elsevier Applied Science, London and New York, 1991, p 25.
- [2] INTERNATIONAL ATOMIC ENERGY AGENCY, *Processing of Nuclear Power Plant Waste Streams Containing Boric Acid*, IAEA-TECDOC-911, Vienna (1996).
- [3] A. Bruggeman and J. Braet, *Method for Separating Boric Acid*, International Patent, Belgium (1995, 1 007 223); United States (1995, 5 468 347), United States (1996, 5 587 047); Europe (1994, 94201610.6); Japan (1994, HEI 6-133238); Korea (1994, 94-24912).
- [4] A. Bruggeman, J. Braet, *Werkwijze en Inrichting voor het Afscheiden van Boorzuur*, Belgian Patent 1012246 (October 1998).
- [5] D. G. Tskhvirashvili and V. V. Galustashvili, *Soviet. At. Energy*, 16, 1, p. 70 (1964).
- [6] A. Bruggeman, J. Braet, F. Smaers, P. De Regge, *Separation Science and Technology*, 32 (1-4), p 737 (1997).
- [7] J. Braet, A. Bruggeman, *Proc. Improving the Economic Performance of Nuclear Power Plants*, Nuclear Engineering International, London, p.197 (1998).

- [8] M. v. Stackelberg, F. Quatram and J. Dressel, *Ztschr. Elektrochem.*, 43, 1, p. 14 (1937).
- [9] J. Braet, A. Bruggeman and R. Van Ammel, "Recovery of Boric Acid from PWR Concentrates", Paper No. 393, presented at the 7th International Conference on Radioactive Waste Management and Environmental Remediation (ICEM'99), Nagoya, Japan, (September 1999).
- [10] J. Braet, A. Bruggeman, R. Van Ammel, "Treatment of Tritiated Methanol Waste." Paper No. 24, presented at the ICEM'99 Conference, Nagoya, Japan (September 1999).
- [11] L. E. Weaner and D. C. Hoerr, "An Evaluation of Laboratory-Scale Oxidation of Radioactive Hazardous Organic Materials to give Legally Disposable Waste." in *Synthesis and Applications of Isotopically Labelled Compounds 1994*, J. Allen, Ed., pp. 897–901, 1995.
- [12] L. E. Weaner, D. C. Hoerr and W. T. Shmayda, " A Practical Approach to the Destruction of Radioactive Organic Mixtures." in *Synthesis and Applications of Isotopically Labelled Compounds 1997*, J.R. Heys and D.G. Melillo, Eds., pp. 79–82, 1998.
- [13] HSC Chemistry For Windows 4.1, Chemical Reaction and Equilibrium Software with Extensive Thermochemical Database, A. Roine, Outokumpu, April 2000.
- [14] R. A. Cloud, "Thermal Treatment for VOC Control", *Chemical Engineering*, July 1998.
- [15] C.M. Schillmoller, "Alloys to Resist Chlorine, Hydrogen Chloride and Hydrochloric Acid", NiDi Technical Series N° 10 020.

DEVELOPMENT OF COMBINED METHOD FOR TREATMENT OF LIQUID WASTE FROM RECONSTRUCTION OF SHALLOW GROUND REPOSITORY

I.G. STEFANOVA, M.D. MATEEVA

Institute for Nuclear Research and Nuclear Energy,
Bulgarian Academy of Sciences,
Sofia, Bulgaria

Abstract. A combined method, based on sorption of radionuclides on inorganic sorbents, chemical precipitation and separation/destruction of organic compounds in liquid waste streams, was developed for the treatment of liquid waste generated during the reconstruction of Novi Han Repository. During the project implementation liquid waste streams were characterised - the chemical and radionuclide composition was identified. Different sorbents were tested. The report summarises the results of research and development work performed.

1. INTRODUCTION

The aim of the study is to develop combined method for treatment of liquid waste that arise during the activities for upgrading of Novi Han Radioactive Waste Repository and even after the repository reconstruction, modernisation and construction of new facilities. The treatment method is combination of two main processes – sorption of radionuclides on natural inorganic sorbent and precipitation of suspended solids and radionuclides, if necessary, depending on the radionuclide inventory of the liquid radioactive waste and it's chemical composition. If necessary, additional method is also included viz; separation of surfactants on modified sorbent.

2. DESCRIPTION OF NOVI HAN REPOSITORY

The Novi Han Radioactive Waste Repository is the only Bulgarian national repository for storage and disposal of radioactive waste, which are generated from nuclear applications in industry, medicine, research and education. The Novi Han Repository comprises of several different disposal vaults and above ground temporary storage structures for solid radioactive waste, biological radioactive waste, spent sealed sources and liquid waste:

- Concrete vault for disposal of low and intermediate level solid wastes, which consist of three separate cells with total volume of 237 m³;
- Concrete vault for disposal of biological wastes — which consist of three separate cells with total volume of 80 m³;
- Special concrete vault for disposal of spent sealed radiation sources of 1 m³;
- Storage facility for liquid radioactive waste, which consists of four stainless steel tanks, 12 m³ each, in a hydro-insulated underground concrete structure.
- Concrete trench for disposal of solid radioactive waste, which consists of eight separate units with total volume of 200 m³.
- Temporary storage structure for low level spent sealed sources, smoke detectors and static electricity eliminators, which consists of four full size metal transport containers with total volume of 136 m³;

- Temporary storage structure for spent sealed sources, which consists of four reinforced concrete structures with total volume of 60 m³;
- Temporary storage structure for radioactive waste that could be released from institutional control, which covers an area of 80 m², covered with a roof.

All disposal and storage units are multibarrier engineered facilities. The disposal facilities and liquid waste storage tanks are constructed according to a modified Russian design (type TP-4891) and commissioned in 1964. The temporary storage structures are constructed in 2000 to store temporarily spent sealed sources until new modern storage facilities are commissioned and solid waste until the disposal in the existing disposal units is licensed.

The installations for treatment and conditioning of radioactive waste, including liquid waste, planned according to the initial design of repository, have not been constructed. Such installations will be constructed at the stage of reconstruction of Novi Han Repository.

Treatment plant for liquid waste, as a part of low and intermediate level waste processing and storage facility, will be constructed in the following years based on the method that was developed under the Research Contract 9631 in the frame of IAEA Co-ordinated Research Programme “Combined Methods of Liquid Radioactive Waste Treatment”. Small mobile installation for treatment of liquid waste that arise during the maintenance and improvement of the existing facilities is under construction.

3. IDENTIFICATION OF KEY RADIONUCLIDES IN THE LIQUID WASTE STREAMS

In contrast to the liquid waste generated in the nuclear fuel cycle, that are characterised with known radionuclide composition, the radionuclide composition of liquid waste streams that arise at Novi Han repository varies in a wide range. Liquid waste, generated by the users of sources of ionising radiation in the industry, research and medicine contribute to minor extent to the total volume of the liquid waste. The Novi Han Repository itself will be the main producer of liquid waste. Based on the radionuclide inventory of the disposal and storage facilities [1,2] and the national radionuclide inventory of the sources of ionising radiation, that are in use in the country, the activity of liquid waste generated at Novi Han Repository will be governed mainly by ¹³⁷Cs, ⁶⁰Co, ⁹⁰Sr and to smaller extent by ²⁰⁴Tl, ¹⁴⁴Ce, ⁶⁵Zn, ⁵⁴Mn, ¹⁴⁷Pm, ²²⁶Ra, ²³⁹Pu, ²⁴¹Am.

4. PRINCIPLES IN THE LIQUID RADIOACTIVE WASTE MANAGEMENT

The national legislation does not allow discharge of any radioactive liquid to the environment [3]. In the environment, only liquids that meet the criteria for drinking water according to the national radiological standards [4] can be released. In addition surface and groundwater protection legislation limits the gross beta activity up to 750 mBq/L [5].

After careful consideration of the activity level, possible radionuclide content, chemical composition and the available treatment technologies, as well as the long term stability of the final waste form, combined method based on precipitation and ion exchange on

natural inorganic sorbents (zeolites) has been selected for decontamination of the radioactive liquid waste that arise during maintenance and improvement of Novi Han Repository and after the reconstruction of the facility. If necessary, separation of surfactants on modified sorbent may be included.

5. SORPTION OF RADIONUCLIDES

5.1. Selection of a sorbent

Several sorbents are studied in order to select the suitable one. All the sorbents are natural zeolites from local deposits.

5.1.1. Description of different sorbents

All the sorbents originate from zeolite deposits located in Northeast Rhodope Mountain in Bulgaria. All of the zeolite deposits are in generic connection with the first and second acidic paleogene volcanism. Actually, most of the zeolite deposits are related to the first acidic paleogene volcanism. The zeolitization is related to the alteration of vitric pyroclastic material under marine conditions. The main products of this process are zeolites (analcime, clinoptilolite, mordenite) and in small quantities other authigenic minerals — mont-morillonite, celadonite, chlorite, adularia, cristobalite, etc. The most promising and thoroughly investigated are the clinoptilolite and mordenite deposits. The chemical composition of monomineral zeolite fractions is given in Table I.

TABLE I. CHEMICAL COMPOSITION OF ZEOLITE SAMPLES FROM DIFFERENT DEPOSITS

Deposit	Beli Plast	Most	Morya- ntzi	Golob- radovo	Kostino	Beli Bair	Lyasko- vetz
Oxides	wt. %	wt. %	wt. %	wt. %	wt. %	wt. %	wt. %
SiO ₂	65.70	65.98	66.00	66.15	64.88	66.66	65.93
TiO ₂	0.10	0.25	0.05	n.d.	n.d.	0.06	0.44
Al ₂ O ₃	11.01	10.71	11.60	11.13	11.91	1.09	0.80
Fe ₂ O ₃	0.37	0.35	traces	0.84	0.12	0.33	1.10
CaO	3.90	3.17	1.83	4.02	3.66	2.10	3.74
MgO	0.65	1.07	0.51	1.01	0.55	0.48	0.48
Na ₂ O	0.20	0.13	3.52	0.67	1.95	2.47	2.02
K ₂ O	2.36	4.46	2.57	1.15	2.30	3.65	1.99
I.L.	15.34	13.40	13.77	14.61	14.20	2.76	13.37
Total	99.63	99.52	99.85	99.58	99.57	99.60	99.87

5.1.2. Comparison of the ion exchange properties

The zeolite samples are crushed and fraction 0.25–0.50 mm is used during the experiments. All the zeolite samples are modified to produce sodium and ammonium exchanged forms. One liter of concentrated solutions of sodium and ammonium nitrate (1N) is passed through columns with 100 grams of zeolite till a full saturation of the sorbent.

Standard procedures are applied to compare the sorption of radionuclides on different sorbents – determination of the ion exchange capacity, construction of sorption isotherms, determination of the distribution coefficients, and kinetics experiments.

Ion exchange capacity

The batch ion exchange capacity is obtained using following procedure – 1 gram crushed and sieved sorbent is equilibrated for 5 days with 100 ml of 0.1 N solution of cesium, strontium or cobalt nitrate, labeled with ^{134}Cs , ^{85}Sr , ^{60}Co , ^{65}Zn , ^{54}Mn , ^{144}Ce . Capacity is calculated according to the equation:

$$K = \frac{(C_0 - C_{eq}) \cdot V_{sol}}{M_{solid}}$$

where K is the exchange capacity, meq/g
 C_0 and C_{eq} are the initial and equilibrium concentration, meq/ml
 V_{sol} is the volume of the solution, ml
 M_{solid} is the weight of the sorbent, g

Results are obtained for natural (untreated) zeolite and for its sodium and ammonium modifications (Table II).

TABLE II. ION EXCHANGE CAPACITIES OF NATURAL UNTREATED AND MODIFIES ZEOLITE SAMPLES FROM DIFFERENT DEPOSITS, $\text{Meq} \cdot \text{g}^{-1}$

Deposit	Exchange form	Cs^+	Sr^{2+}	Co^{2+}	Zn^{2+}	Cd^{2+}	Pb^{2+}	Mn^{2+}	Ce^{3+}
Moryantzi	Natural	0.97	0.69	0.15	0.25	0.42	1.12	0.17	0.12
	Sodium	1.36	0.91	0.19	0.37	0.51	1.29	0.32	0.16
	Ammonium	1.22	0.76	0.16	0.18	0.30	1.20	0.21	0.10
Kostino	Natural	1.35	0.73	0.18	0.40	0.40	1.15	0.21	0.14
	Sodium	1.39	0.92	0.25	0.48	0.40	1.30	0.46	0.06
	Ammonium	1.49	1.04	0.23	0.32	0.33	1.24	0.29	0.16
Beli Plast	Natural	1.34	1.14	0.22	0.34	0.43	1.40	0.23	0.16
	Sodium	1.44	1.28	0.41	0.52	0.60	1.60	0.56	0.19
	Ammonium	1.52	1.26	0.35	0.31	0.37	1.56	0.36	0.16
Golobra-dovo	Natural	0.47	0.18	0.09	0.18	0.25	0.54	0.08	0.12
	Sodium	0.71	0.53	0.13	0.26	0.34	0.83	0.21	0.14
	ammonium	0.78	0.57	0.12	0.25	0.25	0.83	0.17	0.12
Most	natural	0.77	0.38	0.08	0.15	0.27	1.01	0.07	0.06
	sodium	0.95	0.59	0.15	0.30	0.36	0.91	0.19	0.10
	ammonium	0.74	0.73	0.14	0.28	0.28	0.61	0.15	0.12
Beli Bair	natural	0.72	0.67	0.23	0.17	0.38	0.87	0.19	0.16
	sodium	0.88	0.84	0.27	0.32	0.38	1.01	0.38	0.17
	ammonium	0.88	0.75	0.26	0.24	0.29	1.00	0.28	0.10
Lyaskovetz	natural	0.85	0.10	0.05	0.07	0.13	0.41	0.03	0.06
	sodium	0.94	0.36	0.14	0.17	0.32	0.64	0.20	0.06
	ammonium	0.95	0.34	0.13	0.18	0.25	0.59	0.16	0.08

Distribution coefficients

Distribution coefficients are obtained for ^{134}Cs , ^{90}Sr and ^{60}Co in wide concentration range from $1 \cdot 10^{-5}$ N solution of the corresponding radionuclides to trace concentration. Different types of simulated waste solutions were used, that are expected to be generated at Novi Han Repository. These included a simulant “Low salt content solution” ($60 \text{ mg} \cdot \text{dm}^{-3} \text{ CaCl}_2$) and

“Higher salt content solution” (0.02 N Na⁺, 0.002N K⁺). The experimental conditions are – 0.25 ml of the sorbent, 500 ml of the solution.

The distribution coefficients are calculated according to the equation:

$$K_d = \frac{A_0 - A_{eq}}{A_{eq}} \cdot \frac{V_{sol}}{M_{solid}}$$

where: A_0 and A_{eq} — activity of the radionuclide in the solution at the start of the experiment and in equilibrium

V_{sol} , M_{solid} — volume of the solution, ml, weight of the sorbent, g

Results are obtained for natural (untreated) zeolite and for its sodium and ammonium modifications (Table III).

TABLE III. DISTRIBUTION COEFFICIENTS FOR ¹³⁴Cs, ⁹⁰Sr AND ⁶⁰Co ON DIFFERENT SORBENTS, ml·g⁻¹

Deposit	Exchange form	Higher salt content solution		Low salt content solution		
		¹³⁷ Cs	⁹⁰ Sr	¹³⁷ Cs	⁹⁰ Sr	⁶⁰ Co
Moryantzi	natural	2.8.10 ³	0.44.10 ³	5.63.10 ⁴	5.84.10 ⁴	1.56.10 ⁴
	sodium	2.5.10 ³	0.52.10 ³	6.25.10 ⁴	8.19.10 ⁴	1.66.10 ⁴
	ammonium	2.5.10 ³	0.41.10 ³	5.38.10 ⁴	4.10.10 ⁴	2.68.10 ⁴
Kostino	natural	2.8.10 ³	0.51.10 ³	3.67.10 ⁴	4.80.10 ⁴	1.34.10 ⁴
	sodium	2.4.10 ³	0.82.10 ³	5.09.10 ⁴	7.38.10 ⁴	1.34.10 ⁴
	ammonium	2.3.10 ³	0.54.10 ³	3.54.10 ⁴	5.30.10 ⁴	1.01.10 ⁴
Beli Plast	natural	2.4.10 ³	0.63.10 ³	3.38.10 ⁴	4.73.10 ⁴	4.31.10 ³
	sodium	2.6.10 ³	0.67.10 ³	6.54.10 ⁴	2.10.10 ⁴	1.20.10 ⁴
	ammonium	2.6.10 ³	0.80.10 ³	3.77.10 ⁴	9.84.10 ⁴	7.73.10 ³
Golobradovo	natural	2.3.10 ³	0.09.10 ³	3.17.10 ⁴	1.18.10 ⁴	9.86.10 ²
	sodium	1.9.10 ³	0.28.10 ³	3.55.10 ⁴	2.72.10 ⁴	1.95.10 ³
	ammonium	2.1.10 ³	0.28.10 ³	3.47.10 ⁴	1.74.10 ⁴	1.78.10 ³
Most	natural	2.8.10 ³	0.02.10 ³	2.67.10 ⁴	1.33.10 ⁴	1.22.10 ³
	sodium	2.4.10 ³	0.39.10 ³	3.24.10 ⁴	4.59.10 ⁴	8.71.10 ³
	ammonium	2.5.10 ³	0.35.10 ³	3.56.10 ⁴	2.92.10 ⁴	4.58.10 ³
Beli Bair	natural	2.1.10 ³	0.50.10 ³	2.49.10 ⁴	2.37.10 ⁴	5.20.10 ³
	sodium	2.6.10 ³	0.48.10 ³	2.93.10 ⁴	3.45.10 ⁴	6.24.10 ³
	Ammonium	2.4.10 ³	0.36.10 ³	2.56.10 ⁴	3.28.10 ⁴	7.34.10 ³
Lyaskovetz	natural	4.0.10 ³	0.29.10 ³	1.28.10 ⁵	4.21.10 ⁴	2.30.10 ³
	sodium	4.2.10 ³	0.44.10 ³	1.18.10 ⁵	1.78.10 ⁴	2.48.10 ³
	ammonium	3.6.10 ³	0.39.10 ³	-	4.10.10 ⁴	1.05.10 ³

Sorption isotherms

Sorption isotherms are plotted for sorption of ¹³⁴Cs, ⁹⁰Sr and ⁶⁰Co from simulated radioactive waste solution on the different sorbents. Although the equilibrium is reached in 3 to 5 months time, depending on the radionuclide, the contact time between the sorbent and the solution was up to 7 months. The same simulant solutions, as for the distributions coefficients determination, were used. The isotherm, given in Fig. 1 and 2, are linear showing constant distribution coefficients in a wide concentration range.

Kinetics of ion exchange

The “thin layer” method is applied for studying the kinetics of ion exchange. Figures 3 and 4 represent the kinetics of sorption for ^{137}Cs and ^{85}Sr on clinoptilolite from the simulated solution with higher salt content.

5.1.3. Discussion and conclusions

The distribution coefficients for ^{137}Cs on mordenite are higher than on clinoptilolite, but for the rest of the radionuclides as ^{90}Sr , ^{60}Co that may be present in the liquid waste, the distribution coefficients on clinoptilolite are considerably higher. Clinoptilolite is characterised with faster kinetics compared with mordenite sorbent. For these reasons clinoptilolite from Beli Plast deposit is preferred as the sorbent for treatment of liquid waste.

Increase of the sorption ability towards the radionuclide of concern (^{137}Cs , ^{90}Sr and ^{60}Co) is obtained by conversion of the natural zeolite into sodium form.

5.2. Sorption of radionuclides on the selected clinoptilolite

5.2.1. Summary of the general sorption properties

Summary of the research on ion exchange properties of the selected zeolite (clinoptilolite from Beli Plast deposit) is given bellow (Table IV) [6–13]. Sorption of different ions (alkali Cs, Rb and K ions, alkali earth Sr and Ba, and transition and heavy metal ions — Co, Mn, Pb, Ag, Zn, Cd, etc.) has been studied. The investigation includes:

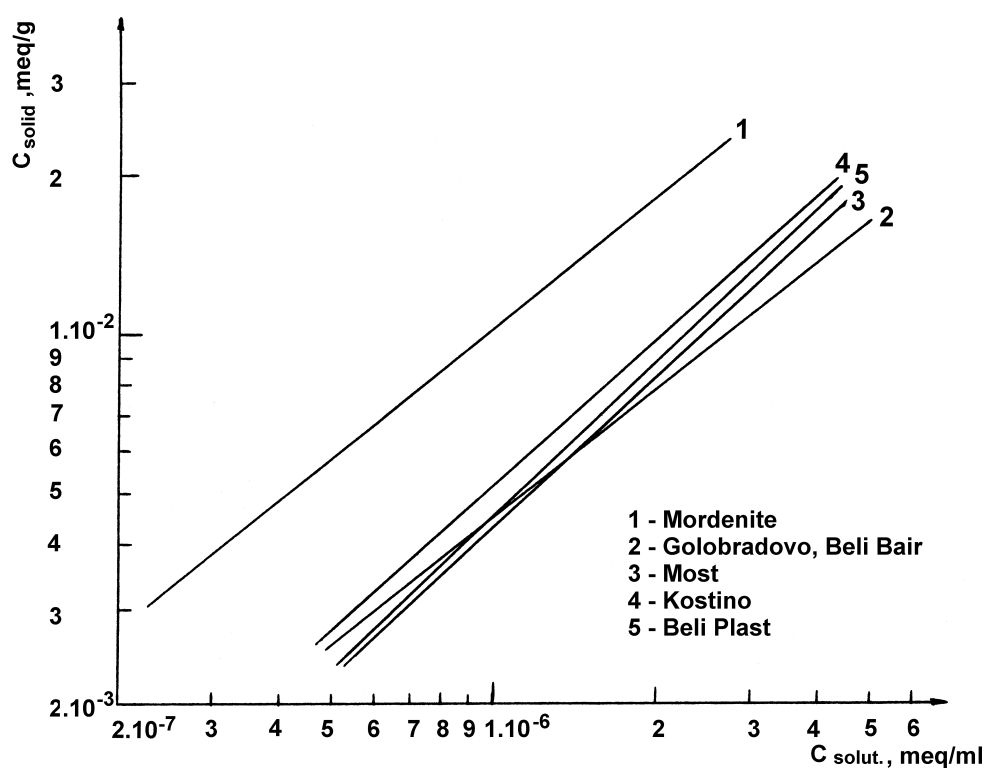


Fig. 1. Sorption isotherms for ^{137}Cs from simulated liquid waste with higher salt content (0.02 N Na^+ , 0.002 N K^+) on zeolites from different deposits.

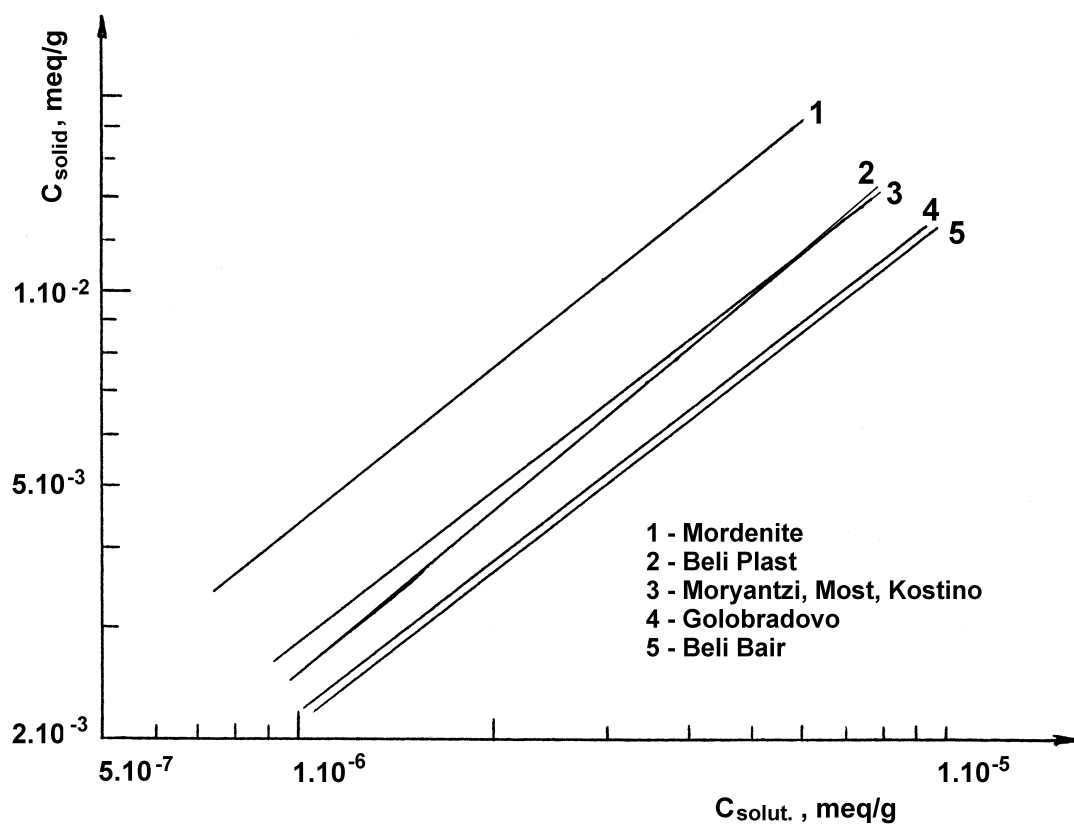


Fig. 2. Sorption isotherms for ^{137}Cs from simulated liquid waste with lower salt content ($60 \text{ mg} \cdot \text{dm}^3 \text{ CaCl}_2$) on zeolites from different deposits.

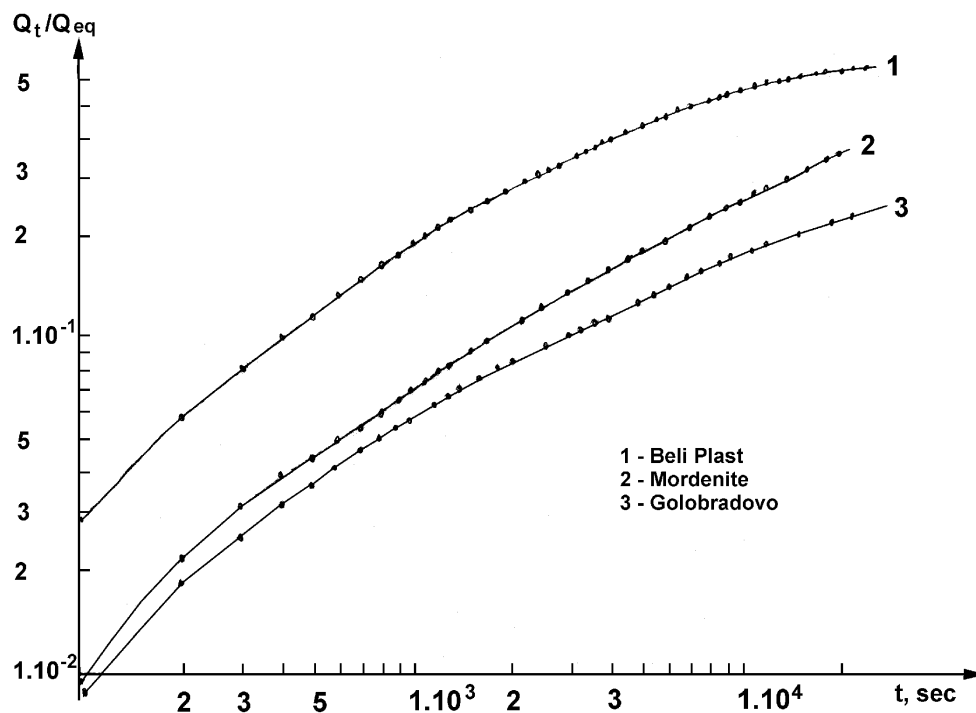


Fig. 3. ^{137}Cs sorption vs. time on zeolites from different deposits.

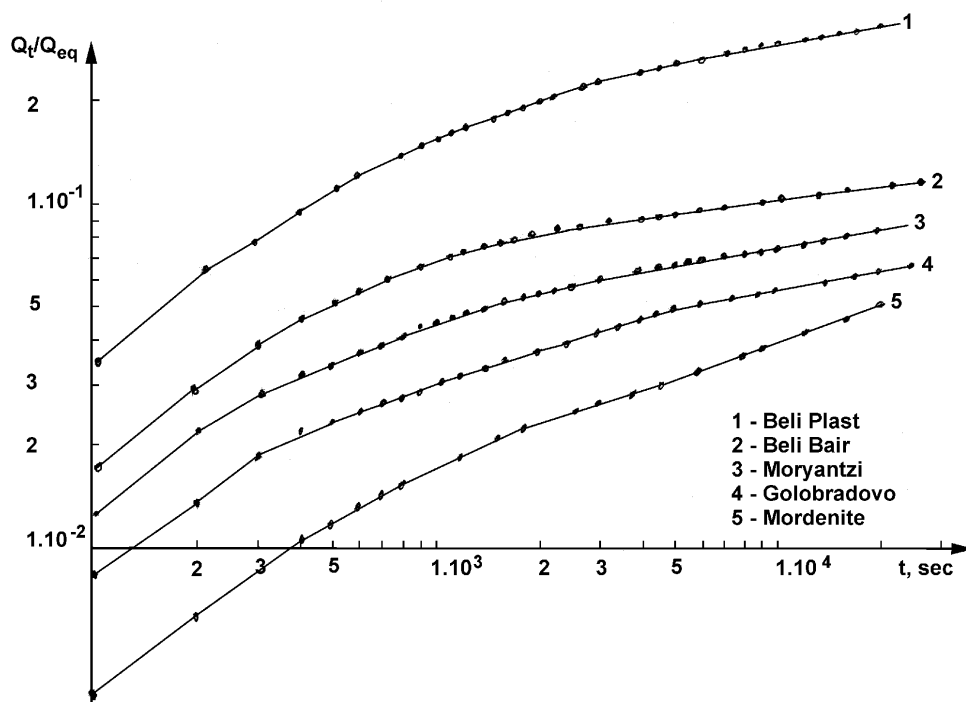


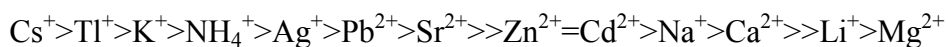
Fig. 4. ^{85}Sr sorption vs. time on zeolites from different deposits.

- the determination of ion exchange capacities under batch conditions,
- the study of the effect of competitive ions, various inorganic substances, both complexing and noncomplexing, organic complexants, pH, temperature, etc.,
- the determination of the thermodynamic and kinetic parameters values, study of the selectivity of zeolites both in standard binary system and for trace amounts of radionuclides, etc.

TABLE IV. SORPTION PROPERTIES OF NATURAL CLINOPTILOLITE

1. Ion exchange capacity	$>1.0 \text{ meq.g}^{-1}$: Cs^+ , Rb^+ , K^+ , NH_4^+ , Sr^{2+} , Ba^{2+} , Ag^+ , Tl^+ , Pb^{2+} , Hg^{2+} ; $0.5\text{--}1.0 \text{ meq.g}^{-1}$: Mn^{2+} , Cu^{2+} , Zn^{2+} , Cd^{2+} ; $<0.5 \text{ meq.g}^{-1}$: Fe^{3+} , Cr^{3+} , Ce^{3+} , Ru^{3+} , Zr^{4+} , Nb^{4+} , Co^{2+}
2. Distribution coefficient	$10^3\text{--}10^4 \text{ ml.g}^{-1}$: ^{137}Cs , $^{110\text{m}}\text{Ag}$, ^{204}Tl , ^{226}Ra , ^{133}Ba $10^2\text{--}10^3 \text{ ml.g}^{-1}$: ^{90}Sr , ^{60}Co , ^{54}Mn , ^{56}Fe , ^{65}Zn , $^{115\text{m}}\text{Cd}$; $<10^2 \text{ ml.g}^{-1}$: ^{144}Ce , ^{106}Ru , ^{95}Zr , ^{95}Nb
3. Selectivity	<div>- in presence of Na, Mg and Ca</div> <div>high: ^{137}Cs, $^{110\text{m}}\text{Ag}$, ^{204}Tl, ^{210}Pb, ^{90}Sr, ^{226}Ra, ^{133}Ba</div> <div>satisfactory: ^{60}Co, ^{54}Mn, ^{56}Fe, ^{65}Zn, $^{115\text{m}}\text{Cd}$;</div> <div>low: ^{144}Ce, ^{106}Ru, ^{95}Zr</div> <div>- in presence of K and NH_4</div> <div>- in presence of citric and tartaric acids</div> <div>high: ^{137}Cs, ^{204}Tl, ^{90}Sr, $^{110\text{m}}\text{Ag}$,</div> <div>high: ^{137}Cs, satisfactory: ^{204}Tl</div> <div>- in presence of oxalic acid</div> <div>high: ^{137}Cs, ^{204}Tl, satisfactory: ^{90}Sr</div>
4. Optimum pH	from 5 to 9
5. Thermal and radiation stability	sufficient for liquid radioactive waste treatment and long term stability in disposal environment

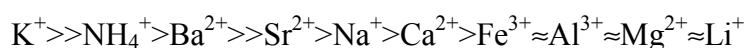
A high sorption capability of clinoptilolite for certain radionuclides, which may be present in radioactive wastes — ^{137}Cs , ^{90}Sr , ^{60}Co , $^{110\text{m}}\text{Ag}$, ^{226}Ra , ^{133}Ba is obtained. The thermodynamic data show that clinoptilolite has high selectivity for Cs, Rb, Ag, Pb, Sr and Ba over Na, Ca and Mg. The selectivity sequence obtained from the values of thermodynamic constants and standard free energies of exchange is as follows:



The radiation stability of clinoptilolite is high. No structural changes or changes in the sorption properties are observed when clinoptilolite is irradiated up to 10^7 Gy. Its thermal stability depends on the type of exchangeable cations and is sufficiently high although high thermal stability is not necessary for decontamination of liquid waste streams.

The sorption of radionuclides from different simulated radioactive waste is studied. The sorption of traces (microquantities) of radionuclides follows linear isotherms. The distribution coefficients are in the range 10^2 – 10^4 ml/g depending on the radionuclide and the composition of the solution.

Leaching of radionuclides from loaded zeolites is an important process that affects their long term stability in the disposal environment, thus reflecting their applicability in liquid waste treatment. The desorption of ^{134}Cs in presence of alkaline, alkaline-earth and polyvalent ions is studied. According to the efficiency of these cations towards desorption of caesium the following sequence is obtained:



The results of desorption of ^{134}Cs by different environmental solutions (potable water, river and sea water, loess water, different brines — MgCl_2 , NaCl , KCl and CaCl_2 , or simplified typical ground waters, which are presented in typical geological strata) confirms that caesium is strongly bound into the clinoptilolite. Significant desorption is observed only in brines. Environmental ground waters as potable water, river and sea water, etc, or simplified typical ground waters desorb insignificant part of the sorbed ^{134}Cs . Similar results are obtained for ^{90}Sr and ^{60}Co . These results confirm that natural clinoptilolite may be used as a sorbent for liquid waste treatment from the point of view of its long term stability in disposal environment.

5.2.2. Sorption of radionuclides from liquid waste, generated at Novi Han Repository

Two main liquid waste streams are generated at the repository:

Diluted solutions with low salt content, close to the salt content of the natural water that is used at Novi Han Repository. These solutions represent the waste stored in the stainless steel tanks and in-cell solution.

Solutions with higher salt content from different decontamination procedures, mainly decontamination of contaminated overalls. Although at present, the volume of such decontamination solutions is low, it will increase with the commissioning of the Low and Intermediate Level Waste Processing Facility and High Level Sealed Sources Processing Facility at Novi Han Repository.

Sorption of radionuclides ^{137}Cs and ^{90}Sr from simulated and real waste solutions that are generated at Novi Han Repository is studied. The study includes:

- Determination of the distribution coefficients from the sorption isotherms
- Kinetics experiments and determination of the internal diffusion coefficients
- Dynamic experiments and construction of the breakthrough curves

Figures 5 to 9 give the sorption isotherms of ^{137}Cs and ^{90}Sr from the simulated waste solutions that contain $1 \cdot 10^{-5}$ N cesium (strontium) labeled with ^{137}Cs (^{90}Sr).

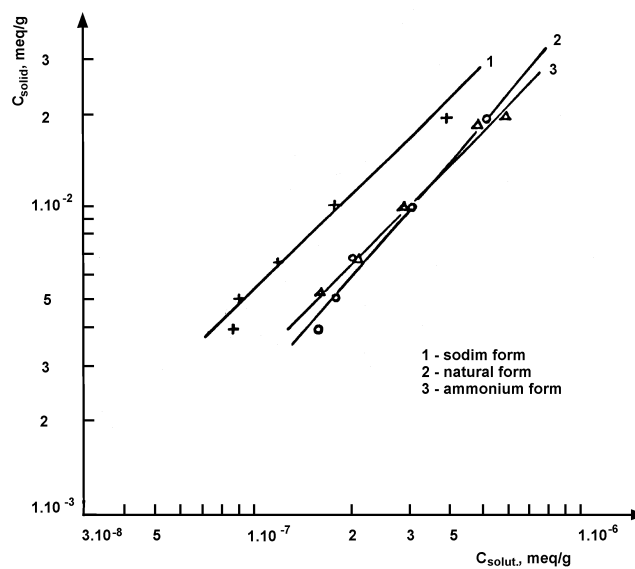


Fig. 5. Sorption isotherms of ^{137}Cs on different cationic forms of clinoptilolite from liquid radioactive waste with low salt content ($60 \text{ mg} \cdot \text{dm}^{-3} \text{ CaCl}_2$).

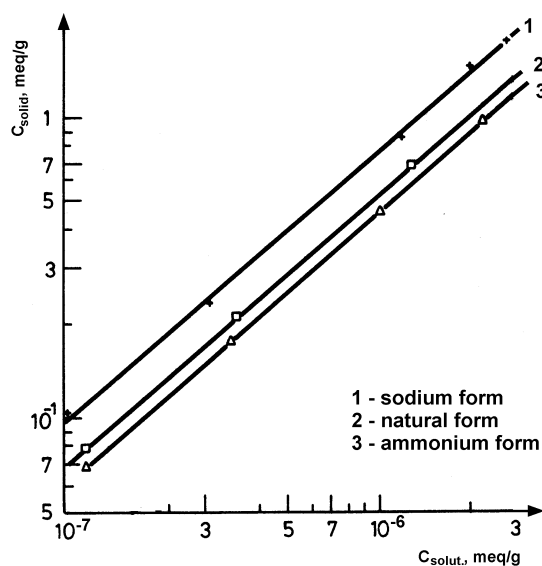


Fig. 6. Sorption isotherms of ^{90}Sr on different cationic forms of clinoptilolite from liquid radioactive waste with low salt content ($60 \text{ mg} \cdot \text{dm}^{-3} \text{ CaCl}_2$).

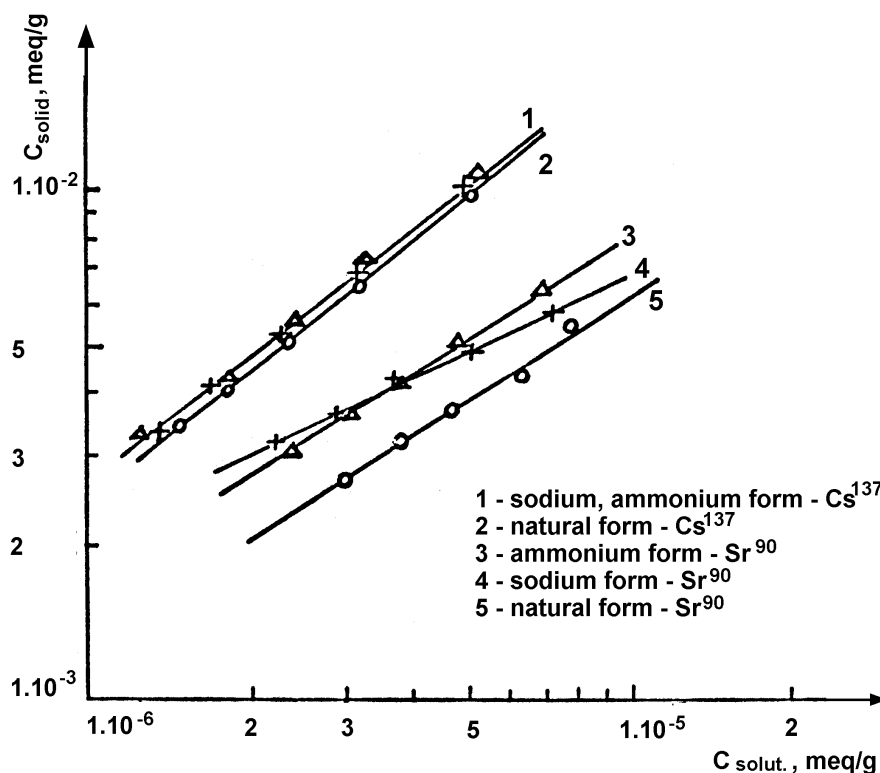


Fig. 7. Sorption isotherms of ^{137}Cs and ^{90}Sr on different cationic forms of clinoptilolite from simulated decontamination waste with higher potassium content (0.02 N Na^+ , 0.005 N K^+).

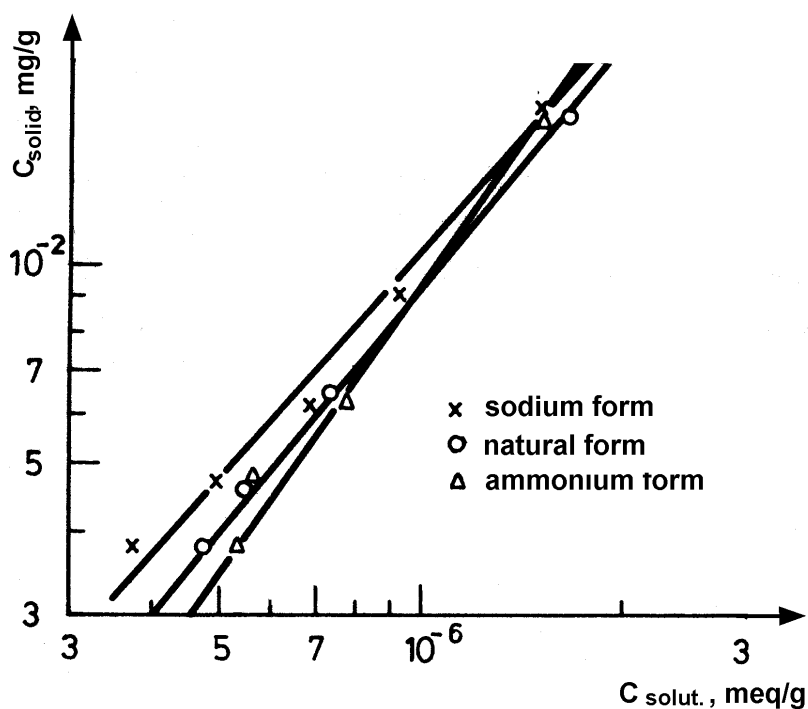


Fig. 8. Sorption isotherms of ^{137}Cs on different cationic forms of clinoptilolite from simulated decontamination waste (0.02 N Na^+ , 0.002 N K^+).

Distribution coefficients determined from the sorption isotherms are given in Table V. Similar results are obtained for ^{60}Co and other radionuclides ^{133}Ba , ^{65}Zn , ^{54}Mn that might exist in the liquid waste.

Figure 10 shows the kinetics of sorption for ^{137}Cs from decontamination solutions. The calculated diffusion coefficients are given in Table VI.

Figures 11 and 12 give the breakthrough curves for ^{90}Sr from liquid radioactive waste with low salt content and from decontamination solution. The influence of the flow rate is given in Figure 13.

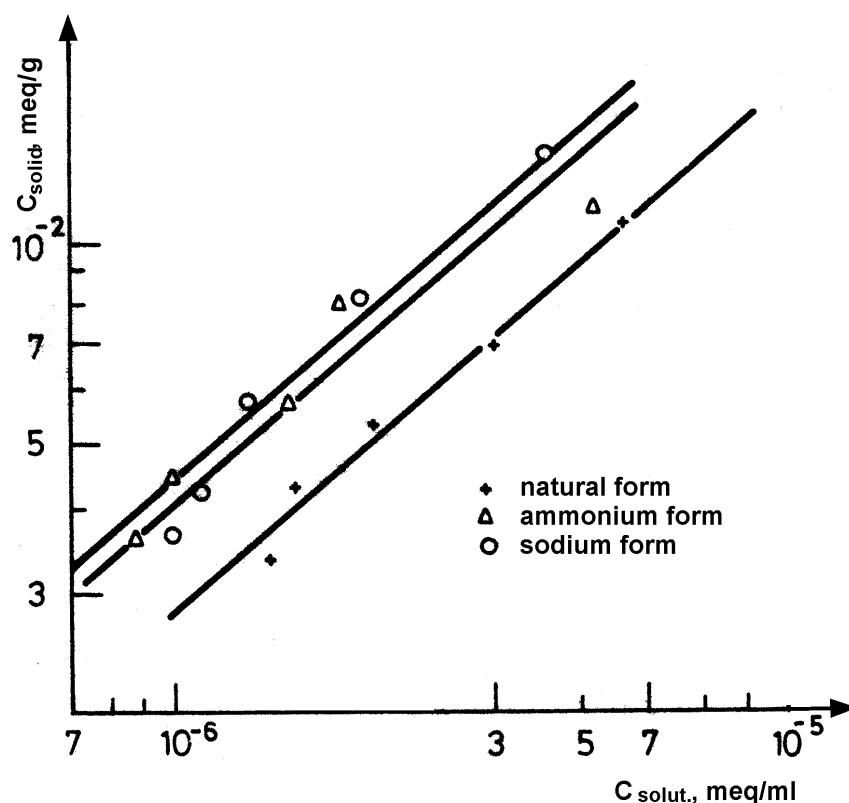


Fig. 9. Sorption isotherms of ^{90}Sr on different cationic forms of clinoptilolite from simulated decontamination waste (0.02 N Na^+ , 0.002 N K^+).

TABLE V. DISTRIBUTION COEFFICIENTS FOR ^{137}Cs AND ^{90}Sr FROM SIMULATED WASTE SOLUTIONS, $\text{Mg}\cdot\text{g}^{-1}$

Solution	Natural clinoptilolite		Sodium clinoptilolite		Ammonium clinoptilolite	
	^{137}Cs	^{90}Sr	^{137}Cs	^{90}Sr	^{137}Cs	^{90}Sr
Low salt content ($60\text{ mg}\cdot\text{dm}^3\text{ CaCl}_2$)	$3.4\cdot 10^4$	$5.7\cdot 10^3$	$5.4\cdot 10^4$	$1.1\cdot 10^4$	$3.3\cdot 10^4$	$1.2\cdot 10^4$
Decontamination solution (0.02 N Na^+ , 0.002 N K^+)	$8.8\cdot 10^3$	$3.8\cdot 10^3$	$9.7\cdot 10^3$	$2.5\cdot 10^3$	$6.7\cdot 10^3$	$3.9\cdot 10^3$
Decontamination solution (0.02 N Na^+ , 0.005 N K^+)	$2.4\cdot 10^3$	$8.1\cdot 10^2$	$2.6\cdot 10^3$	$1.1\cdot 10^3$	$2.6\cdot 10^3$	$1.1\cdot 10^3$

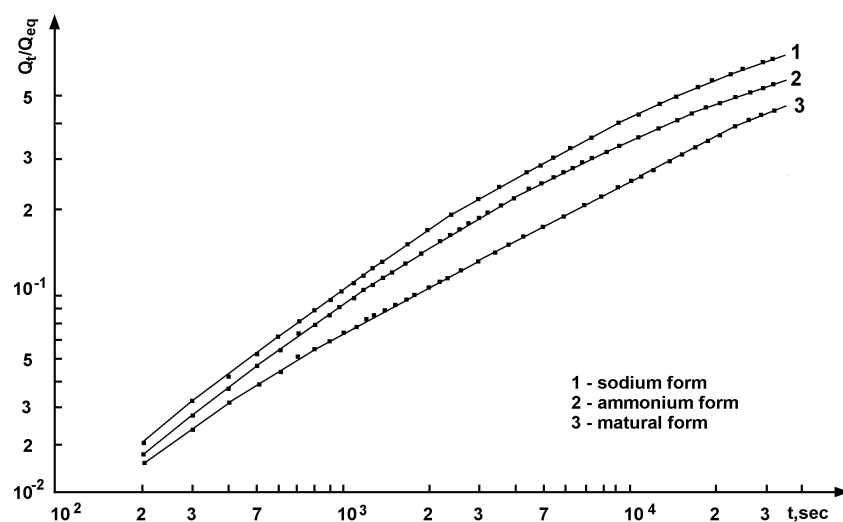


Fig. 10. Kinetics of sorption of ^{137}Cs (Q/Q_{eq} vs. time) on different forms of clinoptilolite.

TABLE VI. DIFFUSION COEFFICIENTS FOR ^{90}Sr AND ^{137}Cs FROM DECONTAMINATION SOLUTION ON DIFFERENT FORMS OF CLINOPTILOLITE, $\text{Cm}^2 \cdot \text{s}^{-1}$

Radionuclide	Natural clinoptilolite	Sodium clinoptilolite	Ammonium clinoptilolite
^{90}Sr	$4.1 \cdot 10^{-11}$	$8.9 \cdot 10^{-11}$	$1.2 \cdot 10^{-10}$
^{137}Cs	$5.2 \cdot 10^{-10}$	$8.2 \cdot 10^{-10}$	$7.3 \cdot 10^{-10}$

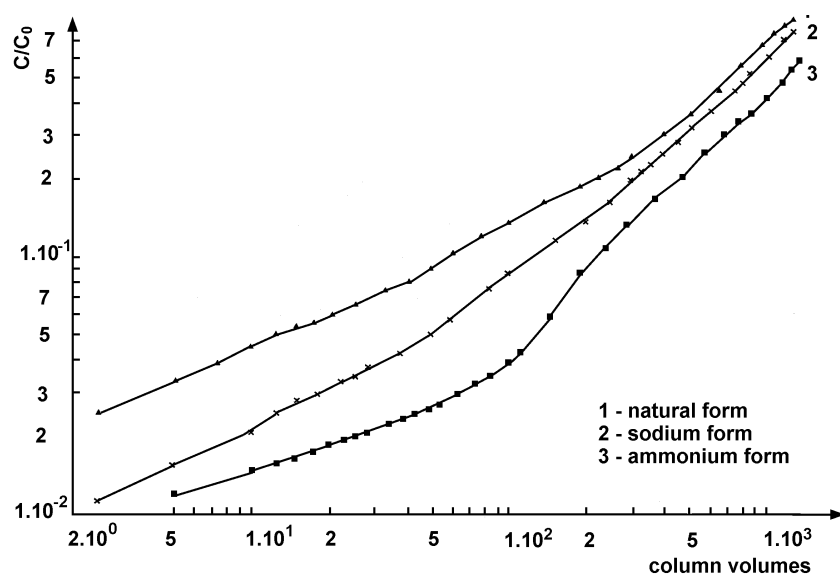


Fig. 11. Breakthrough curve for ^{90}Sr (C/C_0) on clinoptilolite from liquid radioactive waste with low salt content, $m_{\text{sorbent}} = 2\text{g}$, $0.25\text{--}0.50\text{ mm}$, $d_{\text{column}} = 0.83\text{ cm}$, $v = 5\text{ ml} \cdot \text{min}^{-1}$.

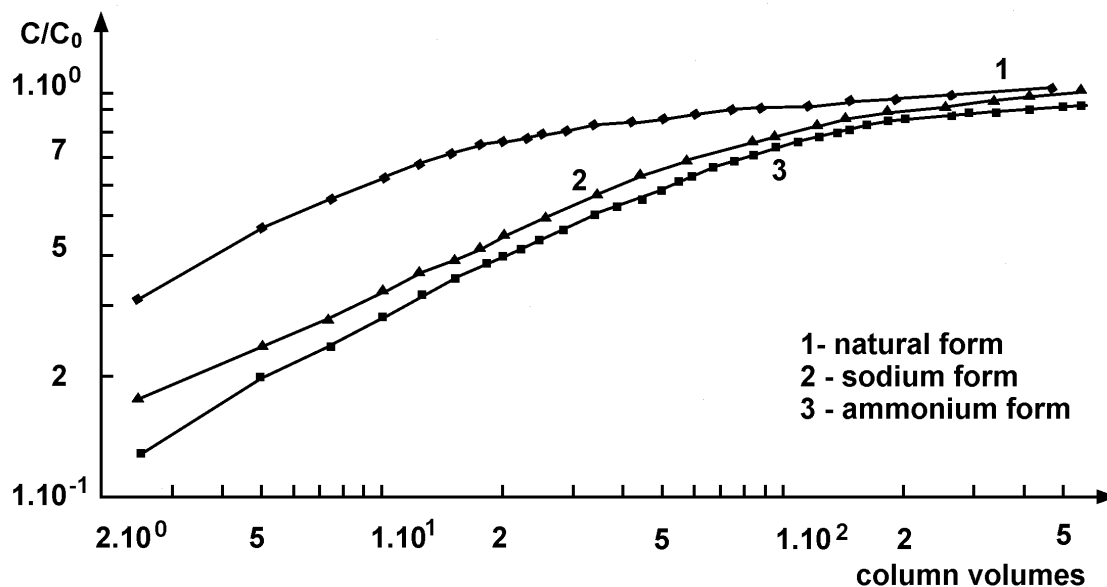


Fig. 12. Breakthrough curve for ^{90}Sr (C/C_0) on clinoptilolite from decontamination solution, $m_{\text{sorbent}} = 2\text{g}$, $0.25\text{--}0.50\text{ mm}$, $d_{\text{column}} = 0.83\text{ cm}$, $v = 5\text{ ml}\cdot\text{min}^{-1}$.

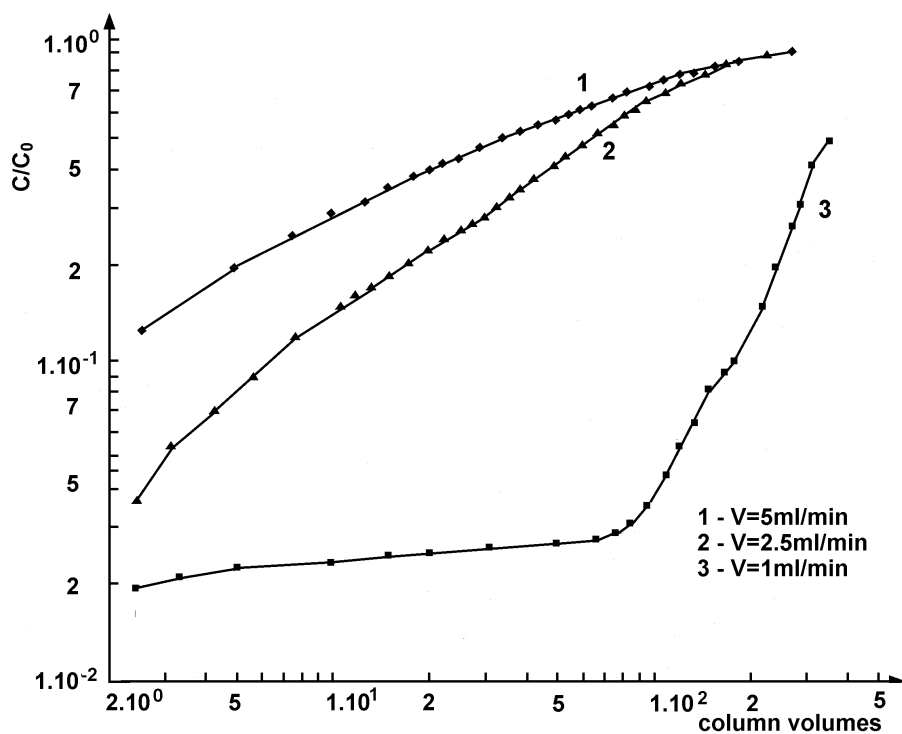


Fig. 13. Influence of the flow rate on breakthrough curve for ^{90}Sr (C/C_0) on clinoptilolite from decontamination solution, $m_{\text{sorbent}} = 2\text{g}$, $0.25\text{--}0.50\text{ mm}$, $d_{\text{column}} = 0.83\text{ cm}$.

Generally, it can be concluded that the results obtained show the applicability of natural clinoptilolite for treatment of liquid waste with radionuclide inventory governed mainly by ^{137}Cs , ^{90}Sr and ^{60}Co that are generated at Novi Han Repository. Further, experiments were also conducted to test the sorbent with real liquid waste from research reactor IRT-2000 and liquid waste that arise during the upgrading of Novi Han Repository.

6. SEPARATION OF CONSTITUENTS DECREASING SORBENT EFFICIENCY

The method that is developed for treatment of liquid waste that arise during the upgrading of Novi Han Repository and waste that will be generated after the construction of new facilities at the site, represents a combined methods. It comprises two separate methods – sorption of radionuclides in ionic form onto natural zeolite and precipitation of insoluble species and radionuclides adsorbed on the suspended solids. For decontamination waste with high surfactants content, additional separation of the detergent with modified kizelgur is envisaged.

6.1. Precipitation of radionuclides

Several precipitation processes are compared and mixed hydroxide – calcium phosphate precipitation is selected as a basic precipitation process applicable for precipitation of radionuclides and flocculation of suspended solids. Table VII gives the decontamination coefficients for ^{85}Sr , ^{60}Co and ^{54}Mn for two simulated waste solutions. The first solution represents waste with very low salt content and the second represents the decontamination waste.

TABLE VII. DECONTAMINATION OF SIMULATED WASTE SOLUTION WITH MIXED HYDROXIDE – CALCIUM PHOSPHATE PRECIPITATION

Waste solution	Precipitants	Concentration	pH	Decontamination coefficient, %				
				^{90}Sr	^{60}Co	^{65}Zn	^{54}Mn	^{144}Ce
Waste with low salt content	FeCl_3	150 mg/l	9.0	97.2	100	97.8	99.8	100
	CaCl_2	50 mg/l						
	Na_2HPO_4	120 mg/l						
Waste with low salt content	FeCl_3	300 mg/l	11.5	98.4	99.7	99.7	100	100
	CaCl_2	100 mg/l						
	Na_2HPO_4	240 mg/l						
Decontamination waste	FeCl_3	150 mg/l	9.0	39.2	100	99.9	99.9	99.7
	CaCl_2	50 mg/l						
	Na_2HPO_4	120 mg/l						
Decontamination waste	FeCl_3	300 mg/l	11.5	49.8	100	100	100	100
	CaCl_2	100 mg/l						
	Na_2HPO_4	240 mg/l						

6.2. Separation of surfactants from liquid waste streams

Separation of surfactants is envisaged, if necessary, for decontamination waste with high surfactants. Adsorption on modified kizelgur is selected as a simple easy and practical method that does not require either sophisticated equipment or special construction materials. The sorbent is prepared in the Institute of Inorganic Chemistry from natural kizelgur under special procedure that includes treatment with sulphuric acid, gel of metacilicic acid, bentonite clay, solution of $\text{Fe}_2(\text{SO}_4)_3$ and thermal treatment to form sorbent with specific surface of $22 \text{ m}^2 \cdot \text{g}^{-1}$ and good mechanical strength of nearly $1.38 \cdot 10^3 \text{ g} \cdot \text{mm}^{-1}$. The modified kizelgur has the following chemical composition — 66.88 wt.% SiO_2 , 12.48 wt.% Al_2O_3 , 4.61 wt.% Fe_2O_3 , 2.17 wt.% CaO , 1.13 wt.% MgO , 5.03 wt.% SO_3 , 2.44 wt.% Na_2O and 1.10 wt.% K_2O .

Simulated waste solution of 10 mg/l surfactant concentration was passed through column with kizelgur. After 2500 bed volumes, the concentration of detergent in the effluent was kept bellow concentration that affects the sorption behaviour of clinoptilolite.

7. PRACTICAL APPLICATION OF THE COMBINED METHOD

The developed method is tested with real liquid waste from research reactor IRT-2000 and liquid waste that arise during the upgrading of Novi Han Repository.

The liquid waste from the research reactor IRT-2000 is extremely low active with low salt content. The activity is governed by the presence of $(6.2-17) \text{ Bq}\cdot\text{dm}^{-3}$ of ^{137}Cs , $(< 5-12) \text{ Bq}\cdot\text{dm}^{-3}$ of ^{90}Sr and $(< 1-4) \text{ Bq}\cdot\text{dm}^{-3}$ of ^{60}Co . The waste is non radioactive waste according to the Regulation No.7 [3], but the environmental protection legislation [5] prohibits the release to the environment of any waste with gross beta activity higher than $0.750 \text{ Bq}\cdot\text{dm}^{-3}$. The experiments show that the total volume of 160 m^3 could be treated with no more than 0.4 m^3 sorbent at decontamination factor 100 and volume reduction factor of at least 400. The treated waste contains $\leq 0.144 \text{ Bq}\cdot\text{dm}^{-3}$ of ^{137}Cs and $\leq 0.1 \text{ Bq}\cdot\text{dm}^{-3}$ of ^{90}Sr .

The liquid waste form the activities related to upgrading of Novi Han Repository is low active with low salt content. The activity is governed by the presence of up to $156 \text{ Bq}\cdot\text{dm}^{-3}$ of ^{90}Sr and traces of ^{137}Cs (bellow $0.51 \text{ Bq}\cdot\text{dm}^{-3}$) and ^{60}Co (bellow $0.47 \text{ Bq}\cdot\text{dm}^{-3}$). The amount of clinoptilolite that is needed for decontamination of the existing waste to activity level that meets not only the requirements of the national radiological protection standard but the environmental protection regulation is 40 dm^3 .

Small mobile installation (see Figure 14) was constructed at Novi Han Repository for their treatment. It consists of two sets of small columns on a mobile platform. The dimensions of the columns conform with their subsequent storage in a concrete lined 200 L drums.

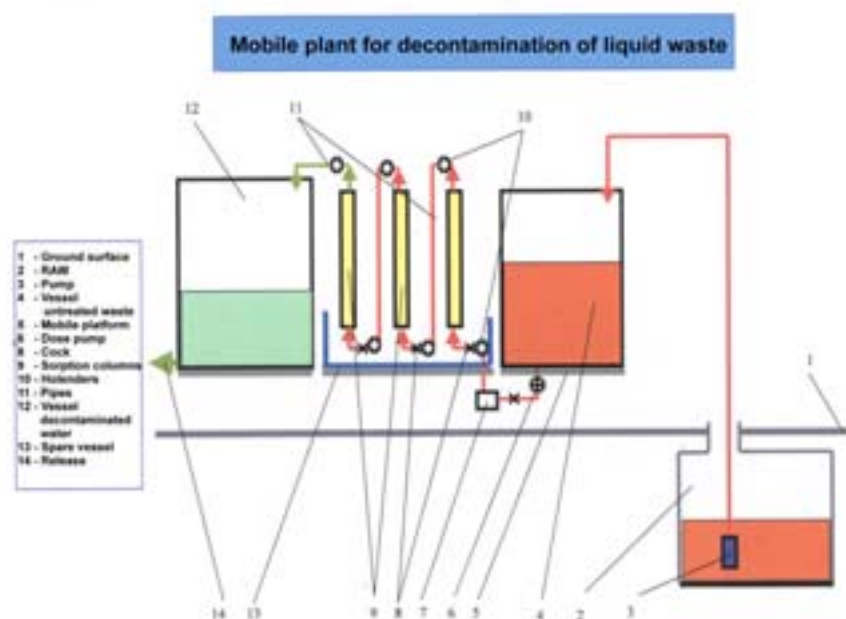


Fig. 14. Mobile installation for treatment of low level liquid waste from upgrading of Novi Han Repository.

Treatment plant for liquid waste, as a part of low and intermediate level waste processing and storage facility will be constructed in the following years based on the method that is developed under the Research Contract 9631 in the frame of IAEA Co-ordinated Research Programme “Combined Methods of Liquid Radioactive Waste Treatment”. It will consist of precipitation and sorption units.

REFERENCES

- [1] STEFANOVA I.G. Characterisation of Radioactive Waste and Identification of Radionuclide Inventory, BUL/4/005, INRNE, Sofia, (1999).
- [2] STEFANOVA I.G., Mateeva M., Radonov G., Nedialkov K., Iovtchev M., Sheherov L., Bekairov P. Temporary storage of radioactive waste at Novi Han Repository, IAEA Workshop on Experience in Upgrading of Novi Han Repository, Borovetz, Bulgaria, 27 – 30 November 2000.
- [3] Committee for Use of Atomic Energy for Peaceful Purposes, Regulation No.7 on Collection, Treatment, Storage, Transport and Disposal of Radioactive Wastes in the Territory of Republic Bulgaria, (1992).
- [4] Committee for Use of Atomic Energy for Peaceful Purposes, Basic norms for radiation protection'2000 (2001).
- [5] Committee on Environmental Protection, Regulation No.7 on Parameters and norms for quality of surface water (1986).
- [6] DJUROVA E., STEFANOVA I., GRADEV G., Geological, mineralogical and ion exchange characteristics of zeolite rocks from Bulgaria, *J. Radioanal. Nucl. Chem., Art.*, **130**(2), 425–432 (1989)
- [7] NIKASHINA V.A., TYURINA V.A., SENJAVIN M.M., STEFANOV G.I., GRADEV G.D., STEFANOVA I.G., AVRAMOVA A.I., Comparative study of the ion exchange properties of natural clinoptilolites from Bulgaria and USSR, Pt1, Study of the equilibrium sorption of caesium and strontium from solutions of different composition, *J. Radioanal. Nucl. Chem., Lett.*, **105**, 175–184 (1986).
- [8] STEFANOVA I.G. AND MILUSHEVA A.G., Natural zeolites as barriers against migration of radionuclides from radioactive waste repositories, In: Proceedings of the International Conference Safewaste'93 (Avignon, Jun.13–18), vol.3, pp.455–461 (1993).
- [9] GRADEV G., AVRAMOVA A., STEFANOVA I., Silver sorption on clinoptilolite and vermiculite and their cation modifications occurrence, in the book Kallo D., Sherry H.S., Eds, Properties and Utilisation of Natural Zeolites, Budapest, pp.463–470 (1988).
- [10] STEFANOVA I.G. AND GRADEV G.D., Sorption of transition ions on natural zeolites, In: Proceedings of the International Conference Ecology'93 (Burgass, Sept. 9–11), pp.322–327 (1993).
- [11] STEFANOVA I.G. AND MILUSHEVA A.G., “Desorption of radionuclides from loaded zeolites”, Proceedings of the International Conference Ecology'94 (Burgass, Sept. 8–10), pp.97–101 (1994).
- [12] STEFANOVA I.G., Natural sorbents as barriers against migration of radionuclides from radioactive waste repositories, NATO Science Series, v.362, pp. 371–380, (1999).
- [13] STEFANOVA I.G., Barriers against migration of radionuclides from radioactive waste repositories, *Trans. Bulg. Nucl. Soc.*, pp.13–17, (1999).
- [14] STEFANOVA I.G., MATEEVA M., MAVRODIEV V., Experimental study on method for decontamination of low level liquid waste from IRT-2000, Annual Conference of Bulgarian Nuclear Society, 25–27 October 2000, Sofia (2000).

APPLICATION OF INORGANIC SORBENTS IN COMBINATION WITH ULTRAFILTRATION MEMBRANE TECHNOLOGY FOR THE TREATMENT OF LOW LEVEL RADIOACTIVE LIQUID WASTE STREAMS.

XIGUANG SU, ZUXI ZHENG, JUN YAO, ZHONGMAO GU
China Institute of Atomic Energy, Beijing, China

Abstract. The purpose of the project was to improve the existing multistage process for treatment of liquid radioactive waste generated at China Institute of Atomic Energy. Sequential application of coagulation/precipitation, evaporation and ion exchange processes is applied for treatment of this waste. To improve efficiency and economics of the process it was proposed to treat the waste by combining the sorption of radionuclides with natural inorganic sorbents (zeolites) and then membrane filtration. At the first stage of the process development, sorption of by radionuclides (^{137}Cs , $^{89,90}\text{Sr}$, RE, ^{106}Ru) on different zeolites has been studied to define the optional procedure for sorbent preparation and conditions for optimization of the sorption process (t °C, pH, influence of solution compositions). Combination of sorption with membrane treatment for solid/liquid phase separation was the next step of the research work. Application of this combined treatment process is discussed in the report.

1. INTRODUCTION

The low level radioactive liquid waste with specific activity of 1×10^2 - 1×10^5 Bq/L generated from radiochemical laboratory, isotopes production, and other activities of nuclear installations, was collected and stored in our institute. Traditionally, this liquid waste is treated by means of a three-stage process, including precipitation, evaporation and organic ion exchange. This treatment process allows achieving satisfactory decontamination factors, but the treatment costs are relatively high.

In seeking more economic methods to treat the low level radioactive liquid waste, many studies on new treatment materials and processes, such as the use of natural or synthetic inorganic sorbents, membranes separation technologies (microfiltration, ultrafiltration, or reverse osmosis) or combinations of these technologies, have been reported [1–5] in the recent years. Especially, there are some scale-up tests on treating the liquid waste [6], which are successful in simplifying treatment process and reducing treatment costs. In our institute, progress in treatment of the liquid waste with inorganic sorbents or reverse osmosis membranes was made [5,7,8]. In the last few years, we have started to use inorganic sorbents in combination with membrane separation technology to treat the liquid waste. This paper mainly focuses on the lab-scale study of liquid waste treatment with inorganic sorbents in combination with membrane separation technology.

2. PROPERTIES OF NATURAL ZEOLITES FOR THE TREATMENT OF LOW LEVEL LIQUID RADIOACTIVE WASTE

2.1. Experimental

As absorbers, three kinds of natural zeolite minerals (ZT-4, ZL-4, and HD-2 sorbents) collected from different areas in China were used. The materials were crushed; the fraction with grain size 80–160 mesh was sieved out for use in the experiments.

In order to improve the exchange properties of the tested materials, influence of the calcination was tested. An appropriate amount of the granular zeolite was added to 3.6 % HCl solution in a 100 ml beaker and soaked for 5–6 min. Then the supernatant was decanted, the zeolite was washed with deionised water, dried and calcined for 6–8 hours at 100–850⁰C. Finally, it was cooled down to ambient temperature for use in the experiment.

For testing the influence of the zeolite form, samples of the materials were converted to NH₄⁺, Na⁺, Ca²⁺, Al³⁺, or H⁺ forms. The conversions were accomplished by mixing certain amounts of natural zeolites with grain size 80–160 mesh with a solution of ammonium (or Na⁺, Ca²⁺, Al³⁺) chloride or hydrochloric acid, respectively. The mixture was then heated in a beaker for 4 hours in a boiling water bath, filtered, washed, and dried.

The experiments were performed with both the simulant and the real low level radioactive liquid waste (LLW) generated in isotopes production and various other activities of nuclear installations. The main compositions are shown in Table I.

TABLE I. COMPOSITIONS OF LLW USED IN THE EXPERIMENTS

Types of liquid waste	pH	Salt content (g/l)	Hardness (mg/l)	Specific activity (Bq/l)	Major nuclides
Simulated liquid waste	6.8	5.3	4.1	5.7×10 ⁴	¹³⁷ Cs, ^{89,90} Sr, RE
Liquid waste generated from CIAE	9.0	4.7	3.7	2.2×10 ³	¹³⁷ Cs, ^{89,90} Sr, ¹⁴⁴ Ce, ¹⁰⁶ Ru

The testing was performed both in static batch and in dynamic column experiments.

For the *static batch experiments*, 0.3 g sorbent (80–160 mesh) from different areas, converted to the desired cationic form, was added to 20 ml of the simulated liquid waste spiked with ¹³⁷Cs. The mixture was then shaken for 1 hour using a shaker. The phases were separated by centrifugation and the supernatant was analysed by gamma ray spectrometry to obtain the distribution coefficients (K_D) of ¹³⁷Cs.

The *dynamic column experiments* were performed in a 10–15 cm long columns with inner diameter of 0.3–0.2 cm packed with 3–5 g of sorbents converted to the desired cationic form. The liquid waste was passed through the column at a flow rate of 2–3 BV/h. The decontamination factor (DF) was obtained by determining the gross beta radioactivity of the effluent.

2.2. Results and discussion

In the first phase, the sorption kinetics was determined for the studied materials. Appropriate amounts of ZT-4, ZL-4 and HD-2 sorbents were added to the simulated liquid waste spiked with ¹³⁷Cs and shaken for up to 4 hours at ambient temperature. The results obtained are given in Fig. 1. The data show that the sorption equilibrium is reached after 1 hour, which indicates that the sorption rate is slow.

The calcining temperature, used for modifying all the three types of sorbents mentioned above, ranged from 100⁰C to 850⁰C. The dependence of the caesium distribution coefficients on the calcining temperature is shown in Fig. 2 for all the materials used. The results show that there is no change of the sorption properties of the materials for calcining temperatures lower than 400⁰C. On the other hand, for the calcining temperatures higher than 400⁰C, the sorption properties of all the sorbents deteriorate. When temperature of 850⁰C is used, the materials

almost lose their ability to sorb caesium. Fig. 2 also indicates that the sorbents from different areas have the same thermal stability.

To check the influence of converting the sorbents to various cationic forms on their sorption properties, distribution coefficients of ^{137}Cs on sorbents converted to NH_4^+ , Na^+ , H^+ , Ca^{2+} , or Al^{3+} forms were determined. The results obtained are listed in Table II. Table II shows that, for the ZT-4 and ZL-4 sorbents, the distribution coefficients of ^{137}Cs on the materials converted to NH_4^+ or Na^+ form are higher than for the remaining forms studied, exceeding the value of $5 \times 10^2 \text{ ml/g}$. Therefore, it can be concluded that the type of the cationic form of the sorbents has an important effect on its sorption properties.

The influence of temperature and pH of the simulated liquid waste on the distribution coefficients of ^{137}Cs on all the three sorbents has been tested. For these experiments, sorbents calcined at the temperature of 350°C were used. The results obtained are shown in Table III and Table IV, respectively.

From the data presented in Table III, it can be seen that the distribution coefficients of ^{137}Cs on all the sorbents slowly decrease with the increase of temperature.

On the other hand, as shown in Table 4, no obvious effect of pH on the ^{137}Cs distribution coefficients was found for any of the sorbents in all the experimental range of pH. Based on these results, it may be suggested that the sorbents are applied at ambient temperature and may be used in a wide range of pH.

In the experiments aimed at determining the sorption capacity of the sorbents, four types of materials (natural, converted to H^+ or NH_4^+ form, or calcined at 350°C and converted to NH_4^+ form) were used. The sorption capacity was determined for various radionuclides; simulated liquid waste was used. The experiments were carried out at ambient temperature. The results obtained are shown in Table V.

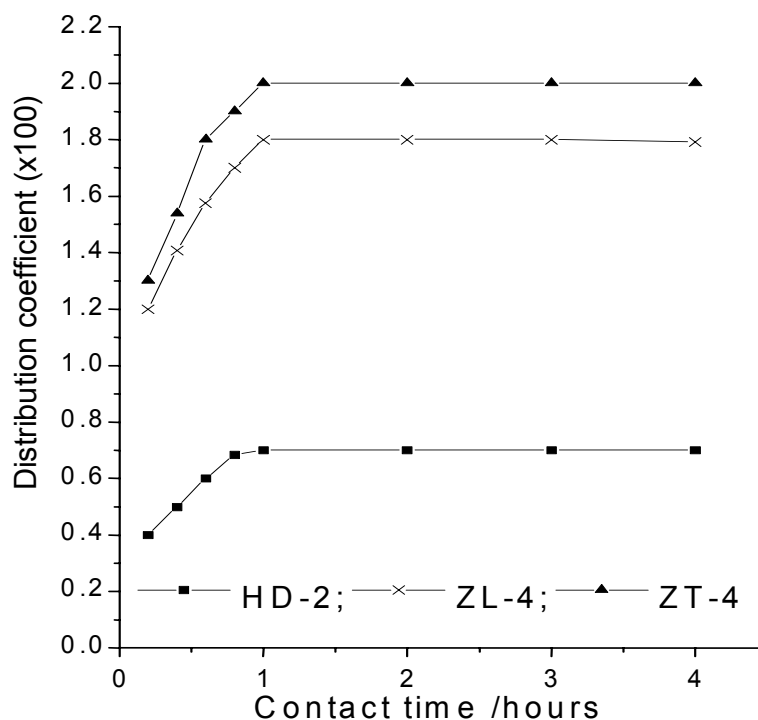


Fig. 1. Sorption kinetics of the sorbents.

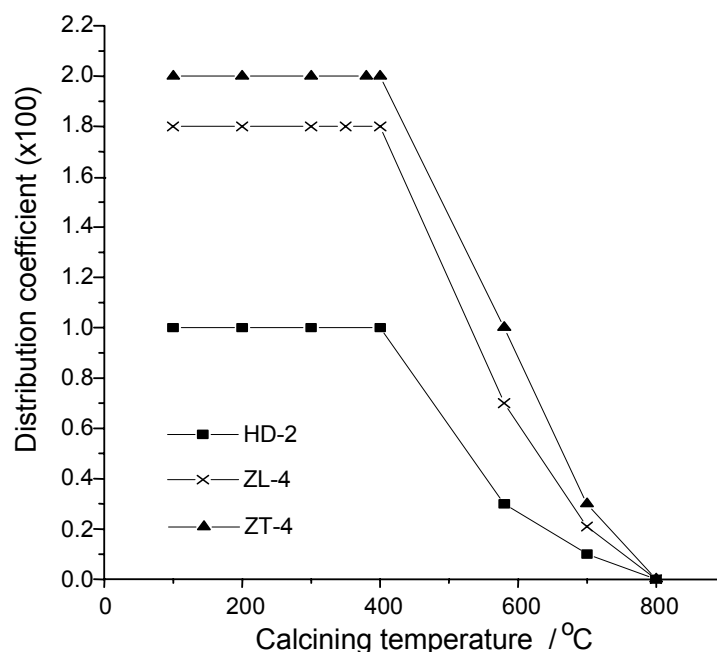


Fig. 2. Influence of calcining temperature on the exchange properties of sorbents.

As shown in Table V, the sorbents from different areas possess different sorption capacities. The sorbents converted to NH_4^+ forms have higher sorption capacities than the natural ones or those in the H^+ forms. This confirms that the conversion of natural zeolite can improve its sorption capacity. From the overall evaluation of the results presented above, it can be concluded that for the treatment of liquid waste, the ZT-4 sorbent in the NH_4^+ form ($\text{NH}_4^+\text{ZT-4}$) is the most prospective.

TABLE II INFLUENCE OF CATIONIC FORM OF THE SORBENTS ON ^{137}Cs DISTRIBUTION COEFFICIENT

Sorbents	Distribution coefficient				
	NH_4^+	Na^+	H^+	Ca^{2+}	Al^{3+}
ZT-4	5.4×10^2	5.7×10^2	1.7×10^2	1.1×10^2	1.6×10^2
ZL-4	5.2×10^2	5.4×10^2	9.5×10^1	7.8×10^1	1.2×10^2
HD-2	1.9×10^2	1.8×10^2	1.4×10^2	5.6×10^1	2.5×10^2

Experimental conditions: ambient temperature; Simulated liquid waste: pH=6.8; Sorbents calcined at 350°C

TABLE III. INFLUENCE OF TEMPERATURE ON ^{137}Cs DISTRIBUTION COEFFICIENT ON THE SORBENTS

Sorbent	Distribution coefficient				
	21 °C	40 °C	59 °C	72 °C	91 °C
ZT-4	5.3×10^2	5.0×10^2	4.8×10^2	4.5×10^2	3.3×10^2
ZL-4	5.0×10^2		3.8×10^2	3.3×10^2	2.8×10^2
HD-2	1.9×10^2	2.0×10^2	1.4×10^2	1.0×10^2	1.0×10^2

TABLE IV. INFLUENCE OF PH ON ^{137}Cs DISTRIBUTION COEFFICIENT ON THE SORBENTS

Sorbent pH	Distribution coefficient			
	4.0	6.6	8.9	10.3
ZT-4	2.0×10^2	2.2×10^2	2.4×10^2	2.4×10^2
ZL-4	1.7×10^2	1.8×10^2		2.1×10^2
HD-2	6.7×10^1	7.3×10^1		7.4×10^1

TABLE V. SORPTION CAPACITY OF THE SORBENTS IN THE SIMULATED LIQUID WASTE

Sorbent	Type	Adsorption-exchange capacity meq/g				
		^{137}Cs	$^{89-90}\text{Sr}$	RE	$^{103-106}\text{Ru}$	^{95}Zr - ^{95}Nb
ZT-4	Natural	0.65				
	NH_4^+	0.86	0.03	0.27	0.03	0.06
	NH_4^+ (350 °C)	0.73	0.06	0.33		
	H^+	0.31				
ZL-4	NH_4^+ (350 °C)	0.82	0.02	0.16		
	H^+	0.42				
HD-2	NH_4^+ (350 °C)	0.46	0.01	0.06		

3. TREATMENT OF LIQUID RADIOACTIVE WASTE BY FLOCCULATION IN COMBINATION WITH SORPTION ON INORGANIC SORBENT OR ‘COATED MATERIALS’

For treatment of real liquid radioactive waste, a combined method was proposed. As the first step, precipitation was initiated by addition of a suitable flocculant to a suspension of inorganic sorbent or ‘Coated materials’ in the treated waste. The supernatant of the precipitation was ultrafiltered (UF) through a UF membrane, and, in the final step, the ultrafiltrate was ‘polished’ by passing it through a column filled with natural zeolite. The scheme was aimed at reaching such decontamination of the waste, as the waste could be discharged to a small river.

3.1. Experimental

The following sorbents and composite materials were used in the experiments:

- C-1----natural zeolite collected from Weichang in Hebei province of China;
- C-2----natural manganese ores collected from Linlin in Hunan province of China;
- C-3----conventional flocculant (FeSO_4 , KMnO_4 , Na_3PO_4);
- C-4----cadmium hexacyanoferrate;
- C-5----FCISM α coated material.
- C-6----FCISM β coated material.

For the combined flocculation/sorption step, the following method was used: Into a LRW A05/2 or LRW A05/3 waste streams, highly selective sorption materials were added followed by the addition of conventional flocculant (FeSO_4 , KMnO_4 , or Na_3PO_4). The mixture was stirred for 5–10 minutes and then allowed to stand for 24 hours. Then, the supernatant liquid was ultrafiltered through a selected ultrafilter membrane, and the decontamination factors and distribution coefficients were determined.

For the distribution coefficients (K_D) determination, following equation was used:

$$K_D = (C_0 - C_I) \times V / C_I \times m$$

where C_0 is the initial activity (concentration) of the ion of interest, C_I is the activity (concentration) of the same ion after the contact between the sorbent and the solution in a batch experiment; V is the volume of solution, and m is the mass of dry sorbent.

The decontamination factors (DF) were defined as a ratio between the initial radionuclide concentration C_0 and its average concentration C_{av} in the total volume of the treated solution, and were accordingly calculated as:

$$DF = C_0 / C_{av} .$$

The experiments were performed in four series. In the first two series, no ultrafiltration was applied. In the third and the fourth series, the supernates were ultrafiltered through membranes with molecular weight cut-off (MWCO) values of 10000 or 5000, respectively. In the respective series, the following sorbents and composite materials, or their combinations were used:

- Series-1: C-3, C-4, C-5, C-6, C-3+C-1, C-3+C-2, C-3+C-4, C-3+C-5, C-3+C-6
 Series-2: C-3+C-1+C-2, C-3+C-1+C-4, C-3+C-1+C-5, C-3+C-1+C-6
 Series-3: (C-3+C-1+C-4), (C-3+C-1+C-5), (C-3+C-1+C-6), (C-3+C-1); the supernate ultrafiltered through membrane with MWCO 10000
 Series-4: (C-3+C-1+C-4), (C-3+C-1+C-5), (C-3+C-1+C-6), (C-3+C-1); the supernate ultrafiltered through membrane with MWCO 5000.

3.2. Ultrafiltration conditions optimization

The UF membrane application is a relatively new method for liquid radioactive waste treatment. In our experiments a polyacrylonitrile (PAN) membrane was used to treat the supernatant of the precipitation. The ultrafiltration system consisted of a source water tank, a pump and a modules of PAN membranes. The schematics of the set-up are shown in Fig. 3.

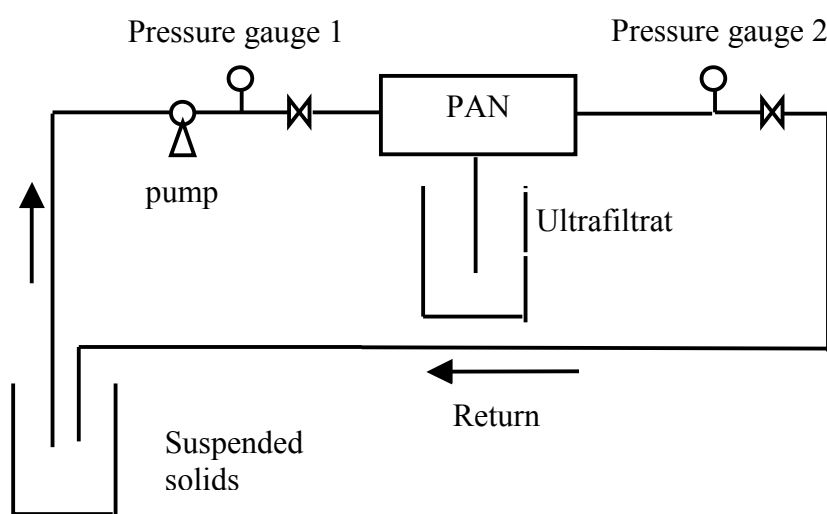


Fig. 3. Flow sheet of ultrafiltration set-up.

Prior the experiments, the UF membrane was soaked for 24 hr in clear water. A preliminary test, performed with distilled water, revealed that the flux through the membrane depends on the pressure used. In the tested range of 0.07 – 0.10 MPa, the flux of the liquid through the module was found to increase with the increasing pressure. Therefore, the operational pressure was selected as 0.1 MPa for all the experiments.

Extensive efforts were undertaken to optimize the procedure for cleaning of the clogged membranes in the module. In the first series of tests, efficiency of various solutions for the cleaning was compared. Backwashing was used in all these experiments. The cleaning solutions tested included H₂O, 0.1N NaOH, 0.1N NaCl, and the membrane permeate liquid. The comparison of the efficiencies of these solutions for membrane cleaning, as obtained in the experiments performed, is given in Fig. 4.

From the results obtained, it can be concluded that after backwashing the membrane with any of the tested solutions, the flux is not decreased significantly and the steady state flux easily reached. Therefore, use of the backwash method for cleaning the UF module can be recommended and should yield desired result.

In the next series of experiments, performance of another technique for washing the clogged membrane — so called ‘alternating clean’ — was tested. It consisted of periodically interchanging the inlet and outlet of the ultrafiltration module whenever the membrane got clogged. The experimental results of these tests have been summarised in Fig. 5.

From the results presented in Fig. 5, it can be seen that the initial flux of the liquid through the module is high. However, after a certain period of time of the operation, the flux through the module is quickly attenuated. This attenuation should be mainly attributed to blocking of the inlet of the module and upper part of the ultrafiltration fibres with solids, that are present in high concentration in the feed. Consequently, by interchanging the inlet and outlet of the module, the blocked part of the module are flushed, the membrane is cleaned, and the flux of liquid through the module returns to its initial value. Hence, if such way of operating of the ultrafiltration module is selected, in which the inlet and outlet are interchanged periodically, higher average flux through the module can be achieved.

Further, an ‘interval cleaning’ method of operating the ultrafiltration module was tested. In this method, after each decrease of the flow, when the concentration effect became poor, the operation was interrupted. Then, the module was backwashed by a suitable cleaning liquid and the operation continued. The experimental result obtained in testing this method is shown in Fig. 6.

From the comparison of the results presented in Fig. 5 and 6, it can be seen that the results of the ‘interval cleaning’ method approach those achieved by the ‘alternating clean’ method, when the inlet and outlet of the module are interchanged periodically. In the ‘interval cleaning’ method, higher average flux can be obtained by selecting optimum times of backwashing. For operational convenience the ‘alternating clean’ method, when the inlet and outlet of the module are interchanged periodically, was selected for the experiments.

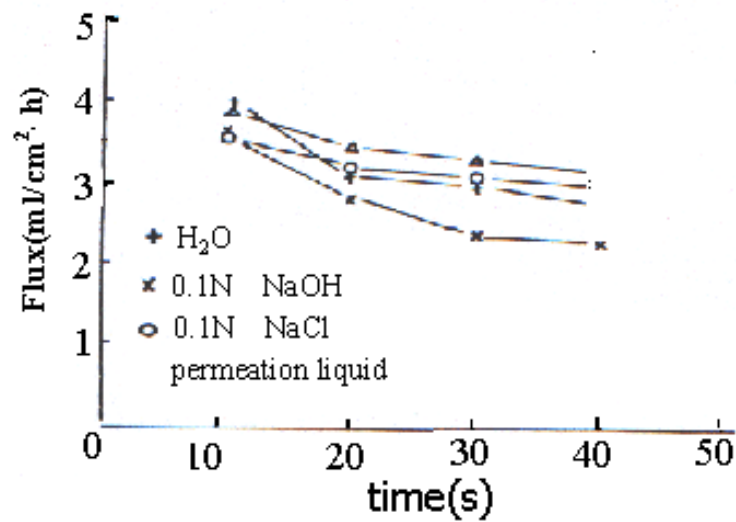


Fig. 4. Time dependence of the flux through the UF membrane after backwashing it with different cleaning solution.

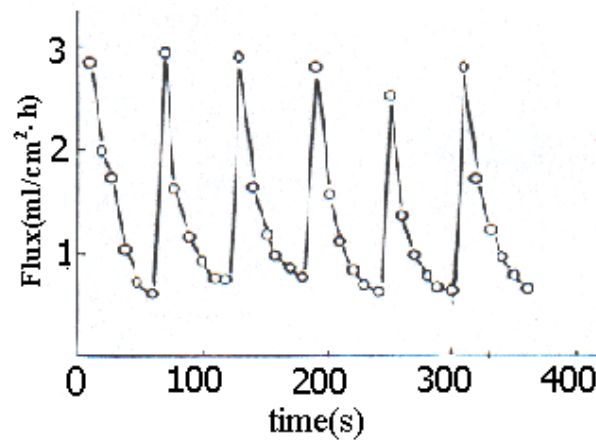


Fig. 5. 'Alternating clean' test results – in the individual periods, the inlet and outlet of the module are interchanged.

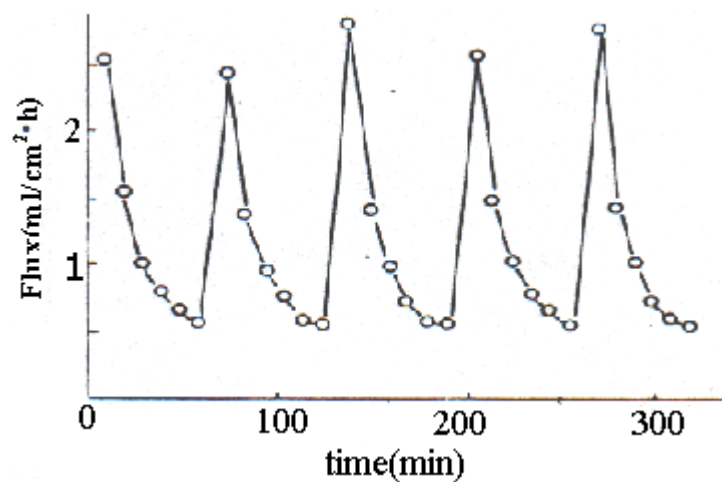


Fig. 6. 'Interval cleaning' test results – after each decrease of the flux, the module is backwashed with a cleaning liquid.

3.3. Results and discussion

For the study of the influence of different grain size of zeolite on DF and K_D , approximately 0.5 g of the zeolite was crushed and sieved into different particles size ranging from 40 to 160 meshes. The sieved materials were added to 20 ml of LRW A05/3 waste that contained three various flocculants – 10–15 ppm of FeSO_4 ; 80–120 ppm of Na_3PO_4 ; and 5–10 ppm of KMnO_4 . The ratio of solid to liquid used was 1:40. The mixture was stirred for 5–10 minutes and allowed to stand for 24 hours. Then, the supernatant liquid was sampled for analysis. The results are given in Table VI.

TABLE VI. INFLUENCE OF THE GRAIN SIZE OF ZEOLITE ON DF AND K_D

Particle size(mesh)	40–60	60–80	80–100	100–120	120–160	Less than 160
pH	10.10	10.07	10.06	10.05	10.03	10.06
DF	32	41	72	1.4×10^2	1.5×10^2	1.5×10^2
K_D	1.2×10^3	1.2×10^3	2.9×10^3	5.6×10^4	6.0×10^4	6.0×10^4

As shown in Table VI, the values of DF and K_D increase with the decreasing particle size till 120–160 mesh. Almost no difference was found between these values measured for the 120–160 mesh fraction and those for particle size less than 160 meshes. Therefore, in the later experiments, zeolite with particle size range 120 to 160 mesh was used.

For the determination of the influence of the amount of zeolite on the values of DF and K_D , different amounts of zeolite were added to 20 ml LRW A05/2 containing conventional flocculant. The mixture was stirred for 5–10 minutes and allowed to stand for 24 hours. Then, the supernatant liquid was sampled for analysis. The results are given in Table VII.

TABLE VII. INFLUENCE OF THE AMOUNT OF ZEOLITE ON THE DF AND K_D VALUES

Amount (g)	0.05	0.1	0.3	0.5	0.8
DF	6.0	12.0	40.0	65.0	98.0
K_D	2.0×10^2	4.4×10^2	1.6×10^3	3.4×10^3	3.9×10^3

As shown in Table 7, the values of DF and K_D increase with increasing amount of zeolite used in the experiments. When comparing the data given in Table 6 with those shown in Table 7, it can be seen that the DF and K_D values measured for zeolite with particle size ranging from 120 to 160 mesh for the A05/3 waste (Table 6) with those found in the same conditions (0.5g zeolite) for the A05/2 waste (Table 7), it can be seen that they are not the same. This difference is should be ascribed to decreased sorption ability of zeolite in the A05/2 waste with higher salt content (when compared with that of the A05/3 waste).

The results of the four series of experiments performed with the highly selective sorbents and composite materials in combination with flocculation are summarized in Tables VIII to X. All the testes were performed with the 20ml batches of the LRW A05/3 waste, after 5–10 minutes stirring, the adjusted samples were allowed to stand for 24 hours.

The experiments in Series-1 were performed by adding the C-3 flocculant (10–15 ppm of FeSO_4 , 80–120 ppm of Na_3PO_4 , 5–10 ppm of KMnO_4), 0.005 g zeolite, 0.05 g coated material, or their mixtures, to the waste. From the results obtained (Table 8) it can be seen that application of the coated sorption materials in combination with the conventional flocculant can increase the DF values. The flocculation itself (C-3 experiment) or the combination of the flocculant and natural manganese ore (C-3 + C-2 experiment) has a low decontamination effect.

TABLE VIII. EXPERIMENTAL RESULTS OBTAINED IN SERIES-1

	C-3	C-4	C-5	C-6	C-3 + C-1	C-3 + C-2	C-3 + C-4	C-3 + C-5	C-3 + C-6
DF	1.1	2.3×10^2	1.4×10^2	1.6×10^2	1.1×10^2	5.9	3.2×10^2	1.6×10^2	2.0×10^2
K _D	40	4.6×10^4	2.8×10^4	3.2×10^4					

TABLE IX. EXPERIMENTAL RESULTS OBTAINED IN SERIES-2

	C-3+C-1+C-2	C-3+C-1+C-4	C-3+C-1+C-5	C-3+C-1+C-6
DF	1.5×10^2	3.6×10^2	2.0×10^2	2.2×10^2

TABLE X. EXPERIMENTAL RESULTS OBTAINED IN SERIES-3 AND 4

MWCO membrane	C-3+C-1+C-4	C-3+C-1+C-5	C-3+C-1+C-6	C-3+C-1
10000	3.6×10^2	2.2×10^2	2.6×10^2	1.3×10^2
5000	5.0×10^2	4.0×10^2	3.6×10^2	1.5×10^2

In Series-2, combination of two types of sorption materials was considered. For the experiments, 0.5 g of zeolite was combined with 0.05 g of one of the C-4, C-5, or C-6 materials. Otherwise, the experiments were performed in the same way as those described in Series-1. From the comparison of the results obtained (Table 9) with those presented in Table 8, it can be seen that addition of 0.5 g of zeolite slightly improves the effectivity of the removal of radionuclides.

The experiments in Series-3 and 4 were performed in the same way as those in Series-2, after 24 hours of standing, the supernatant was ultrafiltered through a ultrafiltration membrane and the DF values were determined. As it can be seen from the comparison of the results in Tables 9 and 10, the values of DF increase a bit after the ultrafiltration. It has been concluded that the ultrafiltration is not a very effective method for waste treatment. The experiments performed with the membrane with higher MWCO value yielded lower decontamination factors, the efficiency of the radionuclide removal could be increased by application of membrane with lower MWCO value.

3.4. Pilot plant test of the method combining sorption precipitation with ultrafiltration and ion-exchange on a zeolite column for treatment of real radioactive liquid waste stream

For this test, 2000 ml portion of the liquid waste was poured into a 3000 ml beaker. The value of pH of the sample was adjusted to pH 7.0–8.0 by addition of diluted nitric acid. Then 5000 mg of the NH₄⁺ZT-4 zeolite with grain size of 80–160 mesh was added and the mixture was stirred with a magnetic stirrer. After the addition of the flocculant to the sample, mixing was continued for 15 minutes. After 24 hours of standing, phase separation was performed by the UF module. The permeate solution from the ultrafiltration was passed through a column filled with zeolite sorbent. After each of the stages, the activity of the solution was measured. The overall results of this treatment process are summarised in Table XI.

TABLE XI. THE RESULT OF THE COMBINED SORPTION PRECIPITATION – ULTRAFILTRATION – ZEOLITE ION-EXCHANGE TREATMENT OF A REAL LIQUID WASTE

Initial specific activity of the waste (Bq.l ⁻¹)	Activity of the solution after sorption precipitation (Bq.l ⁻¹)	Activity of the solution after ultrafiltration (Bq.l ⁻¹)	Activity of the effluent from the zeolite column* (Bq.l ⁻¹)
2.18×10 ⁴	4.4×10 ²	3.1×10 ¹	0.29

* zeolite column only through 1%

From the results presented in Table XI it follows that the efficiency of the combined treatment process consisting of sorption precipitation, ultrafiltration, and ion-exchange on zeolite is very efficient. Its use was successfully demonstrated and it may contribute to simplifying treatment process and reducing treatment costs. The effluent of the process met all the regulatory criteria and was discharged into a smaller river.

4. CONCLUSIONS

- (1) By investigating the thermal stability and sorption properties of natural zeolites and these materials converted to various cationic forms, it was concluded that the NH₄⁺ ZT-4 sorbent possesses the highest sorption capacity.
- (2) The increase of temperature of the liquid waste was shown to slightly deteriorate the sorption ability of the sorbents. However, the pH of the liquid waste has almost no influence on their sorption properties.
- (3) The sorption precipitation process was demonstrated to be suitable for the treatment of low level radioactive liquid waste containing higher concentrations of ¹³⁷Cs and ¹³⁴Cs.
- (4) The separation of the solids and solution can be effectively reached by ultrafiltration. In the arrangement, where the ultrafiltration module inlet and outlet are interchanged during the operation, higher average flux can be achieved.
- (5) It is obvious that the process for waste treatment that combines sorption precipitation with ultrafiltration and ion-exchange on zeolite column can be successfully used for the simplification of waste treatment and treatment costs reduction.

REFERENCES

- [1] L.L. AMESJR. Hw-62607. 1959.
- [2] SEHULZ, W.W. et al. Application of inorganic sorbents in actinide separation processes, Actinide separation, p. 17, 1979.
- [3] DOSCH, R.G., The use of titanates in decontamination of defense waste, SAND-78-0710.
- [4] BUCKLEY, L.P., KILLCEY, R.W.E., VIJAYAN, S. and WONG, C.F., Treatment of Groundwater and soil-wash eachate solution containing mixed waste contaminants, In Proceedings of SPECTRUM Hazardous Waste Management International Meeting, Boise, Idaho, August 23–27, 1992.
- [5] LU XIAOFENG, et al., Treating of laboratory radioactive waste water by reverse osmosis, Technology of water treatment, 14(3), 1998.
- [6] Nucl. Eng. Des., 44(3), p.413–420, 1977.
- [7] LU XIAOFENG, et al., Treating the radioactive waste water by UF, RO and EO combination, Technology of water treatment, 19(1), 1993.
- [8] LI KAIJUN, et al., Study on Preprocessing and Membrane Cleaning Methods for Reverse Osmosis, Membrane Science and Technology, 2(3), 1983.

STUDY OF COMBINED PROCESSES FOR THE TREATMENT OF LIQUID RADIOACTIVE WASTE CONTAINING COMPLEXING AGENTS

F. ŠEBESTA, J. JOHN, A. MOTL, K. ROSÍKOVÁ

Czech Technical University in Prague, Department of Nuclear Chemistry,
Prague, Czech Republic

Abstract. The project aimed to develop a process for the removal of organic complexants and/or separation of radionuclides from spent decontamination solutions and evaporator concentrates. Following studies were carried out: 1) Study of options for direct separation of radionuclides from spent decontamination solutions and evaporator concentrates. Performance of a series of inorganic and composite absorbers for radionuclides separation from the AP-CITROX decontamination solutions and evaporator concentrates was investigated. 2) Study and optimisation of the performance of combined processes of organic components degradation and sorption of radionuclides. Organic complexants photodegradation was optimised for the acidic decontamination and electrolytic decontamination wastes. Total degradation of both citric and oxalic acids can be achieved in less than 12 hours. Study of photocatalytic degradation of metal complexes of oxalic and citric acids showed, that degradation of Co-citrate, Fe-citrate, and Fe-oxalate complexes proceeds significantly more rapidly than the degradation of the pure complexants themselves.

1. INTRODUCTION

In advanced technologies for liquid radioactive waste treatment, it is usually mandatory to achieve as high decontamination factors (D_f) as possible, typically $D_f > 10^3$ are required. For fulfilment of such requirements in real aqueous liquid waste, the presence of various chemical species of radionuclides - ionic forms, colloids, complexes, etc. - often plays a very important role. Reaching sufficiently high decontamination factors in single-stage processes, like ion exchange, may often not be possible because of the presence of significant concentrations of non-ionic or complexed species.

The presence of organic substances forming complexes with the radionuclides is one of the most significant and most complicating factors in the treatment of real aqueous liquid wastes. From such media, separation of the radionuclides may be rather difficult. In addition, the presence of organic complexants in solidificates of radioactive wastes may result in elevated leachability and higher mobility of the cationic contaminants. This effect significantly negatively influences the quality of the final solidificates.

In the Czech Republic, liquid radioactive wastes containing organic complexants are produced during decontamination of various equipment at the NPPs with VVER-type reactors. In the final stage, these wastes are cumulated and concentrated in evaporator concentrates, usually together with the borate-containing wastes. New, advanced, and safer technologies for treatment of these types of waste would require to remove both the organic complexants, and the radionuclides. Development of such processes would also facilitate potential future regeneration of boric acid from evaporator concentrates.

Among the many options for removal of the organic complexants from liquid radioactive wastes, photo-oxidation by means of UV-irradiation has been recently extensively studied. In modern processes, its effectiveness is often enhanced by heterogeneous catalysis [1]. The most efficient material used to catalyse the photodegradation of organic materials by means of UV radiation is titanium dioxide - TiO_2 . The same chemical compound - titanium dioxide - is widely used as one of the most efficient inorganic ion-exchangers for a broad scale of radionuclides such as radiostrontium, radiocobalt, and plutonium [2]. Ideal solution of the problem of the removal of organic complexants and radionuclides from liquid waste would

hence be a single-stage combined process, in that the titanium dioxide used would serve both as the photocatalyst, and as a sorbent for the radionuclides released from the complexes.

However, the requirements towards properties of TiO_2 photocatalyst may differ significantly from those towards properties of TiO_2 ion exchanger. Moreover, there are several important radioactive contaminants that do not sorb well on TiO_2 . Therefore, for the treatment of such waste, a two-stage process may be considered in that the photodegradation of organic complexants is combined with successive removal of the radionuclides on optimised PAN-based composite absorbers [3].

Based on these considerations, the main objective of the research performed was to ***Develop and Test Process(es) for Removal of Organic Complexants and/or Separation of Radionuclides from Spent Decontamination Solutions and/or Evaporator Concentrates***. To reach this objective the research was carried out in the following main directions:

- Study of photocatalytic degradation of organic complexants used in decontamination solutions including EDTA, oxalic and citric acids. Study of photocatalytic degradation of complexes of these complexants with metal ions.
- Background study of options for direct separation of radionuclides from model and real solutions, including testing of prospective composite inorganic-organic absorbers with polyacrylonitrile binding matrix. Some of these materials were developed specifically for these purposes.
- Study and optimisation of the performance of combined processes comprising:
 - Photocatalytic degradation of organic complexants combined with sorption of the released metal ions on the TiO_2 photocatalyser-absorber and/or other inorganic absorbers added to the reaction mixture.
 - Photocatalytic degradation of organic complexants combined with subsequent treatment of the filtrated solution by sorption on optimised PAN-based composite absorbers.

The study was performed with both simulants and real liquid waste from NPPs in the Czech or Slovak Republics. Four types of waste were considered throughout the study. They included:

- Acidic spent decontamination solution from the second stage of the AP-CITROX process (further referred to as "KDR solution").
- Liquid waste from electrochemical decontamination (further referred to as "Electrolysate solution").
- Alkaline spent decontamination solution from the first stage of the AP-CITROX process.
- Evaporator concentrates.

The most intense research targeted to the first two types of wastes. The results, as discussed below in detail, demonstrated the advantages and perspectiveness of combined treatment approach for these types of waste.

The alkaline spent decontamination solution from the first stage of the AP-CITROX process (alkaline permanganate solution) does not contain any organic complexants. Therefore, for this waste only a principle possibility of direct separation of some radionuclides was demonstrated. In this study, TiO -PAN composite absorber was demonstrated to be preferable to the NaTiO -PAN one (titanium dioxide or sodium nonatitanate active components, respectively) for strontium separation [4].

Significant efforts were carried out in the treatment of the real evaporator concentrates from the NPP Dukovany, Czech Republic [5]. The studies performed were directed namely to

estimation of the possibility of direct separation of radionuclides from this solution. A comparison of 11 inorganic absorbers showed that for caesium separation simple cobalt or potassium-cobalt hexacyanoferrates displayed the highest K_D values. A series of dynamic column experiments was performed with a new (TiO₂+FC212)-PAN composite absorber containing a mixture of titanium dioxide and potassium-cobalt hexacyanoferrate active components. The possibility to prepare composite absorber containing a mixture of non-interacting active components for simultaneous separation of caesium and strontium was confirmed. For radiocobalt separation, a method combining sorption with magnetic field action was considered. Efforts towards development of novel magnetic absorbers for this purpose were performed [6,7]. Sorption properties of magnetite, as the magnetic component of these absorbers, have been thoroughly investigated to yield background data for the comparison of the performance of the materials with and without the magnetic field [8]. Within this project, it was not possible to finish development of this technique. Therefore, the results are not discussed here in detail.

2. STUDY OF PHOTOCATALYTIC DEGRADATION OF COMPLEXANTS AND COMPLEXES

2.1. Introduction

Photochemical mineralisation of organic materials by UV radiation has been known as a prospective method for waste water treatment⁹. The photodegradation efficiency can be further enhanced by introduction of a heterogeneously dispersed semiconductor photocatalyst into the system [1,9-11]. Several simple oxide and sulfide semiconductors have band gap energies sufficient for catalysing a wide range of chemical reactions. These include TiO₂, ZnO, CdS, WO₃, SnO₂, ZrO₂ and MoO₃. In general, ZnO and TiO₂ have been shown to be most efficient [1,10]. The photocatalytic properties of titanium dioxide semiconductor photocatalysts depend on many various parameters such as crystalline structure (anatase or rutile) or presence of any dopants, and on the method employed in their preparation, that influences namely the porosity and specific surface area of the resulting materials [1].

The aim of this study was to test the efficiency of several titanium dioxide samples for the mineralisation of organic complexants and complexes, the presence of which in radioactive waste makes separation and concentration of the radionuclides from such waste often impossible. The results obtained in this study were presented namely at the 4th and 5th International Symposium and Exhibition on Environmental Contamination in Central and Eastern Europe that took place in Warsaw and Prague in 1998 and 2000 and were published in several papers [12-17].

The irradiation experiments were carried out in a small immersion well photochemical reactor of 80 mL capacity with a 6 W low-pressure mercury lamp (Photochemical Reactors, U.K., models 3210 or 3006 respectively). The suspension was bubbled with air by using a membrane pump, the temperature was maintained by a thermostat. Membrane filtration (pore diameter 0.40 µm) was used for the separation of the photocatalysts from the reaction mixture. Two types of blank experiments were performed. In the first one, degradation of the complexants or complexes was followed in absence of photocatalyst (BE 1). In the second one, the experiments were performed in presence of titanium dioxide but without irradiation (BE 2).

Five different titanium dioxide samples were used as semiconductor photocatalysts. They included TiO₂-M material (prepared at the Department of Nuclear Chemistry of the CTU in Prague from an intermediate in the production of titanium white), Degussa P25 (commonly used standard, DEGUSSA AG, Germany), HTO material (hydrated titanium dioxide

suspension in water prepared by AEA Technology, Harwell Laboratory, UK), and two commercial materials - Pretiox AV-01 and Pretiox RG-14 (Precheza, a.s., Prerov, Czech Republic) that consist of pure anatase with no rutile admixtures or surface modification, or pure rutile (content of the rutile larger than 98.5 %) with its surface modified by aluminium and silicon oxides. All the samples were characterized by Surface Area Analysis (BET LN₂ method), Powder X-Ray Diffraction, Fourier Transform Infrared Spectroscopy, and Scanning Electron Microscopy. The characteristics of the samples are summarized in Table I. It can be seen that the most distinct difference between the samples is represented by their specific surface areas. The admixtures in the AV – 01 and RG – 14 samples result probably from their surface modification while those found in the TiO₂ - M sample come most probably from imperfect washing of the agents used in the production of this material.

TABLE I. CHARACTERISTICS OF THE TiO₂ PHOTOCATALYSTS USED

Catalyst	Specific surface area [m ² /g]	Crystallinity	Particle size	Admixtures
Degussa P 25	49.4	70 % anatase, 30 % rutile	~ 0.5 µm	-
TiO₂ – M	247.3	100 % anatase	1 µm	Al, S
HTO	174.0*	amorphous	-	-
AV – 01	8.6	100 % anatase	1 µm	Al, K
RG – 14	18.3	100 % rutile	1 µm	Al, Si

* determined for vacuum dried (at room temperature) sample crushed approximately to the original grain size

2.2. Photocatalytic degradation of EDTA and oxalic or citric acids

Since the information on photocatalytic degradation of EDTA and oxalic or citric acids in literature is rather scarce [18-20], a thorough study aimed at the investigation of the conditions and mechanism of their photodegradation was carried out. The TiO₂-M photocatalyst was used throughout this study.

The mechanistic study revealed [14] that all the three complexants can be effectively degraded in the studied system. In agreement with the general literature data [1], the kinetics of the photodegradation process was confirmed to be of the first order for all the three complexants.

Surprisingly, the rate of the degradation was found to be temperature-dependent. The experimental data obtained allowed calculation of the apparent activation energy E_A of the photomineralization process. Its values for HOx, HCit or EDTA were found to be as low as $E_A = 18.1, 15.8$ or 14.8 kJ/mole, respectively. These values unambiguously indicate that the rate-determining step of the process are transport phenomena.

Experiments performed to establish the influence of different amount of the photocatalyst revealed that the proportion of HOx, HCit and EDTA degraded increases rapidly with the increasing amount of TiO₂ in the reaction mixture. However, the blank experiments performed revealed that for the case of EDTA significant part of this degradation is only apparent. The decrease of EDTA concentration in the solution was namely ascribed to its sorption onto the surface of the photocatalyst. This was confirmed in parallel experiments performed with the TiO₂-M and Degussa P25 photocatalysts that differ above all by their specific areas (247.3 and 49.4 m²/g, respectively). In the blank experiments performed with the suspension of 1 g of titanium dioxide in 80 mL of 0.005M EDTA, its apparent decomposition was about 7 times lower for the Degussa P25 catalyst than for the TiO₂-M one, which is in a good agreement with the ratio of their specific surface areas.

The effect of pH on the photocatalytic activity of different samples of TiO_2 was studied because the pH of pure solutions of oxalic or citric acids is rather low, which is not ideal for the prospective removal of ions from the solution by sorption on the TiO_2 photocatalyst/absorber. Also, some literature data²¹ indicate rather strong dependence of the photocatalytic activity of the TiO_2 photocatalysts on pH.

The results show (see Fig. 1) that the photocatalytic activity of TiO_2 -M for HOx and HCit degradation increases with increasing pH up to pH ~ 3 . At neutral and alkaline pH, the degradation is generally rather low. The results obtained for the EDTA differed from the above data again by the blank experiments results. While all the blanks were negligible in the experiments with HOx and HCit, the value of the blank experiment performed under irradiation but without addition of titanium dioxide was found to increase significantly with increasing pH. These results could have been explained by correlating the blank experiments values with the dependence of the abundance of EDTA species on pH. It was concluded that the dissociated ions HY^{3-} , Y^{4-} and NaY^{3-} are highly photolabile, while the lower charged EDTA species are, in absence of titanium dioxide, rather photoresistant.

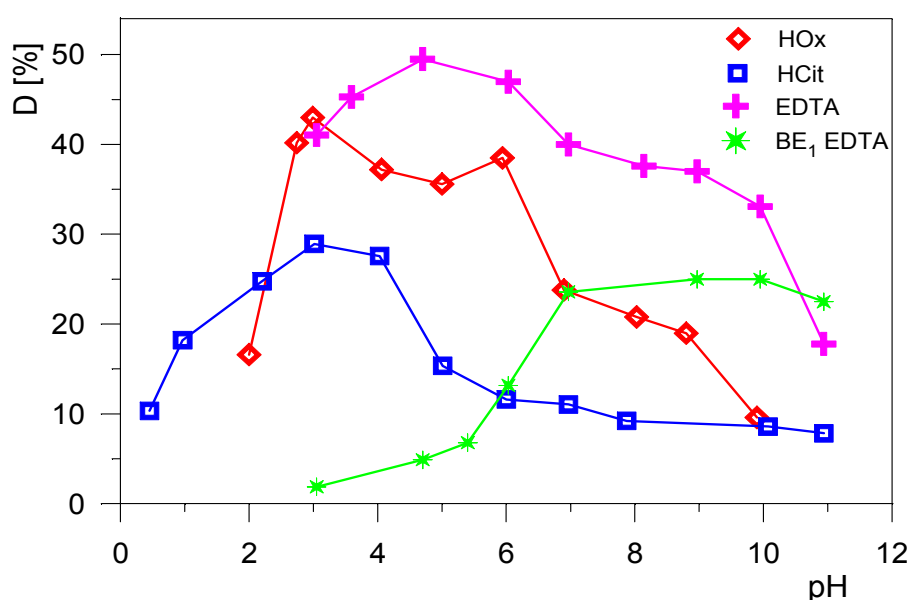


Fig. 1 Decomposition (D) of HOx, HCit and EDTA and the value of blank experiment for EDTA (BE₁, decomposition in absence of TiO_2) as a function of pH (0.01 M HOx, 0.005M HCit, or 0.005M EDTA, $t_{\text{irr}} = 1, 2$, or 2 hrs, respectively, 1.25 g TiO_2 -M/l, $t = 25^\circ\text{C}$, $v_{\text{air}} = 25 \text{ l/hr}$)

Additional experiments allowed to ascribe the decrease of the photocatalytic activity of the TiO_2 -M catalyst towards all the complexants at pH higher than pH ~ 4 –6 to suppression of one of the main degradation mechanisms – direct oxidation of the substrates sorbed onto the surface of the photocatalyst. At pH higher than the value of the isoelectric point of the photocatalyst, the surface of the material bears a negative charge and hence cannot sorb the negatively charged ions of dissociated complexants.

The experiments performed in systems saturated with nitrogen instead of air confirmed the important role of oxygen in the photo-degradation processes. In the absence of oxygen, the degradation rates of oxalic acid are approximately one half of those found for the same systems saturated with air. For HCit and EDTA, the influence of absence of the oxygen was even more pronounced – the degradation rates in nitrogen saturated systems have not exceeded one third or one quarter, respectively, of those achieved in oxygen saturated

systems. This different behaviour of the individual complexants has been ascribed to different contribution of various reaction mechanisms to the resulting degradation.

In the presence of H_2O_2 in the system, significant increase of EDTA degradation was observed. However, when performing the blank experiments, it turned out that virtually all the degradation observed is due to the presence of the H_2O_2 in the system. The role of the catalytic action of TiO_2 in such combined systems was found to be negligible.

2.3. Photocatalytic degradation of metal complexes

The results presented above demonstrated that both the EDTA and oxalic or citric acids may be degraded with a high yield in a photocatalytic process. However, degradation of metal complexes may be significantly different. Therefore, such a study has been initiated. As model systems for this study, degradation of cobalt(II) and chromium(III) complexes with EDTA or cobalt(II) and ferric complexes with citric or oxalic acids, that were of direct interest for this project, has been selected. The results obtained for the citric or oxalic acids complexes were presented at Prague 2000 symposium [16], a comparison of the degradation of the complexes and free complexants is discussed in another paper [17].

As a background study, behaviour of Co^{2+} or Cr^{3+} under photocatalytic conditions was investigated. Significant sorption of both cobalt or chromium on the TiO_2 -M photocatalyst was observed in the BE 2 blank experiments (with TiO_2 , without irradiation) at $\text{pH} > 5.5$ or $\text{pH} > 5$, respectively. At higher pH, precipitation of the ions was observed. Under the irradiation in the presence of the photocatalyst, no significant enhancement of the deposition or sorption suppression of either cobalt or chromium on TiO_2 was observed when compared with the respective blank experiment (BE 2).

Photocatalytic degradation of complexes of EDTA with Co(II) was studied for EDTA and CoCl_2 concentration 0.005 mole/L in the pH range $\text{pH} \sim 3 - 11$. The degradation of organic compounds in this system was found to be very low (4 - 10 % over 1 hr of illumination) when compared with EDTA degradation. Another difference is that the degradation of the EDTA - Co complex decreases with increasing pH. This result correlates well with the earlier finding that the most photosensitive are the free dissociated EDTA ions (see above), the concentration of which is obviously very low in complexed systems and decreases with increasing pH. Regardless of the pH of the solutions studied, the concentration of cobalt decreased by approximately 12 - 15 % during all the photodegradation experiments.

Photocatalytic degradation of complexes of EDTA with Cr(III) was performed in excess of EDTA (the solution of 0.0075 mole/L EDTA and 0.00125 mole/L CrCl_3 was used). The pH range tested was the same as for the experiments with Co(II) ions. The results obtained were also similar to those obtained for the EDTA - Co complexes. The degradation of EDTA - Cr complex was generally low (2 - 8 %) and decreased with increasing pH. Taking in account the 6-fold excess of EDTA over Cr^{3+} ions, this finding is unexpected. The suggested explanation for this effect is an inhibitive influence of chromium to the photocatalytic activity of TiO_2 .

Photocatalytic degradation of complexes of HCit with Co(II) was studied in the pH range $\text{pH} \sim 2 - 12$ (initial pH), the corresponding pH values at the end of the experiment ranged from 2 to 9. In Fig. 2, the results obtained are compared with the degradation of pure HCit. The most striking difference of the curves is the increased efficiency of photocatalytic degradation of HCit in the presence of cobalt ions. Similarity to the experiments with pure Co solutions, significant deposition of cobalt onto the photocatalyst was observed at $\text{pH} > \sim 5$ (at $\text{pH} \sim 9$ more than 60 % of cobalt was removed from the solution during irradiation).

Photocatalytic degradation of complexes of HOx or HCit with Fe(III) yielded data similar to those obtained for the of HCit - Co complexes. At any pH value, the degradation of both HCit and HOx in the presence of ferric ions is several times more efficient than that of the pure complexants. Similarly to cobalt, significant deposition of iron from the HCit - Fe(III) system onto the TiO₂ photocatalyst was found in neutral and alkaline pH range (80 to 85 % of the amount of iron originally present in the solution was removed during the irradiation).

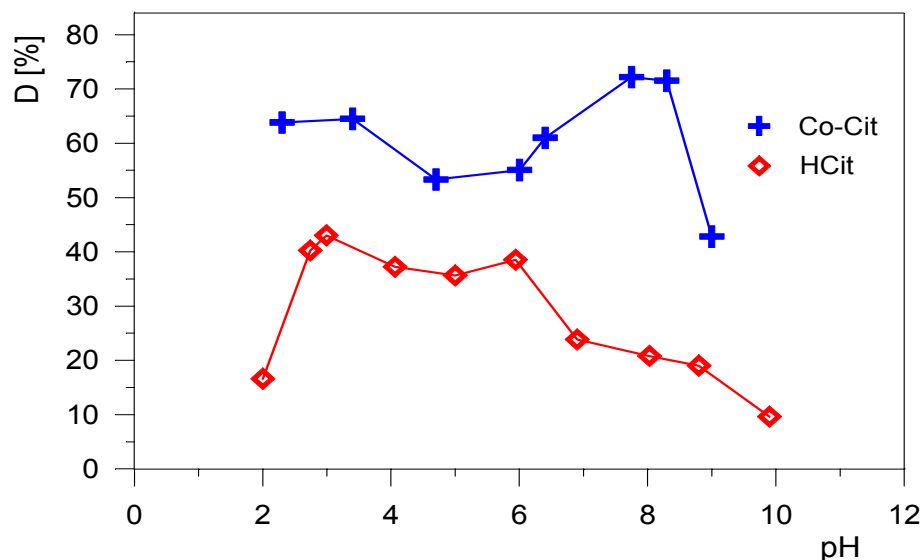


Fig. 2. Degradation of citric acid (HCit) and HCit-Co(II) complexes (D) in the presence of TiO₂-M photocatalyst as a function of pH at the end of the experiment. (0.005M HCit or 0.005M HCit + 0.005M Co(NO₃)₂, $t_{irrad} = 1$ hr, 1.25 g/L TiO₂-M, $t = 25^{\circ}\text{C}$, $v_{air} = 20$ L/hr)

When comparing the photodegradation of EDTA - Co(II) complexes with that of both ferric and cobalt complexes with HCit or HOx, a significant difference can be seen. While the presence of metal ions strongly suppresses the EDTA degradation, the degradation of HCit or HOx in such systems is much more efficient than in their pure solutions. A potential explanation of these effects may be connected with the chemical and photostability of the respective complexes. The highly chemically stable EDTA complexes, the proportion of which increases with increasing pH, seem to be also rather photostable which is corroborated by the decrease of their photodegradation with increasing pH. On the other hand, the increase of photodegradation of HCit and HOx in the presence of Fe(III) or Co(II) may result from metal deposition onto the surface of the photocatalyst. This process is known to result in photocatalyst properties modification^{19,22}, sometimes leading to their activation. In this case, the metals are most probably deposited from their free ionic forms, the proportion of which is much higher in weaker complexing HOx or HCit solution than in the EDTA solutions, rather than from the complexes photodegradation.

2.4. Comparison of the Photocatalytic Activities of TiO₂ of Various Origin

The photomineralization rates of HOx, HCit and EDTA in their pure solutions on various photocatalysts were studied at the natural pH of the solution used (pH = 2, 2.7, or 4.7, respectively) and at pH = 7 and 10. The results obtained were presented at Warsaw 2000 symposium¹⁴. The main general conclusion, that could be drawn from these results, is that the activity of the photocatalysts is not directly proportional to their specific surface area.

When comparing the photodegradation of the individual complexants on various photocatalysts, the following conclusions can be done:

- The activity of AV-01 and RG-14 photocatalysts is generally low.
- The order of the activity of the three more active photocatalysts is different at different values of pH for any of the materials.
- The order of their photocatalytic activity towards the complexants differs at different values of pH.
- The activity of the HTO materials is the most dependent on the value of pH. For the HOx and HCit degradation, its activity at low pH is very high, while it is very low at neutral and alkaline pH range. Its activity towards EDTA degradation is low at any pH.
- The only complexant that can be efficiently photodegraded even at higher pH values is EDTA, the most effective photocatalyst for its degradation is Degussa P25.
- The activity of the Degussa P25 material towards HCit degradation is rather low, even though it is the most active material for the HOx and EDTA degradation at any pH.
- In average, the most consistent properties towards photodegradation of any of the complexants at any pH value displays the $\text{TiO}_2\text{-M}$ material.

In the next step, the photodegradation of metal complexes with various titanium dioxide samples was compared. For the *EDTA - Co* or *EDTA - Cr* complexes, the degradation of EDTA was low with any of the studied materials. Moreover, the order of activities of the photocatalysts is completely inconsistent with their order for the pure EDTA degradation.

For the *HCit - Co* complexes^{16,17}, the comparison of different types of photocatalysts was performed at two different pH values – pH ~ 2 and pH ~ 7. The results obtained are shown in Fig. 3. From these data, it can be seen that at pH ~ 2 the efficiency of photodegradation depends strongly on the type of photocatalyst. Contrary to this, the activity of most of the photocatalysts in neutral pH range is low (only some 15 – 20 % of HCit degraded during 2 hours of irradiation). The only exception to this rule is the $\text{TiO}_2\text{-M}$ photocatalyst, the activity of which is not influenced by pH of the solution. The order of activities of the photocatalysts is again completely inconsistent with their order for the pure HCit degradation.

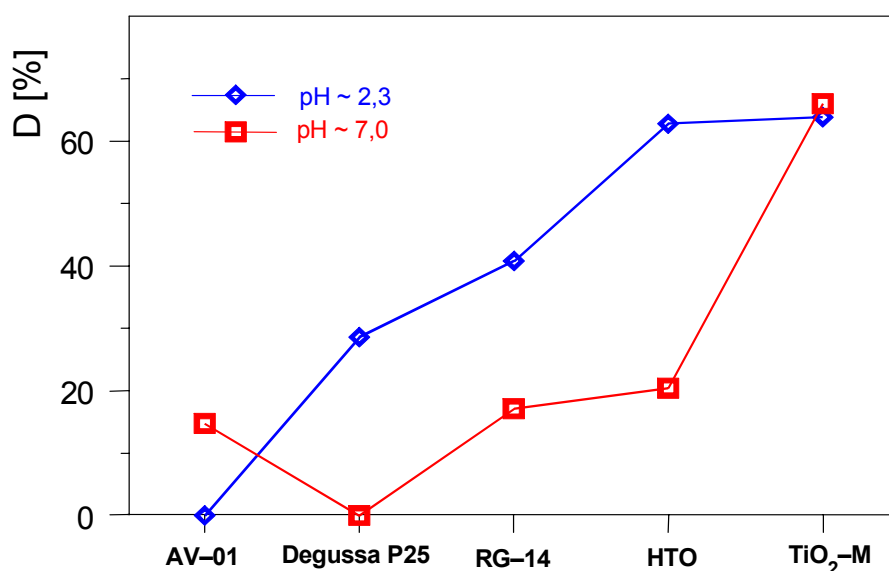


Fig. 3 Degradation of HCit-Co complexes in the presence of various photocatalyst at two different pH
(0.005M HCit + 0.005M $\text{Co}(\text{NO}_3)_2$, $t_{\text{ir}} = 2$ hrs, 1.25 g/L $\text{TiO}_2\text{-M}$, $t = 22^\circ\text{C}$, $v_{\text{air}} = 20$ L/hr)

For the *HCit - Fe* or *HOx - Fe complexes*^{16,17}, the efficiency of the two of the most effective photocatalysts – TiO₂-M and Degussa P25 – was compared in neutral and acidic region. Because of Fe(OH)₃ precipitation, the system HOx – Fe(III) could have been studied in the acidic region, only. No significant difference between the two materials could be seen for any of the systems at any conditions.

3. DIRECT SEPARATION OF RADIONUCLIDES FROM THE SPENT DECONTAMINATION SOLUTIONS

3.1. Introduction

This study was performed to yield background data on the possibility of direct separation of radionuclides from spent decontamination solutions and on the performance of prospective inorganic ion exchangers or composite inorganic-organic absorbers with polyacrylonitrile binding matrix. Some of these materials were developed specifically for these purposes. Parts of the results obtained were presented at the NRC 5 or SIS'01 symposia [23,24], the data has been summarised in a paper contributed to the 14th Radiochemical Conference [25].

The study was performed with both two types of waste. They included ed:

- *Acidic spent decontamination solution from the second stage of the AP-CITROX process (further referred to as "KDR solution").*

This solution represented a real spent decontamination solution generated in the decontamination process of steam generators and main circulating pumps at NPP Dukovany (Czech Republic). It contained 10 g/L of HCit and 8.2 g/L of HOx, the main radionuclidic contaminants were ^{110m}Ag, ⁶⁰Co, ⁵⁸Co, ¹²⁴Sb, ⁵⁹Fe and ⁵⁴Mn.

- *Liquid waste from electrochemical decontamination (further referred to as "Electrolysate solution").*

The model electrolysate solution simulated the solution generated in the „in situ“ electrolytic decontamination of steam generators and main circulating pumps at the NPP Dukovany. Its approximate composition was: 0.029M HOx, 0.017M HCit, 0.014M Fe³⁺, 3.7.10⁻³M Ni²⁺, and 1.8.10⁻³M Cr³⁺. This simulant was prepared in a laboratory electrolyser with the electrodes made of the same stainless steel as used in the primary circuit of VVER type NPPs (STN 41 7241 standard). The same conditions as in the operational electrochemical decontamination were used (current density 130 mA/cm² of the anode surface, total charge per volume unit of electrolyte 44 C/mL and the ratio between the volume of electrolyte and the decontaminated area ~ 31.5 mL/cm²). The initial composition of the fresh electrolyte was 10 g/L of the oxalic and 5 g/L of the citric acids, during the electrolysis, some 60 % or 25 % of which were degraded, respectively. The resulting solution is highly unstable in time, formation of a precipitate starts to take place after few hours since the end of electrolysis and cooling the solution down. For the experiments, the solution was labelled with ^{110m}Ag, ⁶⁰Co, ⁵⁹Fe, ⁵⁴Mn and ⁸⁵Sr.

The performance of a set of inorganic ion-exchangers - prospective active components of composite absorbers - for direct separation of radionuclides from the spent solution was studied. Zirconium phosphate (ZrP), sodium titanate (NaTiO), synthetic zeolite (Na-Y) and mordenite (M 315), iron sulphide (FeS), crystalline polyantimonic acid (CSbA), sodium-nickel hexacyanoferrate (FC 301), zirconium oxide (ZrO), and titanium dioxide (TiO) were selected for this study. These materials were tested in batch experiments at various values of pH. Their chemical stability was evaluated and distribution coefficients (K_D) of the main radionuclides were determined in experiments performed at volume of solution to mass of the absorber ratio V/m = 500 mL/g, 20 hrs of contact time and separation of phases by

centrifugation (10 minutes at 3.000 rpm) was used. Any pH adjustments to the samples were done 15 hours prior the start of the sorption experiments with use of 10M NaOH.

In the dynamic sorption experiments, performance of inorganic-organic composite absorbers, prepared from the inorganic ion-exchangers that performed the best in batch experiments, was tested and compared with standard OSTION KS806 cation exchanger (Spolchemie, Czech Republic). The experiments were performed in SUPELCO Rezorian Cartridges equipped with polyethylene frits both at the bottom and the top of the bed of the absorber (ID ~ 0.86 cm, bed volume BV = 1.2 ml), the downward direction of the feed flow was used. The percentage break-through of the radionuclides in single fractions of the effluents was then calculated and plotted vs. the volume of treated solution expressed in the units of bed volumes of the absorbers (BV).

3.2. Separation of Radionuclides from KDR solution

The results of the *batch experiments* are summarised in Table II. From these data, it can be seen that chemical stability of several of the absorbers tested was insufficient, namely at lower values of pH. At pH ~ 1.3 (original pH of the real solution) ZrP and NaTiO materials completely, and the FeS one partially dissolved. The zirconium phosphate dissolved completely even at pH ~ 3.5. Only at pH ~ 7, all the absorbers tested were chemically stable.

Generally, the highest K_D values and the best conditions for the group separation of the radionuclides of interest were found at pH ~ 1.3. In this case the most prospective is the nickel hexacyanoferrate, followed by ferrous sulphide and synthetic zeolite or mordenite. At neutral pH, the sodium titanate absorber exhibited by far the best sorption properties, while the worst conditions for the separation were at pH ~ 3.5.

A series of *dynamic column experiments* was performed with FC301-PAN, FeS-PAN, or NaY-PAN composite absorber prepared from the respective active components. The original solution with non-adjusted pH was used. Significant break-through of all the radionuclides was observed since the early stages of the experiments with all these materials. The main limiting factor for the direct separation of radionuclides from spent decontamination solution was found to be the insufficient chemical stability of the active components of the composite absorbers tested.

In comparative experiments performed with the OSTION KS806 cation exchanger, the initial break-through of most of the radionuclides was relatively low. However, the break-through occurred so early that it disqualifies even this strongly acidic cation exchanger for direct separation of the radionuclides from the KDR solution.

3.3. Separation of Radionuclides from Electrolysate Solution

The results of the *batch experiments* carried out with the original non-pH-adjusted (pH = 1.75) electrolysate solution and the same solution with its pH value adjusted to pH = 4.37 are summarised in Table III. In the table, the absorbers are sorted following their "performance index", defined as the mean value of logarithms of K_D values for the major radionuclidic contaminants of the real waste (^{54}Mn , ^{59}Fe , ^{60}Co , $^{110\text{m}}\text{Ag}$), at the original pH.

From these results, and their comparison with the data obtained for the KDR solution, several main conclusions follow:

- Contrary to the KDR solution, the chemical stability of the absorbers is relatively good.

TABLE II. K_D VALUES OF VARIOUS RADIONUCLIDES FROM KDR SOLUTION (V/M = 500, 20 HOURS OF CONTACT, SEPARATION OF PHASES BY CENTRIFUGATION FOR 10 MIN; INITIAL PH VALUES 1.37, 3.58 OR 7.08, RESPECTIVELY)

Sorbent	Stability	pH*	K_D					
			^{54}Mn	^{124}Sb	^{59}Fe	^{60}Co	^{58}Co	$^{110\text{m}}\text{Ag}$
ZrP	A	1.36	<i>absorber dissolves</i>					
	A	3.67	<i>absorber dissolves</i>					
	C	7.09	187	6.1	6.2	0.1	< 1	3980
NaTiO	A	1.34	<i>absorber dissolves</i>					
	C	3.88	17	< 1	< 1	< 1	< 1	10058
	C	8.15	955	1209	41	2208	2205	5613
Na-Y	C	1.39	78	80	242	597	97	2117
	C	3.84	< 1	2.1	< 1	< 1	< 1	$> 4.4 \cdot 10^5$
	C	7.43	1.4	11	< 1	< 1	2.1	434
M 315	C	1.36	82	56	266	605	99	1695
	C	3.60	< 1	< 1	< 1	< 1	< 1	1546
	C	7.40	< 1	< 1	9.0	< 1	< 1	$> 4.5 \cdot 10^5$
FeS	B	1.30	70	67	1192	641	89	$> 6.9 \cdot 10^5$
	C	3.88	< 1	< 1	< 1	< 1	< 1	4988
	C	7.50	52	77	122	19	18	$> 4.5 \cdot 10^5$
CSbA	C	1.34	266	3.1	61	67	61	$> 6.9 \cdot 10^5$
	C	3.52	33	< 1	< 1	< 1	< 1	6409
	C	6.44	93	20	5.1	2.1	4.6	12987
FC 301	C	1.35	158	67	906	1760	642	$> 6.9 \cdot 10^5$
	C	3.57	211	< 1	< 1	394	394	$> 4.3 \cdot 10^5$
	C	7.46	42	< 1	60	100	98	$> 4.8 \cdot 10^5$
ZrO	C	1.35	184	3.8	44	176	170	$> 6.9 \cdot 10^5$
	C	3.63	< 1	< 1	< 1	< 1	< 1	2859
	C	8.15	142	553	5.4	37	39	2690
TiO	C	1.35	50	1.0	33	43	8.5	$> 6.9 \cdot 10^5$
	C	3.57	< 1	< 1	< 1	< 1	< 1	$> 4.3 \cdot 10^5$
	C	7.08	186	979	68	14	7.5	$> 4.8 \cdot 10^5$

A – absorber dissolves

B – absorber partially dissolves

C – no dissolution observed

* - pH measured at the end of contact

- The K_D values measured are generally low, the only interesting value is that obtained for strontium and the CSbA absorber in the solution with non-adjusted pH (initial pH = 1.75) – $K_D = 2.4 \cdot 10^5$ obtained even in the presence of organic complexants is extraordinarily high.
- In the solutions with pH adjusted to pH = 4.37, iron precipitation occurs in some cases.
- As confirmed by blank experiments, significant amounts of $^{110\text{m}}\text{Ag}$ are lost from the system by non-specific sorption. This effect is negligible for all the other radionuclides.

Taking in account the fact that the K_D values measured were even lower than those found for the KDR solution, where the direct separation of the radionuclides was unsuccessful, no *dynamic experiments* with inorganic-organic composite absorbers were performed. Two experiments with the OSTION KS806 cation exchanger were run with the original

non-pH-adjusted (pH = 1.75) solution or a solution with its pH value adjusted to pH = 4.37. As an example, the break-through curve measured the original solution is shown in Fig. 4. As can be seen, ^{59}Fe did break through since the start of the experiment, the other radionuclides did also break through rather soon. Similar results were obtained for the solution with its pH adjusted to pH = 4.37.

A general conclusion that can be drawn from this data is that the results obtained in the earlier experiments with the KDR solution were fully confirmed. Direct separation of cations from the electrolyte solution onto an ion-exchanger, composite absorber, or cation resin is not possible.

TABLE III. K_D VALUES OF RADIONUCLIDES OF INTEREST FROM ELECTROLYSATE SOLUTION NOT TREATED BY PHOTOCATALYTIC DEGRADATION OF ORGANIC COMPLEXANTS (V/m = 500 ml/g, 20 HOURS OF CONTACT, INITIAL pH = 1.75, SEPARATION OF PHASES BY CENTRIFUGATION FOR 10 MIN).

Absorber	pH**	Absorber Stability	Iron Precipit.	K_D [ml/g]					Mean $\log(K_D)^*$
				^{54}Mn	^{59}Fe	^{60}Co	$^{110\text{m}}\text{Ag}$	^{85}Sr	
CSbA	2.48	A	–	1415	44	83	74441	244500	2.90
	4.11	A	–	480	13	49	< 49	11565	1.79
TiO	2.65	A	–	31	28	78	889	285	1.94
	4.37	A	–	63	13	16	< 49	837	1.45
NiFC	3.01	A	–	< 6	22	38	9659	52	1.92
	4.40	A	–	111	< 11	159	< 49	39	1.74
ZrO	3.22	A	–	36	< 16	52	1331	2118	1.90
	4.58	A	–	47	< 11	10	< 49	1406	1.35
ZrP	3.47	B	–	29	< 16	17	3245	115	1.85
	4.55	A	–	2309	< 11	64	< 49	2420	1.97
Mordenite	2.98	A	–	< 6	< 16	10	12996	12	1.77
	4.44	A	–	12	< 11	< 5	< 49	382	1.13
NaTiO	3.97	A	–	21	< 16	28	1042	320	1.75
	4.71	A	–	657	22	34	< 49	2774	1.85
FeS	3.03	A	–	< 6	< 16	< 8	2394	12	1.56
	4.53	A	?	24	19	26	< 49	52	1.44
Na-Y	3.99	A	–	< 6	< 16	< 8	67	< 6	1.18
	4.81	A	+	< 7	< 11	< 5	< 49	352	1.08

* – without the ^{85}Sr value

** – pH measured at the end of contact

A – no dissolution observed

B – absorber partially dissolves

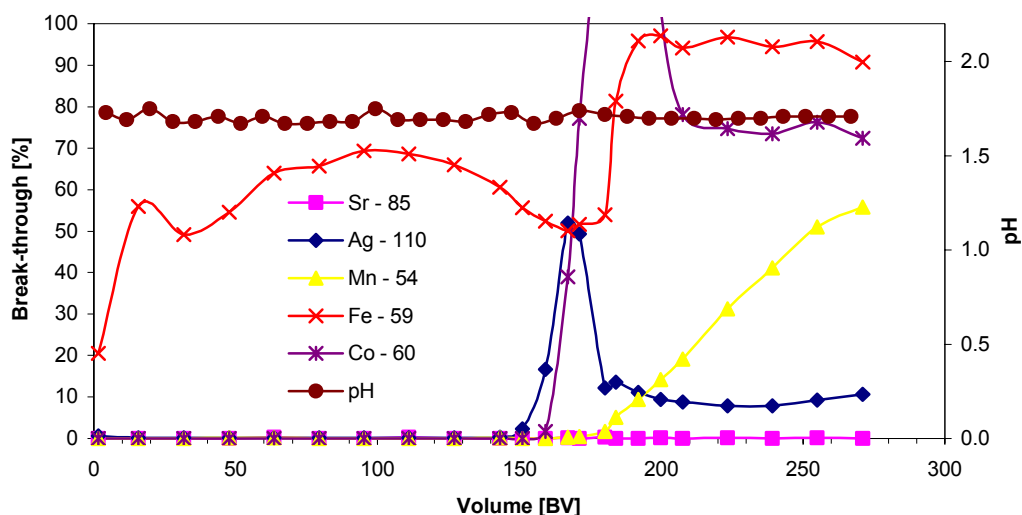


Fig. 4 Break-through curves of selected radionuclides through a column of OSTION KS806 cation exchanger from the electrolysate solution ($pH = 1.75$) and the dependence of pH of the effluent on the volume of the treated solution ($BV = 1.2$ ml, absorber grain size 0.08 - 0.16 mm, flow rate 5.9 BV/hr)

4. DEVELOPMENT OF A PROCESS COMBINING PHOTOCATALYTIC DEGRADATION OF THE ORGANIC COMPLEXANTS WITH CONCURRENT OR SUBSEQUENT SORPTION OF THE RADIONUCLIDES ON THE TiO_2 PHOTOCATALYST / ABSORBER

4.1. Optimisation of the conditions of photocatalytic degradation of the complexants in spent decontamination solutions

The aim of this work was to achieve quantitative degradation of the complexants. Preliminary experiments revealed that, in standard conditions, the degradation of HOx and HCit in their more concentrated solutions proceeds slowly. Among the most interesting results of these experiments, the possibility to increase the photocatalytic activity of the TiO_2 by partially converting it to peroxotitanates, should be listed (in a 4-hours irradiation experiment, the amount of the HOx degraded was more than doubled). Therefore, additions of hydrogen peroxide were included among the parameters during the conditions optimisation.

In the optimisation, the individual experimental parameters – aeration rate (v_{air}), amount of the photocatalyst, temperature, and presence of hydrogen peroxide – were varied on the basis of the knowledge of their impact on the overall photodegradation rate, as gained in the above discussed study of the degradation of organic complexants. The experimental techniques used were the same as described in the chapter 2.1. Parts of the results obtained were presented at the NRC 5 or SIS'01 symposia [23,24], all the data has been summarised in a paper contributed to the Prague 2000 conference [16].

4.1.1. KDR solution

A series of tests was run for the KDR solution. The four sets of experimental conditions tested were as follows:

Conditions	Photocatalyst	Temperature	Aeration Rate	H_2O_2
"Standard"	1.25 g TiO_2 -M/L	$T = 22^{\circ}C$	$v_{air} = 25$ L/hr	–
"High m+T"	3.15 g TiO_2 -M/L	$T = 45^{\circ}C$	$v_{air} = 50$ L/hr	–

"No TiO ₂ "	no TiO ₂ added	T = 45 ⁰ C	v _{air} = 50 L/hr	1 mL each 2 hours
"Peroxide"	3.15 g TiO ₂ -M/L	T = 45 ⁰ C	v _{air} = 50 L/hr	1 mL each 2 hours

The "No TiO₂" conditions correspond to homogeneous photocatalysis with H₂O₂. The results obtained for the HCit or HOx degradations are shown in Figs. 5 and 6. From the results gained, it can be seen that, under the optimum ("Peroxide") conditions, all the oxalic and citric acids can be quantitatively degraded within 12 hours. It can also be seen that in the "Modified" and Optimum" conditions, the photodegradation proceeds in two steps - in the initial phase, only HOx is degraded, and only when its concentration significantly decreases, the HCit degradation starts to proceed. Another experiment confirmed that quantitative degradation of both the complexants can be achieved even in the "modified" conditions (no H₂O₂ addition). However, 28 hours are needed to accomplish the degradation.

Using the optimised procedure, organic complexants in several batches of the real spent KDR solution from NPP Dukovany were quantitatively photodegraded. The resulting solution was then used for the study of radionuclides separation onto a set of prospective inorganic sorbents (see below).

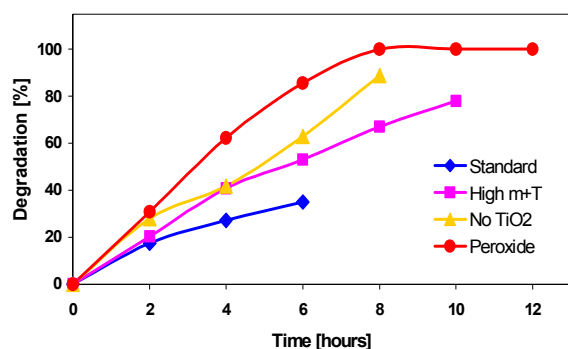


Fig. 5 Degradation of oxalic acid in the KDR simulant solution in various conditions as a function of the time of irradiation
(For conditions definitions see text)

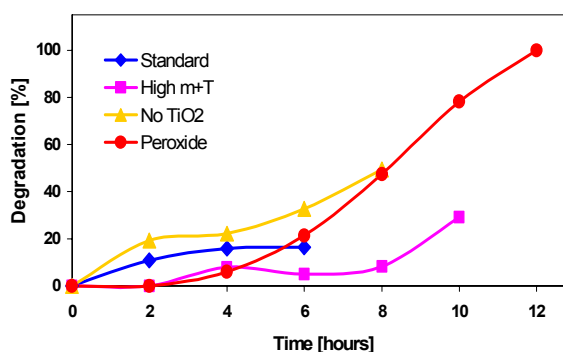


Fig. 6 Degradation of citric acid in the KDR simulant solution in various conditions as a function of the time of irradiation
(For conditions definitions see text)

4.1.2. Electrolysate solution

A similar set of experiments was carried out with a simulant of the spent electrochemical decontamination process solution. The preliminary experiments performed revealed problems caused by plugging the frit of the photoreactor at elevated temperatures. Therefore, in all the testing conditions defined above, the temperature was kept at the standard value of 22⁰C (the respective modified conditions were labelled as "High m" or "Peroxide", respectively). From the results gained (see Figs. 7 and 8) and their comparison with the data for the KDR solution, it can be seen that, namely in its initial stages, the degradation of the electrolyte solution is significantly faster than that of the KDR solution. This difference might be potentially associated with the modification of the TiO₂ photocatalyst properties with iron, since some 80 % of the iron present in the electrolyte are deposited onto the catalysts in the early stages of the process which results in loading the catalyst with more than 200 mg of iron per gram of TiO₂. Some 10 hours of irradiation are needed to quantitatively degrade both the oxalic and citric acids in the electrolyte solution.

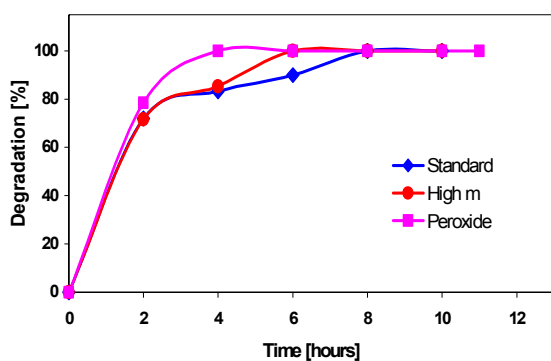


Fig. 7 Degradation of oxalic acid in the electrolyte solution in various conditions as a function of the time of irradiation
(For conditions definitions see text)

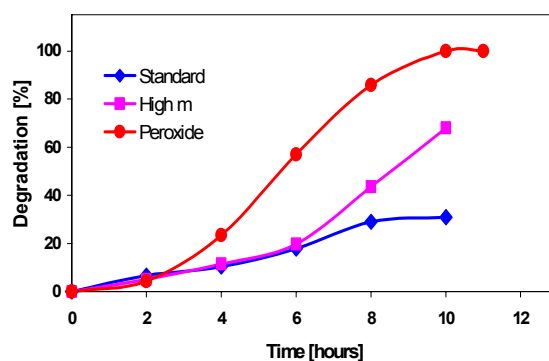


Fig. 8 Degradation of citric acid in the electrolyte solution in various conditions as a function of the time of irradiation
(For conditions definitions see text)

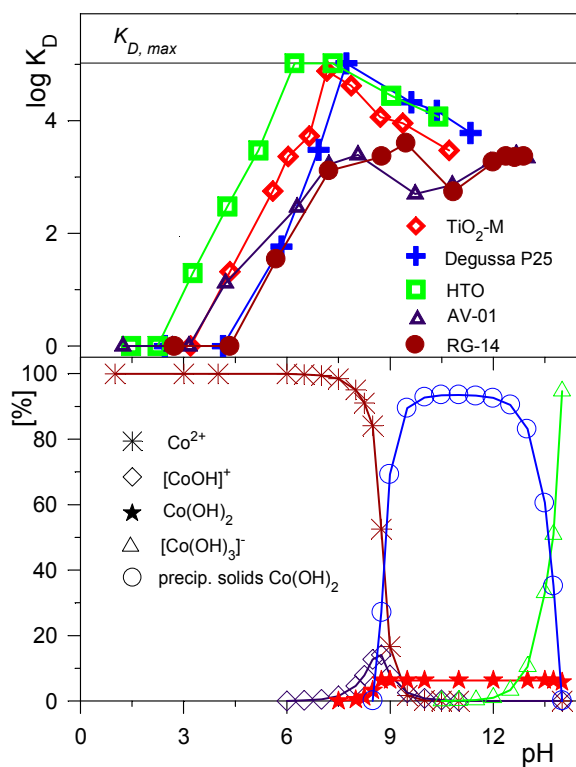


Fig. 9 Dependence of the distribution coefficient K_D of cobalt ions and of the abundance of cobalt ion species on pH
($0.1M Na^+$, $c_{Sr} = 10^{-5}$ mole/l,
 $V/m = 100$ ml/g, 20 hours of contact)

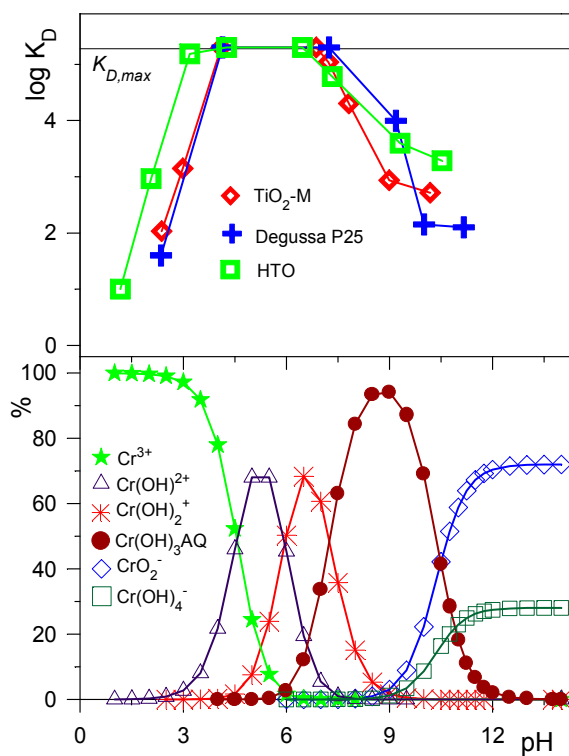


Fig. 10 Dependence of the distribution coefficient K_D of chromic ions and of the abundance of chromic ion species on pH
($0.1M Na^+$, $c_{Cr} = 10^{-5}$ mole/l,
 $V/m = 100$ ml/g, 20 hours of contact)

Using the optimised "Mixed-H₂O₂" procedure, HOx and HCit was quantitatively photodegraded in four batches (per 90 ml) of the electrolysate solution, thus preparing the solution for the determination of the distribution coefficients of the radionuclides of interest onto a set of prospective inorganic sorbents. Later, 800 ml of such solution was successfully prepared for the dynamic column sorption experiments.

4.2. Study of Sorption Properties of Various Titanium Dioxide Materials

4.2.1. Introduction

This study was aimed mainly at the estimation of the performance of the second stage of the studied combined process – sorption of radionuclides and metal ions from the solution after photocatalytic degradation of the organic complexants onto various TiO₂ photocatalyst / absorbers. An option of pH adjustment of the solution after the photodegradation and prior the sorption removal of the released metal ions. To reach these aims, dependences of the metal ions distribution coefficients on pH have been determined for all the TiO₂ materials, earlier studied as photocatalysts. The results have been correlated with the metal ions speciation. As examples of typical radionuclidic contaminants present in decontamination solutions or evaporator concentrates strontium, cobalt, mercury, and chrome (both chromic ions and chromate) were selected. The detailed results of this study were published in the proceedings of the 13th Radiochemical Conference [26].

Hydrated titanium dioxide is one of the "classical" inorganic ion-exchanger [27]. In alkaline solutions, it acts as a cation exchanger, while in acidic solutions, it behaves as an anion exchanger. Therefore, the isoelectric point (or point of zero charge) of the TiO₂ sorbents is one of their important characteristics. For various materials, it may range [28,29] from pH ~ 1 to pH ~ 6. Generally, sorption properties of hydrated titanium dioxide depend on many factors, not all of which are known in sufficient detail.

The distribution coefficients (K_D) were determined in batch experiments. As absorbers, all the five photocatalysts described in chapter 2.1 above were used. Prior the K_D determination, the "titration curves" were constructed. Each of the materials was contacted with a set of solutions with Na⁺ concentration equal to 0.1 mole/L and varying concentrations of NaOH or HNO₃. Volume of solution to mass of the absorber ratio $V/m = 100$ mL/g and time of contact 43 hours were used. For the K_D determination, solution mixtures (0.1M Na⁺) were selected for each of the absorbers from its respective titration curve so as to cover pH range from 0.1M HNO₃ to 0.1 M NaOH in nearly equidistant way. The absorbers were contacted with the solutions at $V/m = 100$ mL/g for 23 hours, then, the labelled stock solution of the metal ion under study was added to all the samples so as not change the Na⁺ concentration and as to reach the final concentration of the respective metal 10⁻⁵ mole/L. Then, the shaking was continued for additional 20 hours. Centrifugation (~ 5 minutes at 3.000 rpm) was used for the separation of phases, the distribution of the metal ions was determined radiometrically. Blank experiments (no TiO₂ added) were performed to estimate the non-specific sorption losses. Calculation of K_D values and their maximum ($K_{D,max}$) or minimum ($K_{D,min}$) determinable values was performed as described elsewhere²⁶.

4.2.2. Titration curves

The titration curves obtained differed by two main parameters – equilibrium values of pH established after contacting them with 0.1 M NaNO₃ solution with no acid or alkali additions, and by slope of the nearly linear close-to-the-neutral-pH part of the curve. For the Degussa P25, AV-01, RG-14 and HTO suspension absorbers the equilibrium pH was close to neutral

(ranging from 5.2 to 7.4), while for the TiO₂-M absorber the pH was as low as pH = 2.6 (see Table IV). This difference is probably caused by the method of preparation. The TiO₂-M absorber is prepared from an intermediate from titanium white production by sulphate process and its "acidic" character may hence be caused by incomplete washing of the acid.

TABLE IV. PARAMETERS OF THE TITRATION CURVES OF THE ABSORBERS
(q - THEORETICAL SORPTION CAPACITY)

Absorber	pH in 0.1M NaNO ₃	Titration curve slope	q [meq/L]
Degussa P25	5.2	14.9	3.3
TiO ₂ -M	2.6	3.5	6.0
HTO	7.4	1.9	10.5
AV-01	6.2	21.4	3.6
RG-14	6.9	19.5	4.4

From the titration curves measured, theoretical sorption capacities of the materials have been estimated, their values are listed in Tab. 4. It can be seen that by far the highest sorption capacity was found for the HTO absorber. For the TiO₂-M material, the sorption capacity is about 40 % lower, while the sorption capacities of the remaining three materials were found to be similar (close to 4 meq/g).

4.2.3. Distribution coefficients

Dependences of distribution coefficients (K_D) of strontium, cobalt, mercury, chromic ions, and chromates on pH were measured in pH range 1–13. For the experimental conditions used, the values of $K_{D,max}$ were $6 \cdot 10^4$ mL/g, $2.6 \cdot 10^5$ mL/g, 10^5 mL/g, 10^5 mL/g, $2 \cdot 10^5$ mL/g, and $7 \cdot 10^4$ mL/g for the Sr, Hg, Co, Cr³⁺, and CrO₄²⁻, respectively. The K_D data were correlated with the dependences of the abundances of individual metal ion species on pH calculated using MINEQL1 code [30]. As an example, the data obtained for cobalt and chromium(III) are shown in Fig. 9 & 10. Generally, the results obtained revealed significant differences in the sorption properties of various TiO₂ materials. With regard to the uptake of cations, the studied materials can be grouped into three groups:

- Group I: HTO suspension
- Group II: Degussa P25 and TiO₂-M
- Group III: Pretiox AV-01 and Pretiox RG-14

Sorption of all cations onto the HTO suspension starts at lowest pH values. The maximum value of K_D are reached already at pH ~ 6 - 7 (divalent cations) or pH ~ 3 (trivalent cations). This material is the only one that can be efficiently used to remove metal cations even from neutral and low-alkaline solutions.

Degussa P25 and TiO₂-M materials exhibit similar sorption properties. The sorption of cations started at pH ~ 4 - 5 and $K_{D,max}$ is reached at pH ~ 7 - 8 (divalent cations) or pH ~ 4 (trivalent cations). Both these materials are prospective for removal of metal ions from alkaline solutions with pH > ~ 9.

Pretiox AV-01 and Pretiox RG-14 are the worse absorbers of the materials studied. They reach the $K_{D,max}$ value for strontium at pH ≥ 12, for cobalt the $K_{D,max}$ values are not reached at all. Hence, these materials could be effectively used for removing metal ions only from highly alkaline solutions.

A brief study of uptake of anions by the materials revealed that for chromates the highest K_D values were achieved for the $\text{TiO}_2\text{-M}$ absorber. Sorption properties of the Degussa P25 and HTO absorbers are similar. The AV-01 material exhibits very poor properties for sorption of chromates.

An important conclusion of this study is that the metal ions speciation plays a crucial role in metal sorption. The decrease of sorption of hydrolysing cations (Co, Hg, Cr) at high pH values correlates well with the decrease of free Me^{n+} ions concentrations.

4.2.4. Isoelectric point

Isoelectric point (or zero point of charge) is an important characteristics of any adsorbing solid. Lehto states[31], that for the materials that can act both as cation and anion exchangers, the isoelectric point may correspond (depending on experimental conditions) to the so called equiabsorption point (EAP) - the value of pH where both cations and anions are exchanged. This study was aimed at deduction of the EAP (or isoelectric points) for our absorbers from the sorption data presented above. For this exercise, the linear portions of the K_D - pH dependences for all the ions studied were plotted for each of the absorbers. An example of such plot is given in Fig. 11. When we define the EAP to correspond to the intercept of the cation and anion K_D - pH dependences, it is obvious from these figure that not a single EAP can be defined.

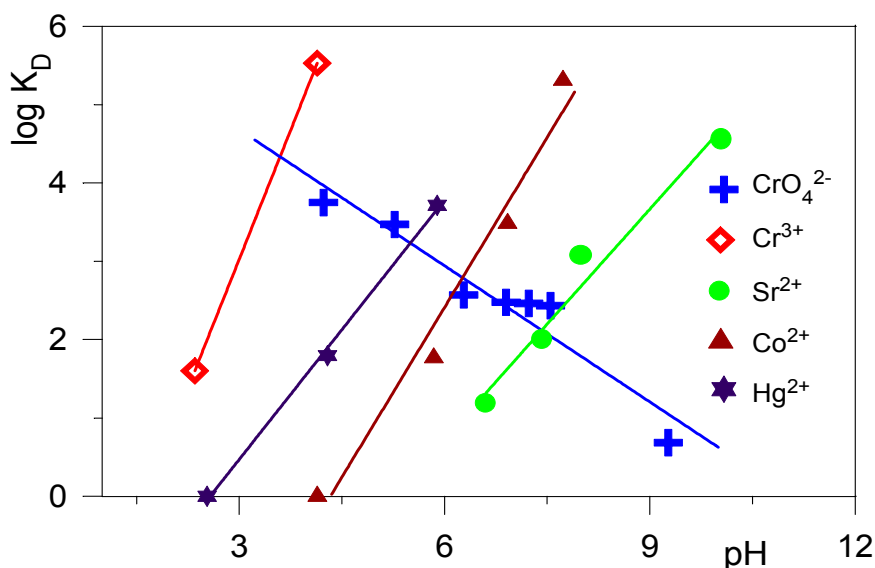


Fig. 11 Dependence of the distribution coefficients K_D of various ions on pH for the Degussa P25 absorber.

This finding has been explained on the basis of theoretical considerations [32]. It was concluded that, when TiO_2 is assumed to behave as a stoichiometric ion exchanger, the EAP (intercept of the cation and anion K_D - pH dependences) will depend on the charge and on the „true“ exchange constant of the respective ions exchanged. The EAP therefore cannot be considered a general characteristics of absorbers.

From the same considerations it follows that the EAP will coincide with the isoelectric point only in the case when the following conditions will be met:

1. The charge of the anion and the cation used is the same
2. The initial concentration of the ions is the same
3. The „true“ exchange constants of anions and cations corresponding to reaction (3) and (13) or (14) are the same
4. The anion sorption capacity of the absorber equals its capacity for the cation sorption.

4.3. Conclusions

From the data discussed above it follows that the proposed technology, combining photocatalytic degradation of the organic substances with sorption of the released radionuclides onto the TiO₂ photocatalyst/absorber, is not very prospective for the treatment of the liquid radioactive waste containing organic complexing agents. The photocatalytic degradation is effective in the acidic pH range, only, while the sorption of the radionuclides proceeds only in the alkaline pH range. From the tested titanium dioxide materials, only TiO₂-M sample or Degusa P25 exhibit significant photocatalytic properties even in weakly basic pH values and HTO sample acceptable sorption properties in the weakly acidic pH range.

If a process is considered that, after the photodegradation step (taking place in acidic solution), includes pH adjustment to alkaline range to improve conditions of the radionuclides sorption, both the TiO₂-M and HTO materials could be prospective. However, decreasing the activity of the waste below the free discharge limit in such a process would be probably difficult to achieve.

5. DEVELOPMENT OF A PROCESS COMBINING PHOTOCATALYTIC DEGRADATION OF THE ORGANIC COMPLEXANTS WITH SUBSEQUENT SEPARATION OF THE RADIONUCLIDES BY SELECTIVE ABSORBERS

The main aim of this study was to develop a process combining the photocatalytic degradation of organic complexants with subsequent treatment of the filtrated solution by sorption. Optimised PAN-based composite absorbers were considered as the first choice for the sorption step. The results obtained in the study of the first stage of this process - optimisation of the conditions of photocatalytic degradation of the complexants in spent decontamination solutions - are given in chapter 4.1 above. Therefore, the data presented here concentrate on the estimation of the performance of the second stage of the combined process – separation of radionuclides and metal ions from the solution after photocatalytic degradation of the organic complexants.

For this study, the set of inorganic ion-exchangers described in the chapter 3.1 was used. The testing comprised both batch and dynamic sorption experiments. The techniques used were the same as described in the chapter 3.1. Prior the sorption experiments, the complexants in both the simulants used were quantitatively photodegraded using techniques described in chapter 4. For the experiments, the solutions were labelled with ^{110m}Ag, ⁶⁰Co, ⁵⁹Fe, ⁵⁴Mn and ⁸⁵Sr. Both the labelling and any pH adjustments were done at least one day before the start of the sorption experiment. Parts of the results were presented at the NRC5 and SIS'01 symposia [23,24], all the data were summarised in a recent contribution to the APSORC'01 conference [33].

5.1. Testing of the Performance of Inorganic Ion-exchangers with KDR Solution Treated by Photocatalysis

In *batch experiments*, the performance of all the tested absorbers was compared on the basis of the distribution coefficients (K_D). The pH of the solution, established after the total photodegradation of the organic complexants (pH = 2.80), has not been adjusted prior the sorption tests. The results obtained are shown in Table 5.

From these results, and their comparison with the data obtained in the original KDR solution not subjected to photodegradation, several main conclusions follow:

- Contrary to the original KDR solution with non-adjusted pH, the chemical stability of all the tested absorbers is good in the solution after the photodegradation of the complexants.
- From the data given in Table 5 it follows that the most prospective absorbers for radionuclide separation from the KDR solution after photodegradation of organic complexants are zirconium phosphate or sodium titanate, followed by crystalline polyantimonic acid.
- When comparing the performance of the absorbers in the original pH-adjusted KDR solution (see Table II) with that in the solution after photodegradation of organic complexants, it can be seen that the distribution coefficients of silver are similar for both the solutions. For the other elements, the separation is much more efficient from the degraded solution. The only exception to this rule is the nickel hexacyanoferrate absorber which uptakes manganese and cobalt more readily from the complexants-containing solution.

TABLE V. K_D VALUES OF VARIOUS RADIONUCLIDES FROM KDR SOLUTION AFTER PHOTOCATALYTIC DEGRADATION OF ORGANIC COMPLEXANTS (V/m = 500, 20 HOURS OF CONTACT, INITIAL pH = 2.80, SEPARATION OF PHASES BY CENTRIFUGATION FOR 10 min).

Sorbent	pH*	K_D [ml/g]				
		Mn-54	Fe-59	Co-60	Ag-110m	Sr-85
ZrP	3.47	3674	1482	2007	$2.1 \cdot 10^4$	3292
NaTiO	3.97	1929	4699	1701	$1.7 \cdot 10^5$	4205
Na-Y	3.99	144	198	172	$1.4 \cdot 10^4$	1064
Mordenite	2.98	299	173	190	$3.2 \cdot 10^3$	6287
FeS	3.03	< 4	30	26	$1.4 \cdot 10^4$	< 2
CSbA	2.48	2106	507	255	$> 2.9 \cdot 10^5$	$> 4.0 \cdot 10^6$
NiFC	3.01	< 4	353	76	$> 2.9 \cdot 10^5$	549
ZrO	3.22	< 4	31	< 8	48	< 2
TiO	2.65	< 4	55	< 8	373	< 2

* - pH measured at the end of contact

When comparing the performance of the absorbers in the non-pH-adjusted original KDR solution (at the end of contact, pH ~ 1.3) and in the solution after photodegradation of organic complexants (at the end of contact, pH = 2.5 – 4), the absorbers may be divided into two groups. The group of the poorly sorbing materials does not display very pronounced differences of their sorption properties in the two media compared while most of the materials that exhibit the highest K_D values in the solution after photodegradation of organic complexants are chemically unstable (dissolve) in the original non-pH-adjusted solution.

Based on these results, two *dynamic sorption experiments* were designed. NaTiO-PAN/SF or ZrP-PAN/SF composite absorbers containing the ZrP or NaTiO active components, that showed the most promising sorption properties in the batch experiments, were used for treatment of the solution prepared and labelled in the same way as described in the previous chapter. With the ZrP-PAN/SF absorber, break-through of all the radionuclides occurred already after treatment of ~ 50 BV of the solution. The results obtained for the NaTiO-PAN/SF absorber (see Fig. 12) were somewhat better. However, even in this experiment all the radionuclides break through the column rather soon, the maximum achievable concentration factor not being higher than 100.

Among the potential reasons of this relatively rapid break-through of all the radionuclides, exhaustion of the sorption capacity of the composite absorbers should be considered. To verify this assumption, another experiment was performed with a standard strongly acidic cation exchanger OSTION KS806. The sorption cycle of this absorber was really found to be significantly longer, virtually no break through of any of the radionuclides was observed during treatment of the solution with volume equal to 250 BV. The decontamination factors of all the radionuclides achieved with this ion-exchanger were virtually the same as those measured in the initial phases of the experiment with NaTiO-PAN/SF but its sorption capacity is obviously much higher. Since at the end of the experiment the colour changes of the bed of the absorber indicated exhaustion of 1/5 to 1/4 of its sorption capacity, practical concentration factors of several hundred to one thousand should be achievable with this material.

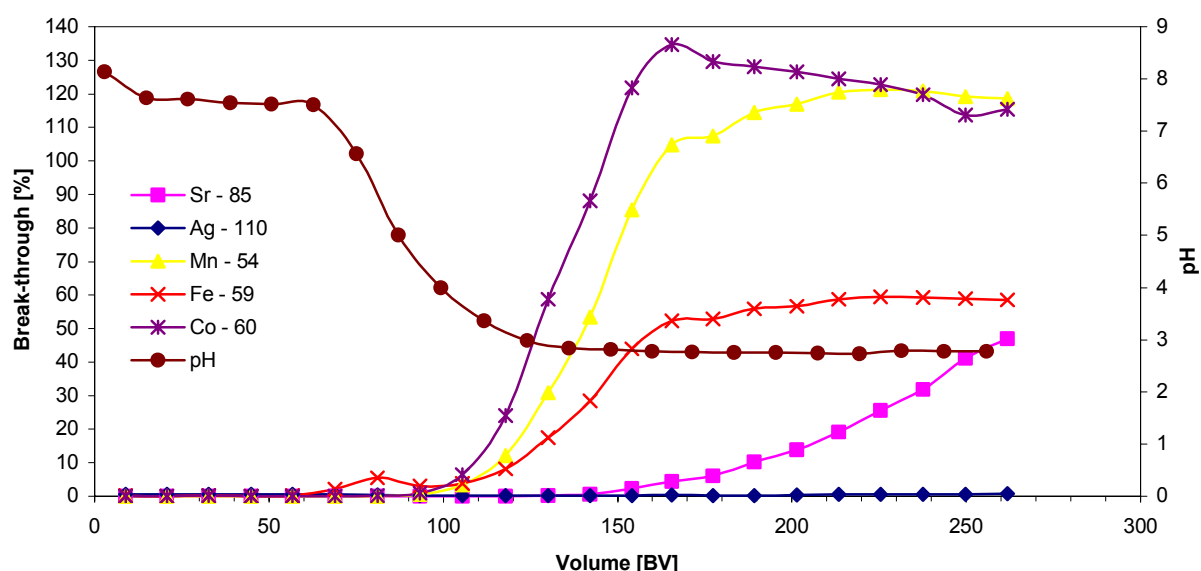


Fig. 12 Break-through curves of selected radionuclides through a column of NaTiO-PAN/SF composite absorber from the real KDR solution after photodegradation of organic complexants and the dependence of pH of the effluent on the volume of the treated solution ($BV = 1.2$ ml, absorber grain size 0.25 - 0.4 mm, flow rate 6.2 BV/hr)

5.2. Testing of the Performance of Inorganic Ion-exchangers with Electrolysate Solution Treated by Photocatalysis

In *batch experiments*, the performance of all the tested absorbers was compared on the basis of the distribution coefficients (K_D). The pH of the solution, established after the total photodegradation of the organic complexants ($pH = 4.37$), has not been adjusted prior the sorption tests. From the data obtained and their comparison with the result obtained without the photocatalytic degradation, influence of the organic complexants degradation on the efficiency of radionuclides separation was evaluated. Correlation was also performed with the

performance of the materials with the KDR solution. The results obtained are summarised in Table 6 together with the "equilibrium" (at the end of contact) pH values. In the table, the absorbers are sorted following their "performance index" (see chapter 3.2).

From these results, and their comparison with the data obtained for the solution without photocatalytic degradation, it can be seen that the photocatalytic degradation of the organic complexants results in significant increase of the distribution coefficients of radionuclides. Taking in account that ^{110m}Ag distribution coefficients are high for any of the absorbers (except for the ZrO one), the most prospective absorbers for radionuclide separation from this solution should be chosen on the basis of their distribution coefficients of ^{54}Mn , ^{59}Fe , and ^{60}Co . From this point of view, the Na-Y absorber (synthetic zeolite) should be selected as the most prospective absorber (mean K_D for the above three radionuclides $K_D \sim 540$). Column application of composite absorbers derived from the other similarly performing materials – NaTiO (sodium titanate, mean $K_D \sim 490$) and ZrP (zirconium phosphate, mean $K_D \sim 340$) might be complicated by the iron precipitation observed in the batch experiments.

When comparing the performance of the absorbers with that in the KDR solution after photodegradation of organic complexants (see Table VI), it can be seen that the absorbers behave in similar way. However, the K_D values measured for the best materials in the electrolyte solution are about 3 to 8 times lower than those measured in the KDR solution.

TABLE VI. K_D VALUES OF RADIONUCLIDES OF INTEREST FROM ELECTROLYSATE SOLUTION AFTER PHOTOCATALYTIC DEGRADATION OF ORGANIC COMPLEXANTS, (V/m = 500 ml/g, 20 hours of contact, initial pH = 4.37, centrifugation for 10 min).

Absorber	pH**	Absorber Stability	Iron Precipit.	K_D [ml/g]					Mean $\log(K_D)^*$
				^{54}Mn	^{59}Fe	^{60}Co	^{110m}Ag	^{85}Sr	
CSbA	3.14	A	–	3716	209	65	20488	7729	3.00
Na-Y	4.82	A	–	497	555	561	2633	4154	2.90
ZrP	4.80	A	+	471	395	148	9197	3653	2.85
NaTiO	4.91	A	+	313	894	262	1852	701	2.78
Mordenite	4.42	B	(+)	189	166	167	636	2259	2.38
NiFC	4.42	A	–	< 6	114	< 7	1299	161	1.70
FeS	4.17	A	?	< 6	29	19	573	< 7	1.57
TiO	3.15	A	–	< 6	32	< 7	1317	< 7	1.56
ZrO	4.59	A	(+)	< 6	67	< 7	46	19	1.28

* – without the ^{85}Sr value

A – no dissolution observed

** – pH measured at the end of contact

B – absorber partially dissolves

? – not estimable

Based on these results, two *dynamic sorption experiments* were designed. NaY-PAN/SF composite absorber containing active component of synthetic zeolite was used for treatment of the solution prepared and labelled in the same way as described above. A parallel experiment was run with the OSTION KS806 cation exchanger (see Fig. 13).

The results obtained confirmed the assumptions drawn from the data obtained in the batch tests. For the NaY-PAN/SF composite absorber, most of the radionuclides break through the column rather soon (after about 125 BV). The maximum achievable concentration factors is hence again relatively low with this absorber. Similarly to the case of the KDR solution, the sorption cycle of the standard strongly acidic cation exchanger OSTION KS806 was found to

be significantly longer. Except for an insignificant break-through of ^{110m}Ag that occurred after treatment of ~ 100 BV of the solution, no radionuclides did break through till more than 200 BV of the solution passed the column. Only then, ^{59}Fe was detected in the column effluent while all the other radionuclides were still fully retained. Hence, practical concentration factor of at least two hundred may be expected to be achievable with this material.

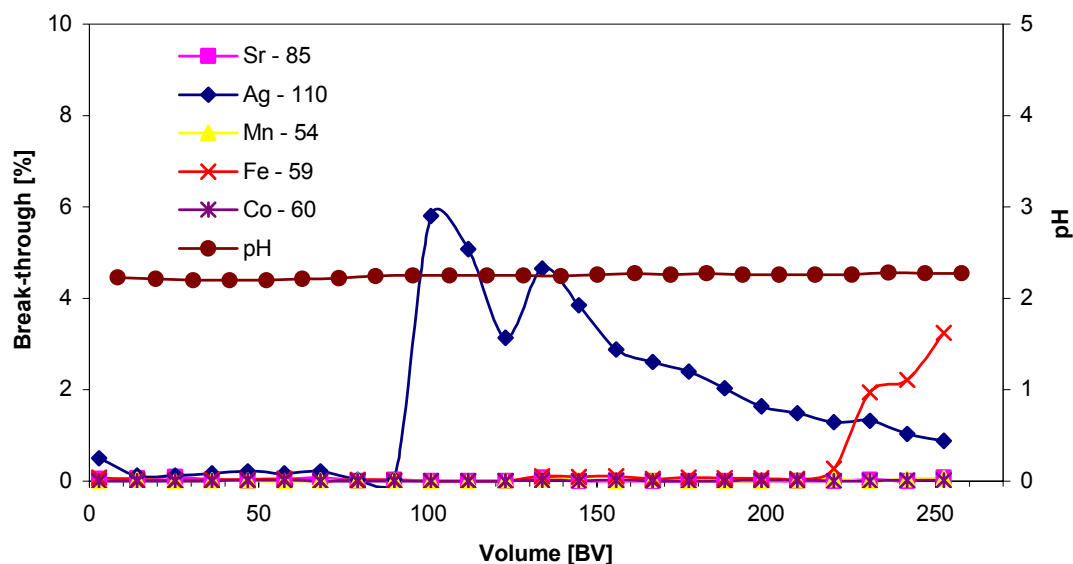


Fig. 13. Break-through curves of selected radionuclides through a column of OSTION KS806 cation exchanger from the electrolyte solution after photodegradation of organic complexants and the dependence of pH of the effluent on the volume of the treated solution. (BV = 1.2 ml, absorber grain size 0.08 - 0.16 mm, flow rate 5.3 BV/hr)

5.3. Conclusions — Process Design

From the data obtained, it can be concluded that a process combining photocatalytic degradation of the organic complexants with subsequent radionuclides separation onto a strongly acidic cation exchanger offers an efficient option for radionuclides separation from the the spent solutions from either chemical or electrochemical decontamination.

A three-step modular process was proposed on the basis of these results, the process modules being:

- photocatalytic degradation module
- phase separation module
- radionuclide sorption module.

Further on, this process was tested with real spent decontamination solutions.

6. VERIFICATION OF THE PROCESSES IN HOT TESTS WITH REAL SOLUTIONS

For the KDR solution, the process development work described in chapter 5.1 was carried on with the real spent decontamination solution. Therefore, the positive results obtained during this phase represent at the same time verification of the developed process.

For the electrolysate solution, the performance of the processes designed was verified in a demonstration experiment performed jointly with a small enterprise AllDeco Trnava, Slovakia. This experiment was carried out at the radiochemical laboratories in the premises of the NPP Jaslovské Bohunice, Slovakia. Waste prepared by standard electrochemical decontamination method of VVER 440 NPP reactor internals was used for the demonstration. The results obtained are reviewed in a recent contribution to the APSORC'01 conference [33].

For the spent electrolysate solution preparation, standard electrochemical decontamination method was used. A contaminated stainless steel tube with external diameter of 0.8 cm and both ends sealed (part of an internal reactor dosimetry "dry channel") was decontaminated in a small electrochemical decontamination system with steel outer cathode. Solution containing 10 g/L of the oxalic acid and 5 g/L of citric acid was used as the electrolyte. The decontamination was performed in standard operational conditions (130 mA/cm² of the anode surface, time of electrolysis 54 minutes). The electrolysate was analysed for the concentrations of oxalic and citric acids, Fe, Ni, and Cr; pH of the solution was measured. Relative specific activity of the gamma-rays emitting radionuclides in the electrolysate was determined by high-resolution gamma-ray spectrometry. An example of the real electrolysate solution composition is given in Table 7 below.

For the photodegradation and sorption experiments, the experimental set-ups and techniques described in chapters 2.1 or 3.1, respectively were used. The "peroxide" conditions (see chapter 4.1.2) were used during the photocatalytic degradation of the oxalic and citric acid in the real electrolysate solution. Sorption removal of the radionuclides was tested in a dynamic sorption experiment with OSTION KS806 cation exchanger in H⁺ form.

6.1. Photocatalytic Degradation of Organic Complexants in the Real Electrolysate Solution

The analyses carried out in the course of the photodegradation of the electrolysate solution revealed that the degradation of the organic complexants and complexes in the real waste proceeds as well as it did in the simulants used in the laboratory experiments, i.e. the degradation was quantitative already after ~ 12 hrs. As an example of the behaviour of the solution during irradiation, results obtained for one of the batches of the treated solution are listed in Table VII.

The first conclusion that follows from these data is that, similarly to the experiments with simulant solutions, significant amounts of both the oxalic and citric acids are decomposed already during the electrolysis. In average, ~ 60 % of the oxalic and ~ 35 % of the citric acid were degraded in this step.

Further investigation of the data reveals that the vast majority of iron (~ 95 %) is removed during the photocatalysis. This removal should be ascribed to iron deposition onto the surface of the photocatalyst. An interesting feature is the rather different behaviour of nickel (~ 20 % removed). Significant amount of chromium is removed, too (~ 70 %).

Out of the radionuclides, quantitative removal during the photocatalysis was observed for ¹²⁴Sb and ¹³⁷Cs. Some deposition/sorption of radiocobalt and ⁵⁴Mn onto the photocatalyst takes place, too. From these findings an important conclusion on the nature of the spent photocatalyst follows. As a result of metal ion / radionuclide deposition, this photocatalyst would collect a significant part of the total radioactivity of the treated solution and would hence represent a secondary waste stream.

TABLE VII. BEHAVIOUR OF RADIONUCLIDES, MACROELEMENTS, COMPLEXANTS AND pH DURING PHOTOCATALYSIS (ELECTROLYSIS/PHOTOCATALYSIS No. 5, TOTAL IRRADIATION TIME 21 hrs)

Nuclide	Peak [keV]	10 ³ cps		D [%]
		Electrolysate	Photocatalysate	
Sb-124	603	175.9	0.0	100.0
Cs-137	661	18.6	0.0	100.0
Co-58	811	92.1	53.7	41.7
Co-60	1332	945.7	723.0	23.5
Mn-54	834	1064.3	903.3	15.1
Element		c [mg/l]		D [%]
		Electrolysate	Photocatalysate	
Fe		7.289	0.293	96.0
Ni		0.941	0.735	21.9
Cr		2.610	0.763	70.8
Complexant		c [mg/l]		D [%]
		Electrolysate	Photocatalysate	
Oxalic acid		4.16	0	100
Citric acid		3.65	0	100
		Electrolysate	Photocatalysate	
pH		1.70	5.11	

D – relative amount removed during photocatalysis

6.2. Sorption removal of radionuclides from the real electrolysate solution treated by photocatalysis

The results of the sorption part of the test are summarised in Fig. 14. In total, some 300 BV (~ 350 mL) of the electrolysate solution treated by photocatalysis were passed through the column of the OSTION KS806 cation exchanger. The experiment could not have been continued because of available laboratory time restriction.

From the data obtained, it can be seen that, except for nickel, no radionuclides or metal ions broke through in the course of all the test. Most of the deviations of the break-through curves from the zero level should be rather ascribed to statistical uncertainties of the measurement of relatively low activities. Visually, the progress of loading the column with metal ions could be followed as a dark zone expanding through the column. At the end of the experiment, some 5 % of the bed of the exchanger (1 mm out of the total length of the bed of 2 cm) has not been loaded, yet. It can be therefore supposed, that significant break-through of the metal ions and/or radionuclides would occur soon. This assumption seems also to be corroborated by a small increase of the iron concentration in the last fraction of the effluent.

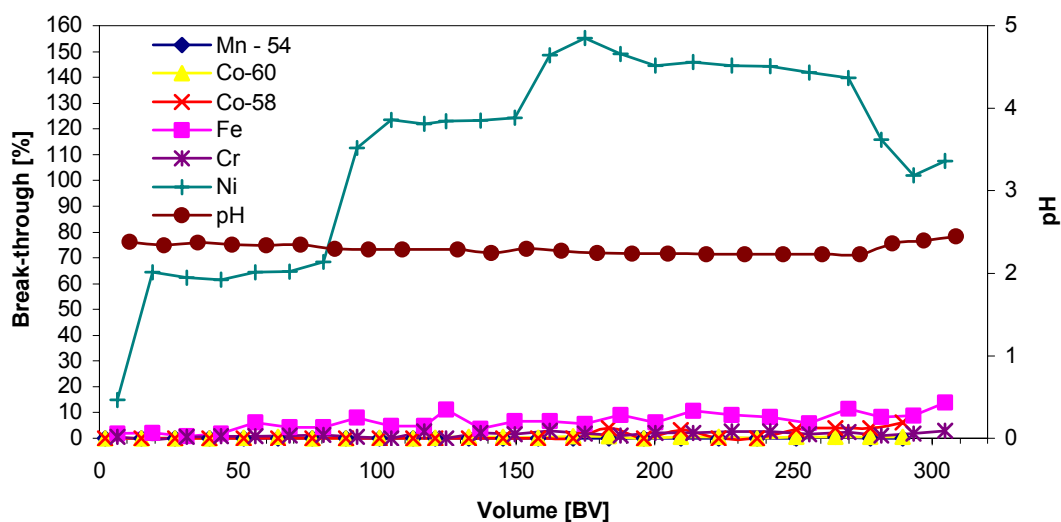


Fig. 14 Break-through curves of radionuclides and metal ions through a column of OSTION KS806 cation exchanger from the real electrolysate solution after photocatalytic degradation of organic complexants and the dependence of pH of the effluent on the volume of the treated solution (BV=1.2ml, absorber grain size 0.08 - 0.16 mm, flow rate 6.0 BV/hr)

At this moment, there is no explanation available for the behaviour of nickel in the process. Contrary to iron or chromium, it is not significantly retained on the photocatalyst during the photocatalysis. In the sorption step, it starts to break through already in the first fractions of the effluent. In the middle part of this test, the concentration of nickel in the effluent exceeded that in the feed. After washing the excess nickel of the column, its concentration in the feed stabilised at the same level as in the feed (100 % break-through).

6.3. Conclusions

The results of verification of the process designed with the waste from electrochemical decontamination were rather promising. Both the photocatalytic degradation and the radionuclide sorption modules performed in the real solution as well as in the preliminary tests with the simulant solutions. Somewhat controversial data were obtained for the behaviour of nickel ions in the system. If considering practical application of this process, attention should be paid to the spent photocatalyst that would represent an additional secondary radioactive waste stream.

7. SUMMARY OF THE RESULTS AND CONCLUSIONS

In this project, potential of two combined processes for the removal of organic complexants and/or separation of radionuclides from spent decontamination solutions was investigated in detail. The processes considered were:

- A single-step process combining photocatalytic degradation of organic complexants with sorption of the released metal ions on the TiO₂ photocatalyst/absorber.
- A two-step process combining photocatalytic degradation of organic complexants combined with subsequent treatment of the filtrated solution by sorption on optimised PAN-based composite absorbers.

The study was performed with both simulants and real liquid waste from NPPs in the Czech or Slovak Republics. The attention concentrated namely on:

- Acidic spent decontamination solution from the second stage of the AP-CITROX process ("KDR solution").
- Liquid waste from electrochemical decontamination ("Electrolysate solution").

In addition to the process development studies, detailed research was carried out in the following directions:

- Study of photocatalytic degradation of organic complexants used in decontamination solutions including EDTA, oxalic and citric acids. Study of photocatalytic degradation of complexes of these complexants with metal ions.
- Study of sorption properties of various TiO_2 materials
- Background study of options for direct separation of radionuclides from model and real solutions, including testing of prospective composite inorganic-organic absorbers with polyacrylonitrile binding matrix.

The general conclusions of the study of *photocatalytic degradation* most important for the process development are:

- All the organic complexants studied (oxalic and citric acids or EDTA) can be effectively photodegraded in the presence of a titanium dioxide catalyst.
- The degradation is more effective in acidic solutions, in neutral and alkaline pH range the reaction rate sharply decreases.
- TiO_2 -M and Degussa P25 samples display the highest activity for catalysing the photodegradation of organic complexants.

The general conclusions regarding the *TiO_2 sorption properties* are:

- Out of the materials tested, the best sorption properties displays the HTO suspension. This material is the only one that can be efficiently used to remove metal cations even from neutral and low-alkaline solutions.
- Degussa P25 and TiO_2 -M materials exhibit similar sorption properties. They are prospective for removal of metal ions from alkaline solutions with $\text{pH} > \sim 9$.
- Pretiox AV-01 and Pretiox RG-14 are the worse absorbers of the materials studied.

Another important conclusions of this study are that the metal ions speciation plays a crucial role in metal sorption and that the correspondence of the isoelectric and equiabsorption points has a rather limited validity.

The study of the options for the *direct separation of cations* from the spent decontamination solutions onto an ion-exchanger, composite absorber, or cation resin revealed that such separation is not possible with any of the materials investigated.

The results of the *process development studies* can be summarized as follows:

- Conditions allowing quantitative photocatalytic degradation of organic complexing agents in spent solutions used for both the chemical and electrochemical decontamination of NPP primary circuit internals have been found.
- The single-step process, combining photocatalytic degradation of organic complexants with sorption of the released metal ions on the TiO_2 photocatalyst/absorber, was found not very prospective for the treatment of the liquid radioactive waste containing organic complexing agents. The photocatalytic degradation is effective in the acidic pH range, only, while the sorption of the radionuclides proceeds only in the alkaline pH range. If a process is considered that, after the photodegradation step (taking place in acidic solution), includes pH adjustment to alkaline range to improve conditions of the radionuclides sorption, both the TiO_2 -M and HTO materials could be prospective.

However, decreasing the activity of the waste below the free discharge limit in such a process would be probably difficult to achieve.

- A two-step process combining photocatalytic degradation of organic complexants combined with subsequent treatment of the filtrated solution by sorption on optimised PAN-based composite absorbers was developed. It was found that separation of the radionuclides released from the organic complexes onto organic resins is preferable to the application of selective inorganic-organic absorbers. The results of verification of the process designed with the waste from electrochemical decontamination were rather promising. If considering practical application of this process, attention should be paid to the spent photocatalyst that would represent an additional secondary radioactive waste stream.

In addition to development of methods for the treatment of spent decontamination solution, significant efforts were carried out in the treatment of the real evaporator concentrates from the NPP Dukovany, Czech Republic. For the contemporary caesium and strontium separation a new (TiO₂+FC212)-PAN composite absorber containing a mixture of titanium dioxide and potassium-cobalt hexacyanoferrate active components was developed. For radiocobalt separation, a method combining sorption with magnetic field action was considered. Within this project, it was not possible to finish development of this technique.

Generally, it can be concluded that the objectives, defined for this project, were fully achieved. The idea of combining photocatalytic degradation of organic complexants with the separation of the released radionuclides by sorption techniques was productive and enabled development and verification of a novel technique for the treatment of two types of spent decontamination solutions. Development of similar techniques for treatment of waste types with different compositions seems to be desirable.

REFERENCES

- [1] SCHIAVELLO, M. (Ed.): Heterogeneous Photocatalysis, Wiley Series in Photoscience and Photoengineering, Vol.3, J.Wiley & Sons, Chichester, 1997.
- [2] CLEARFIELD, A., (Ed.): Inorganic Ion Exchange Materials, CRC Press Inc., Boca Raton, Florida, 1982.
- [3] ŠEBESTA, F.: Composite absorbers consisting of inorganic ion-exchangers and polyacrylonitrile binding matrix. I. Methods of modification of properties of inorganic ion-exchangers for application in column packed beds, J. Radioanal. Nucl. Chem., 220, 1997, pp. 77–88.
- [4] ŠEBESTA, F.-JOHN, J.-MOTL, A.: Removal of Cesium and Strontium from Highly Saline Acidic or Alkaline HLW Using PAN-Based Composite Absorbers, In: BAKER, R. - SLATE, S. - BENDA, G., eds.: ICEM'97 Proc. Sixth International Conference on Radioactive Waste Management and Environmental Remediation, Singapore, October 12-16, 1997, ASME International, New York 1997, pp. 241–244.
- [5] ŠEBESTA, F.-JOHN, J.-MOTL, A.-ROŠÍKOVÁ, K.: Study of Combined Processes for the Treatment of Liquid Radioactive Waste Containing Complexing Agents, Progress Report of the Research Contract No.9585/R2 between the International Atomic Energy Agency and the Czech Technical University in Prague, Czech Republic; CTU Prague, July 2000, 37 + 21.

- [6] COTTEN, G.B.-NAVRATIL, J.D.-ŠEBESTA, F.: New Magnetic-Enhanced Adsorption Process for Wastewater Treatment, In: KURUC, J.-RAJEC, P., eds.: Separation of Ionic Solutes, Vol. VIII, Abstracts of the 8th Int. Conf. SIS'99, Stará Lesná - High Tatras, Slovakia, September 11-16, 1999, Omega Info, Bratislava 1999, pp. 73–74.
- [7] ŠEBESTA, F.: Composite Absorbers – Properties and Potential for Separations in Magnetic Field (in Czech), In: Proc. Magnetic Separations in Biosciences and Biotechnologies, September 14–15, 1999, České Budějovice, Czech Republic, Institute of Landscape Ecology, Academy of Sciences of CR, České Budějovice 1999, pp. 84–87.
- [8] MOTL, A. - HLAVICOVÁ, J. - ŠEBESTA, F. - NAVRATIL, J.D.: Sorption of cobalt from aqueous solutions onto magnetite, J. Radioanal. Nucl. Chem., to be published.
- [9] LEGRINI, O. - OLIVEROS, E. - BRAUN, A.M.: Photochemical Process for Water Treatment, Chem Rev. 93, 1993, pp. 671–698.
- [10] HOFFMANN, M.R. - MARTIN, S.T. - CHOI, W. - BAHNEMANN, D.W.: Environmental Applications of Semiconductor Photocatalysis, Chem Rev. 95, 1995, pp. 69–96.
- [11] TANAKA, K. - HISANAGA, T. - HARADA, K.: Efficient Photocatalytic Degradation of Chloral Hydrate in Aqueous Semiconductor Suspension, J. of Photochem. and Photobiol., A: Chemistry, 48, 1989, pp. 155–159.
- [12] DANAČÍKOVÁ, E. - JOHN, J. - ŠEBESTA, F. - HOOPER, E.W.: Degradation of Organic Complexants Using Photo-Oxidation Processes, In: Proc. Workshop 97, Prague, January 20–22, 1997, Part I., Chemistry, ČVUT Prague, 1997, pp. 155–156.
- [13] JOHN, J. - DANAČÍKOVÁ, E. - ŠEBESTA, F. - MOTL, A. - ROSÍKOVÁ, K. - HOOPER, E.W.: Study of Separation of Radionuclides and Heavy or Toxic Metals from Complexants-Containing Solutions (in Czech), In: Proc 50th Chemical Societies Congress, Zlín, Czech Republic, September 8-11, 1997, Chem. listy, 91(9), 1997, pp. 770–771.
- [14] DANAČÍKOVÁ-POPELOVÁ, E. - JOHN, J. - ROSÍKOVÁ, K. - ŠEBESTA, F. - HOOPER, E.W.: Mineralization of Organic Pollutants in Mixed Waste by UV Radiation, In: Proc. Warsaw'98 Fourth International Symposium and Exhibition on Environmental Contamination in Central and Eastern Europe, September 15–17, 1998, Warsaw, Poland; CD ROM Edition, Florida State University, Tallahassee, FL, 1999, Paper No. 170.
- [15] ROSÍKOVÁ, K. - JOHN, J. - DANAČÍKOVÁ-POPELOVÁ, E. - ŠEBESTA, F. - HOOPER, E.W.: Study of EDTA Photodegradation, In: Proc. Warsaw'98 Fourth International Symposium and Exhibition on Environmental Contamination in Central and Eastern Europe, September 15–17, 1998, Warsaw, Poland; CD ROM Edition, Florida State University, Tallahassee, FL, 1999, Paper No. 107.
- [16] ROSÍKOVÁ, K. - JOHN, J. - ŠEBESTA, F.: Photocatalytic Degradation of Metal Complexes and Spent Decontamination Solutions, in Proc. Prague 2000 – Fifth International Symposium and Exhibition on Environmental Contamination in Central and Eastern Europe, September 12–14, 2000, Prague; CD ROM Edition, Florida State University, Tallahassee, FL, USA, 2000, paper No. 897, 7 pp.
- [17] ROSÍKOVÁ, K. - JOHN, J. - ŠEBESTA, F.: Comparison of Photocatalytic Degradation of Organic Complexants and Metal Complexes Thereof (in Czech), In: Proc. 52nd Chemical Societies Meeting, September 17–20, 2000, České Budějovice (Czech Republic), Chem. listy, 94(9), 2000, pp. 852–853.
- [18] HERRMANN, J.M. - MOZZANEGA, M.N. - PICHAT, P.: J. Photochem., 1983, 22, pp. 333–343.
- [19] SERPONE, N. - LAWLESS, D. - DISDIER, J. - HERRMANN, J.-M.: Langmuir, 1994, 10, pp. 643–652.

- [20] LITTER, M.I. - NAVIO, J.A.: J. Photochem. Photobiol, A.: Chem., 1994, 84, pp. 183–193.
- [21] MALINKA, E.A.-KAMALOV, G.L.: J. Photochem. Photobiolog. A: Chem., 1994, 81, pp. 193–197.
- [22] MILIS, A. - PERAL, J. - DOMENECH, X. - NAVIO, J.A.: J. Mol. Catal., 1994, 87, 67–74.
- [23] ROSÍKOVÁ, K.-JOHN, J.-ŠEBESTA, F.-MOTL, A.: Separation of Radionuclides from Organic Complexants Bearing Wastes, In: NRC5 – 5th International Conference on Nuclear and Radiochemistry, September 3–8, 2000, Pontresina, Switzerland; Paul Scherrer Institute and University Bern, Switzerland, 2000, Vol. 2, pp. 569–572.
- [24] ROSÍKOVÁ, K. - JOHN, J. - ŠEBESTA, F. - MOTL, A.: Separation of Radionuclides from Electrochemical Decontamination Waste, In: J. Kufcaková, ed.: Separation of Ionic Solutes, Abstracts of the 9th Int. Conf. SIS'01, June 5-10, 2001, Bratislava, Modra-Harmonia, Slovakia, Comenius University, Bratislava 2001, pp. 66–69.
- [25] ROSÍKOVÁ, K. - ŠEBESTA, F. - JOHN, J. - BUCHTOVÁ, K. - MOTL, A.: Separation of Radionuclides from Spent Decontamination Solutions onto Selective Inorganic-Organic Composite Absorbers, In: Proc. 14th Radiochemical Conference, 14–19 April 2002, Mariánské Lázně, Czech Republic; Czech J. Phys., to be published.
- [26] DANAČÍKOVÁ, E. - JOHN, J. - MOTL, A. - ŠEBESTA, F. - HOOPER, E.W.: Study of Sorption Properties of Various Titanium Dioxide Materials, In: Proc. 13th Radiochemical Conference, 19–24 April 1998, Mariánské Lázně - Jáchymov, Czech Republic; Czech J. Phys., 49/S1, 1999, pp 789–795.
- [27] AMPHLETT, C.B.: Inorganic Ion Exchangers, Elsevier Publishing Co., Amsterdam, 1964.
- [28] LEHTO, J. et al.: Advanced Separation of Harmful Metals from Industrial Waste Effluents by Ion Exchange, J. Radioanal. Nucl. Chem., Articles, 208, 1996, pp. 435–443.
- [29] SAMANTA, S.K.: Hydrated Titanium (IV) Oxide as a Granular Inorganic Sorbent for Removal of Radiostrontium, J. Radioanal. Nucl. Chem., Articles, 209, 1996, pp. 235–242.
- [30] WESTALL, J.C. - ZACHARY, J.L. - MOREL, F.M.M.: MINEQL, A Computer Program for the Calculation of Chemical Equilibrium Compositions of Aqueous Systems. Tech. Note 18, Dept. Civil. Eng., Massachusetts Institute of Technology, Cambridge 1976, USA.
- [31] LEHTO, J.: Sodium Titanate for Solidification of Radioactive Waste - Preparation, Structure and Ion Exchange Properties, Academic Dissertation, Report Series in Radiochemistry 5/1987, University of Helsinki, Finland, 1987.
- [32] MOTL, A.-ŠEBESTA, F.-JOHN, J.: Sorption of Cobalt on Hydrous Manganese Dioxide - Mechanistic Considerations, in Proc. Warsaw'98, Fourth International Symposium and Exhibition on Environmental Contamination in Central and Eastern Europe, September 15-17, 1998, Warsaw, Poland, CD ROM Edition, Florida State University, Tallahassee, FL, USA, paper No. 109.
- [33] ROSÍKOVÁ, K. - JOHN, J. - ŠEBESTA, F.: Separation of Radionuclides from Chemical and Electrochemical Decontamination Waste, in Proc. APSORC 2001, 30 October–2 November 2001, Fukuoka, Japan; J. Radioanal. Nucl. Chem., to be published.

THE VOLUME REDUCTION OF LIQUID RADIOACTIVE WASTE BY COMBINED TREATMENT METHODS

T. SZÁNYA^c, P. TILKY^a, B. KANYÁR^b, G. MARTON^c, J. SCHUNK^a, J. VISZLAY^a,
L. HANÁK^c, Z. NÉMETH^b

^a NPP Paks, Hungary

^b University of Veszprém, Department Radiochemistry, Hungary

^c University of Veszprém, Department Chemical Engineering, Hungary

Abstract. A new combined method (adsorption, ion-exchange) and a mobile treatment equipment was developed for the regeneration of AP-CITROX decontamination reagents. Columns containing activated carbon, cation- and anion-exchange resins are used. For the acidic (reductive) (citric acid, oxalic acid, H₂O) liquid, the experimental results revealed that the ⁵⁴Mn, ⁵⁸Co and ⁶⁰Co radioisotopes are strongly concentrated on the Varion KSN cation-exchanger, while the ^{110m}Ag is accumulated mainly in the activated carbon and cation-exchanger layer. Since the decontamination factors for the radionuclides with long half-lives (⁵⁴Mn, ⁶⁰Co, ^{110m}Ag) are high, and the radionuclides with short half-lives (⁵¹Cr, ¹²⁴Sb, ⁹⁵Nb) decay to small activities during the storage, the purified liquid can be recycled in the decontamination processes. The volumetric reduction factor at the tested volume (227 dm³) was as high as 45.4.

1. INTRODUCTION

Owing to corrosion processes and neutron activation, the equipment of the primary circuit of a nuclear power plant operating at high pressure (regenerative heat exchangers, steam generators, pipelines, pumps etc.) become radioactive. As a result of the corrosion processes and the neutron activation a corrosion layer containing such radionuclides as ⁵¹Cr, ⁵⁴Mn, ⁵⁸Co, ⁶⁰Co, ^{110m}Ag, ⁵⁹Fe, ¹²⁴Sb, and ⁹⁵Nb are formed on the inner surface of the equipment at the welded joints.

There are radionuclides with long half-life are ⁵⁴Mn (312 days), ⁶⁰Co (5.26 years) and ^{110m}Ag (250 days), and radionuclides with shorter half-life are ⁵¹Cr (28 days), ⁵⁸Co (71 days), ⁵⁹Fe (45 days), ¹²⁴Sb (60 days), and ⁹⁵Nb (66 days) in this solution.

In the case of the nuclear power plants operating at high pressure (PWR) it is necessary to decontaminate the equipment every 3–5 years. At WWER-400 type-reactors the decontamination of equipment of the primary circuit is carried out by using the AP-CITROX process. During the AP-CITROX process as a first step the surface to be decontaminated is treated under alkaline conditions by KMnO₄ solution at 90–95°C. (During the newest LOMI process a V²⁺, Cr²⁺, EDTA, gluconic acid, picolinic acid containing complex forming decontamination is used).

The alkaline oxidative and the acidic reductive decontamination solutions originated from the AP-CITROX process are usually stored in containers without any treatment. In these containers, the short lived radionuclides decay during the long storage time, however the longer lived radionuclides (⁵⁴Mn, ⁶⁰Co and ^{110m}Ag) have still the concentration above the discharge limit of 1 kBq/dm³ and are not allowed to be discharged in the environment even after several years of storage.

A problem in the treatment of such a waste lies in the mixing of alkaline oxidative and acidic reductive decontamination solutions. In this case, due to the oxalic acid — KMnO₄

reaction the MnO_2 precipitate is formed, which settles as radioactive slurry in the container. The decontamination solution (especially the alkaline oxidative one) may also contain several undesired organic compounds (oils, fats, detergents etc.), solid grains and colloid impurities that can be considered as carriers of radioactive nuclides.

A usual practice for the processing of such a waste at nuclear power plants is evaporation followed by solidification of the evaporation concentrate by either cementation, bituminization or vitrification.

The objective of the study was to develop a new combined adsorption-ion-exchange method for the treatment of alkaline, oxidative (NaOH , KMnO_4 , H_2O) acidic reductive (citric acid, oxalic acid) and LOMI (V(II)EDTA) radioactive decontamination solutions using active carbon adsorbent, cation exchanger, anion exchanger packing at an increased temperature. The details of this method are published in [1,2].

2. TREATMENT OF THE ALKALINE OXIDATIVE DECONTAMINATION SOLUTION

An alkaline oxidative radioactive decontamination solution (the composition is given in Table I) was pumped in through a column downwards ($300 \text{ cm} \times 5.5 \text{ cm}$ diameter) at 95°C with the flow rate of $100\text{--}400 \text{ cm}^3/\text{min}$. The 180 cm upper part of the column was filled with activated carbon (Top-Sorb type, University of Veszprém, Dep. Chem. Eng.). Physical characteristics of the adsorbent are given in Table II. The bottom part of the column was filled with 40 cm of Varion-KSN cation resins (particle size: $0.4\text{--}1.2 \text{ mm}$) in the Fe(II) form, with 40 cm of Varion-KSN cation resins (particle size: $0.4\text{--}1.2 \text{ mm}$) in the H^+ form and with 40 cm Varion-ATN anion exchange resins in the OH^- form (Nitrokémia Ipartelepek, Balatonfuzfo; particle size: $0.4\text{--}1.2 \text{ mm}$) from top to bottom.

TABLE I. THE INITIAL COMPOSITION OF THE ALKALINE OXIDATIVE DECONTAMINATION SOLUTION (KMnO_4 contents in the solution is 5 g/L , NaOH - 10 g/L)

^{51}Cr (kBq/L)	^{54}Mn (kBq/L)	^{58}Co (kBq/L)	^{60}Co (kBq/L)	$^{110\text{m}}\text{Ag}$ (kBq/L)	^{124}Sb (kBq/L)	^{95}Nb (kBq/L)	Σ (kBq/L)
82	15.4	2.9	1.6	520	77.7	230	929.6

TABLE II. PHYSICAL CHARACTERISTICS OF THE ADSORBENT

Specific surface area S_{BET} (m^2/g)	701.63
Pore volume (cm^3/g)	0.5027
Average pore diameter (nm)	2.866
Particle size (mm)	1–3

The radionuclide composition of the solution leaving the column as a function of the effluent volume is given in Table III. The radioactivity measurements were carried out by using Canberra Series 80 gamma-spectrometer.

TABLE III. THE RADIONUCLIDE COMPOSITION OF THE SOLUTION LEAVING THE COLUMN

	Activity concentration, kBq/L							
Volume, L	⁵¹ Cr	⁵⁴ Mn	⁵⁸ Co	⁶⁰ Co	^{110m} Ag	¹²⁴ Sb	⁹⁵ Nb	$\Sigma^{54}\text{Mn}+^{60}\text{Co}+^{110m}\text{Ag}$
24	0.22	0.08	0.04	0.24	0.26	1.02	0.04	0.58
57	0.4	0.16	0.1	0.36	0.38	1.94	0.12	0.90
77	0.56	0.08	0.06	0.16	0.52	4.8	0.12	0.76
93	0.58	0.06	0.06	0.14	0.16	5.4	0.08	0.36
113	1.16	0.02	0.06	0.12	0.1	6.78	0.06	0.24
136	1.76	0.08	0.08	0.22	0.28	8.06	0.08	0.58
152	3.56	0.16	0.24	0.22	0.30	10.46	0.44	0.68
173	3.24	0.14	0.22	0.24	0.16	10.74	0.36	0.54

The axial activity in the liquid phase during the treatment was measured. Samples from the liquid phase at differential axial length of the column were taken. The samples have been analyzed by using Camberra Series 80 gamma-spectrometer.

At the end of the treatment (the total volume of the treated liquids is 173 L) the activity of the solid phase was measured (dried at 100°C until the constant weight) with Canberra Series 80 gamma-spectrometer. The results of the measurements are given in Table IV.

TABLE IV. THE AXIAL ACTIVITY DISTRIBUTION IN THE SOLID PHASE AFTER TREATMENT

Axial Position cm	Packing	Activity concentration, Bq/kg packing						
		^{110m} Ag	⁵⁸ Co	⁶⁰ Co	⁵⁴ Mn	¹²⁴ Sb	Σ^*	Σ^{**}
0	Active Charcoal	$3,8.10^7$	$2,1.10^5$	3.10^5	4.10^5	4.10^5	$3,87.10^7$	$3,97.10^7$
30	Active charcoal	2.10^6	$1,4.10^4$	$5,1. 10^3$	$2,2.10^4$	8.10^4	$2,078.10^6$	$2,1218.10^6$
60	Top-Sorb Active charcoal	10^7	$3,7.10^4$	$7,3.10^4$	$2,8.10^5$	$3,3.10^5$	$1,0.53.10^7$	$1,0720.10^7$
90	Top-Sorb Active charcoal	$1,2.10^7$	$2,6.10^4$	$1,4.10^5$	$3,7.10^5$	$3,7.10^4$	$1,2384.10^7$	$1,2447.10^7$
90	Active charcoal	$8,8.10^6$	$1,4.10^4$	$7,8.10^3$	$1,4.10^5$	$1,7.10^4$	$8,3218.10^6$	$8,4788.10^6$
120	Active charcoal	$1,1.10^7$	$1,8.10^4$	10^4	$2,3.10^5$	$2,9.10^5$	$1,124.10^7$	$1,2548.10^7$
150	Top-Sorb Active charcoal	$1,1.10^6$	$5,7.10^3$	$3,5.10^3$	$1,1.10^4$	$5,7.10^4$	$1,1145.10^6$	$1,1772.10^6$
180	Top-Sorb Active charcoal	$1,52.10^4$	$3,3.10^3$	$2,3.10^3$	2.10^3	$5,1.10^3$	$1,93.10^4$	$2,77.10^4$
210	Fe ²⁺ form Varion-KSN	$1,8.10^4$	3.10^3	$2,7.10^3$	$1,6.10^3$	$3,6.10^3$	$2,23.10^4$	$2,89.10^4$
240	H ⁺ form Varion-KSN	$1,3.10^3$	960	$1,1.10^3$	825	830	$3,225.10^3$	$5,01.10^5$
270	OH ⁻ form Varion-ATN	$8,1.10^3$	$1,9.10^3$	$1,6.10^3$	626	$3,7.10^4$	$5,326.10^3$	$4,42.10^4$
300	OH ⁻ form Varion-ATN	$2,6.10^3$	$1,5.10^3$	$1,5.10^3$	740	$3,3.10^4$	$4,34.10^4$	$3,93.10^4$

Where $\Sigma^* = \Sigma^{110m}\text{Ag}+^{60}\text{Co}+^{54}\text{Mn}$

$\Sigma^{**} = \Sigma^{110m}\text{Ag}+^{58}\text{Co}+^{60}\text{Co}+^{54}\text{Mn}+^{124}\text{Sb}$ The measurement results are given in Figs. 1–9.

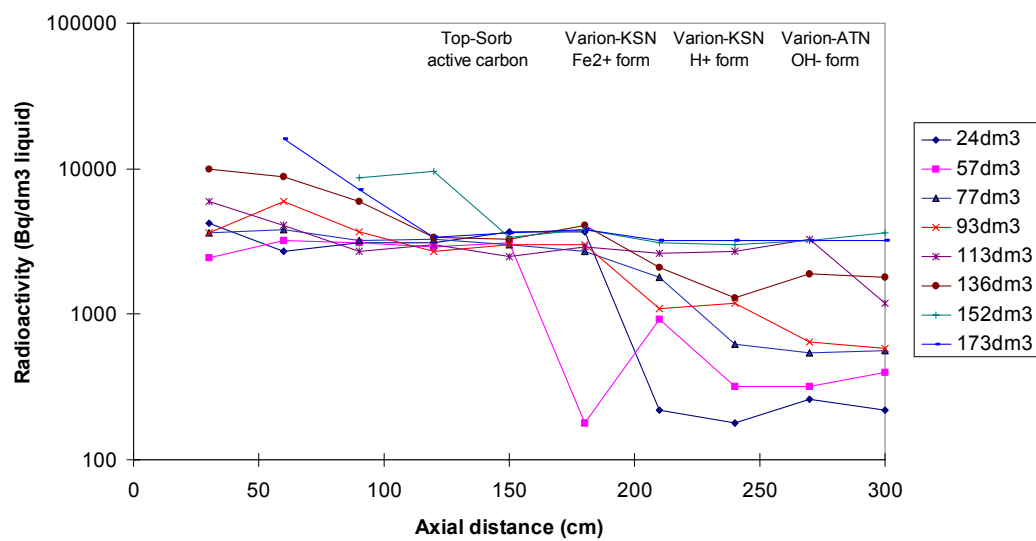


FIG. 1. The ^{51}Cr distribution at differential purified volumes in the liquid phase.

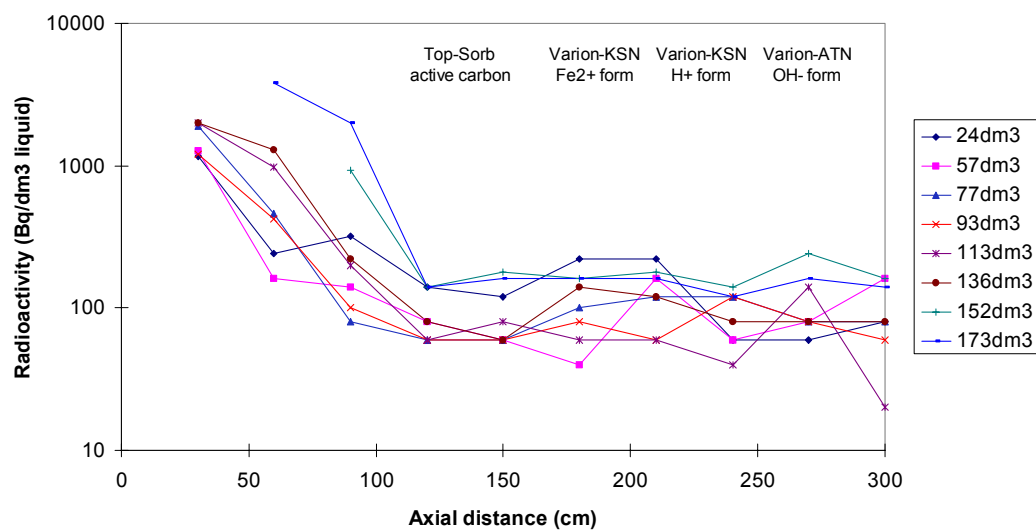


FIG. 2. The ^{54}Mn distribution at differential purified volumes in the liquid phase.

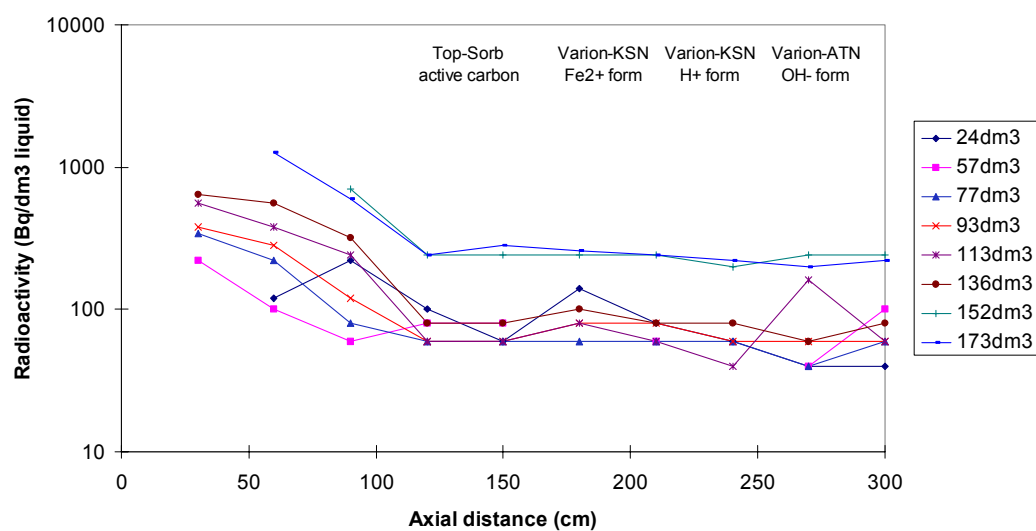


FIG. 3. The ^{58}Co distribution at differential purified volumes in the liquid phase.

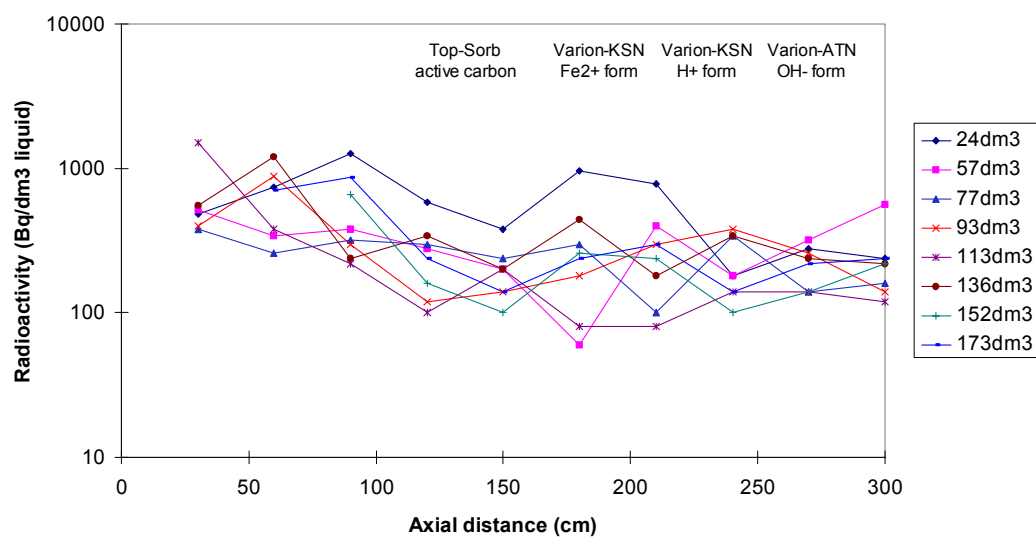


FIG. 4. The ^{60}Co distribution at differential purified volumes in the liquid phase.

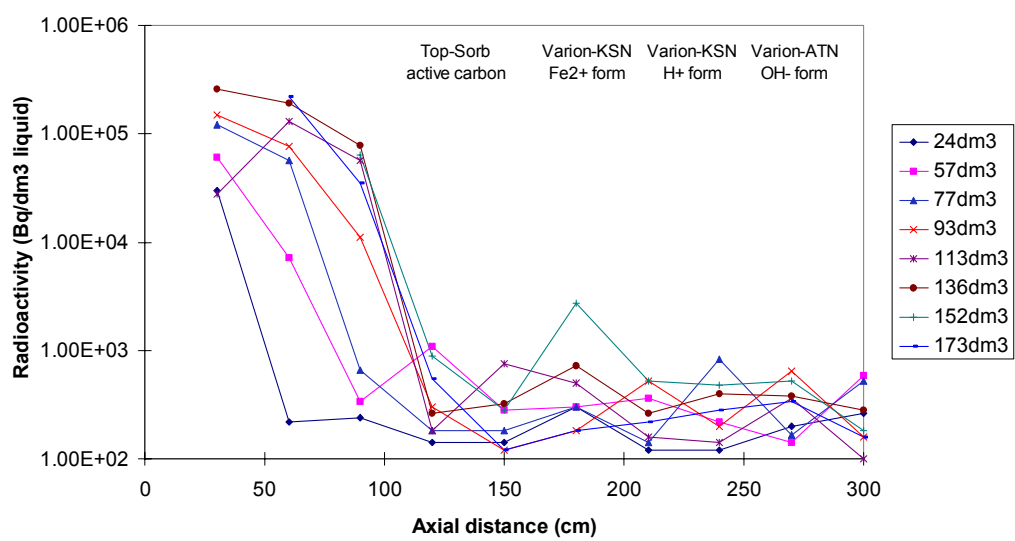


FIG. 5. The ^{110m}Ag distribution at differential purified volumes in the liquid phase.

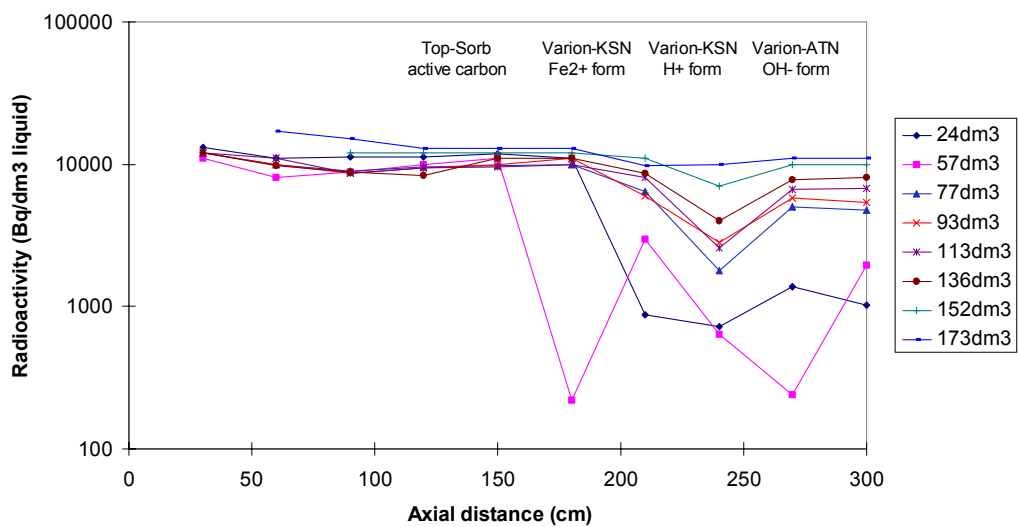


FIG. 6. The ^{124}Sb distribution at differential purified volumes in the liquid phase

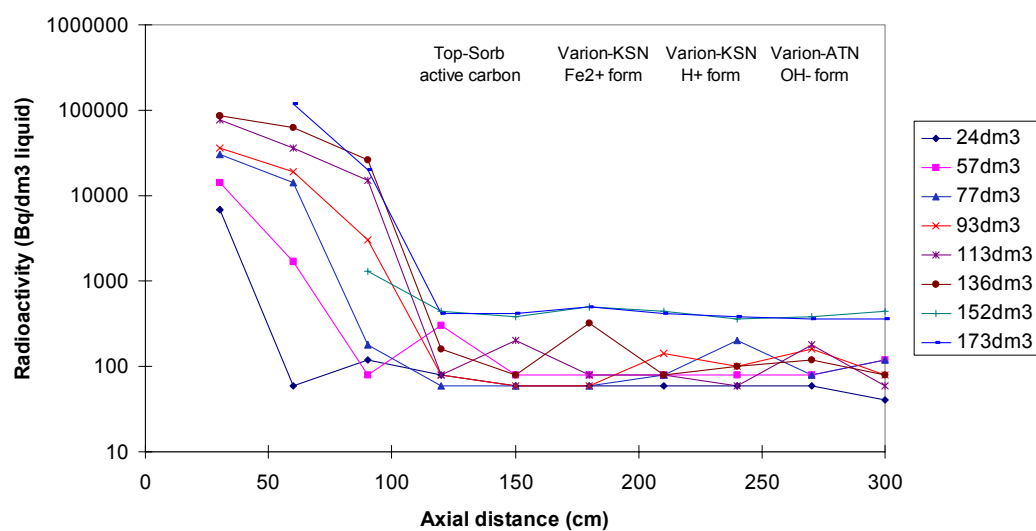


FIG. 7. The ^{95}Nb distribution at differential purified volumes in the liquid phase.

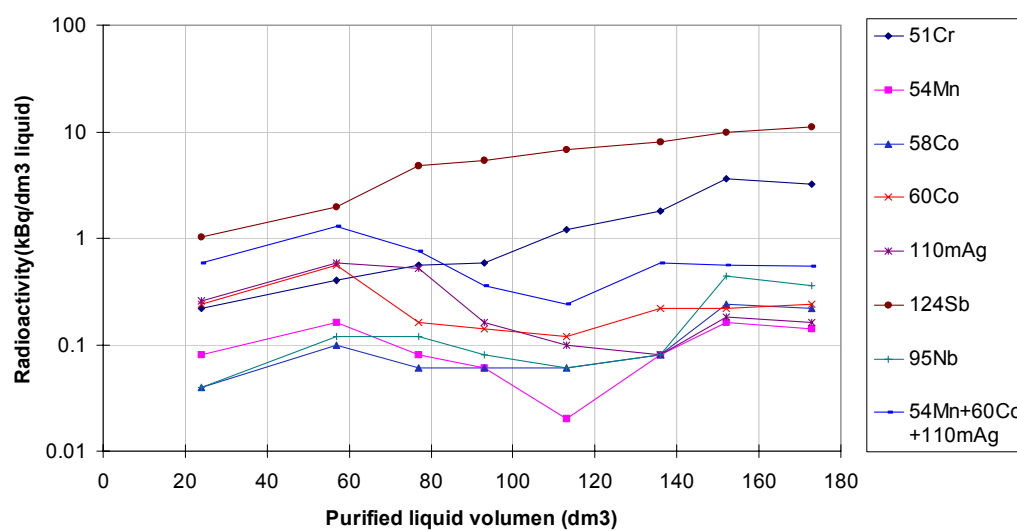


FIG. 8. The activity of the treated solution for different volumes.

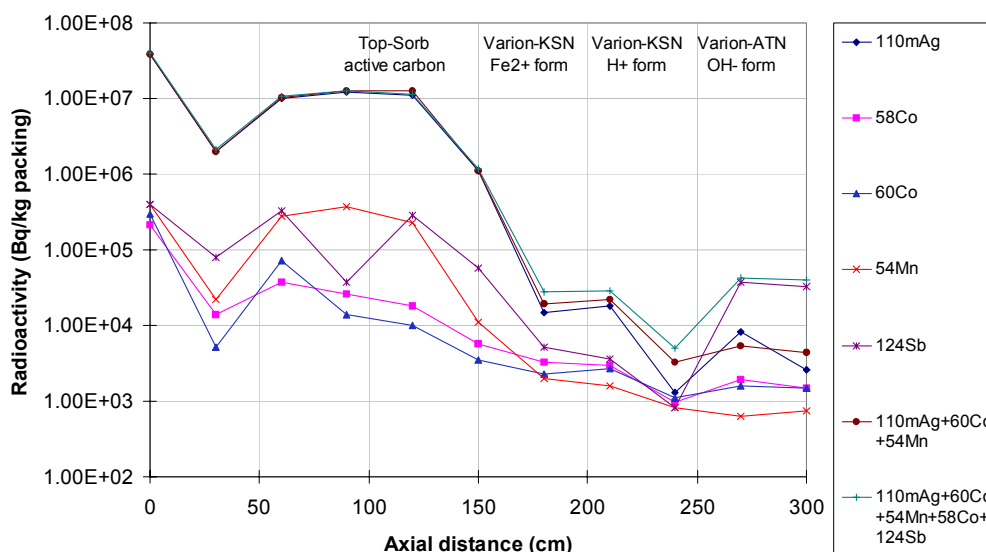


FIG. 9. The activity of the solid phase after 173L purified liquid volume.

The results of the experiments show that ^{54}Mn , ^{58}Co , ^{60}Co , ^{124}Sb and $^{110\text{m}}\text{Ag}$ radioisotopes are concentrating on the Top-Sorb active charcoal adsorbent. The concentration of ^{54}Mn , ^{60}Co , $^{110\text{m}}\text{Ag}$ for the 173 L volume is below 1 kgBq/L.

The decontamination factors (DF) are as follows:

Radionuclide	DF
^{51}Cr	256
^{54}Mn	107
^{58}Co	13.2
^{60}Co	6.7
$^{110\text{m}}\text{Ag}$	3250
^{124}Sb	7.1
^{95}Nb	639
$^{54}\text{Mn} + ^{60}\text{Co} + ^{110\text{m}}\text{Ag}$	993

The volume reduction factor (VRF) for the whole column is 24,3 for the active charcoal adsorbent layer is 40,5.

3. TREATMENT OF THE ACIDIC REDUCTIVE RADIOACTIVE SOLUTION

An acidic decontamination solution (the composition of the solution is given in Table V) was pumped through a column system (2100 mm length \times 55 mm diameter) downwards with the flow rate of $200 \text{ cm}^3 \cdot \text{min}^{-1}$ at 90°C .

The 900 mm upper part of the system was filled with activated charcoal (Top-Sorb type, University of Veszprém, Dept. of Chemical Eng.; specific surface area S_{BET} : $701.63 \text{ m}^2 \cdot \text{g}^{-1}$, pore volume: $0.5027 \text{ cm}^3 \cdot \text{g}^{-1}$, average pore diameter: 2.866 nm, particle size: 1–3 mm). A middle part of the system (800 mm) contained Varion-KSN cation exchange resins (from

Nitrochemical Works, Balatonfuzfo; particle size: 0.4–1.2 mm, in H^+ form) and the third part of the column was filled with 400 mm of Varion-ATN anion exchange resins (from Nitrochemical Works, Balatonfuzfo; particle size: 0.4–1.2 mm, in OH^- form) from top to bottom.

TABLE V. THE INITIAL RADIONUCLIDE CONCENTRATIONS ($kBq \cdot L^{-1}$) IN THE ACIDIC SOLUTION (citric acid and oxalic acid contents of the solution is $10 g \cdot L^{-3}$)

Radionuclide	^{51}Cr	^{54}Mn	^{58}Co	^{60}Co	^{110m}Ag	^{124}Sb	^{95}Nb	Σ
Activity concentration	38	280	280	940	108	16	47	1709

To determine the axial radionuclide distribution in the liquid phase during the purification, samples were taken from the liquid phase at different axial length (300, 600, 900, 1200, 1500, 1800, 2100 mm) of the column at a given purified liquid volume (18, 55, 89, 106, 126, 146, 227 L). The samples were analysed by γ spectrometry with a Ge-Li detector and a multichannel analyser (Canberra, Series 80).

The axial radionuclide distributions are shown in Figs. 10–16. The radionuclide composition of the solution leaving the column as a function of the effluent volume is plotted in Fig. 17.

To determine the axial radionuclide distributions in the solid phase after the purification, the solid phase was also analyzed following the complete drying (at $100^\circ C$ until the constant weight) with the same detector system. The radionuclide distribution curves in the solid phase can be seen in Fig. 18.

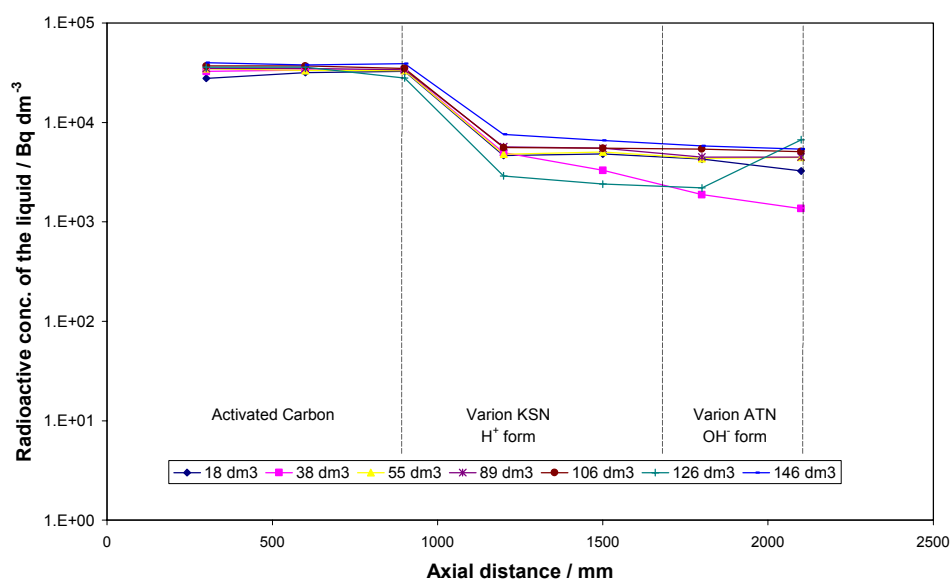


FIG. 10. The ^{51}Cr distribution in the liquid phase at different purified volumes.

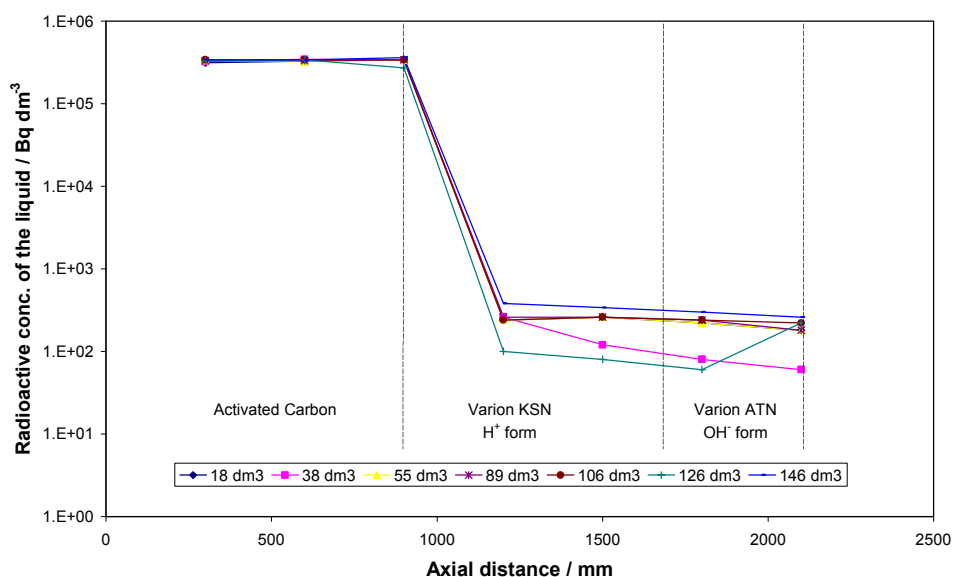


FIG. 11. The ^{54}Mn distribution in the liquid phase at different purified volumes.

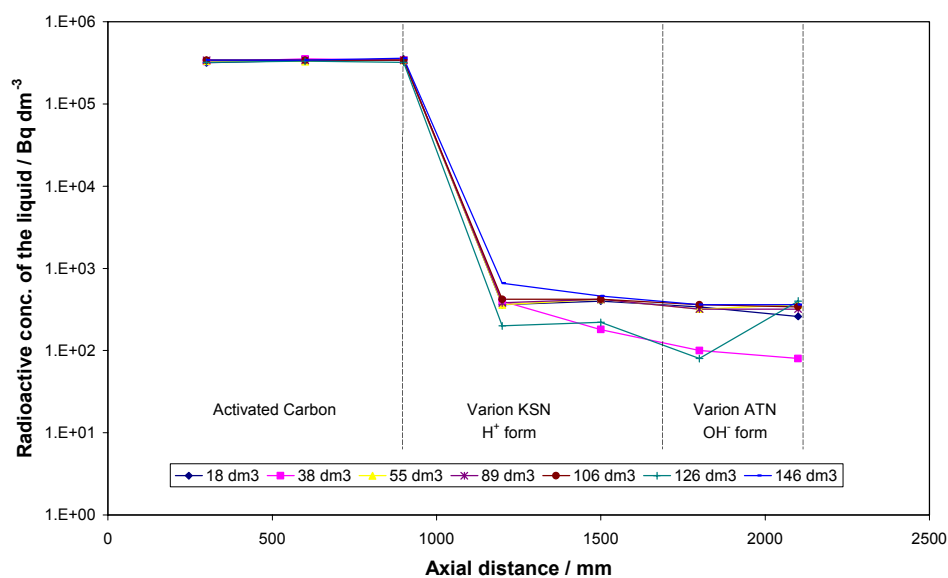


FIG. 12. The ^{58}Co distribution in the liquid phase at different purified volumes.

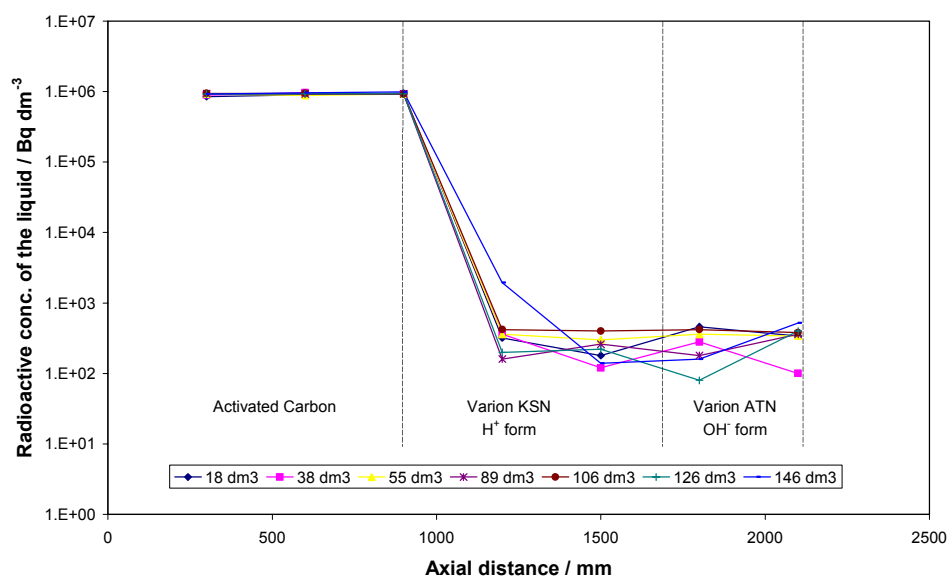


FIG. 13. The ^{60}Co distribution in the liquid phase at different purified volumes.

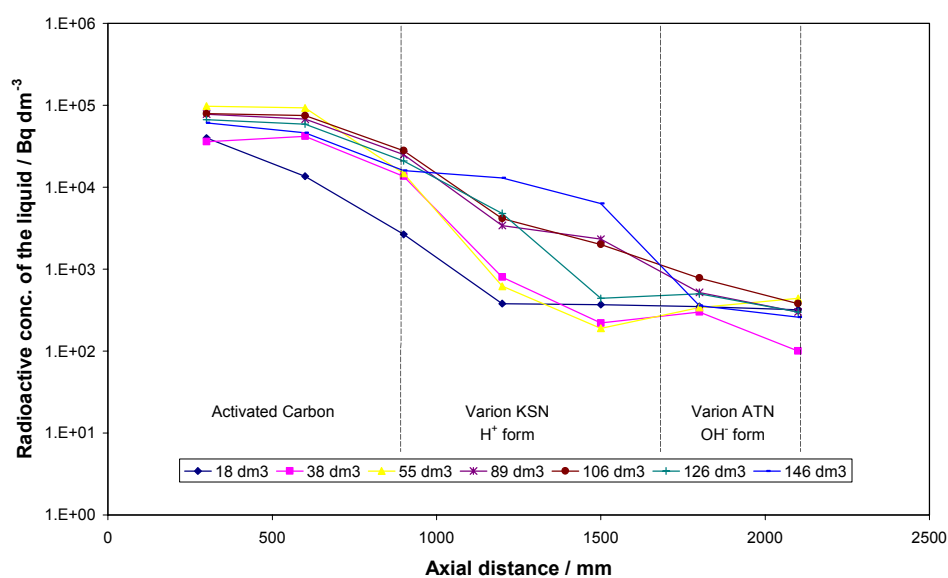


FIG. 14. The ^{110m}Ag distribution in the liquid phase at different purified volumes.

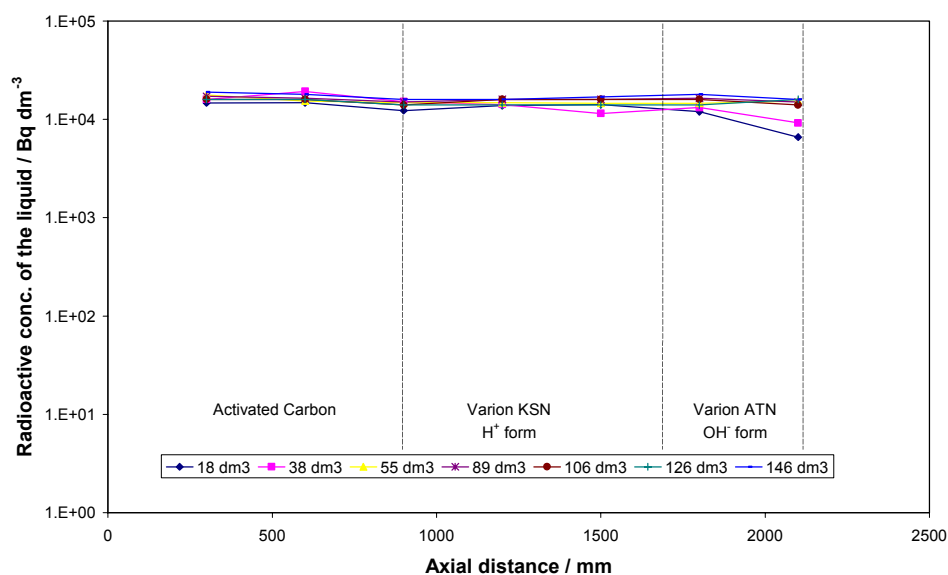


FIG. 15. The ^{124}Sb distribution in the liquid phase at different volumes.

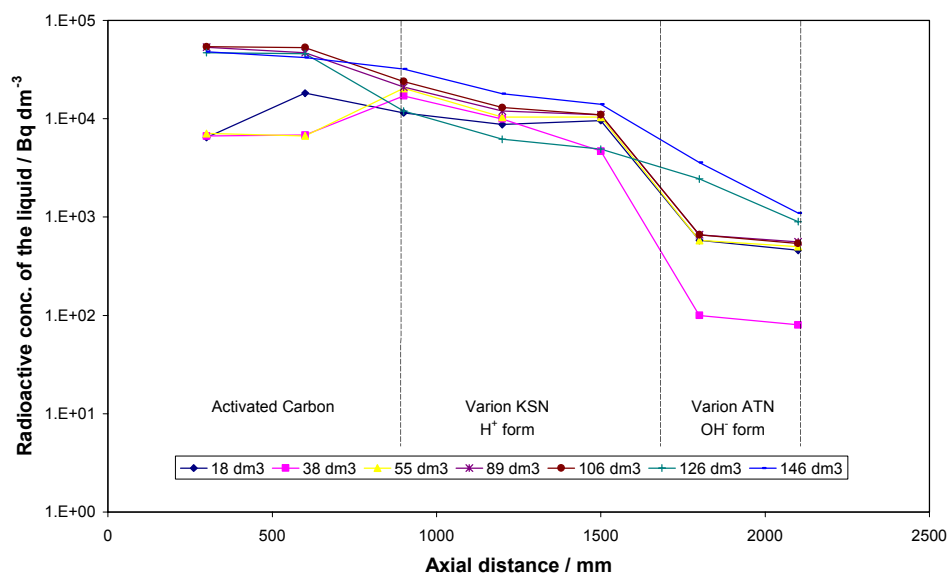


FIG. 16. The ^{95}Nb distribution in the liquid phase at different purified volumes.

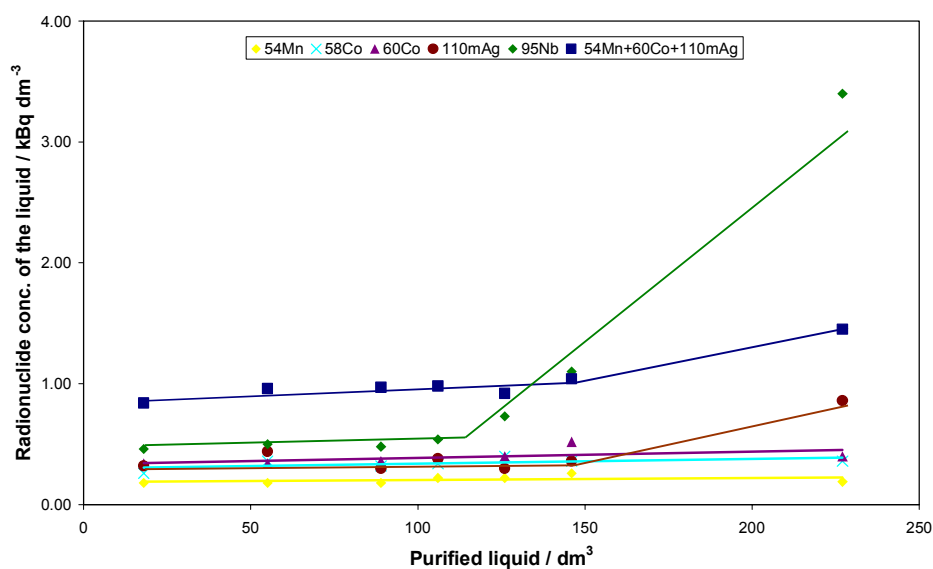


FIG. 17. The radionuclide concentration in the treated solution at different purified volumes.

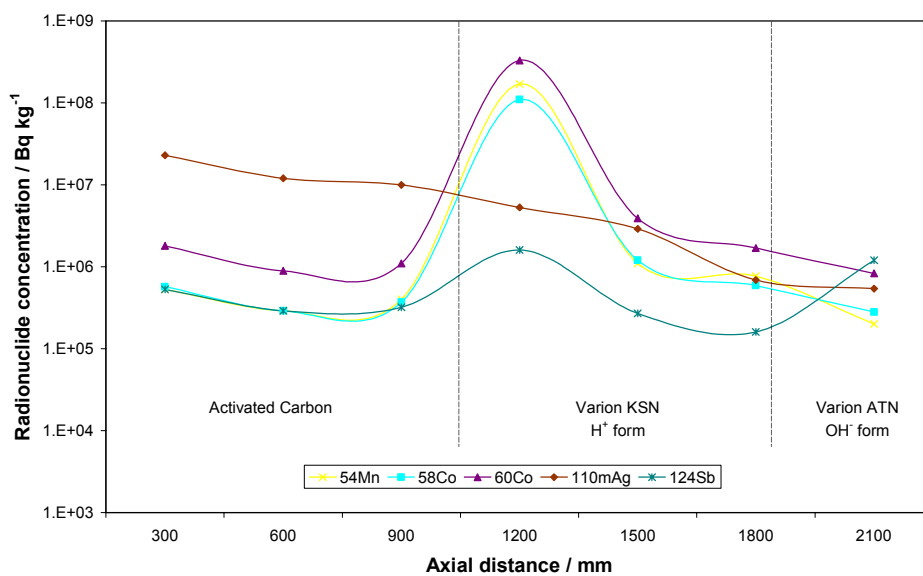


FIG. 18. The radionuclide concentration in the solid phase at 227 L purified liquid volume.

TABLE VI. THE CALCULATED DFs FOR TWO PURIFIED VOLUMES (126 AND 227 L)

Isotope	⁵¹ Cr	⁵⁴ Mn	⁵⁸ Co	⁶⁰ Co	^{110m} Ag	¹²⁴ Sb	⁹⁵ Nb	Σ ⁵⁴ Mn+ ⁶⁰ Co+ ^{110m} Ag
DF ₁₂₆	8	1273	700	2350	360	1	52	1443
DF ₂₂₇	10	1474	778	2350	126	1	14	916

The calculated VRF values are $VRF_{126} = 25.2$ and $VRF_{227} = 45.4$, respectively. (The volume of the packaging is 5 L).

4. TREATMENT OF THE LOMI RADIOACTIVE DECONTAMINATION SOLUTION

At NPP Paks, after the alkaline oxidative and acidic reductive decontamination steps, the LOMI (Low Oxidation Metal Ion) decontamination is used. (V(II) formiate 0,002–0,004 mol/dm³, EDTA 0,005–0,05 mol/dm³, NH₄OH buffer pH4,5–5 in water at 90–95°C temperature).

A radioactive decontamination LOMI liquid (the composition is given in Table VII and VIII) was pumped through a multi-layered column at 80°C.(PAV/VAN/EDTA/1 measurement)

Column I	64 cm ³ 2:1 volume ratio Varion-KSN in H ⁺ form and Top-Sorb activated carbon I.D= 1cm L=80 cm
Column II	64 cm ³ 2:1 volume ratio Varion-KSN in H ⁺ form and Top-Sorb activated carbon I.D= 1cm L=80 cm
Column III	64 cm ³ Varion-ATN in OH ⁻ form I.D= 1cm L=80 cm
Column IV	64 cm ³ Top-Sorb activated charcoal supported with K ₂ (CuFe(CN) ₆ I.D= 1cm L=80 cm

Top-Sorb activated charcoal (d_p=1–3 mm) was produced at University of Veszprém, Dep. Chem:Eng. Varion-KSN, Varion-ATN (d_p=0,4-1,2 mm) are products of Nitrokémia Works Balatonfuzfo, Hungary.

TABLE VII. THE INITIAL RADIOCHEMICAL COMPOSITION OF THE LOMI RADIOACTIVE DECONTAMINATION SOLUTION (Bq/L)

⁵¹ Cr	⁵⁴ Mn	⁵⁹ Fe	⁵⁸ Co	⁶⁰ Co	⁶⁵ Zn	⁹⁵ Zr	⁹⁷ Nb	⁹² Sr	¹²⁴ S	⁷² Ga	^{110m} Ar	Σ
30,1	1277	37,4	2119	486	24	92	65	28	468	134	68	6271

TABLE VIII. THE INITIAL CHEMICAL COMPOSITION OF THE LOMI RADIOACTIVE DECONTAMINATION SOLUTION

EDTA total	9,24 mmol/liquid /dm ³ liquid
EDTA free	2,53 mmol/liquid /dm ³ liquid
EDTA metal complex	6,71 mmol/liquid /dm ³ liquid

Metals, compounds: mg/L

Na	V	Fe	NH ₃	Mn	Ni
425	238	77.5	625	0.3	0.3

Co, Cr below the detectable limit <0,1 mg/L

The radionuclide composition of the solution leaving the different columns (I, II, III, IV) are given in Figs. 19–22.

According to the previous experimental data up to the 4330 cm³ treated volume the summarized radioactivity of ⁵⁴Mn, ⁶⁰Co, and ^{110m}Ag is below 1 kBq/dm³. VRF for columns I, II, III, IV is VRF=16,4, for the summarized ⁵⁴Mn, ⁶⁰Co, and ^{110m}Ag DF=277.

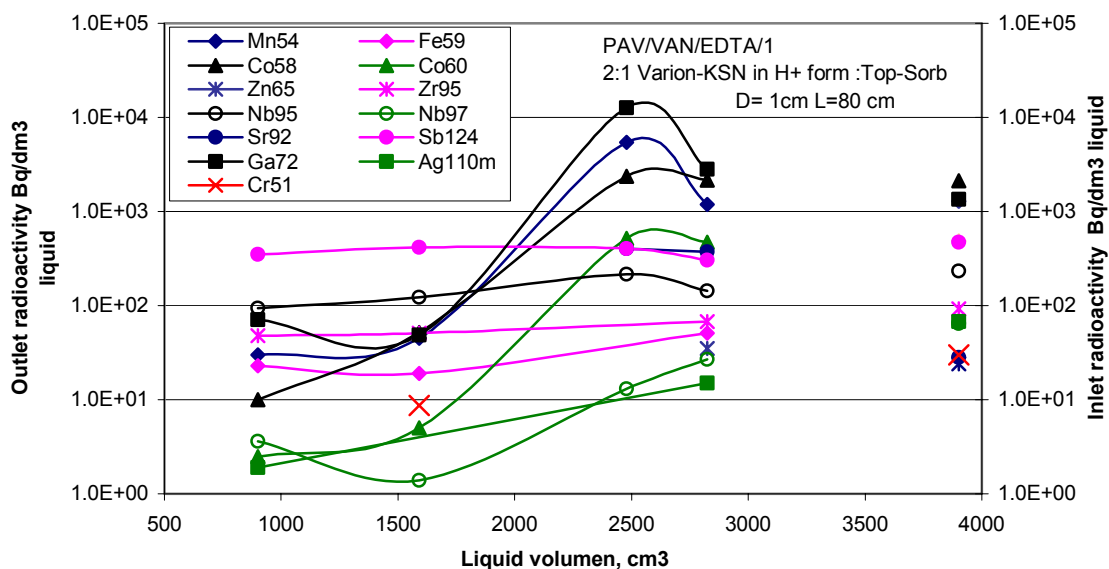


FIG. 19. Breakthrough curves of the column I.

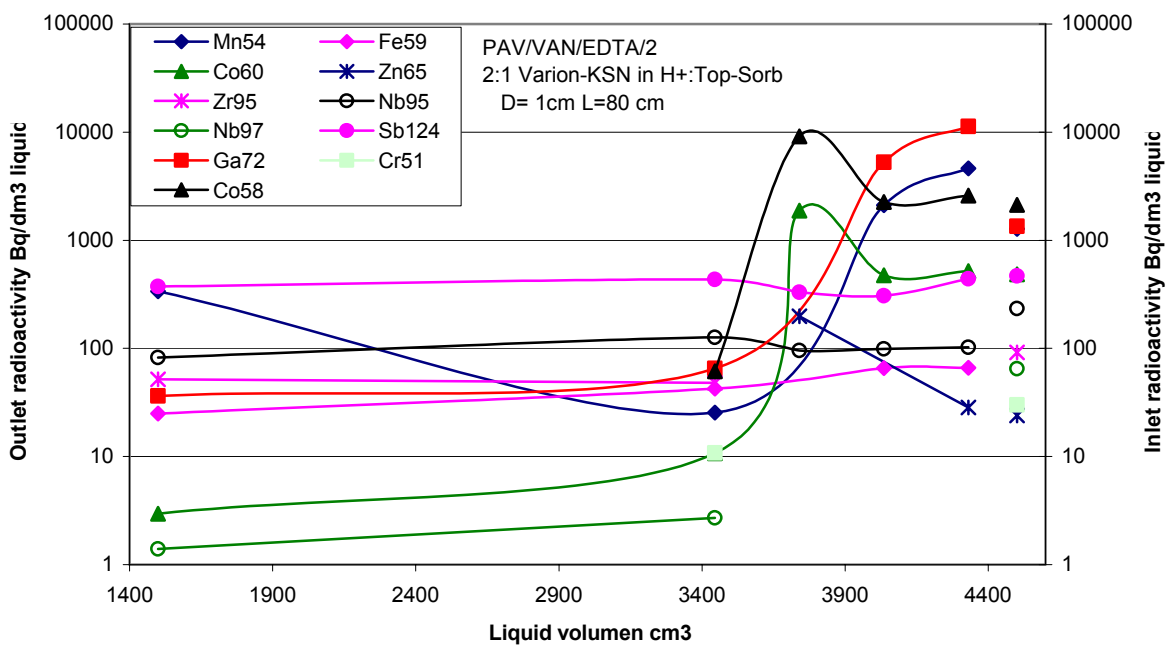


FIG.20. Breakthrough curves of the column II.

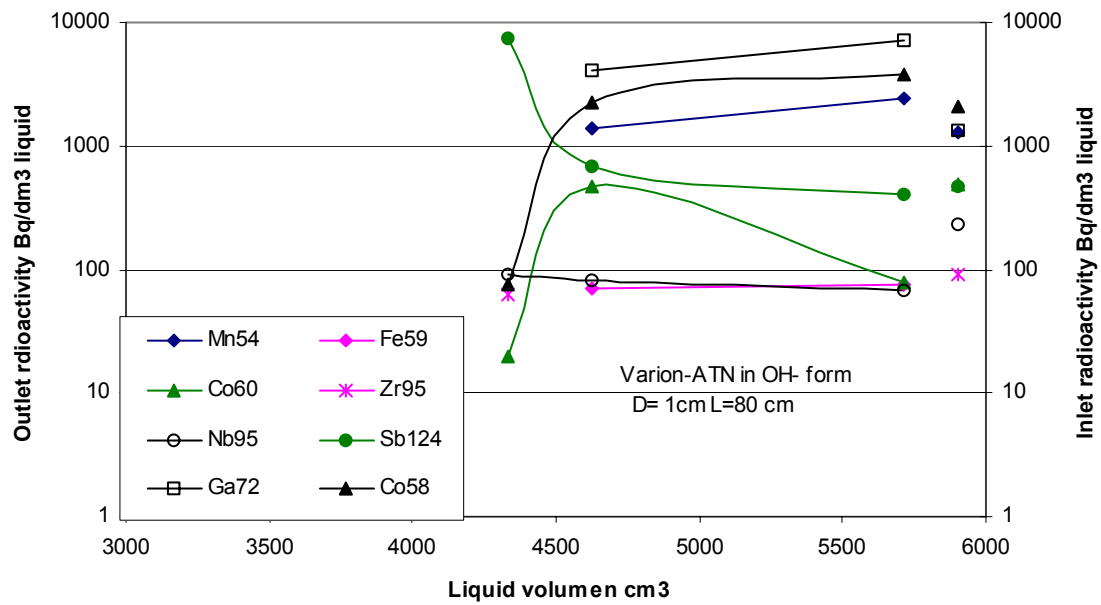


FIG. 21. Breakthrough curves of the column III.

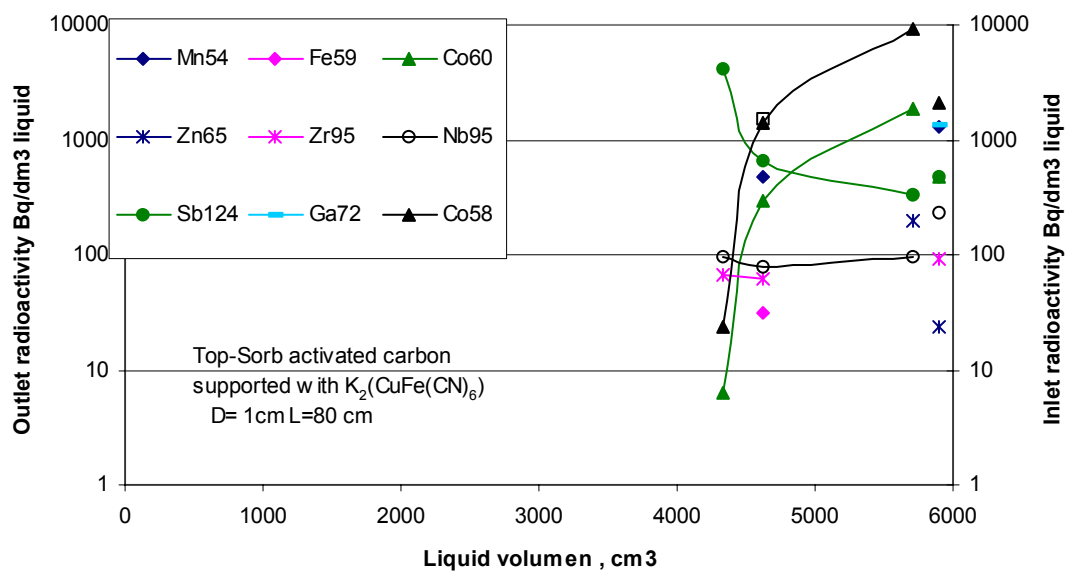


Fig. 22. Breakthrough curves of the column IV.

5 SUMMARY

The combined adsorption, ion-exchange processes for the treatment of radioactive decontamination liquids. (alkaline oxidative, acidic reductive, and complex compound containing LOMI liquids, multi-layered adsorption ion-exchange columns) have been studied. The most important results are as follows:

Alkaline oxidative radioactive decontamination liquid

DF=993 for $^{54}\text{Mn} + ^{60}\text{Co} + ^{110m}\text{Ag}$

VRF=40,5 for activated carbon column

VRF=24,3 activated carbon+ cation exchanger+ anion exchanger columns

Acidic reductive radioactive decontamination liquid

DF=916 for $^{54}\text{Mn} + ^{60}\text{Co} + ^{110\text{m}}\text{Ag}$

VRF=454 for cation exchanger layer

VRF=45,4 for active carbon+ cation exchanger+ anion exchanger columns

Complex compound (EDTA) containing LOMI radioactive decontamination liquid

DF=277 for $^{54}\text{Mn} + ^{60}\text{Co} + ^{110\text{m}}\text{Ag}$

VRF=16,4 for the activated carbon+ cation exchanger+ anion exchanger columns

As a result these studies a mobile treatment facility can be used after the in situ decontamination processes (AP-CITROX-LOMI) at the Nuclear Power Plant Paks, Hungary.

REFERENCES

- [1] MARTON, GY., SZÁNYA, T., HANÁK, L., SIMON, G., HIDEG, J., MAKAI, J., SCHUNK, J., Chem. Eng. Sci, 51 (11), 2655–2660, (1986).
- [2] SZÁNYA, T., HANÁK, L., SIMON, G., MARTON, GY., ARGYELÁN, J., MALECZKY, E., VARGA, I., MAKAI, J., SCHUNK, J., TILKY, P., II. Int. Sem. On Prim. Sec. Side Water Chemistry of NPP 19–23. Sept. (1995) Balatonfüred, Hungary.

COMBINED PROCESSES AND TECHNIQUES FOR PROCESSING OF ORGANIC RADIOACTIVE WASTE

P.K. WATTAL, D.S. DESHINGKAR, C. SRINIVAS, D.B. NAIK, S. MANOHAR
Bhabha Atomic Research Centre,
Mumbai, India

Abstract. To improve the existing practice for treatment of organic waste, in particular spent TBP/dodecane solutions, oxalic acid and spent ion exchange resins, new processes have been selected and studied. Alkaline hydrolysis was investigated as alternative to wet oxidation for processing of spent TBP solutions. Photo-degradation of oxalic acid and photo-catalytical destruction of spent ion exchange resins have been studied to process these particular types of waste. A combination of wet oxidation in association with photo-oxidation appears to be promising. In this case consumption of H_2O_2 is limited to dissolution of ion exchange resin only, and further oxidation can be achieved by photo-oxidation. The same type of treatment has been effectively applied to a solution of oxalic acid in 3M HNO_3 . Hydrolysis of TBP using NaOH mainly leads to formation of sodium salt of di-butyl phosphate (DBP) and butanol. DBP is more stable towards hydrolysis, so sodium salt of DBP, being aqueous compatible, can be directly immobilised into cement. Electrochemical oxidation in combination with other oxidation/treatment methods was also studied.

1 INTRODUCTION

Various types of radioactive organic waste emanate in the nuclear fuel cycle. Organic waste represent the risk not only from the radioactivity viewpoint but also due to their chemical nature. Any acceptable process should address these both concerns. Management options considered globally for this waste include storage, incineration, chemical destruction and even direct immobilization in matrices like cement, polymers etc.

The storage option for this waste can only be considered as an interim measure and not the final management option. In general, most of the organic wastes are not compatible with presently known immobilization matrices. Immobilization, wherever practiced for specific cases, may lead to a large increase of the volume of the final waste form. This is on account of very low waste loading acceptable by the matrix. Even though incineration of organic waste, in general, appeared attractive in the past, its adoption gets limited on account of elaborate off-gas treatment to meet authorized discharge limits for the environment. Besides, waste streams like spent TBP solvents, ion-exchange resins etc., if incinerated, generate corrosive reaction products like P_2O_5 , SO_2 , HCl etc., which not only demand special materials of construction for their handling but also generate large secondary waste volumes.

Destruction of organic waste is an attractive option as it leads to reduction in toxicity, and waste volumes thereby making waste treatment more effective, eco-friendly and economical. Variety of different destruction methods exists, the optimum method being dependent on the nature of the specific waste. These involve *chemical destruction, wet oxidation and other advanced oxidation methods*. Appropriate application of these techniques and their judicious combination can result in very effective solutions for troublesome waste streams.

Chemical destruction employing wet oxidation catalyzed with hydrogen peroxide can completely mineralize spent TBP solvents and ion exchange resins. However, higher consumption of hydrogen peroxide and the aqueous waste volumes generated thereby make it less attractive.

Other advanced oxidation processes utilizing photo/electro/sono energy in conjunction with the oxidants (hydrogen peroxide/ozone) substantially reduce the requirements of the

oxidants and in turn the volumes of the aqueous waste generated. Use of energy in these forms in conjunction with hydrogen peroxide provides higher concentration of hydroxyl radicals and also alternative oxidation reaction pathways thereby improving the decomposition kinetics. Besides, mineralization can be carried out under moderate temperatures thereby preventing self-decomposition of hydrogen peroxide.

The purpose of this study was the development of processing options for the following waste streams:

- (a) Spent *Purex solvents* generated during spent fuel reprocessing;
- (b) Spent *organic ion-exchange resins* from nuclear power plants and other waste management operations;
- (c) Spent *complexing agents* (EDTA, citric acid, and oxalic acid) from decontamination operations.

2 SPENT PUREX SOLVENTS

Purex process is widely used for recovery of plutonium and uranium from spent fuel. TBP in n-paraffin diluent (mostly n-dodecane) is used as solvent during this extraction process. The solvent undergoes chemical and radiolytic degradation during its repeated use and thus adversely affects its performance. This is then discarded as organic radioactive waste.

The typical radiochemical composition of the spent solvent (30% TBP in n-Dodecane) tried for these studies are given in Table I

TABLE I. RADIOCHEMICAL COMPOSITION OF SPENT SOLVENTS

Type of radiation	Activity concentration (Bq/mL)
Gross alpha*	740–1200
Gross beta/gamma	28,000–40,000
<i>Major fission products</i>	
Ru-106	27,000–37,000
Cs-137	30–90

*(*Pu+Am; Pu/Am= 10*)

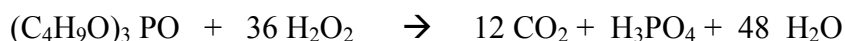
Processes investigated for the treatment of this waste stream include wet oxidation and alkaline hydrolysis.

2.1 WET OXIDATION PROCESS:

Wet oxidative mineralization using hydrogen peroxide was studied at temperatures of 95–100°C in the presence of the ferric salt catalyst (*Fenton-type oxidation*).

In the laboratory experiments, it was observed that only TBP component undergoes oxidation reaction. The dodecane portion does not take part in this reaction and separates out as the top layer in the reaction product mixture. This is on account of the fact that n-dodecane, being a saturated alkaline is normally refractory towards wet oxidative destruction.

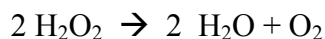
Mineralization reaction of TBP is represented by the following equation:



Laboratory experiments were conducted with non-radioactive solvent up to one litre and ferric salt as a catalyst. The reaction was carried out under constant agitation and total reflux mode. The feed streams for the experiment were as following:

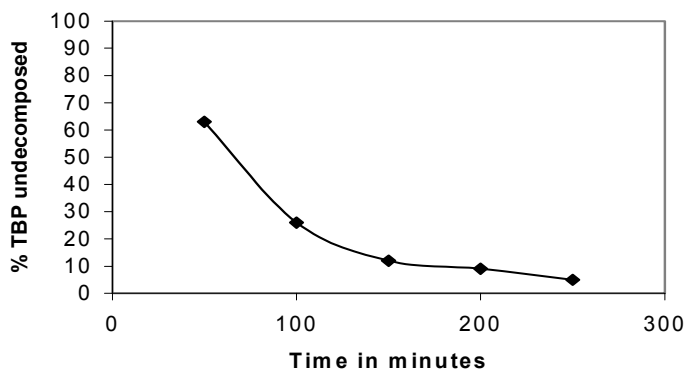
Feed solvent	35% TBP in n-dodecane
Concentration of H ₂ O ₂	35% (w/v)
Concentration of the ferric salt catalyst	0.1M
Reaction temperature	95–100°C
Addition rate of hydrogen peroxide	50–60 mL/min/L of solvent

As expected, the diluent quantitatively separated from the aqueous portion and formed the top layer of the reaction mixture. H₂O₂ consumption in the reaction was 100% in excess of the stoichiometric level. Mineralization of pure TBP (conversion to water-soluble reaction products) was very gradual giving rise to nearly heterogeneous reaction conditions. This made the oxidation very sluggish and inefficient leading to excessive consumption of hydrogen peroxide following self-decomposition side reaction:



The kinetics of the TBP mineralization is given in Fig. 1.

FIG. 1. Percent decomposition of TBP by wet oxidation



As can be seen in Fig. 1, nearly 96% of the total TBP present initially got oxidized in around 4.2 hours.

The experiments with active solvents showed similar behaviour. The TBP portion was selectively mineralized leaving the diluent portion virtually unaffected. The diluent portion formed a separate layer in the product mixture and its recovery was quantitative. Nearly 95% mineralization of TBP could be achieved in 4 hours at 95–100°C in the presence of ferric salt catalyst under reflux and constant agitation by gradual addition of hydrogen peroxide. The hydrogen peroxide demand in the reaction was 100% in excess of the stoichiometric level.

With regard to the distribution of radioactivity, the recovered diluent had an activity in the range of 2–3 Bq/mL for gross alpha and 1000–1200 Bq/mL for gross beta/gamma. The aqueous portion of the oxidation reaction mixture contained the remaining radioactivity. The

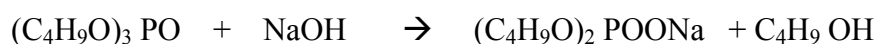
recovered diluent had high residual beta/gamma activity as against alpha. This would impose difficulties in case of diluent to be recycled and reused.

Even though the process is amenable to quantitative recovery and recycle of the diluent (n-dodecane) with less activity, excessive consumption of hydrogen peroxide and the multifold (10–12 times volume of the original waste) generation of aqueous wastes with nearly all the activity of the original solvent, makes the process less attractive for its adoption on a plant scale.

2.2 ALKALINE HYDROLYSIS PROCESS

In view of the above limitations with regard to excessive consumption of hydrogen peroxide and high aqueous waste generated thereby, an alternative process employing an alkaline hydrolysis route for destruction of TBP was investigated.

TBP being an ester of phosphoric acid is susceptible to hydrolysis. Hydrolysis of TBP using NaOH mainly leads to the formation of sodium salt of dibutyl phosphoric acid (NaDBPO₄ or HDBP, respectively) and butanol. The governing equation is:



HDBP is more stable towards hydrolysis in alkaline medium and its further hydrolysis occurs to a limited extent. The reaction products of alkaline hydrolysis, being aqueous-compatible, can be further immobilized in cement.

During alkaline hydrolysis of TBP in n-dodecane, the diluent does not take part in the reaction and separates out as top phase in the product mixture. The products of the reaction are water-soluble and get separated out of the dodecane phase rendering it free of TBP. The degradation products of TBP are also converted to their respective sodium salts and get into the aqueous phase along with most of the activity associated with these degradation products. A very small amount of activity is associated with the diluent degradation products.

Laboratory experiments with inactive simulated waste followed by actual radioactive waste were conducted for studying the alkaline hydrolysis of the solvents. Known volumes of the solvent to be hydrolyzed were mixed with 50% (w/v) aqueous NaOH solution keeping mole ratio of NaOH:TBP as 3:2 under constant agitation and total reflux conditions at 125–130°C for nearly 7 hours.

After the completion of the reaction, three distinct layers were observed in the product mixture. Top diluent layer contained, typically, less than 100 ppm of TBP. The volume of the top diluent layer did not match with the theoretically expected volume indicating thereby that the diluent separation from the bottom phase was not complete. The unaccounted portion of the diluent was observed to be present in the middle aqueous layer. The middle layer also contained entire butanol formed during the reaction. Though products of hydrolysis, viz., NaDBP, Na₂MBP and Na₃PO₄ formed in the reaction, and excess alkali were contained mostly in the bottom layer, fractions of these were also observed in the middle layer. Complete separation of the diluent entrapped in the middle layer could be achieved only after addition of water to the reaction product mixture. Addition of water equivalent to 40–50% of the volume of the original waste was found necessary for complete separation of the diluent at room temperature. This separation is on account of the vast difference in the solubility of butanol and dodecane in water.

TBP conversion and the activity distribution in the diluent phase during alkaline hydrolysis for a typical run with actual spent solvents up to a batch of 7 L is shown in Fig. 2.

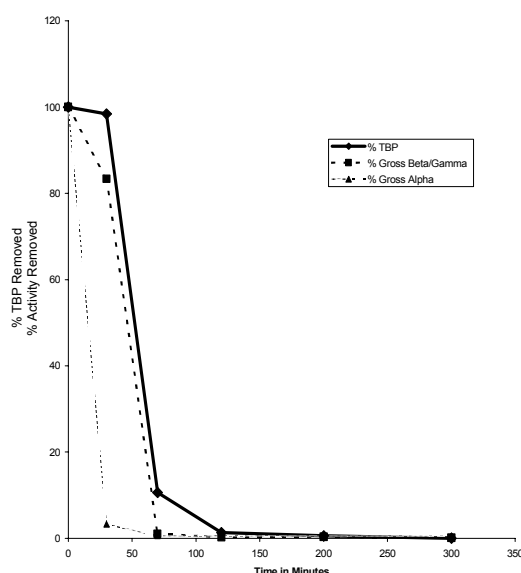
2.3 ENGINEERING SCALE DEMONSTRATION FACILITY FOR ALKALINE HYDROLYSIS OF SPENT SOLVENTS

Laboratory studies with active solutions up to 7-L scale had established the feasibility of the process. The process results in the conversion of TBP into aqueous soluble products, namely NaDBP and butanol. Based on the studies carried out, a full-scale demonstration facility (200 L/batch) was set up to establish the process on a plant scale.

2.3.1 Demonstration facility description

The plant housed a reaction kettle of 500-L capacity provided with a jacket for steam heating and a mechanical agitator mounted on top of the kettle. The reaction kettle was designed to provide 100% free board space for safe operation.

FIG. 2. TBP decomposition & decontamination achieved



A shell and tube type condenser connected to the vapor line of the reaction kettle was provided to ensure complete reflux of all vapors generated during the reaction. All inlet ports were provided on top of the kettle for feeding of waste & chemicals. These ports were provided with liquid seals in the form of loops to prevent the escape of vapors during the reaction. A bottom outlet was provided to facilitate complete draining of the contents into a separation tank located below the reaction kettle. The separation tank was provided with interphase sensing to facilitate separate draining of the two phases into designated waste collection tanks. The equipment was located at requisite elevations so as to effect gravity draining in most of the cases thereby avoiding transfer modes involving moving parts. All vessel off-gas lines/vents were connected to a common header that was routed to the exhaust blower. All the equipment was equipped with adequate instrumentation. Pneumatically operated bellow seal valves were used to demonstrate remote operability of the facility. Figure 3 shows the schematic of the process.

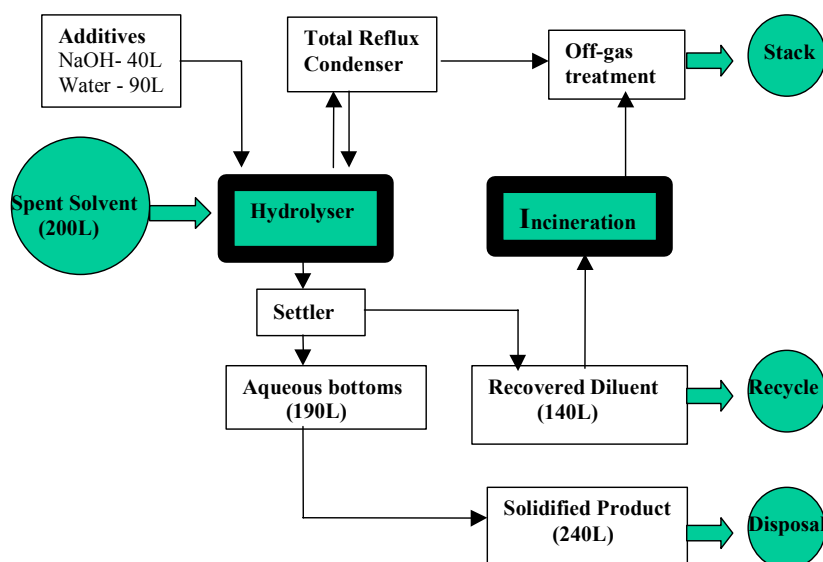


FIG. 3. Schematic of the alkaline hydrolysis process.

2.3.2 Operation of the demonstration facility

The feed to the reaction kettle consisted of 200 L of organic solvent and 40 L of 12.5 M NaOH. The organic solvent was transferred to the reaction kettle by an airlift. 40 L of NaOH was subsequently gravity drained into the reaction kettle. The contents of the kettle were continuously agitated to keep the alkali dispersed in the organic solvent. The reaction vessel was maintained below the atmospheric pressure through the condenser vent connected to the exhaust blower.

Supply of steam to the jacket of the reaction kettle was started only after ensuring the desired level of vacuum in reaction kettle and checking for closure of all inlet and outlet ports to the reaction kettle. The desired reaction temperatures were maintained by ON/OFF control of steam.

After about 5 hours of reaction at temperature in the range of 98–116°C, samples were drawn under constant agitation. On standing, these samples separated into three phases. Water was subsequently added into the reaction kettle and post reaction agitation was carried out for about 30 minutes for enabling dissolution of the middle phase. Two distinct phases were then detected by the interphase sensing probes which were concurred by the density probes provided in both the phases. The density of the top phase had decreased from about 0.80 g/cm³ (corresponding to 30% TBP in n-dodecane) at the start of the reaction to about 0.74 g/cm³ (corresponding to n-dodecane) indicating near completion of reaction. The total contents of the reaction kettle were drained into a separation tank where the phases were allowed to separate. The separated phases were collected into designated tanks for the aqueous bottoms and the recovered diluent. The results of the runs are given in Table II.

TABLE II. SUMMARY OF THE PLANT SCALE ALKALINE HYDROLYSIS RUNS

a) Operational parameters and feed streams.

Run No.	Batch vol. (L)	Additives			Reaction temp. (°C)	Reaction time (h)	Heating media steam (psig) *	System pressure (kPa)
		Alkali (L)	(Conc.)	Water (L.)				
1	200	48.0	12.20M	90.0	95–114	5.0	20–30	97.4–98.3
2	200	37.0	13.00M	90.5	95–116	5.0	15–30	97.4–98.3
3	200	36.5	12.45M	90.0	95–114	5.0	15–30	97.4–98.3

*Although steam pressure up to 20 psig is sufficient for the process, pressures up to 30 psig were used to check the adequacy of the condenser with respect to higher boil up rates (at the end of reaction time).

b) Conversion and recovery after hydrolysis

Run No.	Batch vol. (L)	TBP hydrolyzed		Dodecane recovered		Water added (L)	Aqueous bottoms for immobilization (L)
		Init. Vol. (L)	%Hydrolyzed.	Init. Vol. (L)	% Recovered.		
1	200	60	100.00	140	98.57	90.0	190
2	200	60	99.98	140	98.31	90.5	187
3.	200	60	99.90	140	98.90	90.0	190

Based on the above experiments a full scale plant for the processing of spent solvents has been built.

2.3.3 Immobilization of the aqueous bottoms

Experimental studies carried out on immobilization of the aqueous waste generated from the treatment step in cement matrices have established the compatibility of the waste with the matrix. Blocks with the waste to cement ratio of 0.4 were seen to set within 24 h with no bleed liquid. After curing for a period of 28 days these blocks were subjected to leach tests. Leaching procedures followed were as per ISO standards. Leaching results for a typical block are given in Fig. 4.

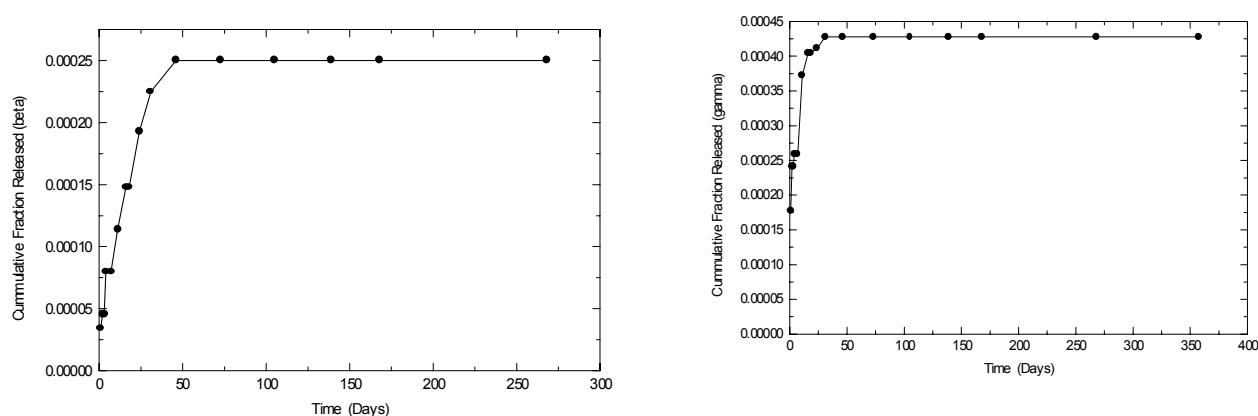


FIG. 4. Leach results of the waste immobilized in cement matrix.

In order to assess operational parameters like sequence of waste and cement addition, mixing time etc., full-scale blocks were made by mixing 150 kg of OPC with 60 L of waste using a nauta mixer. These experiments have established process parameters with regard to good homogenization of mix at water to cement ratio of 0.4. No bleed liquid was observed after 24 hours and the blocks had set well. Core drilled samples of these cured blocks were subjected to compressive strength tests and the average strength of these blocks were found to be around 18 MPa.

3 SPENT ORGANIC ION EXCHANGE RESINS

3.1 INTRODUCTION

Processing of spent ion exchange resins (polystyrene divinyl benzene) by traditional encapsulation in cement is associated with problems such as setting, swelling and disintegration. Direct incineration is also not attractive in view of elaborate off-gas treatment and large amount of secondary waste generated.

Conversion of organic resins into inorganic products by oxidative decomposition appears to be an attractive option as it converts the unstable organic waste into a chemically inert inorganic waste, which is further amenable to conventional waste management practices.

Wet oxidation of ion exchange resins using catalyzed hydrogen peroxide (Fenton-type reaction) needs to be conducted at elevated temperature of 95–100°C in order to obtain significant reaction rates. However, as seen in the wet oxidation of Purex solvent, this leads to wasteful decomposition of hydrogen peroxide requiring its use in large stoichiometric excess. This can be minimized if the reaction is conducted at lower temperature, preferably at ambient temperature. Ambient temperature operation not only minimizes H₂O₂ self-decomposition but also enhances process safety and simplicity. Alternatively, uses of UV to enhance these reactions have yielded significant increase in the rate of reaction. This being an ambient temperature operation, it leads to high efficiency in the use of hydrogen peroxide. Besides a number of photo induced reactions are also possible which help in mineralizing the organic content. All in all it leads to sub-stoichiometric requirement of hydrogen peroxide.

For photo-Fenton reaction to be effective, it has been observed that the spent ion exchange resins have to be in the form of dissolved solutions. This necessitates that the solid form of ion exchange resins be converted to a solution form. This has been achieved by dissolution of the resin beads in hydrogen peroxide to form a clear homogeneous solution. Therefore these solid ion exchange resins are converted to water-soluble products by reaction with sub-stoichiometric quantity of hydrogen peroxide. The second stage involves the eventual mineralization of the dissolved resin products.

3.2 PARTIAL OXIDATION OF ION EXCHANGE RESINS

It was decided to adopt a chemical method of dissolution of resins using catalyzed hydrogen peroxide followed by photo-Fenton mineralization. Experiments were conducted to optimize this initial dissolution process with regard to minimum hydrogen peroxide consumption and the temperature for cation, anion and mixed resins.

The dissolution reaction can be represented as follows:



Parallel reactions during dissolution include:

- (a) Dissolution of the solid resins;
- (b) Oxidation of the dissolved resins in the aqueous phase;
- (c) Wasteful self-decomposition of hydrogen peroxide.

Second and third reactions need to be minimized and the hydrogen peroxide employed should be utilized only for dissolution of the resins. The dissolution reaction was too slow at ambient temperature (30°C) requiring 10–24 hours and was highly dependent on the catalyst and the hydrogen peroxide concentration. The summary of the laboratory results obtained up to 2 kg at temperatures in the range of 95–100°C is given below in Table III.

TABLE III. DISSOLUTION OF ION EXCHANGE RESINS BY CATALYZED HYDROGEN PEROXIDE

Run No.	Resin type	Dry resin wt (g)	Catalyst/Additives	H ₂ O ₂ (mL)	Reaction time (h)	Volume of unreacted resin (mL)
1	Cationic	1000	CuSO ₄ : 12.5 g Free water : 3000 mL	8400	8.0	0
2	Cationic	1000	CuSO ₄ : 12.5 g Free water : 125 mL	1000	2.0	240
4	Cationic –30% Anionic – 70%	1000	CuSO ₄ : 12.5 g Free water : 1000 mL	1000	5.0	400
5	Cationic –30% Anionic – 70%	1000	CuSO ₄ : 12.5 g Free water : 1000 mL	2900	5.0	450
6	Cationic –30% Anionic – 70%	2000	CuSO ₄ : 25 g Free water : 500 mL	5300	5.0	860

In case of cation resins, the unreacted portion of resins could be dissolved by further addition of hydrogen peroxide. However, in the case of undissolved resins arising from mixed resins, further addition of the oxidant did not effect the desired dissolution. This could be, partly, on account of the fact that the functional group of anion resins dissociates at higher temperature rendering the polymer backbone hydrophobic.

The same reaction when conducted at 50–60°C under similar conditions led to complete dissolution of cation resins. The complete dissolution of anion resins required their conversion into the chloride form. This could be due to the known reaction of OH radical intermediates with chloride ion. It was noticed, in the case of mixed resins, that the cation portion could be selectively dissolved without affecting the anion portion. The anion portion after separation from the dissolved cation resins solution could be completely oxidized. The dissolution experiments showed that proper temperature control and adequate agitation of the reaction mixture are essential for the successful dissolution of resins.

3.3 PHOTO-FENTON MINERALIZATION OF THE DISSOLVED RESINS

The photo-Fenton process was selected for the mineralization of the dissolved resins solutions on the basis of the following considerations:

- (a) Absorption spectrum of the dissolved resins.
- (b) High total organic carbon (TOC) and chemical oxygen demand (COD) of the resin solution.
- (c) Advantage of conducting the reaction in the homogeneous liquid phase.
- (d) Moderate radiant power requirement by this reaction.

3.3.1 Laboratory-scale photochemical experiments

Laboratory experiments were conducted at room temperature in an immersion-type photochemical reactor equipped with a double walled quartz well and Hg vapor lamp. The experiments showed that the dissolved resin mineralization could be achieved in 3 to 5 hours time with stoichiometric quantity of H_2O_2 in the presence of ferrous sulphate as catalyst. The extent of mineralization by photo-Fenton reaction was observed by following the drop in TOC from an initial value of 30 g/L with time. Ferrous sulphate having concentration of 3000 ppm was used as catalyst. Figure 5 shows the kinetics of oxidation for dissolved cation and anion resins.

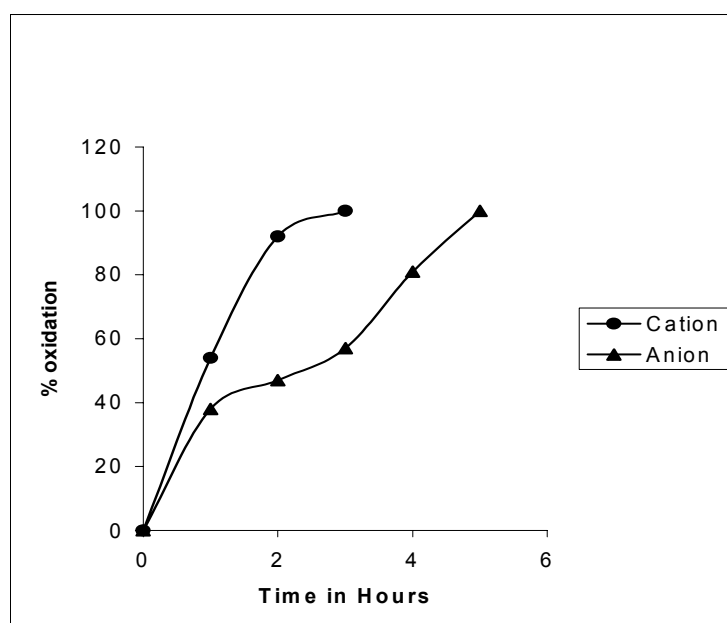


FIG. 5. Photo-Fenton oxidation of ion exchange resins.

3.3.2 Pilot scale photo-Fenton experiments

Based on the successful laboratory studies, pilot scale experiments were conducted in an immersion type photo-reactor of 50 L capacity equipped with the high pressure mercury vapor lamp of one kW capacity. The feed solutions used had initial COD of 100 g/L. A batch of 18 L of this solution was subjected to photo-Fenton reaction. Near complete mineralization was achieved after about 8 h of reaction time and about 10 L of 50% hydrogen peroxide was added during the reaction. The temperature maintained during the reaction was in the range of 30–50°C. The extent of mineralization expressed in terms of COD values of the solution with time is given in Table IV.

TABLE IV. MINERALIZATION OF RESIN SOLUTIONS IN THE IMMERSION TYPE BATCH REACTOR

Time (hours)	COD (g/L)
0.0	100
2.7	63*
4.0	30
6.0	27
8.5	2

* 50% of the stoichiometric value of hydrogen peroxide introduced

The pilot experiments in the immersion reactor clearly demonstrated that photo-Fenton reaction is effective for mineralizing high TOC dissolved resins. However, the use of high-pressure Hg lamps in these reactors has normally the drawback of low radiation efficiency. Also, the heat generated by these lamps requires proper cooling arrangements.

Alternatively, it is more advantageous to use flow type of systems, which have better adaptability for plant scale operations. In view of this, the tubular type of flow reactors was used to study its performance for photo-Fenton reaction. This reactor was equipped with UV and visible light sources instead of the high pressure Hg lamp.

For photo-oxidation processes alone it is reported that the flow stirred batch reactors are more efficient than tubular flow reactors. This is probably because of the liquid elements continuously sweeping the radiating surface thereby giving much greater utilization of the photons. Whereas in the tubular flow reactors, operating in the laminar flow range, the photon flux attenuates rapidly from the radiating surface. However, for a photo-Fenton reaction, the performances for both the reactors were more or less comparable.

The experiments conducted on dissolved cation resin solutions are summarized below. Figure 6 gives the photograph of the tubular flow system used in this study.

Solution volume	12.5 L
Initial COD	11.0 g/L
Final COD	1.1 g/L
Reacton temperature	25–35°C
Reaction time	3.3 hours
50% H ₂ O ₂ added	1.0 L



FIG. 6: Photograph of the tubular photochemical reactor

3.3.3 Decontamination studies

The solutions obtained after initial dissolution of ion exchange resins using sub-stoichiometric catalyzed hydrogen peroxide were treated by chemical precipitation for removal of radioactivity. This was attempted with the objective of minimizing down stream activity for further processing, involving photo-Fenton reactions. These solutions had the organic contents equivalent to 55 g/L of chemical oxygen demand (COD) and pH in the range of 2–2.5. The significant radionuclides in these solutions are typically activation products ^{60}Co , $^{55,59}\text{Fe}$, ^{54}Mn and ^{51}Cr and fission products $^{137,134}\text{Cs}$ and ^{90}Sr .

Chemical precipitation of transition metal radionuclides (^{60}Co , $^{55,59}\text{Fe}$, ^{54}Mn and ^{51}Cr) involved the use of their respective carriers along with potassium hexacyanoferrate and 8-hydroxy quinoline for effective decontamination. In presence of hexacyanoferrates ^{137}Cs is removed by ion exchange. Barium chloride added reacts with copper sulphate already present in solution (catalyst during initial dissolution by wet oxidation) to form barium sulphate which acts as co-precipitation agent for decontamination of Sr.

The optimized composition of the precipitating agent and the DFs achieved are given in Table V.

TABLE V. CHEMICAL PRECIPITATION REAGENTS AND DFs ACHIEVED

Reagents and tracers added per litre of resin solution

$\text{K}_4\text{Fe}(\text{CN})_6$	125 mili moles
Ni(II), Co(II), Mn(II)	100 mg each,
BaCl_2	100 mili moles
8-hydroxy quinoline	25 mili molar
Tracers	0.01-0.1 micro curies/L

Decontamination factors obtained

Radionuclide	DF
^{137}Cs	60000
^{60}Co	29500
^{54}Mn	365
^{59}Fe	700
$^{85+89}\text{Sr}$	71

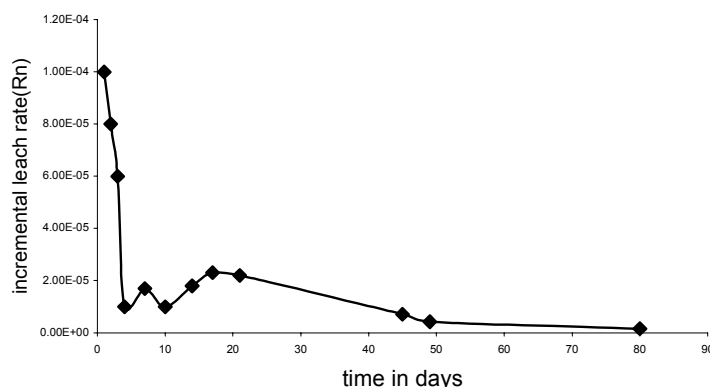
These results clearly show that chemical precipitation can be effectively used to achieve high DFs for activation and fission products from high COD aqueous solutions resulting from resin dissolution. The precipitation reagent concentrations used were higher than those generally employed for treatment of LLW. The supernant having COD of 55 g/L can be subjected to photo-Fenton reaction for effective destruction of organics. Subsequently, these potentially active wastes free of organics can be treated as LLW waste. The sludges generated during precipitation can be incorporated in cement based matrices.

3.3.4 Immobilization of sludges generated during chemical precipitation of radionuclides from dissolved resin solutions

$^{134,137}\text{Cs}$ and ^{60}Co are predominant radionuclides in the sludges generated from chemical precipitation. After adjusting the pH to 9.0, the sludge was incorporated into OPC with additives that included vermiculite, activated charcoal and silica fumes in different

proportions for improving leachability, especially for ^{60}Co and ^{137}Cs . Loading of the sludge up to 40 wt. percent was tried. After curing for 28 days, the leaching test was carried out as per ANSI 16.1 The composition of additives was optimized by making a number of blocks to achieve low leach rates.

FIG. 7. Incremental leach rate (Cs) for cement blocks incorporating sludge



The results show that activated charcoal, vermiculite and silica fumes were highly effective for reducing the leaching of ^{60}Co and ^{137}Cs . Since the ^{60}Co is known to have high leach rates from cement matrix in the presence of organic complexing agents like carboxylic acids, combination of additives such as vermiculite, charcoal and silica fumes were used to improve upon the leach behavior. For cesium, vermiculite alone was an effective additive. The incremental leach rates of the cement blocks incorporating the ^{60}Co and ^{137}Cs traced sludges are indicated in Fig. 7. The leachability indices calculated for the ^{60}Co and ^{137}Cs blocks were 13.0 and 13.6 respectively against the minimum acceptable value of 7.

Based on these developments, a treatment scheme which can be envisaged as an alternative to direct immobilization is shown in Fig. 8

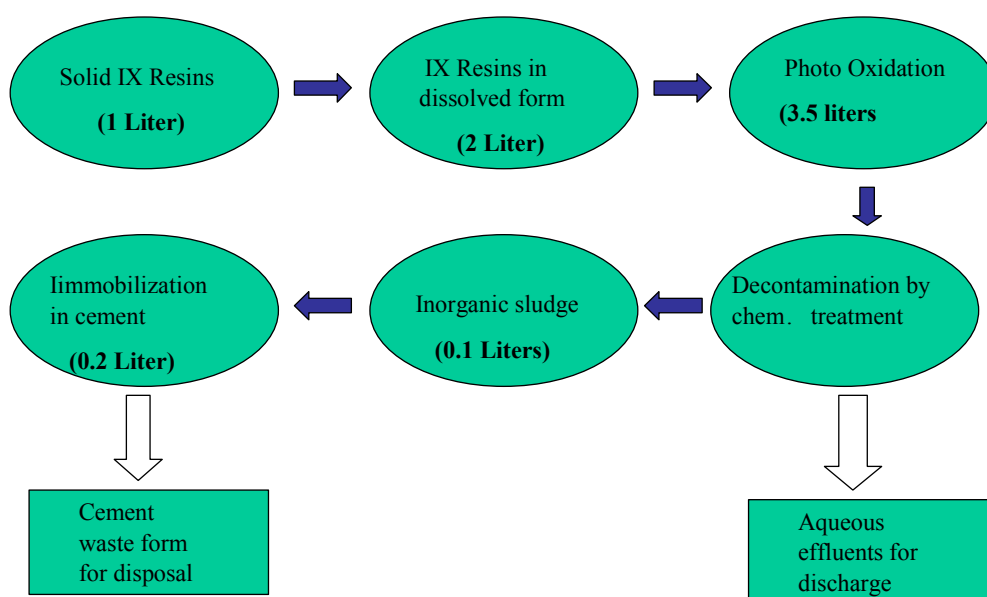


FIG. 8. Treatment scheme and waste volumes (ion exchange resins.)

4 SOLUTIONS OF COMPLEXING AGENTS (EDTA, CITRIC AND OXALIC ACIDS)

Chemical decontamination is widely used employing aqueous solutions of organic acids such as EDTA, citric acid, oxalic acid and ascorbic acid for complexation and dissolution of various radioactive ions from metal surfaces. Radioactive aqueous wastes containing 100–1000 ppm concentration of these complexants are generated during decontamination operations at nuclear reactors. Oxidative destruction of these compounds facilitates subsequent steps in the treatment and disposal of these aqueous wastes. Photochemical oxidation method is ideally suited for this kind of waste. Experiments were conducted in the laboratory scale immersion type photoreactor and the pilot scale tubular photoreactor employing simulated solutions of these formulations.

4.1 LABORATORY EXPERIMENTS IN IMMERSION-TYPE PHOTO REACTOR

The experiments showed that the photo-Fenton reaction is superior in terms of faster kinetics to UV-hydrogen peroxide method for mineralization of this waste stream. It may be on account of the high photosensitivity of various carboxylate complexes of ferric ion over a broad wavelength range. The laboratory experiments were conducted on individual constituents as well as the composite solutions containing EDTA, citric acid and ascorbic acid (ECA). The irradiation was effected by 200-watt high-pressure mercury vapor lamp. Experiments were conducted on 500 mL of sample solutions. Mineralization of ECA formulation under photo-Fenton conditions in the laboratory immersion reactor is shown in Fig. 9. The results demonstrate that it is feasible to mineralize these formulations rapidly at ambient conditions.

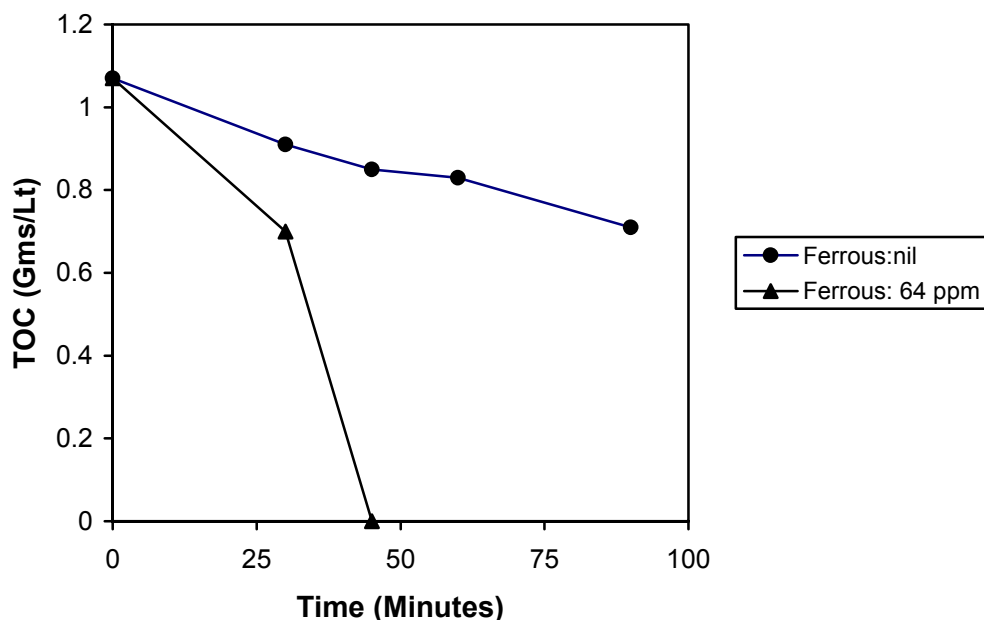


FIG. 9. Mineralization of organic decontamination formulation, EDTA-citric acid-ascorbic acid under photo-Fenton conditions.

4.2 PILOT SCALE EXPERIMENTS IN THE TUBULAR FLOW PHOTO REACTOR ON THE SOLUTIONS OF COMPLEXING AGENTS

These experiments were conducted using UV-hydrogen peroxide method in a recirculatory mode at ambient temperature.. The details of the feed solutions and the conditions were as under.

Dissolved organic solute concentration: 1000 ppm
Lamp used: low pressure mercury vapour lamp: 39 W
Temperature: Ambient
Hydrogen peroxide (40%): 100–200 mL

These results also confirmed the need for photo-Fenton conditions for faster kinetics to be achieved for mineralization of these organic substrates.

Typical results are summarized in the Table VI.

TABLE VI. PHOTOCHEMICAL OXIDATION OF ORGANIC COMPLEXING AGENTS IN TUBULAR FLOW PHOTO REACTOR BY UV-H₂O₂ METHOD

Substrate	Volume of aqueous solution (L)	Flow rate (mL/min)	Recirculation time (hours)	Oxidation (%)
Citric acid	15	70–80	4	65
Citric acid	7	320–340	5	92
Citric acid	15	10–20 L/min	2	85–90*
EDTA	15	70–80	5	20
EDTA-Na salt	7	320–340	5	80
Oxalic acid	7	70–80	5	64
Oxalic acid	7	320–340	5	90

* This experiment was conducted in the presence of ferrous sulfate catalyst

5 CONCLUSIONS

As is the case with aqueous radioactive waste, organic waste also quite often requires combination of processes to meet the requirement both for radioactivity as well as organic content. Appropriate choice of processes and their combination have yielded significant reduction not only in the waste volumes but have also reduced the organic contents for final disposal/discharge.

For spent solvent wastes, alkaline hydrolysis results not only in the conversion of TBP into aqueous soluble reaction products but also recovers the diluent practically free of TBP and radioactivity. The radioactivity consolidated into the aqueous phase can be immobilized in cement based matrices.

Advanced oxidation methods appear to be a prudent choice for waste streams like spent ion exchange resins and other organic complexing agents (used for decontamination purposes). Organic ion exchange resins in the bead form are highly resilient to decomposition by oxidation. For these resins a combination of processes involving catalytic wet oxidation for solubilising these resin into aqueous media followed by mineralization using photo-Fenton

reactions is very effective. This combination of processes results in substantial reduction in the oxidant used and also minimum secondary volumes. These solutions are also amenable to decontamination by conventional methods such as chemical precipitation etc., which results in minimum volumes for waste disposal/discharge. A generalized schematic for organic waste could be envisaged as given in Fig. 10.

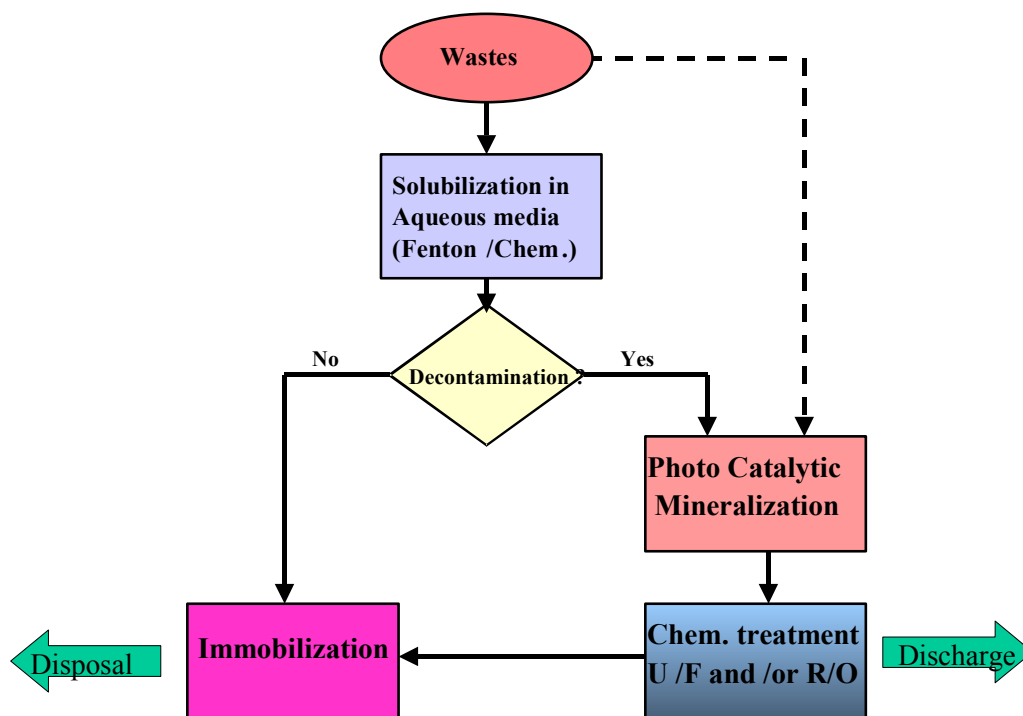


FIG. 10. Combined treatment of organic wastes.

COMBINED TREATMENT OF AQUEOUS RADIOACTIVE WASTE CONTAINING URANIUM, THORIUM AND RADIUM RADIONUCLIDES BY CHEMICAL PRECIPITATION AND LATERITE SOIL SORPTION

SYED HAKIMI SAKUMA, NIK MARZUKEE, MOHD KHAIRUDDIN
Malaysian Institute for Nuclear Technology Research (MINT), Malaysia

Abstract. A combination of methods was investigated to treat waste streams containing soluble uranium, thorium and radium. 1) A chemical precipitation pretreatment of the liquid waste streams studied resulted in nearly 100% removal of radium, thorium and uranium at the optimum pH 9.9 (decontamination factors 391, 234 and 80, respectively). Thorium hydroxide ($\text{Th}(\text{OH})_4^0$) were the dominant species forming the precipitate, for uranium in absence of carbonate the solubility limiting species was $\text{UO}_2(\text{OH})_2$ while radium precipitated as radium sulphate. Addition of a coagulant was found to aid in improving the separation of the supernatant from the precipitate formed. 2) Soil column experiments were conducted to further decrease the radionuclide level of the supernatant stream. A saturated porous laterite soil column was used for the tests. The supernatants, adjusted to pH 4.0 after the chemical treatment at the optimum pH 9.9, showed zero concentration of all the three radionuclides, after having passed through such soil column. From the experiments performed it could be concluded that the combined treatment of liquid waste streams containing soluble uranium, thorium and radium by chemical treatment and soil column offers good decontamination of the radionuclides. Both the combined treatment methods are cheap and the precipitate wastes produced can be easily managed.

1 INTRODUCTION

There is a need to develop technological processes for the treatment of aqueous radioactive waste from the decontamination of mineral processing facilities. The main radionuclides in this waste are ^{238}U , ^{232}Th and ^{226}Ra . The activity concentration is usually small but the total activity might be high due to the large volume of radioactive waste generated. The chemical composition in which the three radionuclides exist in the aqueous waste needs to be known to select or develop a proper treatment method.

1.1. Thorium

The major source of thorium is monazite (Ce, La, Y, Th) PO_4 that is essentially a phosphate of rare earth metals. The thorium contents range from 3% to 20% as ThO_2 . Since thorium exists in the solution as a highly charged cation, it undergoes an extensive interaction with water and with many anions. A free Th^{4+} ion dominates at pH below 3. From pH 3 to pH 4.5, the 1:1 and 1:2 hydroxyl complexes predominate. Above pH 4.5, $\text{Th}(\text{OH})_4^0$ is the major and most important chemical combination. The insoluble compounds of thorium, which form precipitates are common and may be suitable for the removal of tracer amounts of thorium from the solution. Thorium can be precipitated as hydroxide from the nitrate, chloride, sulfate, acetate, bromide and iodide solutions either directly or by addition of hydroxyl ions. pH at which the precipitation of thorium hydroxide begins is almost independent on the concentration of thorium salt and anions in the solution. The completeness of the precipitation depends on the amount of precipitant added; quantitative precipitation is achieved by the addition of 3.5 equivalents of the precipitant. Thorium hydroxide is a highly insoluble compound forming a gelatinous precipitate when alkali or ammonium hydroxide is added to an aqueous solution of Th^{4+} . The solubility in water is very low with the solubility product of 10^{-39} . Since hydroxide carrier precipitates are non-specific, they should be counted

only to remove thorium from a simple mixture of contaminants or as a group separation to be followed by more specific chemical purification steps.

A thorium ion is largely hydrolyzed at pH above 3.2, and the hydroxyl complexes are involved in the sorption process. The adsorption of thorium onto clays, oxides and organic matter increases with increasing pH and is complete at pH6.5. In neutral to acid solutions, the thorium adsorption is less complete onto clays than onto solid humic acid. Studies were also conducted on the effects of pH, ionic strength and carbonate alkalinity on the thorium adsorption by goethite in the 0.1M NaNO₃ electrolyte. The mobility of thorium for different thorium species at certain pH conditions in natural water at low temperature has also been investigated. The dissolved thorium is almost invariably complexed in natural water. Complexing increases the solubility of thorium bearing heavy minerals below pH8.

1.2. Uranium

The studies on the influence of temperature, bicarbonate concentration and uranium concentration on the sorption of uranium onto a number of pure minerals have been conducted while the idealized distribution coefficients being calculated from Freundlich Isotherms. The studies on the sorption of uranium onto well characterized goethite, amorphous ferric hydroxide and haematite soils have been carried out and experimental data were modeled in the carbonate free solutions assuming that mainly UO₂OH⁺ and (UO₂)₃(OH)₅⁺ aqueous complexes were absorbed. The study also included the influence of pH on the sorption of ferric oxides from the 0.1M NaNO₃ solutions. There was a steep adsorption edge between pH2 and pH5, with the adsorption rising from zero at pH1.8 to 100% (complete adsorption) on goethite and amorphous Fe(OH)₃.

1.3. Radium

Radium among the three radionuclides is the most toxic element and is mobile in soil. The radionuclide is potentially hazardous for humans from the external irradiation and ingestion viewpoints. The Ra²⁺ ion is probably the most important radium species in the natural water. The compounds formed by radium and their solubility are similar to barium. Radium is expected to co-precipitate with BaSO₄, carbonates and ferric hydroxides (the radius of Ra²⁺ ion is 0.00052 μm as compared with 0.000143 μm for Ba²⁺). Of the alkaline-earth elements radium shows the least tendency for complex formation, although 1:1 complex with citric, tartaric, succinic and several other acids were detected at pH 7.2 to 7.4. The behaviour of radium in solution is expected to be similar to that of strontium and barium and that sorption will occur mainly by ion exchange.

It is very important to understand the adsorption behavior of ²²⁶Ra on different local soils and clay minerals. The sorption of radium is mainly due to ion exchange reaction. It is more dependent on the composition and structure of minerals than on their specific surface area. On most materials, there is an adsorption edge at which sorption increases sharply. The minimum and maximum values and the steepness depend on a particular material and on a sorption mechanism.

2 OBJECTIVE AND GENERAL APPROACH

The objective of this study was to improve the efficiency of removal of dissolved thorium, uranium and radium from mineral processing waste by the application of combined treatment methods. The treated effluent will have to meet the requirements for release to the

environment set by the national regulatory body. The study was planned both on a laboratory and a pilot scale.

The following approach has been selected for the study.

For the laboratory scale treatment

- 1) Comparison of adsorption of uranium and thorium on different clay minerals and local soils by a batch method to select a best sorbent,
- 2) Batch experiments to determine the sorption capacity of the selected sorbent for ^{226}Ra , and relative sorption using different masses of the soil sorbent,
- 3) Chemical treatment of aqueous solutions at different pH to investigate precipitation of thorium, uranium and radium,
- 4) Soil column experiments with the selected sorbent to adsorb any remaining thorium, uranium and radium radionuclides.

The experimental data obtained from the laboratory scale studies were planned to extrapolate to the pilot plant scale treatment. The objective of the treatment at a pilot scale facility (combined treatment by chemical precipitation and soil column) was to clean the waste stream till the level acceptable for discharge into the environment in compliance with the authorized discharge limits.

For the pilot plant scale treatment:

- 1) Setup of a pilot scale facility for in situ treatment for real radioactive waste streams,
- 2) Determination of optimal process parameters, and
- 3) Determination of the treated water parameters to comply with the authorized discharge limits.

3 BATCH EXPERIMENTS

3.1 Comparison studies

The batch experiments were conducted to determine the adsorption of thorium and uranium on clay minerals and local soil sediments. The soil materials were dried by air and then filtered to the size of 0.250–0.350 μm .

The waste samples containing dissolved thorium and uranium species were prepared from the actual waste stream to produce similar chemical characteristics and concentration and then filtered through a 0.2 μm micro pore filters. pH of the radioactive solution was selected 4.9.

For each sample, preparations, procedures and conditions were the same in order to produce reproducible results and make a correct comparison. Prior to the experiments, the background concentration of thorium and uranium in the samples were determined by neutron activation analysis. Each experiment was conducted in a 40 mL polycarbonate centrifuge tube. Clay minerals and soil sediments of 2.5 g were precisely weighed and added into their respective tubes. 35 mL of the soluble solution was then added into each tube. All the tubes were equilibrated for 14 days at room temperature. After the equilibration period, the solid sediments were removed from each tube by filtering through a 0.45 μm . micro pore filter and then were allowed to dry. All solid and liquid samples collected at end of experiments were subjected to neutron activation analyses.

3.2 Sorption of ^{226}Ra on the sorbents with a different mass

The batch experiments were conducted to investigate the sorption of ^{226}Ra on sorbents with eight different masses ranged from 0.25 g to 3.50 g. 15 mL of the radium solution and the respective soil mass were added into a 20 mL vial. All the vials were equilibrated during 2 weeks after shaking at room temperature. After the equilibration period, all the vials were centrifuged and the 10 mL solution samples were collected and transferred into containers for gamma counting. The solid sediments were removed from each vial by filtering through a 0.45 μm filter and then the sediments were allowed to dry. The solid sediments were also transferred to counting containers of the same geometry for gamma counting. The counting containers were sealed by a tape.

3.3 Determination of sorption capacity of the soil sorbents

A batch experiment was conducted using the solution containing ^{226}Ra with the activity in the range $74\text{--}9 \times 10^2$ Bq. A soil sorbent with the mass of 0.11 g and 15 mL of the solution containing Ra were added into the vial. Six vials with a different radium concentration were equilibrated during 2 weeks at room temperature and then centrifuged. The samples of 10 mL volume were collected and transferred into containers for gamma counting. The solid sediments were removed from each vial by filtering the solution through a 0.45 μm filter, allowed to dry, and then transferred to the counting containers for gamma counting. All the solutions and the sediments were collected into counting containers of the same geometry and sealed by a tape.

4 SOIL COLUMN EXPERIMENTS

The soil sorbents that had demonstrated the highest radionuclide adsorption were selected to form a soil column. Preliminary studies were conducted to determine the hydraulic conductivity of the soil column prior to the treatment process. The soil materials (size 0.250–0.350 μm) with addition of a small amount of 0.250 mm size sand were packed into polyethylene rings forming a column (10.0 cm diameter, height 45.0 cm). The packed column was saturated and then conditioned with the pre-equilibrated effluent (pH4.0) for three days for optimum removal of the thorium and uranium radionuclides. This enables a maximum contact between the solution and the soil.

Before introduction of the aqueous radioactive solution, the steady state effluent water downward flow through the soil layer was maintained for 14 days. The effluents from the column were collected into bottle vials by using a fractional collector apparatus continuously in fractions for every one hour and then analyzed for the thorium and uranium concentration.

The soil column was divided into layers at 1 cm interval along the height to determine the thorium and uranium radionuclides adsorbed on the soil layer. Each interval sample was mixed thoroughly for neutron activation analysis to determine the concentration of thorium and uranium adsorbed at different depths.

4.1 Combined treatment

In the combined aqueous waste treatment, chemical precipitation was followed by soil column treatment.

Chemical precipitation

Chemical precipitation was a first treatment process for the aqueous waste stream containing uranium, thorium and radium. Prior to the treatment, an optimum pH had to be determined. At a laboratory scale, ten 30 mL waste samples were prepared in a 40 mL polycarbonate tube. The concentrated sodium hydroxide was added and pH of the solution was adjusted ranging from 7.00 to 12.41. 3 mL of 1M magnesium chloride were added in each sample to improve the coagulation process. Stirring had to be very slow during the addition of the sodium hydroxide and magnesium chloride in order to avoid breaking up any precipitate form. The supernatant was filtered through a 0.45 micro pore filter and the filtrate then collected. 10 mL of each sample filtrate was sent for the ICPMS analysis to determine the concentration of uranium and thorium. The background concentration of thorium and uranium were also determined by ICPMS.

3 mL each of 1M barium chloride and 2M ammonium sulphate were added to the balance of 20 mL filtrate in each sample. A coagulant aid was then added in order to separate the filtrate from the formed precipitate. The solution was stirred very slowly and then filtered through a 0.45 micro pore filter. 15 mL of each sample filtrate and the background solution of radium were sent for gamma counting using a Hyper pure germanium detector.

Sorption

In the second treatment process, the selected soil sorbent was used in the soil column. The soil materials (size 0.250–0.350 mm) with addition of 0.250 mm size sand (ratio 1:1, respectively) was packed into polyethylene rings forming a column (3.0 cm diameter, height 8.0 cm). The packed column was conditioned with a pre-equilibrated effluent (pH4.0) for 1 day to allow a maximum contact between the solution and the soil.

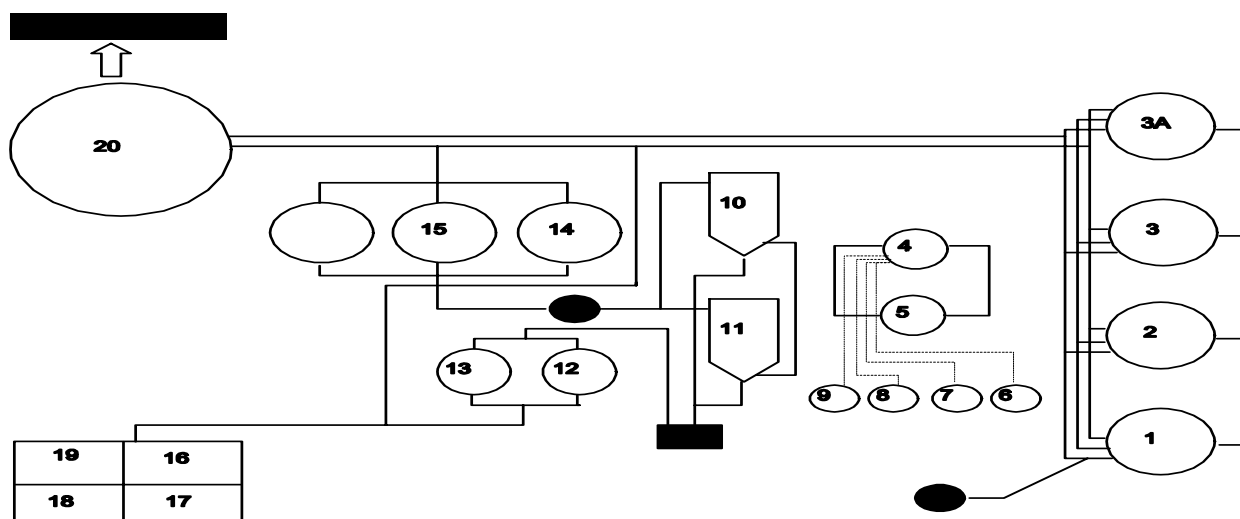
From the chemical treatment, 15 mL of the effluent from the optimum pH condition treatment was adjusted to pH4 and allowed to flow into the soil column. The effluent was collected by using a fractional collector apparatus into bottle vials in fractions for every 1 minute continuously. The samples were analyzed for the concentration of thorium and uranium by ICPMS and radium by a Hyper pure germanium detector. Each sample was subjected for the 5 hours counting period.

A pilot scale facility for treatment of raw radioactive waste

A pilot scale facility for the treatment of aqueous radioactive waste is shown in Fig. 1. The facility consists of collection tanks, mixing tanks, chemical tanks, clarifiers, retention tanks, settling tanks, a sludge collection point, solar beds and a holding pond. The facility has the capacity to treat 20 m³ of aqueous waste per day. Then the treated effluent was allowed to pass through a soil column from the holding pond for the second treatment before discharge.

5 RESULTS AND DISCUSSION

Table I and Fig. 2 shows the results of comparison adsorption studies by batch experiments on different pure clay minerals and soil sediments. 9 clay minerals adsorbed more uranium than thorium at pH ranging from 3.74 to 5.74. The adsorbed uranium concentration ranged from 7.83 ppm to 49.52 ppm. The Ca-montmorillonite has the highest adsorption value of 49.52 ppm. The range of the thorium concentration being adsorbed is 0.02–6.7 ppm. Smectite has an average adsorption value of 6.7 ppm and 24.6 ppm for thorium and uranium, respectively. Yellow soil at pH 3.91 shows high adsorption concentration 27.04 ppm uranium and 33.1 ppm thorium. For brown soil the adsorption was 23.27 ppm for uranium and 50.18 ppm for thorium at pH3.79.



Soil column treatment

FIG. 1. A pilot scale facility for the chemical treatment of aqueous radioactive waste containing ^{226}Ra , ^{232}Th and ^{238}U (1, 2, 3, 3A - collection tanks, 4, 5 - mixing tanks, 6, 7, 8, 9 - chemical tanks, 10, 11 - clarifiers, 12, 13 - settling tanks, 14, 15 - retention tanks, 16, 17, 18, 19 - solar bed, 20 - holding ponds).

Table II shows the types of clay minerals and the minerals present in the yellow laterite soil. The yellow soil was selected for the soil column treatment study because of its high adsorption and abundant present in the environment. The presence of goethite minerals, suitable pH 3.9 condition and presence of good clay adsorbents in the yellow soil contributed to high adsorption. Figure 3 shows high adsorption for thorium and uranium radionuclides. Most of thorium radionuclides were adsorbed at the distance 0–4.4 cm from the surface. The initial concentration 27.2 ppm at the surface was decreased to about 23 ppm at the 4.4 cm distance. At a higher distance depth, the background level of the thorium concentration (21.5 ppm) was observed in the soil. The initial concentration of uranium sharply decreased from 15.2 ppm at the surface to about 3.3 ppm at 1 cm depth.

Most of uranium and thorium radionuclides were adsorbed on the soil surface. The analysis of the effluent samples at different time intervals shows a near background concentration level which indicates that most of the radionuclides have been adsorbed. Figure 4 shows that the distribution coefficient for the soil sorbent laterite decreases with the increase of the sorbent mass. The sorption dropped rapidly when the mass of sorbents was in the range of 0 to 1.0 g and remained constant from 1.0 g to 4.0 g. The mass of sorbent less than 0.25 g was suitable for the adsorption of the radium radionuclides.

Figure 5 shows that the distribution coefficient increases with the increase of the concentration of ^{226}Ra up to 27.4 Bq/mL. The adsorption capacity of the soil sorbent for radium was quite high - 7.4×10^3 Bq/g.

TABLE I. ADSORPTION OF URANIUM AND THORIUM ON CLAY MINERALS AND SOILS

No	Clay minerals/soil clay	U(ppm)	Th(ppm)	B. G.	B. G.	adsorbed	adsorbed	pH
				U (ppm)	Th(ppm)	U(ppm)	Th(ppm)	
1	Haematite	19.30	4.50	0.50	0.50	18.80	4.00	4.63
2	Ca-montmorillonite	52.40	25.60	2.88	24.29	49.52	1.31	5.43
3	Illite bearing shale	31.70	13.60	4.61	13.50	27.09	0.10	4.16
4	Vermiculites	40.90	3.00	0.98	2.98	39.92	0.02	5.74
5	Smectites	25.20	8.80	0.60	2.10	24.60	6.70	5.43
6	Kaolin well crystallised	11.70	33.80	3.87	27.50	7.83	6.30	3.84
7	Na-illite	26.00	11.50	12.53	9.62	13.47	1.88	3.74
8	Sand with Fe-oxide	14.80	3.40	0.84	2.53	13.96	0.87	4.27
9	Zeolite	22.70	18.80	5.29	18.60	17.41	0.20	4.60
10	Yellow soil sediments	29.60	55.40	2.56	22.3	27.04	33.1	3.91
11	Brown soil sediments	25.50	57.10	2.23	6.92	23.27	50.18	3.79
12	Dark red soil sediments	21.80	16.20	2.49	13.82	19.31	2.38	4.15

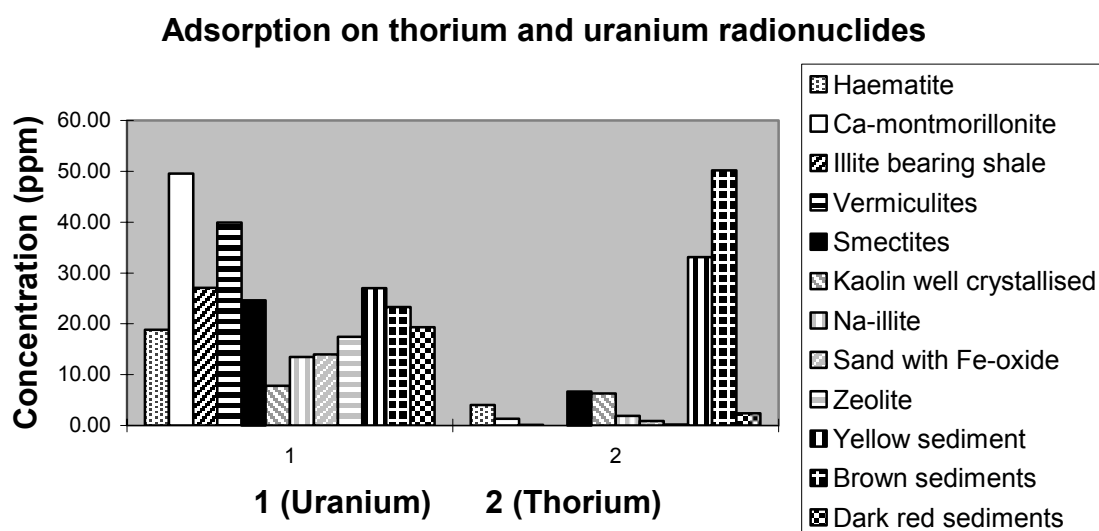


FIG. 2. Adsorption of thorium and uranium by different clay minerals and soil sediments.

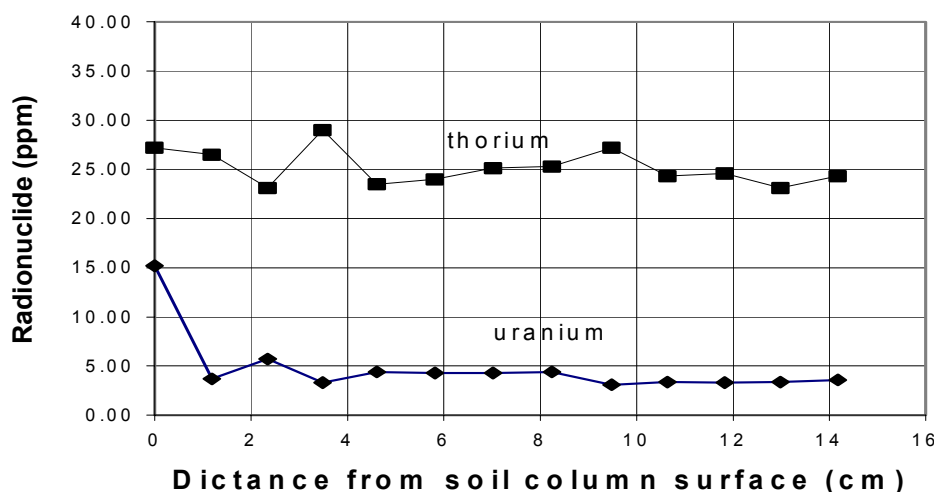


FIG. 3. Adsorption of thorium and uranium radionuclides from soil surface.

TABLE II. TYPES OF CLAY MINERALS AND MINERALS PRESENT IN THE YELLOW LATERITE SOIL SEDIMENTS

Clay minerals and minerals	Composition
Kaolinite Md	$\text{Al}_2\text{Si}_2\text{O}_5(\text{OH})_4$
Quartz	SiO_2
Illite M	$\text{KAl}_2(\text{Si}_3\text{AlO}_{10})(\text{OH})_2$
Vermiculite	$(\text{Mg,Fe,Al})_3(\text{Si,Al})_4\text{O}_{10}(\text{OH})_2 \cdot 4\text{H}_2\text{O}$
Clinocllore	$\text{Mg}_5\text{Al}(\text{Si}_3\text{Al})\text{O}_{10}(\text{OH})_8$
Chlorite	$\text{Al}_6(\text{AlSi}_3)\text{O}_{10}(\text{OH})_8$
Goethite	FeO_2

In combined treatment at a laboratory scale, the waste streams containing thorium, uranium and radium were first treated by chemical precipitation. The effluent analysis shows the decrease of the concentration and activity counts of the solution after the treatment. The precipitation of thorium hydroxide from the nitrate solutions (with sodium hydroxide as precipitant) increases with the increase in the number of hydroxyl groups in the molecule. A transparent colloidal solution of negatively charged thorium hydroxide was formed. The coagulation of thorium hydroxide was improved further by addition of the magnesium chloride. At pH 9.9, the thorium hydroxide $\text{Th}(\text{OH})_4$ species were the dominant species which form precipitate. For uranium, the hexavalent species dominate in the solution.

In absence of carbonate the solubility limiting species in oxic systems are $\text{UO}_2(\text{OH})_2$ which were in a solid form. The addition of the sodium hydroxide solution did not lead to the precipitation of radium.

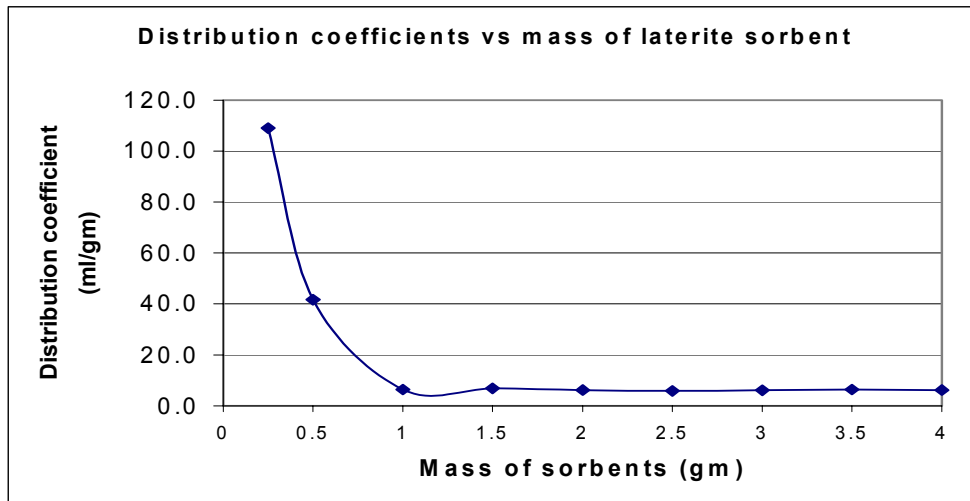


FIG. 4. The distribution coefficient against the mass of sorbents.

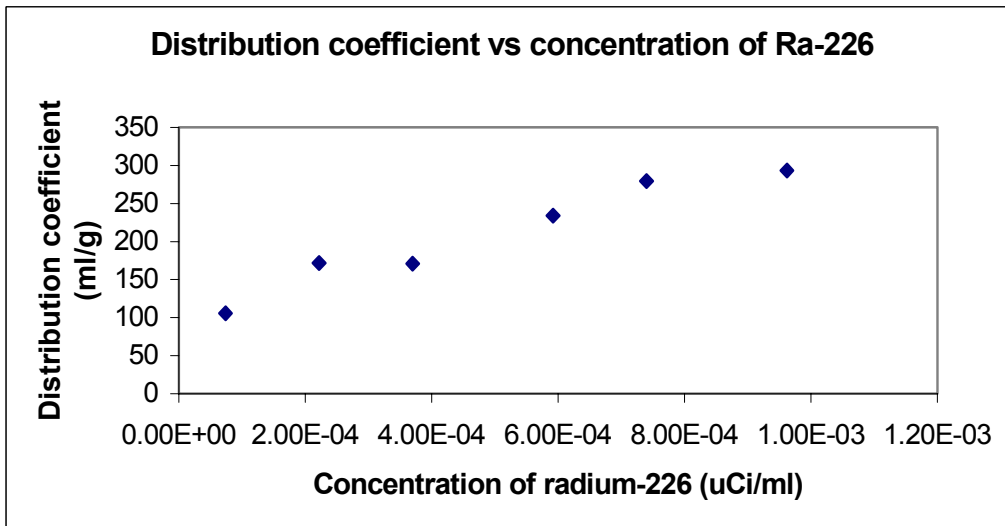


FIG. 5. The distribution coefficient against the concentration of ^{226}Ra .

The concentration of uranium and thorium in the filtrate shows the tremendous decrease. For the thorium treatment, shown in Fig. 6, at optimum pH ranged from 9.9 to 11.2, there was the reduction of the concentration to from the initial background 4.67 $\mu\text{g/L}$ to 0.05 $\mu\text{g/L}$. Figure 7 shows that at optimum pH9.9, the concentration of uranium has decreased from initial background concentration of 49.4 $\mu\text{g/L}$ to 0.62 $\mu\text{g/L}$.

During the treatment of radium, white precipitates were formed that consisted of barium sulphate and radium sulphate. The gamma analysis of the filtrate has demonstrated the reduction of activity from 0.0781 to 0.0002 counts per second. From Fig. 8, the high decontamination factor of 391 was obtained for radium at optimum pH ranged from 9.6 to 9.9. Addition of a coagulant aid to the filtrate improved the separation of the liquid phase from the precipitate by flocculation coagulation process.

In Fig. 9, the comparison of the decontamination factors for the three radionuclides shows that DF for radium is the highest (391), for thorium - 234 and for uranium - 80. The optimum pH value 9.9 was the same for the three radionuclides. The percentage removal was 99, 100, 100 for uranium, thorium and radium, respectively. This indicates that high decontamination of the waste streams can be achieved at the proper pH and the chemical concentration.

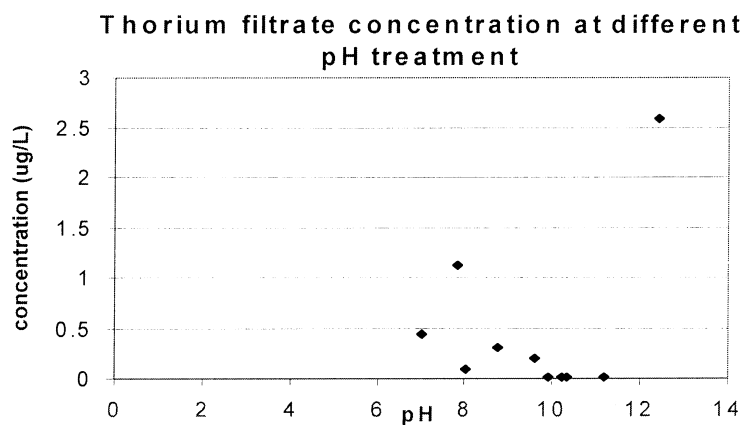


FIG. 6. The thorium filtrate concentration at different pH.

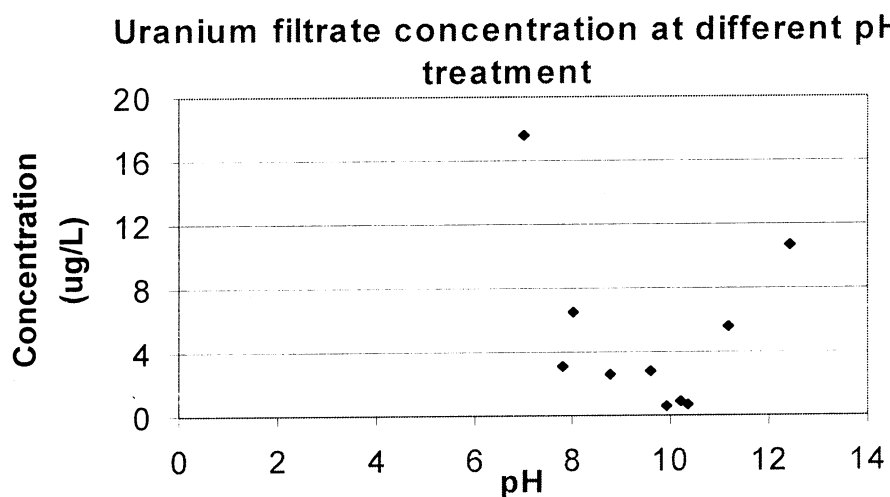


FIG. 7. The uranium filtrate concentration at different pH.

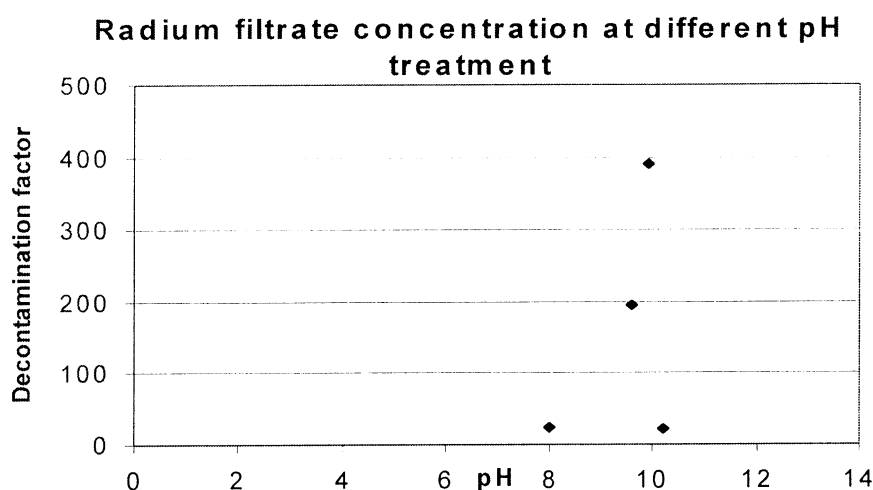


FIG. 8. Decontamination factor for radium at different pH.

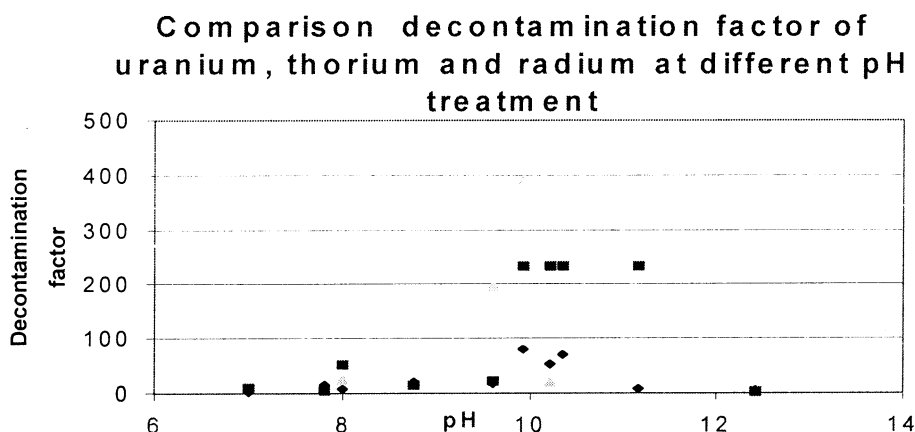


FIG. 9. Comparison of the decontamination factors for uranium, thorium and radium at different pH.

After the soil column treatment, the ICPMS method could not detect any uranium or thorium in the filtrate. That indicates that the two radionuclides remained in the solution after chemical precipitation were adsorbed by the soil. The radium radioactivity counts also cannot be detected even after 5 hours counting period.

The laboratory results were extrapolated for the treatment of actual radioactive waste in the pilot plant shown in Fig. 1. The experiments have shown that the critical process parameters should be strictly followed to obtain good results. The most critical parameter for high decontamination is pH of the aqueous waste. The chemical treatment was carried out in the mixing tanks where the chemicals with a required concentration were added. The chemicals should be added exactly at the same concentration as followed from the laboratory scale results. Mixing of the chemicals must be slow enough in order not to disturb the precipitate formed in the mixing tank. The precipitate and supernatant were separated by two

clarifiers and then the supernatant was pumped out into two retention tanks while the precipitate was pumped out into a settling tank. The supernatant in the retention tank must satisfy the respective water quality environmental limits established by the national regulatory body. If the resulted supernatant activity was too high it can be pumped back into the collection tank for the second chemical precipitation treatment. For final treatment the effluent was passed through a porous laterite soil column to remove any remaining radionuclides. The activity of the effluent must be less than the authorized discharge limits. Other parameters of the effluents important for the discharge are pH, conductivity, COD, BOD, the presence of soluble solids, total solids, suspended solids, the color, presence of toxic metals, temperature, hardness of water and smell. Such parameters as BOD, COD, total solid and suspended solids values were within the authorized discharge limits. The activity contents was less than the discharge limit. Other parameters can be tolerated even those were slightly above the limits and can be discharged in a control manner.

6 SUMMARY AND CONCLUSION

Combined chemical treatment and adsorption can successfully treat the given radioactive waste stream. The chemical treatment resulted in the very high percentage removal (nearly 100%) of the radionuclides, while the soil column treatment can remove completely any remaining radionuclides after the chemical treatment. The treated effluent for discharge must comply with the discharge procedures set up in the Malaysian Environmental Quality Act 1974 and recommendations of the World Health Organization (WHO). The activity concentration was less than 37 kBq/L and thus can be discharged into the environment according to the release limit recommended by the IAEA. The conclusion is that the combined treatment has achieved the objectives of the study.

However, it is recognized that the treatment performance of large volumes of radioactive waste will not be the same when treating a small volume. The treatment in a laboratory scale is usually carried out in ideal conditions whereas for large volumes conditions are not so ideal. There are such factors as the presence of carbon dioxide in the air which will effect the precipitation, mixing speed during mixing of chemicals and precipitate formed, chemicals concentration used, separation, etc., which will effect the treatment. In the soil treatment there may occur soil clogging which will affect the flow of effluent. The effective porosity of the soil must be high to avoid clogging and to provide conditions for a good contact between the liquid and the soil surface. The study indicated that a large volume of waste could be treated within a site which produced the waste. The volume of waste after the treatment will be small, highly concentrated but easily to handle.

REFERENCES

- [1] CORNELIUS, K., HURLBUT, JR. and CORNELIUS, S., Manual of Mineralogy, 20th edition, John Wiley and Sons, (1985).
- [2] AMES, L.L., McGARRAH, J.E. and WALKER, B.A., Sorption of trace constituents from aqueous solutions onto secondary minerals II. Radium, Clays and Clay Minerals, vol. 31, (1983a), p. 335–342.
- [3] AMES, L.L., McGARRAH, J.E. and WALKER, B.A., Sorption of uranium and radium by biotite, muscovite and phlogopite, Clays and Clay Minerals, vol. 31, (1983b), p. 343–351.

- [4] HIS, C.K., LANGMUIR, D., Adsorption of uranyl onto ferric oxyhydroxides; application of the surface complexation site binding model. *Geochimica et Cosmochimica Acta*, vol. 49, (1985), p. 1931–1941.
- [5] KEITH, A.H., DAVID, J. H. and LEE, K. C., Equilibrium Adsorption of Thorium by Metal Oxides in Marine Electrolytes, *Geochimica et Cosmochimica Acta* Vol. 52, (1987), p. 627 – 636.
- [6] BRIAN, D. L and JAMES, W.M., Solid/Solution Interaction: the Effect of carbonate Alkalinity on Adsorbed Thorium, *Geochimica et Cosmochimica Acta* Vol. 51, (1986), p. 243 – 250.
- [7] DONALD, L. and JANET, S.H., The Mobility of Thorium in Natural Waters at Low Temperatures, *Geochimica et Cosmochimica Acta* Vol. 44, (1980), p. 1753 – 1766.
- [8] GOBBETT, D.J. and HUTCHISON, C.S., *Geology of The Malay Peninsula*, The Geological Society of Malaysia, Wiley-Interscience, New York, (1973).
- [9] Batch-Type Procedures for Estimating Soil Adsorption of Chemicals, Technical Resource Document EPA/530/SW-87/006-F, United States Environmental Protection Agency, Washington, (1992).
- [10] BRADY, N.C., *The Nature and Properties of Soils*, Macmillan Publishing Company, New York, (1990).
- [11] SYED, H.S., Competitive Adsorption of Strontium-90 on Soil Sediments, Pure Clay Phases and Feldspar Minerals, *Appl. Radiation Isotop* , Vol. 46, No. 5, (1994), p. 287 – 292.
- [12] HIGGO, J.J.W., Review of Sorption Data Applicable to the Geological Environment of Interest for the Deep Disposal of ILW and LLW in the UK: Safety Studies, Nirex Radioactive Waste Disposal, NSS/R162, British Geological Survey, Nottingham, (1988).
- [13] HYDE, E.K., *The Radiochemistry of Thorium*, National Academy of Sciences, National Research Council, Nuclear Science Series, U.S. Atomic Energy Commission, January 1960.
- [14] LANGMUIR, D. AND HERMAN, J.S., The mobility of thorium in natural waters at low temperatures, *Geochimica et Cosmochimica Acta* Vol. 44, pp. 1753, (1980).
- [15] INTERNATIONAL ATOMIC ENERGY AGENCY, *Disposal of Radioactive Wastes into Rivers, Lakes and Estuaries*, Safety Series No. 36, Vienna (1971).
- [16] AMERICAN WATER WORKS ASSOCIATION, Inc., *Water Quality and Treatment*, Third Edition, A Handbook of Public Water Supply, McGraw Hill, New York (1971).
- [17] AMERICAN PUBLIC HEALTH ASSOCIATION, *Standard Methods for the Examination of Water and Waste*, 15 Edition American Water Works, Water Pollution Control Federation, (1981).
- [18] ECKENFELDER, W.W Jr., *Principles of Water Quality Management*, CBI, Boston, (1980).
- [19] CLARK, J.W., VIESSMAN, W.JR., AND HAMMER, M.J., *Water Supply and Pollution Control*, Third Edition, Harper and Row Publishers, (1970).
- [20] INTERNATIONAL ATOMIC ENERGY AGENCY, *Chemical Treatment of Radioactive Wastes*, Technical Report Series No.89 (1968).
- [21] INTERNATIONAL ATOMIC ENERGY AGENCY, *Chemical Precipitation Processes for the Treatment of Aqueous Radioactive Wastes*, Technical Report Series No 337, (1992).
- [22] RUBIN, A.J., *Chemistry of Waste Water Technology*, Ann Arbor Science Publisher, Inc., Michigan, 246–267 (1968)

COMBINED LIQUID WASTE TREATMENT PROCESSES INVOLVING INORGANIC AND ORGANIC SORBENTS, REVERSE OSMOSIS AND MICRO/ULTRAFILTRATION

HO-YEON YANG*, JONG-HYUN HA, MYUNG-JAE SONG

Nuclear Environment Technology Institute,

*Korea Hydro & Nuclear Power Co., Ltd,

Daejeon, Republic of Korea

Abstract. Cesium and cobalt removal from borated liquid radioactive waste from NPP was studied. Chemical and radiochemical analyses were undertaken for samples from Kori No. 2 NPP in order to understand the characteristics of the liquid waste. Cesium and cobalt were the dominant radionuclides in the NPP's liquid waste. Various commercial sorbents were tested. Of these sorbents, DT-10, -90 and Durasil -70 are activated carbon for cobalt removal, whereas Amberlite IRN-77 is an organic resin and DT-30 and Durasil-230 are inorganic sorbents used for cesium removal. Since liquid radioactive waste contains large amounts of Na^+ , experimental tests were specifically focused on the removal of cesium and cobalt from the liquid waste in the presence of sodium ions. The test results showed that the inorganic sorbents were high effective for cesium removal in the presence of Na^+ . For cobalt removal, DT-10 and Amberlite IRN-77 showed the best results. They both are less affected at presence of sodium ions. Detergent destruction by photocatalysed oxidation using TiO_2 sorbents was studied. Processes for the decontamination of boric acid bearing concentrates using suitable processes which includes consideration of ion exchange, membrane filtration and volatilization crystallization, used both singly and in combination is considered.

1. INTRODUCTION

Liquid radioactive wastes generated from nuclear power plants comprise the floor and equipment drains, chemical wastes, laundry wastes etc. Evaporation for these radioactive liquid wastes has been employed in the Korean PWR nuclear power plants. Though evaporators employed give satisfactory decontamination and volume reduction factors, the chemicals and impurities present in these wastes cause problems such as corrosion and scaling for the evaporators and foaming during evaporation. These problems also markedly decrease the decontamination and also could reduce the evaporator life. Maintenance costs also increased [1, 2].

Since 1986, about 60% of waste evaporators in US PWR's have been replaced by ion exchange processes, in order to overcome these problems [3]. Despite the successful application of the organic ion exchanger in giving high waste volume reduction, their costs and high personnel radiation exposures need to be addressed [4].

Studies have been carried out on the use of processes such as ion exchange, ultrafiltration, and reverse osmosis and have even been partially adopted in many nuclear power plants. Since no single unit process can treat the liquid waste of varied physico-chemical characteristics, the combined technology consisting of several unit processes as above may be more effective in treating these radioactive wastes.

New combined radioactive waste treatment processes have also to address removal of organics or oils usually contained in the liquid wastes. This has to be carried out as a pre-treatment step, more specifically for laundry wastes generated from the washing of the contaminated protective wears and showers from nuclear power plants.

The radioactivity of the laundry waste varies between 10^{-7} – 10^{-4} $\mu\text{Ci/mL}$ with the total annual generation of approximately 4,000 m^3 per each reactor in Korean NPPs. This comprises nearly 60% of the entire radioactive liquid waste generated from the reactor [5]. As mentioned above, evaporation is the only treatment employed presently.

Feasibility studies on processing units such as the fibre filters (FF), UF membranes, RO membranes, and selective ion exchange resins (SIES) were carried out for the treatment of these wastes. This paper summarizes the results of the lab-scale experiment using these combined processes for the removal of radionuclides such as cobalt and cesium and the organics in the simulated waste solutions. The demonstration tests employing these combined processes were also carried out with actual radioactive waste to verify the effective DFs achieved and the removal of organics. Besides permeation in the RO unit was also carried out occupies Boric acid exists predominantly and in large concentrations in the treated effluents after the evaporation process. RO process was also studied to find out the possibility for the removal of boron. Removal of cesium was also studied in these unit processes.

2. STATUS OF COMBINED PROCESS DEVELOPMENT

Liquid radioactive waste generated from Korean nuclear power plants can be largely divided into three kinds: borated wastes, laundry wastes and laboratory-chemical wastes. Their treatment methods and characteristics are shown in Table I.

Korea Electric Power Research Institute (KEPRI) carried out research on using inorganic ion exchangers and organic ion exchange processes as an alternative to evaporation process during the period of November 1993 to April 1996 in co-operation with Korea Atomic Energy Research Institute (KAERI). A pilot scale process ($1\text{m}^3/\text{h}$) for liquid radioactive waste treatment was built at Kori NPP No. 2 in 1996[6].

For the treatment of the laundry wastes, KERPI has carried out research on using reverse osmosis between May 1995 and October 1998. A pilot scale RO facility ($1\text{m}^3/\text{h}$) for laundry waste was built for assessing its performance at Yonggwang NPP No. 4 [7].

KAERI also carried out research for the treatment of laundry waste using reverse osmosis and micro/ultrafiltration, but no pre-treatment process and post-treatment process have been studied and therefore, further studies on these processes are required.

Other countries also have made all the efforts to develop and employ new processes for the treatment of these liquid radioactive wastes. The prominent systems developed are selective inorganic ion exchangers, regenerative organic ion exchangers and unit processes such as ultrafiltration, reverse osmosis and inorganic membrane etc.

3. SYSTEM DESCRIPTION

The reverse osmosis (RO) system was developed as a water purification technology that relies on applying pressure to force water through a semi-permeable membrane. The membranes used in RO let water to pass but retain most of the dissolved solids. Typical RO process flow diagram for the liquid radioactive waste system is shown in Fig. 1.

TABLE I. CHARACTERISTICS OF LIQUID RADIOACTIVE WASTE GENERATED FROM KOREA NPPs [8].

LIQUID WASTE	TREATMENT METHOD	CHARACTERISTICS
<ul style="list-style-type: none"> HIGH TDS BORATED WASTE 	<ul style="list-style-type: none"> EVAPORATION 	<ul style="list-style-type: none"> OBTAIN HIGH DF, ACHIEVE ZERO-RELEASE, HOLD THE DISCHARGE OF BORON DETERGENT AND OILY WASTE WITHIN LIQUID RADIOACTIVE WASTE DECREASE THE CAPABILITY OF EVAPORATOR NEED LARGE INITIAL INVESTMENT COSTS AND MAINTENANCE
<ul style="list-style-type: none"> LOW TDS BORATED WASTE 	<ul style="list-style-type: none"> ORGANIC ION EXCHANGER 	<ul style="list-style-type: none"> INCREASE OF SPENT RESINS BY ADSORPTION OF NON-RADIOACTIVE IONS DIFFICULTIES FOR THE ACHIEVING ZERO-RELEASE DIFFICULTIES FOR SOLIDIFICATION OF SPENT RESINS
<ul style="list-style-type: none"> LAUNDRY WASTE 	-	<ul style="list-style-type: none"> DIRECT DISCHARGE, IF SATISFIED WITH THE RELEASE CRITERIA DIFFICULT FOR THE ACHIEVING ZERO-RELEASE POSSIBILITY FOR CONTAMINATION OF ENVIRONMENT BY DETERGENTS
<ul style="list-style-type: none"> LABORATORY CHEMICAL WASTE 	<ul style="list-style-type: none"> ORGANIC ION EXCHANGER 	<ul style="list-style-type: none"> POSSIBILITY TO DISCHARGE HEAVY METALS INTO THE ENVIRONMENT DIFFICULT FOR THE SOLIDIFICATION OF SPENT RESINS

*TDS: Total dissolved solids

g

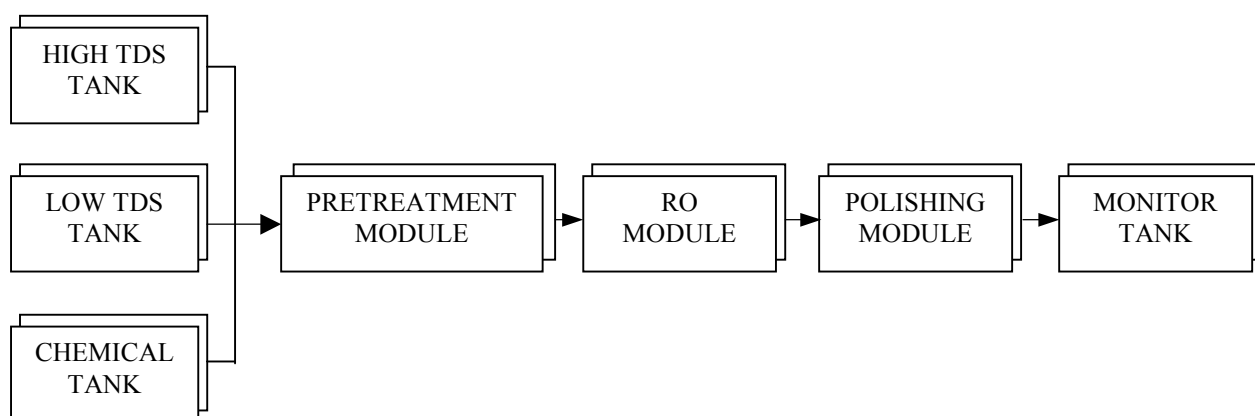


FIG. 1. Flow diagram of laboratory scale combined processes.

Liquid radioactive wastes are passed through a pre-treatment module, where all the impurities are removed and thus maintain the optimal performance for the RO system. The effluents after pre-treatment are routed through the RO modules for the removal of soluble species and the permeates are passed through a polishing module.

3.1. Pre-treatment module

Proper pre-treatment of the waste solutions to the RO system is critical so as to maintain its optimum performance and to minimize the operating costs. To achieve these objectives, the pre-treatment module is designed to minimize or prevent fouling, scaling and degradation of the membrane. Table II provides general guidelines used to prevent or minimize fouling, scaling, and degradation of RO membranes, as well as their pre-treatment techniques [9].

TABLE II. SUGGESTED FEED WATER QUALITY GUIDELINES AND PRE-TREATMENT TECHNOLOGY

Item	Guidelines	Pre-treatment
Foulants		
Solids	SDI ^{*1} < 5 Turbidity < NTU ^{*2}	Clarification, multimedia filtration, Coagulation
Iron	<0.05 ppm	Oxidation, manganese greensand
Manganese	<0.05 ppm	Filtration
Organics (TOC)	<10–15 ppm	Chlorine, activated carbon
Microorganisms	Not specified	Chlorine, biocides
Scalants		
Calcium carbonate	LSI ^{*3} <1 (concentrate)	Softening, antiscalants, pH
Barium	< 0.05 ppm	
Srortium	< 0.1 ppm	
Silica	50 – 150 (concentrate)	Hot lime softening

*1. SDI: Silt Density Index

2. NTU: Nephelometric Turbidity Unit

3. LSI: Langelier saturation Index(or LI or SI)

In conventional filtration, the liquid passes directly through the filter medium with the solids accumulate on the filter surface. The solid filter cake thus formed is a porous structure and removes solids. However, the solids act as an additional barrier to be continued passage of fluid, both through the cake structure and through interface with the filter medium and fine particles begin to block the pores. For a given pressure, the throughput decreases as the solids get collected. For the liquid with fine particulates and colloidal materials, the rate can be extremely rapid.

3.2. RO module

Reverse osmosis is a process whereby the phenomenon of osmosis is reversed by the application of pressure to concentrated solution in contact with a semi-permeable membrane. If the applied pressure is in excess of the solution's natural osmotic pressure, the solvent will flow through the membrane to form a dilute solution on the opposite side and a more concentrated solution on the side to which pressure is applied. If the applied pressure is equal to the solution's natural osmotic pressure, no flow will occur. If the applied pressure is less than its natural osmotic pressure, there will be a flow from the dilute solution to the concentrated solution.

Typical RO system consists of either spiral wound or hollow fibre membranes housed in a pressure vessel to prevent leakage [10]. These devices are connected in parallel and/or in series to achieve the desired quality of product water.

RO membranes are commercially available in spiral wound or hollow fibre configurations and, to a lesser extent, in tubular and plate and frame configurations. The following are desirable characteristics in a membrane device [11]:

- Safe operation at high pressure;
- No internal or external leaks;
- Easy to flush or clean;
- Minimal pressure drops on permeate and brine sides;
- Made from inert, corrosion-resistant materials;
- Long term reliable operation.

3.3. Ion exchange module

The use of ion exchange materials to remove soluble contaminants is a well-established and very effective technique. The effluent simply passes through a bed of absorption material, which could be a manufactured resin or a natural zeolite, and the contaminant is removed. When exhausted, the ion exchange bed is removed and replaced.

The operating cost of such a system is usually very depending on the volume of ion exchange material consumed, and its basic cost, its subsequent handling and disposal costs. The consumption of ion exchange material depends on three key factors:

- The suitability of the material for the effluent being treated;
- The selectivity of the material for the contaminant or contaminants of concern;
- The chemical conditions in which the system is operated.

A poor choice in any of the three areas can lead to a significant increase in materials consumption and consequent increase in its processing cost.

NETEC has been testing the performance of different exchange materials under different chemical conditions and with different effluent streams for many years. Our test experiences, both nuclear and non-nuclear, suggests appropriate materials and conditions for the treatment of most of the effluents [14].

The ion exchange module will utilize two ion exchangers to polish RO permeates. In general, there will be two treatment steps: one is designed as makeup ion exchange, and the other designated as a polishing ion exchange unit. [10]. The makeup ion exchange unit consists of separate selective ion exchange resin beds. The second ion exchange unit is always a mixed bed type, which is necessary to obtain the lowest possible level of ionic impurities [10, 11]. The ion exchange units have the capacity to remove substantial amounts of organic and particulate matter in addition to ions.

4. MATERIALS AND METHODS

4.1. Materials

4.1.1. Simulated waste solutions

The simulated radioactive waste was made using tap water, detergent and chemicals such as CsCl, CoCl₂, etc. Simulated wastes were used for the laboratory experiments but real radioactive waste was used for the demonstration test at Yonggwang nuclear power plant. Floor drains waste was also simulated. The properties of liquid radioactive waste in Korean nuclear power plants are given in Table III.

4.1.2. Lab-scale Unit

The lab-scale combined process consisted of the fibre filter system, UV/H₂O₂ Photo-Oxidation system, UF and RO modules and selective ion exchange beds. Each unit process was designed for treatment capacity except of 100 L/h of that the flow velocity for Selective Ion Exchange System was kept at 0.176 L/min (flow rate: 60 L/h) This was done to ensure sufficient retention time in the column. Fibre filter was used for the removal of suspended solids and organics in the waste. The material, thickness and pore size of polyester filter were, 0.6 mm and 1 μ m, respectively.

The UV/H₂O₂ Photo-Oxidation system comprised a 15W UV lamp, cylinder-type glass reactor (22cm H x ϕ 4cm ID), three) kW UV reactor (Gaya, Korean manufacturer) and the stainless steel reactor of 45 L volume.

TABLE III. PROPERTIES OF LIQUID RADIOACTIVE WASTE IN KOREAN NUCLEAR POWER PLANTS

	Properties	Range	Properties	Range
Chemical & Physical Properties	pH	5.85 ~ 8.91	Cl ⁻ (ppm)	13 ~ 25
	COD (ppm)	16 ~ 141	NO ²⁻ (ppm)	0.5 ~ 4.5
	Na ⁺ (ppm)	10 ~ 15	SO ₄ ²⁺ (ppm)	6.8 ~ 8.8
	K ⁺ (ppm)	0.2 ~ 1.4	SS (ppm)	75 ~ 155
	Mg ²⁺ (ppm)	1 ~ 2	Non-ionic	(<10 μ m)
	Ca ²⁺ (ppm)	3.4 ~ 6.0	Surfactant (ppm)	65 ~ 153
Specific Activity	Co-58(μ Ci/ml)	2.69E-5 ~ 5.99E-3	Cs-34(μ Ci/mL)	1.80E-5 ~ 4.58E-2
	Co-60(μ Ci/ml)	1.92E-5 ~ 2.91E-3	Cs-37(μ Ci/mL)	2.42E-5 ~ 5.63E-2

During the test (continuous or batch), 125 mL of the waste in the reactor was used. H₂O₂ and pH controls by NaOH or HCl added directly in the waste tank were maintained. This waste was injected to the reactor by a peristaltic pump. The system was equipped for recirculation with the flow rate of 100 L/h. The surface of the glass reactor was wrapped by aluminum foil for protection from UV radiation.

The UF process for a throughput of 100 L/h consisted of a UF module, waste feed pump, backwashing pump and control box. The module type of UF process comprised the hollow fibre with molecular weight cut-off (MWCO) of 10,000. The material of UF membrane was that of polysulfone.

The cellulose acetates and Thin Film Composite(TFC) and polyamide RO membrane in spiral wound type were compared for their performance. Table IV shows the characteristics of the two types of these RO membranes and Table V shows the operating conditions for the laboratory studies.

4.1.3. *Methods*

The laboratory tests were carried out for the optimum condition of the system under the batch mode with a variation of pH, pressure, boron concentration and temperature.

The simulated waste in the waste tank I is pumped up into the fibre filter unit and the permeate is also pumped into the UF unit. The permeate of UF unit goes to RO unit and finally the permeate of RO unit is treated by the ion exchange unit (See Fig. 2). 150 L of waste water solutions were used on once-through mode.

TABLE IV. THE CHARACTERISTICS OF CELLULOSE ACETATE (CA) AND TFC* POLYAMIDE RO MEMBRANES (PA)

Item	CA	PA
Maker (model)	Osmone (192 SR CA)	Filmtec Co., USA (SW 30HR)
Module	Spiral wound	Spiral wound
Material	Cellulose acetate	TFC* polyamide
Size (inches)	30 x 2	40 x 2.4
pH range	4–7	2–11
Surface area (m ²)	1.0	1.5

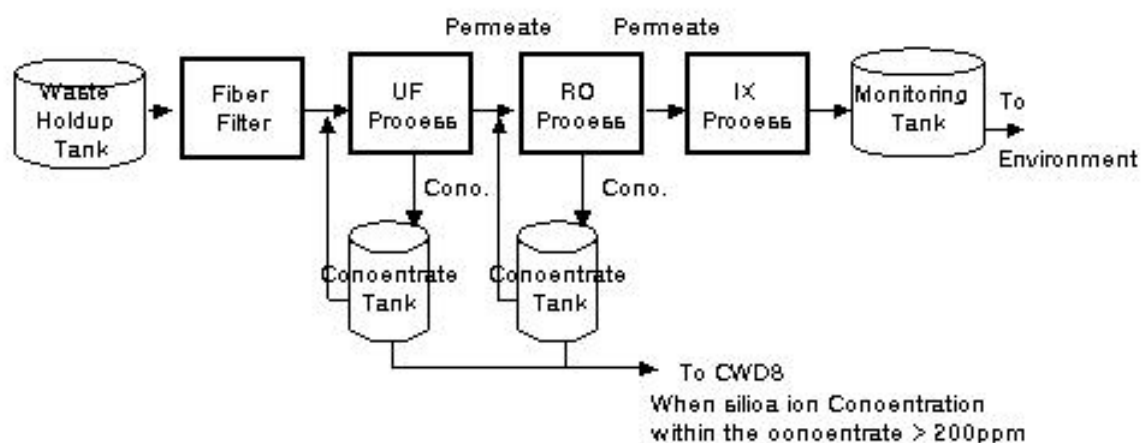
*TFC: Thin Film Composite

Co and Cs in the permeate and in the rejected waste were measured by Atomic Absorption Spectrophotometer (Thermo Jarrell Ash Co. Ltd. USA). Surfactant was analyzed using TOC analyzer (TOC-5000A, Shimadzu Co. Ltd., Japan). Boron was also measured by 0.1N-NaOH Titration-Mannitol method. Suspended solids were analyzed by the centrifuge particle analyzer (BTC, USA).

TABLE V. OPERATION CONDITION IN THE LAB

Item	Operation
Pressure (psi)	0–300
pH range	4–9
Temperature (°C)	25–45
Turbidity (NTU*)	1 less

*NTU: Nephelometric Turbidity Unit



Function	Removal of SS and Organic	Removal of fine particles and organic	Removal of Ion materials	For Ca
Target	Capacity: 100 L/hr DF: 2-10	Capacity: 100 L/hr DF: 10-20	Capacity: 100 L/hr DF: 10-20	Capacity: 100 L/hr DF: 10-100
Operational conditions	Differential pressure	Operational pressure: 40psi pH: 9-10	Operational pressure: 200psi pH: 7-10	Flow velocity: <0.178m/min

FIG. 2. Schematic diagram of lab-scale combined process.

5. RESULTS

5.1. Fibre filter process test

Most of suspended solids and organic materials in the waste were removed through the FF process.

5.1.1. Suspended solid removal

More than 93% of suspended solids, in the sizes ranges between 0~5 μm , were filtered by the FF unit within 15 minutes, and nearly 99.8% of the suspended solids were removed within 45 minutes (Fig. 3).

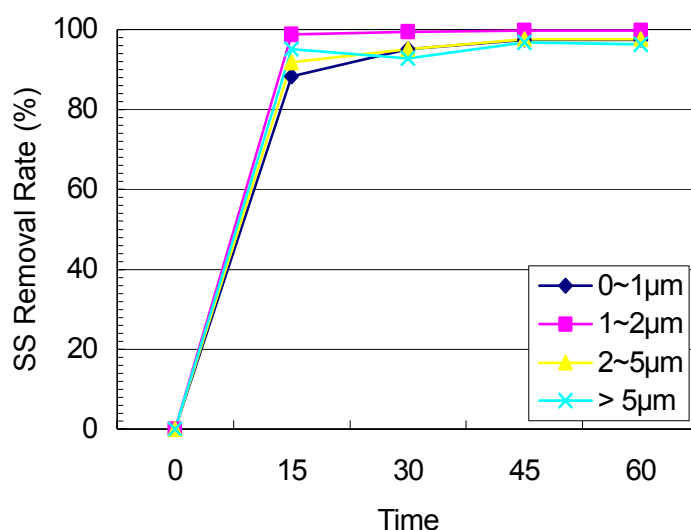


FIG. 3. Suspended solids removal by Fibre Filter.

5.1.2. Organics removal

The organic removal by the FF was quite effective. The initial TOC was nearly 50 to 53ppm (oil:surfactant = 1:4). About 82% of the organic materials including oil and surfactant were removed within 15 minutes. The removal rate after 15 minutes was almost constant up to 90 minutes. The flow rate was also not much reduced during the filtration. The flow rate was 2.4 L/min after 90 minutes whereas the initial flow rate was 2.6 L/min.

The permeates from the FF was pumped into the UF unit. The RO membrane separated the residual organic materials and cobalt.

5.2. UV/H₂O₂ photo-oxidation test

The 3 kW of UV lamp with 180–400 nm wavelength was tested for the experimental data with the UV lamp having long range of wavelength. Simulated solutions having TOC up to 85 ppm made of surfactants and tap water were employed. Effect of hydrogen peroxide was optimum at 1000 ppm, and at a pH9.5 (Figs. 4 and 5).

The lab-test results using 15 W and 3 kW of UV lamps revealed that for the removal of TOC more than 85%, the UV lamp of minimum 28.6 kW~30 kW would be required.

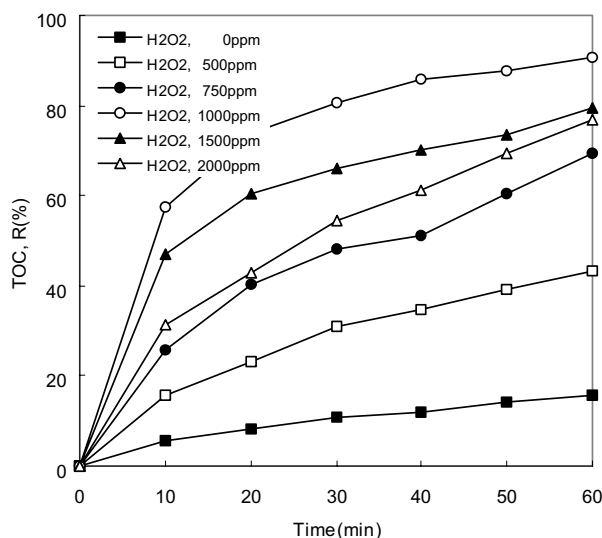


FIG. 4. TOC removal rate with H_2O_2 injection volume variation using 3 kW UV lamp.

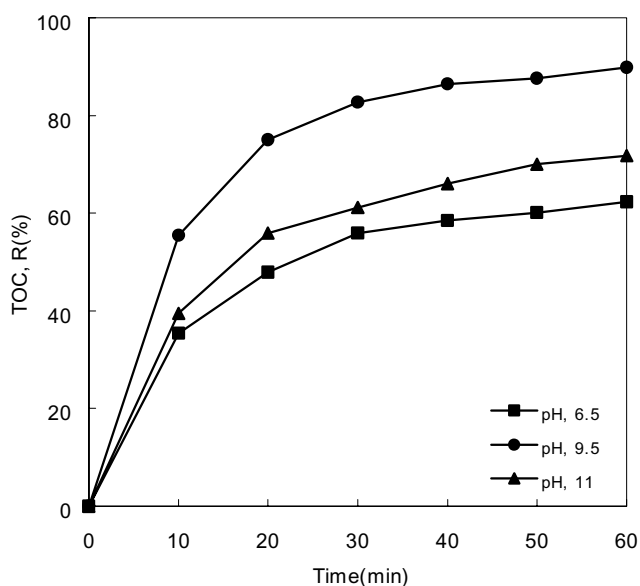


FIG. 5. TOC removal rate with pH variation using 3 kW UV lamp.

During the reactor maintenance period, the laundry waste is produced in the amount of nearly 19.4 ton/day. To process this waste volume, the UV pre-treatment system requires at least more than 30 kW UV reactor for 1 ton/h of treatment capacity. Minimum of three to five of 5 kW lamps in series would be desirable to reduce the TOC removal efficiently.

UV photo degradation system is also expected to remove foam and entrainment generated from the detergent wastes.

5.3. UF process test

To find out the optimum operational parameters during UF process, tests were carried out varying the flow rates, pressures and backwashing intervals, which could effect the salt rejection rate and throughputs. The rejection rate of cobalt was increased by about 2 – 4% as flow rate increased and radionuclide rejection was also slightly increased with increasing of the operating pressure (see Fig. 6).

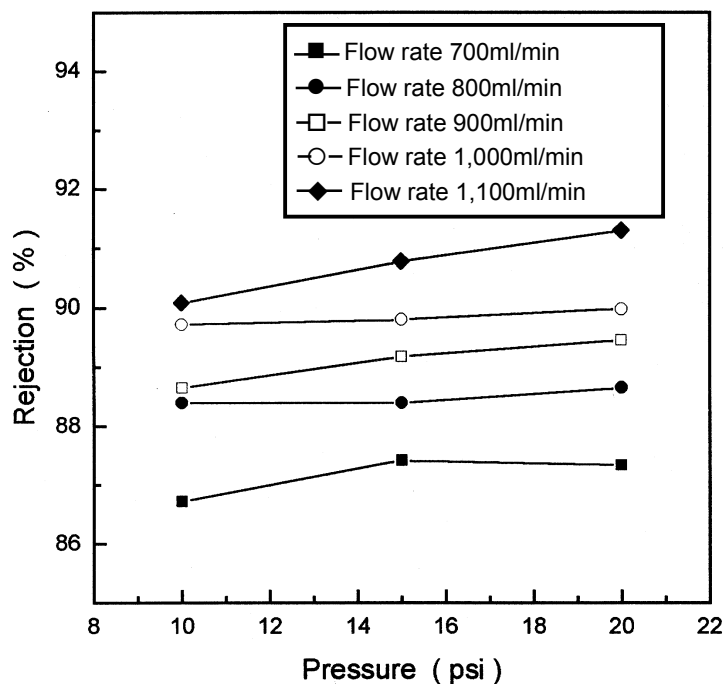


FIG. 6. Co rejection rate as a function of pressure and flow rate.

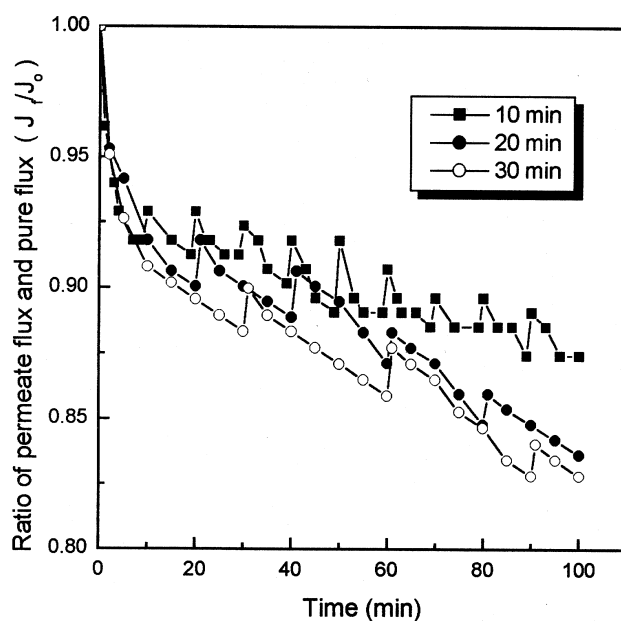


FIG. 7. Variations in the permeate flux as a function of backwashing interval (backwashing time: 1min, backwashing solution: permeate solution).

The permeation flux variation by backwashing was tested. From the results of the experiments (Fig. 7), the permeate flux reduced with time and was practically zero as the time passed. With the shorter time interval of backwashing, reduction of the permeate flux was not so fast. However, the permeate flux rate rapidly decreased after 20 min.

5.4. RO process test

To have knowledge of the optimum operational parameters of the RO process, tests were carried out depending on the variations of pH, pressure and temperature, that could effect the salt rejection rate and flow. Tests on the boron permeation were also carried out with variations in pH and temperature. Two different kinds of membrane, CA and PA, were tested for comparison purposes to study the effect on radionuclide rejection.

5.4.1. Effect on membrane types

To confirm the difference between the two types of RO membrane in its radionuclide removal efficiency, distilled water with cobalt and cesium was used and the concentration adjusted for studying their rejection variation rate during the test. Figures 8 and 9 show the results from the test on radionuclide rejection rates using CA and PA types of membranes. The cobalt and cesium rejection rates on PA type membranes were more effective.

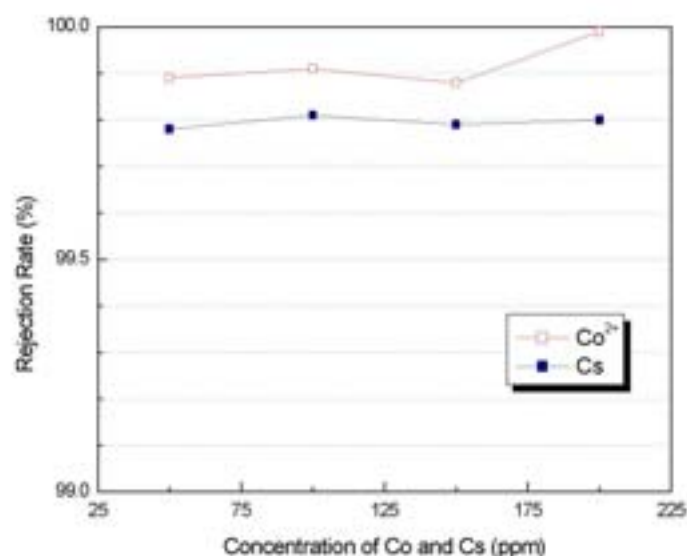


FIG. 8. Effect on the radionuclide rejection rate in PA membrane system at 25 °C and 4.5Mpa.

The rejection rates for cobalt and cesium were 99.9% and 99.8% with PA type membranes whereas about 91~93% and 87~89% in CA type membranes respectively. The rejection rates in CA type showed wide difference between cobalt and cesium. It appears that the fixed charge generated by carboxylic group in CA membrane rejects more strongly the cobalt on account of their ionic valence.

The rejection rates for Co and Cs in PA gave DF more than 1000 and 500, respectively. The Thin Film Composite PA membrane was only used for further tests due to its better efficiency in radionuclide rejection.

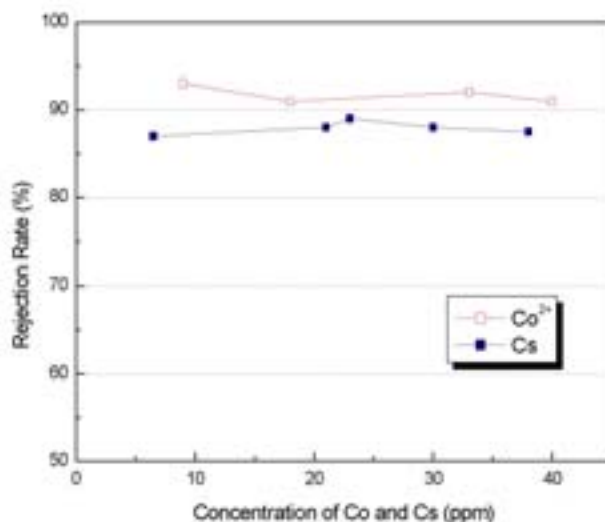


FIG. 9. Effect on the radionuclide rejection rate in CA membrane system at 25 °C and 1.43 Mpa.

5.4.2. pH effect

The experimental tests with PA membrane were carried out for the pH variation on Co, Cs, surfactant rejection and boron permeation rates. The tests were carried out at 25°C and at the pressure of 50 psi. The pH was controlled at 4, 7 and 9. The rejection rates of Co, Cs and surfactant increased as the pH increased. The optimum condition for rejection rates was at pH9. The rejection rates at pH9 were about 98% for Co, 93% for Cs and 90% for the surfactant. Besides, boron permeation rate rapidly decreased as pH increased, and the highest boron permeation rate was 81.2% at pH4 [15].

In general, 10 ~ 30% of cobalt contained in liquid radioactive waste were filtered by 0.4µm filter and the rest of it was dissolved in the waste. This dissolved cobalt is mostly cationic with a valency of 2 and are present as $\text{Co}(\text{OH})_2$ in the pH range of 8–9. $\text{Co}(\text{OH})_2$ stays in the colloidal phase and easily combines with the surfactant. On the other hand, the surfactant in the waste produces micelle which has high charge density and electric potential on to its surface, so as to produce the complex with $\text{Co}(\text{OH})_2$ having low solubility [12–13]. Therefore, the rejection rates of Co and surfactant increases as pH increases.

Boron in the waste is present as $\text{B}(\text{OH})_3$ with high solubility in water at a pH below 5. As the pH increases, low soluble anionic species such as $\text{B}(\text{OH})_4^-$, $\text{B}_3\text{O}_3(\text{OH})_4^-$ and $\text{B}_3\text{O}_3(\text{OH})_5^{2-}$ are produced from the hydrolysis of $\text{B}(\text{OH})_3$. Accordingly, $\text{B}(\text{OH})_3$ under the low pH can permeate RO membrane easily.

5.4.3. Operation pressure effect

The rejection rates using the PA membrane for cobalt, cesium and surfactant in the waste at 25°C and at pH9 were tested as a function of pressure varied at 50, 100, 150, 200, 250 and 300 psi respectively (see Fig. 10). As the pressure increased, the rejection rates of Co, Cs and surfactant also increased. Above 200 psi, the rejection rates for Co and Cs were 100% and 93.1%, respectively, and that of the surfactant almost 91.8%. The boron permeation rate at pH4 and at 25°C was decreased as the pressure increased.

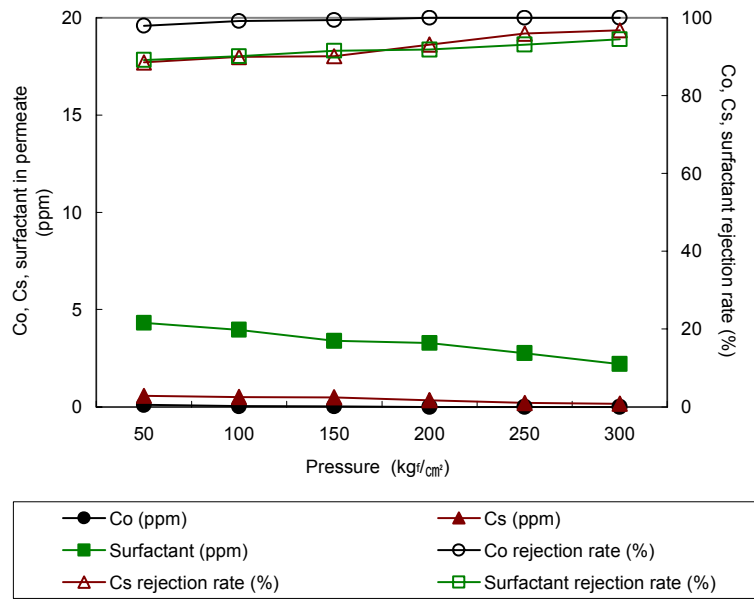


FIG. 10. Rejection rate variation of Co, Cs and surfactant as a function of pressure.

The velocity of solute as a function of pressure is affected by solute diffusion coefficient in the membrane and partition coefficient between membrane and solution. Therefore, as the pressure in the RO increases, rejection rates of Co, Cs and surfactant also increase but boron permeation rate is decreased.

The test results on the variation of permeation volume and volume reduction factor according to pressure variations are shown in Fig. 11. The permeation volume increased as the pressure increased. However, the concentration volume also decreased. Ratio of the concentration volume to the permeation volume defined as a volume reduction factor gradually increases as the pressure increases.

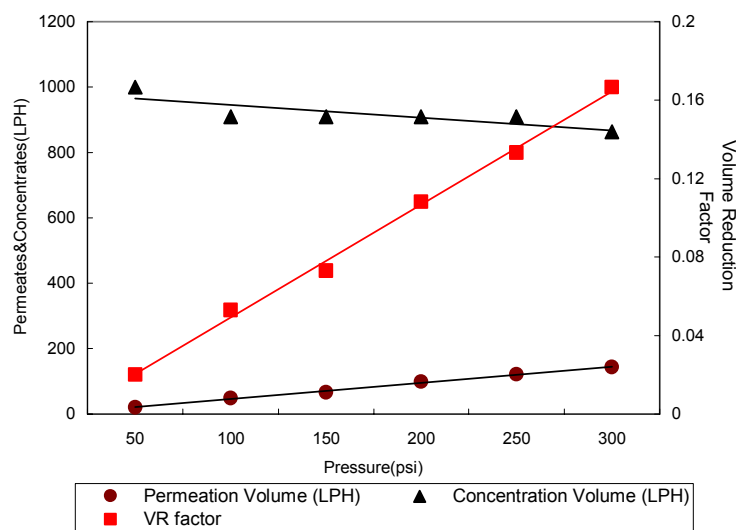


FIG. 11. Variation of permeation and concentration volumes.

5.5. Boron concentration effect

The optimum boron permeation rate has been tested with the PA membrane for the waste solutions under the condition of pH4, pressure 50 psi and temperature 25°C. The boron concentration for these tests were varied as 500, 1000, 1500, 2000 ppm (Fig. 12). The boron permeation rate increased as a function of boron concentration. Generally, salt permeation volume depends on the difference of salt concentration being present on both sides of the membrane [16].

5.5.1. Temperature effect

Boron permeation rate as well as the rejection rates of cobalt and surfactant depends strongly on the waste temperature. The tests for rejection rates of cobalt, cesium and surfactant were carried out for the simulated waste solutions at pH9 and pressure of 200 psi with variation of temperatures at 25, 35, 45 °C, respectively. The rejection rates of surfactant were 99.2% at 45°C.

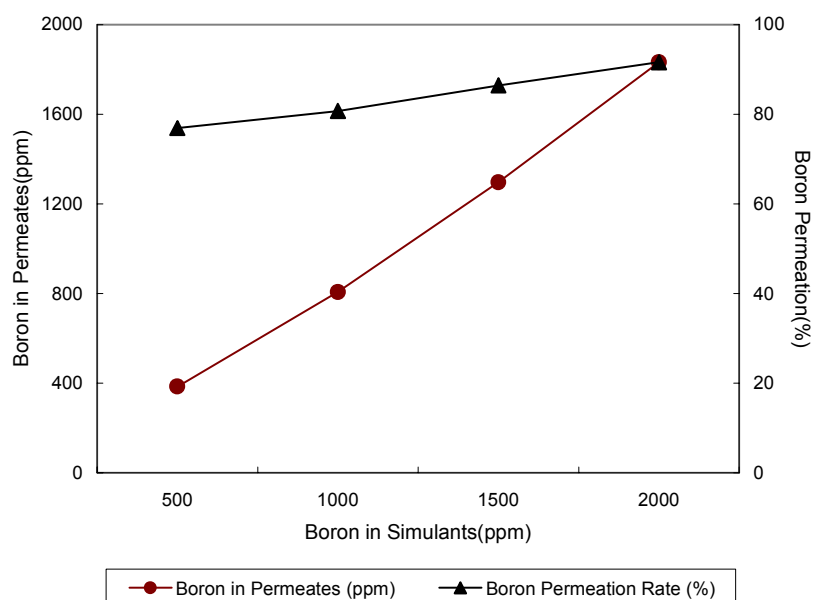


FIG. 12. Variation of the boron permeation rate as a function of boron concentration.

Boron permeation tests were carried out under the temperature variation of 25°C, 35°C and 45°C and under pH4 and pressure of 50 psi. It was observed that the boron permeation rate increased as a function of temperature. The permeation rates were 81.2% at 25°C, 86.2% at 35°C and 92.2% at 45°C. The permeation rates of solute and solvent increase as the osmotic pressure increases, and also the viscosity of solvent gets lower as a function of temperature.

6. DEMONSTRATION TESTS

The lab-scale combined treatment facility for liquid radioactive waste was installed at Younggwang nuclear power plant and demonstration tests using actual liquid radioactive waste were carried out to verify the performance of the combined system. The system consisted of FF, UF module, RO module and SIES.

6.1. Tank module

The tank module consisted of 120 L capacity waste tanks for FF, 60 L for UF and RO membranes. The radioactive waste was obtained from the high TDS tank to FF tank. FF was placed in front of the UF membrane module for the removal of colloidal solids to prevent frequent fouling of UF and RO. Pressure drop was the criteria for rejecting the filter.

6.2. Test with actual radioactive waste

The liquid waste in FF tank was processed with fibre filter, UF and RO membrane, and SIES. The total activity concentration of actual waste was 8.199×10^{-4} mCi/mL and the initial concentration of each nuclide is shown in Table VI. The activity of permeate was lower than LLD (Lower Limit of Detection) and the decontamination factor (DF) was of the order of 5,000 for these liquid radioactive waste.

TABLE VI. DATA SHEET OF THE DEMONSTRATION TEST

ISOTOPE	WHUT (μ CI/CC)	FF	DF	HFUF	DF	SRO	DF	SIES	DF
Na-24	4.466E-07	5.609E-07	-	1.525E-07	2.9	1.00E-08	15.25	1.00E-08	1.0
Mn-54	2.845E-05	1.215E-05	2.3	1.027E-05	1.2	1.00E-08	1,027	1.00E-08	1.0
Fe-59	3.968E-06	1.235E-06	3.2	7.228E-07	1.7	1.00E-08	71.3	1.00E-08	1.0
Co-58	2.567E-04	1.120E-04	2.3	1.050E-04	1.1	1.00E-08	10,500	1.00E-08	1.0
Co-60	1.849E-04	8.875E-05	2.1	8.238E-05	1.1	1.00E-08	8,238	1.00E-08	1.0
Zr-95	5.015E-06	1.00E-08	506.1	1.00E-08	1.0	1.00E-08	1.0	1.00E-08	1.0
Zr-97	4.312E-06	1.157E-06	3.7	1.00E-08	115.7	1.00E-08	1.0	1.00E-08	1.0
Nb-95	6.341E-06	1.00E-08	634.1	1.00E-08	1.0	1.00E-08	1.0	1.00E-08	1.0
Ru-106	1.623E-05	1.00E-08	1623.0	1.00E-08	1.0	1.00E-08	1.0	1.00E-08	1.0
Ag-110m	7.051E-05	2.119E-05	3.3	1.00E-08	2119.0	1.00E-08	1.0	1.00E-08	1.0
Sb-124	1.014E-05	4.056E-06	2.5	1.829E-06	2.2	1.00E-08	1,829	1.00E-08	1.0
Sb-125	7.890E-06	3.015E-06	2.6	1.381E-06	2.2	1.00E-08	1,381	1.00E-08	1.0
Xe-133m	5.914E-06	1.00E-08	454.9	1.00E-08	1.0	1.00E-08	1.0	1.00E-08	1.0
Cs-136	4.802E-06	1.178E-06	4.1	1.00E-08	117.8	1.00E-08	1.0	1.00E-08	1.0
Cs-137	3.794E-06	1.593E-06	2.4	1.325E-06	1.2	1.677E-07	7.9	1.00E-08	17
Ba-137m	2.104E-04	1.00E-08	21,040	1.00E-08	1.0	1.00E-08	1.0	1.00E-08	1.0
Sum	8.199E-04	2.519E-04	3.3	2.063E-04	1.2	3.167E-07	651.4	1.600E-07	2.0

NOTE: 1.00E-08 is used for minimum detectable activity(MDA) for calculating DF's

7. CONCLUSIONS

- (a) The combined system with fibre filter (FF) unit and reverse osmosis membrane module was successful to achieve the DF more than 1000 for cobalt. The rate of removal of organic materials and suspended solids in this FF met the pre-treatment requirements of the RO process.
- (b) The use of 3 kW UV lamp (180~400 nm wavelength) showed the removal of nearly 85% of TOC with 1000 ppm of H₂O₂ consumption.
- (c) The radionuclide rejection rate for the UF unit increased as the flow rate increased and also increased slightly with the increase of the operating pressure.
- (d) The cobalt and cesium rejection rates were higher in polyamide membrane than cellulose acetate membranes. However, the boron permeation rate was higher for the CA membrane.
- (e) The rejection rates of Co, Cs and surfactant showed the best result at pH9. The boron permeation rate showed good results at pH4. The boron permeation rates increased with the increase of the boron concentration.
- (f) The permeation rate of Co, Cs, surfactant, and boron showed best results at 45°C.
- (g) The demonstration tests with actual radioactive waste showed the activity of the permeate was lower than LLD (Lower Limit of Detection) and the overall decontamination factor (DF) was nearly 5,000 for these wastes with the activity concentration of 8.199×10^{-4} mCi/cm³.

REFERENCES

- [1] MOGHISSI, A. A., Radioactive Waste Technology, ASME, pp. 223– 274 (1986).
- [2] INTERNATIONAL ATOMIC ENERGY AGENCY, Treatment of Low and Intermediate Level Liquid Radioactive Wastes, Technical Report Series No. 236, IAEA, Vienna, pp 91–113 (1984).
- [3] ELECTRIC POWER RESEARCH INSTITUTE, Radioactive waste Generation Survey Update, EPRI/NP-5526, Vol. 2(1988).
- [4] BILAU, A., RUTAR, F., Liquid Radioactive Waste Processing History at Fort Calhoun Nuclear Station, Waste Management '89, Vol. 2 (1989).
- [5] Yongkwang Nuclear Power Plant I, “Scheme of Management Improvement on Radioactive Liquid Laundry Waste” (1994).
- [6] SONG, M. J. et al., Development of an Inorganic Ion Exchanger Utilization Process for Treatment of Liquid Radioactive Waste, KERPI-93N-J04, Korea Electric Power Research Institute (1996).
- [7] PARK, J. K. et al., Development of Liquid Radioactive Waste Treatment Technology with Reverse Osmosis Membrane, TR.96NS12.S1998.83, Korea Electric Power Research Institute (1998).
- [8] KOREA ELECTRIC POWER CORPORATION, Annual Summary Reports of Radiation Management in 1998, KEPSCO (1999).
- [9] KUCERA, J., Practical Application of Reverse Osmosis, EPRI International Low Level Waste Conference & Exhibit Show, 1997, United State Filter Corporation (1997).
- [10] ZAHID AMJAD, Reverse Osmosis (1993).
- [11] BIPIN S. PAREKH, Reverse Osmosis Technology (1988).
- [12] YANG, H. Y. et al., Cobalt and Organics Removal Effect Using Fiber Filter/Reverse Osmosis Combination Process For LLRW from Korean PWR NPP, ICONE-9, Nice, France (2001).

- [13] YANG, H., Y. et al., Pretreatment of Radioactive Laundry Waste UV Photo-Oxidation Process Optimum Operation of RO Membrane Process, WANO-TC Workshop, Matsue, Japan (2000).
- [14] PARK, S.M et al., An Experimental Study on Liquid Radioactive Waste Treatment Process Using Inorganic Ion Exchanger, J. Environ. Sci. Health, A34(4), 767– 793 (1999).
- [15] WONG, J. M., Boron Control in Power Plant Reclaimed Water for Potable Reuse, Environ. Progress, Vo. 3, No. 1, pp. 5– 11 (1984).
- [16] KIKUCHI M. and SUGIMOTO, Y., Development of a Laundry Waste Treatment System, Nuclear Engineering and Design, 44, 413 (1977)

ELABORATION OF A COMBINED ELECTROSORPTION METHOD FOR TREATMENT OF LLRW

Yu. KARLIN, R. ILIASOV, I. SOBOLEV
Moscow State Enterprise — MosNPO “Radon”,
Sergiev Posad, Russian Federation

Abstract. The basic principles of electrosorption were described and the terms “contact” and “non-contact electrosorption” were explained. A mathematical model of electrosorption was developed to describe the kinetics of the sorption processes in a sorbent layer in an electrical field.

A laboratory installation for an experimental study of electrosorption was designed and constructed. ^{137}Cs electrosorption on the sorbent “Fenix-A” (nickel hexacyanoferrate precipitated on silica gel - a production MosNPO “Radon”) was studied. Comparison of theoretical and experimental results has shown a satisfactory correspondence (on the qualitative level).

Electrosorption of ^{90}Sr on a BaSO_4 colloidal sorbent and electrosorption of ^{137}Cs , ^{90}Sr and ^{238}U on chitin-chitosan sorbents in the laboratory installation was investigated. A pilot scale facility for treatment of real liquid radioactive waste from tanks at MosNPO “Radon” was constructed.

1 INTRODUCTION

Various sorption processes are widely used for the treatment of contaminated water and liquid radioactive waste. [1]. There are two main regimes of sorption: a static regime and a dynamic regime. In the static regime, a sorbent and water to be cleaned are mixed together. The admixture is distributed between the solution and the sorbent (sometimes to the thermodynamic equilibrium), whereupon the sorbent is separated from the solution. In the dynamic regime, the water is filtered through an unmovable or less movable layer of sorbent. Dynamic sorption is often realized in column apparatus.

Only sorbents with certain properties can be effectively used for treatment. They must be sufficiently strong, should have low hydraulic resistance, low adhesion to suspended and colloidal admixtures, and also a well developed surface for fast internal diffusion of ions. The latter requirement explains the fact that a most widespread type of sorbents is a granular sorbent. The size of granules may be different, but frequently it varies from 100 μm up to several millimeters. Powdered and colloidal sorbents (for instance, freshly prepared BaSO_4), sorbents with low mechanical toughness, and stringy (scaly) sorbents are not applicable for treatment.

Electrosorption is more flexible regarding the properties of sorbents since this method does not require filtration of the solution through a sorbent layer and even does not need a direct contact between them. The basic principles of electrosorption are described elsewhere, e.g. in [2–3]. A sorbent is placed between two porous diaphragms (for instance, between microfiltration or ultrafiltration membranes), the treated solution washes these diaphragms outside, and electrical current is passed through the solution and the sorbent layer (perpendicular to the surfaces of diaphragms or membranes). Under the electrical field, ions move through the sorbent layer and, in the porous space of the sorbent, are redistributed between the sorbent and the water phase.

The nearest analogue of electrosorption is electrodialysis with dialysate chambers filled with ion-exchangers [4–6], however there is a principle difference between the two methods. There is no movement of the solution through the sorbent layer at electrodialysis.

In spite of its simplicity, electrosorption was not explained theoretically, and there is no information on its practical use. Within this study, an attempt was made to develop

theoretical aspects of electrosorption on the basis of electrochemical kinetics, and compare theoretical assumptions with experimental results for the solution $K^+-Cs^+-H^+-OH^--NO_3^-$, as well as a variant of its practical realization in a multichamber electromembrane device. was proposed.

2 THEORY

As the processes involved in electrosorption are quite complicated, a simple mathematical model was proposed to explain the transport of ions. The following conditions were considered (Fig.1):

the water solution of electrolyte $K^+-Cs^+-H^+-OH^--NO_3^-$ was considered (electrosorption on an inorganic sorbent in this system was studied experimentally),

the sorbent layer and two diffusion layers near the sorbent layer were assumed,

the Nernst model was used for describing the diffusion layers,

the sorbent layer was considered as a solution of single-charge unmovable ion-exchange groups R^- , having a homogeneous distribution and always being in certain cation forms,

at the sorbent layer in any system spot there is a point of thermodynamic equilibrium for the cation distribution between the ion-exchange groups and the water phase,

one-dimension non-stationary electrodiffusion of ions through the sorbent and the diffusion layers was considered,

it was assumed that the electrodes are sufficiently separated from the considered system (to neglect the influence of electrode reaction products),

the composition of an external solution is defined by the condition of material balance (the given volumes of the solution and the sorbent layer are considered).

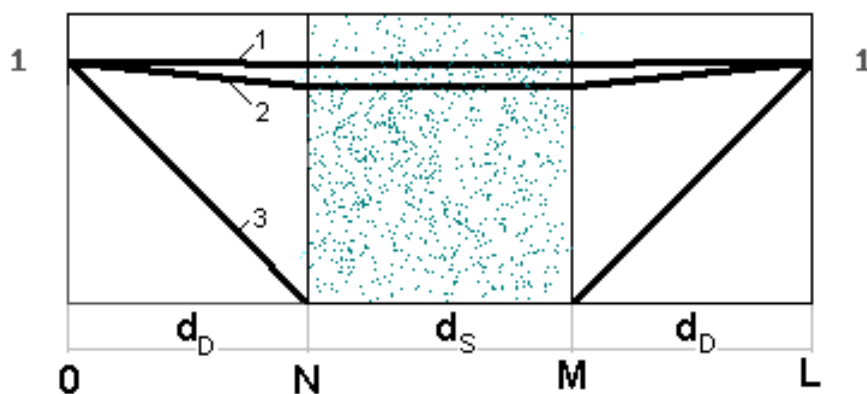


FIG. 1. The profiles of the relative ion concentration in the diffusion layers and in the sorbent layer during electrosorption of the solution $0,02M KNO_3+0,002M CsNO_3$ (pH 7): 1 - NO_3^- ; 2 - K^+ ; 3 - Cs^+ .

In Fig.1 the ion concentrations are given in the relative form:

$$\bar{C}_i = \frac{C_i}{C_{oi(V)}} \quad (1)$$

where

C_i is the concentration of i-th type of ion in the accounting area,

$C_{oi(V)}$ is the concentration of i-th type of ion in the volume of the solution at an initial period.

A system of non-stationary electrodiffusion equations, written for each type of ion, was used for the description of ion transport. This system was complemented by a condition

of electroneutrality of the solution and a condition of conservation of the total concentration of ion-exchange groups in the sorbent layer.

The above assumptions allow to suppose that only three types of ion exchange reactions are possible in the sorbent layer:



A trivial system of differential equations was used for the description of ion transport in the diffusion layers:

$$\frac{\partial C_i}{\partial t} = \text{div}(J_i) \quad (5)$$

$$\frac{\partial(C_H - C_{OH})}{\partial t} = \text{div}(J_H - J_{OH}) \quad (6)$$

$$J_i(X) = -D_i \frac{dC_i}{dX} - Z_i D_i C_i \frac{d\Psi}{dX} \quad (7)$$

$$I = F \sum_{i=1}^N Z_i J_i \quad (8)$$

$$C_K + C_{Cs} + C_H = C_{NO_3} + C_{OH} \quad (9)$$

$$C_H C_{OH} = K_w \quad (10)$$

where

- C_i is the concentration of i-th type of ions,
- J_i is the specific flow of i-th type of ions,
- Z_i is the charge of i-th type of ions,
- D_i is the diffusion coefficient of i-th type of ions,
- t is the time,
- X is the coordinate, directed perpendicular to the surfaces of the membrane,
- $\Psi = \frac{\phi F}{RT}$ is the relative electrical potential,
- F is the Faraday number,
- R is the universal gas constant,
- T is the temperature,
- I is the density of electrical current,
- K_w is the constant of water dissociation,
- $N=5$ is a number of types of ions in the considered system.

The system of equations, which was used for the description of ion transport in the sorbent layer, looks much more complex:

$$\frac{\partial C_K}{\partial t} = \text{div}(J_K) + k_{H/K} C_H C_{RK} + k_{Cs/K} C_{Cs} C_{RK} - k_{K/H} C_K C_{RH} - k_{K/Cs} C_K C_{RCs} \quad (11)$$

$$\frac{\partial C_{Cs}}{\partial t} = \text{div}(J_{Cs}) + k_{H/Cs} C_H C_{RCs} + k_{K/Cs} C_K C_{RCs} - k_{Cs/H} C_{Cs} C_{RH} - k_{Cs/K} C_{Cs} C_{RK} \quad (12)$$

$$\frac{\partial(C_H - C_{OH})}{\partial t} = \text{div}(J_H - J_{OH}) + k_{K/H} C_K C_{RH} + k_{Cs/H} C_{Cs} C_{RH} - k_{H/K} C_H C_{RK} - k_{H/Cs} C_H C_{RCs} \quad (13)$$

$$\frac{\partial C_{NO_3}}{\partial t} = \text{div}(J_{NO_3}) \quad (14)$$

$$\frac{\partial C_{RK}}{\partial t} = k_{K/H} C_K C_{RH} + k_{K/Cs} C_K C_{RCs} - k_{H/K} C_H C_{RK} - k_{Cs/K} C_{Cs} C_{RK} \quad (15)$$

$$\frac{\partial C_{RCs}}{\partial t} = k_{Cs/H} C_{Cs} C_{RH} + k_{Cs/K} C_{Cs} C_{RK} - k_{H/Cs} C_H C_{RCs} - k_{K/Cs} C_K C_{RCs} \quad (16)$$

$$\frac{\partial C_{RH}}{\partial t} = k_{H/K} C_H C_R + k_{H/Cs} C_H C_{RCs} - k_{K/H} C_K C_{RH} - k_{Cs/H} C_{Cs} C_{RH} \quad (17)$$

$$J_i(X) = -D_i \frac{dC_i}{dX} - Z_i D_i C_i \frac{d\psi}{dX} \quad (18)$$

$$I = F \sum_{i=1}^N Z_i J_i \quad (19)$$

$$C_K + C_{Cs} + C_H = C_{NO_3} + C_{OH} \quad (20)$$

$$C_{RK} + C_{RCs} + C_{RH} = C_X \quad (21)$$

$$C_H C_{OH} = K_W \quad (22)$$

In equations (11–22): $\overrightarrow{k_{i/j}}$ and $\overleftarrow{k_{j/i}}$ is the constant of ion-exchange rate for the exchange of j-th and i-th sort of ions, respectively, in the sorbent layer according to equations (1) – (3); C_X is the concentration of ion-exchange groups in the sorbent layer.

The considered model of electrosorption systems could be summarized by a material balance equation for each type of ions:

$$V \frac{dC_{i(V)}}{dt} = (J_i^L - J_i^0) S \quad (23)$$

and the condition of pH stability in the external solution

$$\begin{aligned} C_{H(V)} &= \text{const} \\ C_{OH(V)} &= \text{const} \end{aligned} \quad (24)$$

where

$C_{i(V)}$ is the concentration of i-th type of ions in the external solution,

V is the total volume of the external solution,

S is the working area of the membrane (or the sorbent layer) surface,

J_i^0 and J_i^L are the specific flows of i-th type of ions in the point 0 and L (Fig.1).

The requirements, expressed by equations (23) and (24), define the border conditions and those have been incorporated for the maximum compliance of the theoretical model with the conditions of the experiment.

The initial conditions were given by the distribution of ion concentrations in the whole transport area and in the volume of the external solution at a zero moment of time. The initial distribution of ion concentrations is shown in Fig.1. At the initial moment the sorbent inheres in K-form mainly. The initial ion concentration profiles in the diffusion layers are linear. In the sorbent layer, the concentration gradient of any ion is zero.

A numerical method was used to solve the differential equations system. A PC was used for the calculations.

A case of point thermodynamic equilibrium between the solution and the sorbent in any accounting mode in the sorbent layer was used for the numerical calculations. For the realization of this condition the absolute values of rate constants of the direct ion-exchange reactions were given arbitrarily greater than the flow rate of ions related to the ion-exchange reaction, and also much larger than the electrodiffusion rate of ions. The values of the rate constants of the reverse ion-exchange reactions were calculated for known values of the rate constants of the direct ion-exchange reactions and the given values of distribution coefficient of ions between the water solution and the sorbent.

The calculation results (Fig.2) show that the rise of the density of electrical current leads to significant intensification of ion transport. The rise of pH of the solution leads to the significant increase of target ion extraction from the treated solution (Fig. 3). There are three stages of electrosorption (Fig.4). In an initial stage, mainly ion exchange processes occur in the sorbent layer on anode. In a second stage, the sorption front is moving through the sorbent

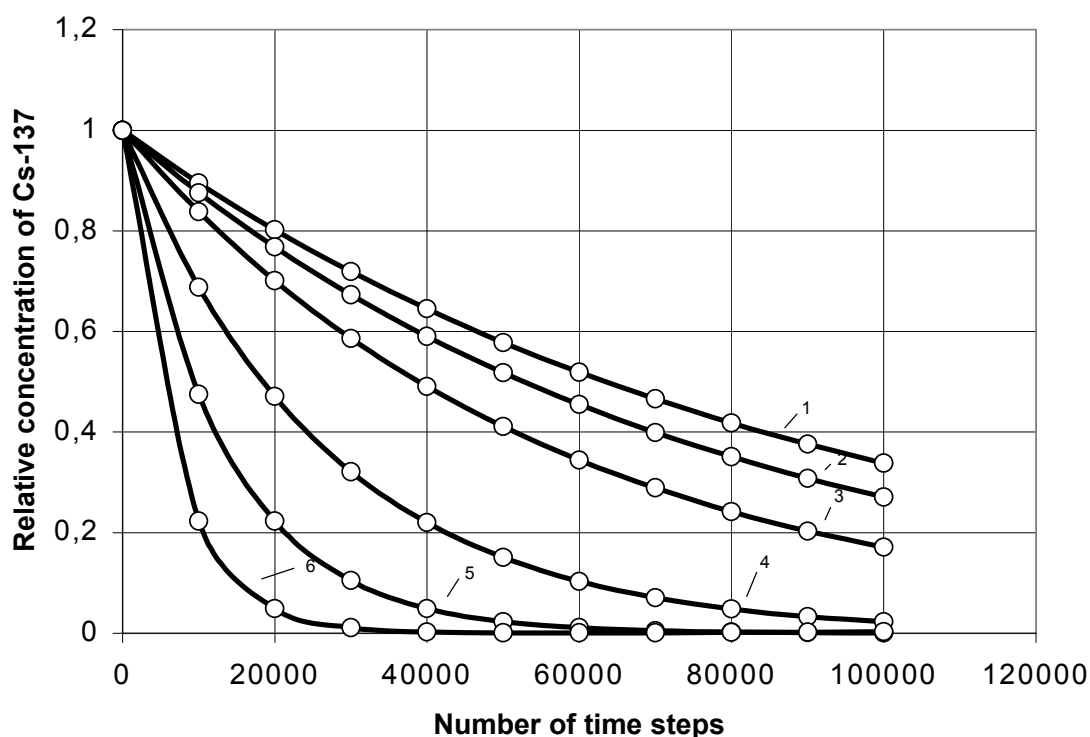


FIG.2. Dependence of the relative concentration of Cs^+ on time in the numerical calculation of electrosorption for the external solution: $0,02\text{M KNO}_3 + 0,002\text{M CsNO}_3$: 1- $I=0 \text{ A/m}^2$, 2- $I=1 \text{ A/m}^2$, 3- $I=2 \text{ A/m}^2$, 4- $I=5 \text{ A/m}^2$, 5- $I=10 \text{ A/m}^2$, 6- $I=20 \text{ A/m}^2$.

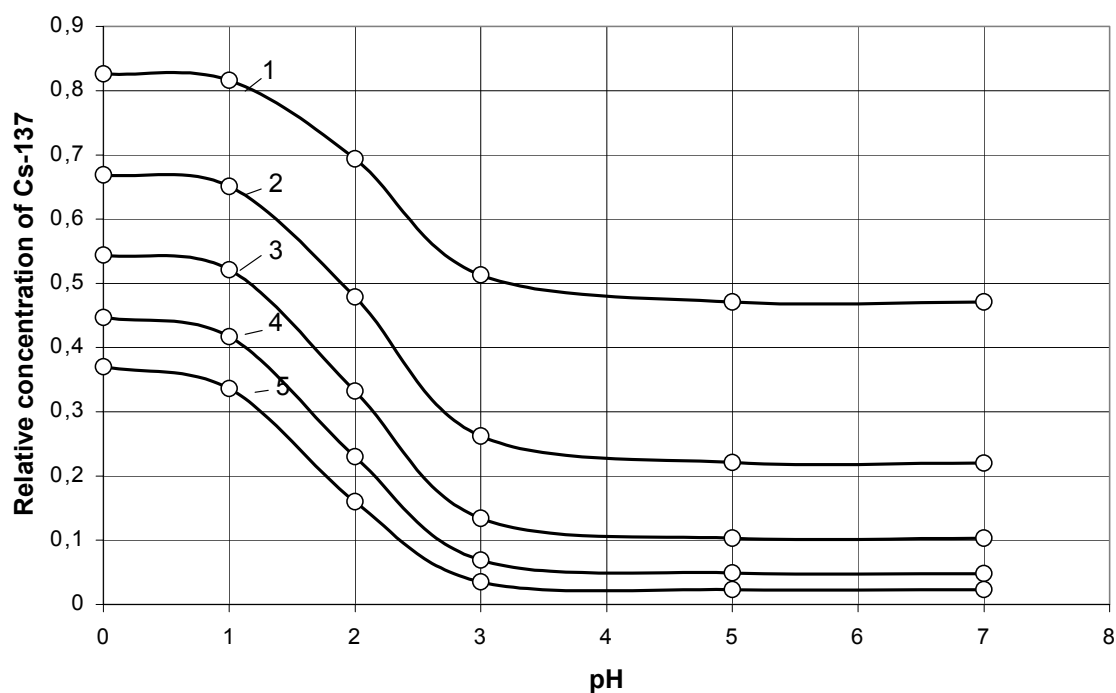


FIG.3. Dependence of the relative concentration of Cs^+ on pH in the numerical calculation of electrosorption for the external solution $0,02\text{M KNO}_3 + 0,002\text{M CsNO}_3$. The number time steps: 1–20000, 2–40000, 3–60000, 4–80000, 5–100000.

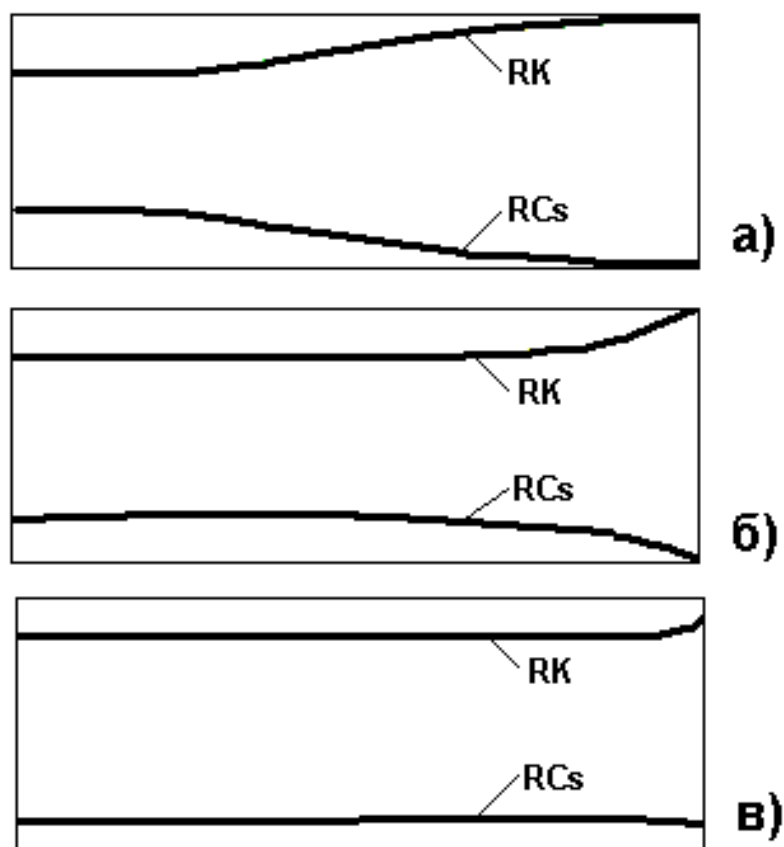


FIG.4. The accounting concentration profiles of RK and RCs in the sorbent layer in the solution $0,02\text{M KNO}_3 + 0,002\text{M CsNO}_3$ ($\text{pH}=7$). The number of time steps is: a) 50000, b) 100000, c) 250000.

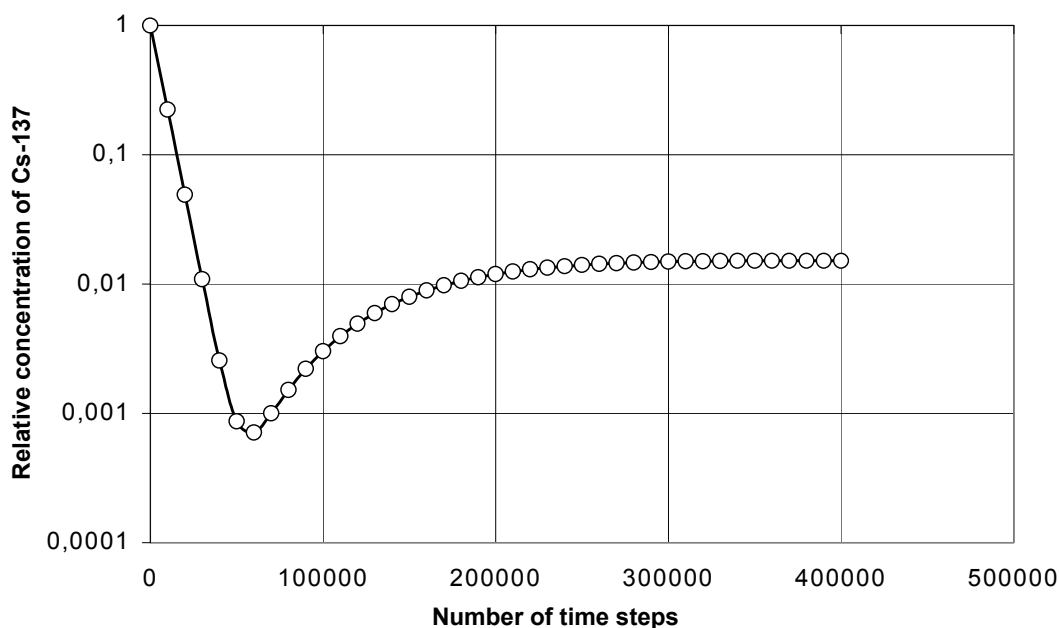


FIG.5. Dependence of \overline{C}_i on the number of time steps for the solution $0,02M KNO_3 + 0,002M CsNO_3$ ($pH=7$).

layer to cathode. At some moment the maximum level of removal of admixture (caesium) is reached (Fig.5), since the sorption regime is close to the dynamic regime. Finally, in a third stage, the concentration profile of the migrating components in the sorbent is leveling - a sorption regime approaches to the static regime, the level of admixture extraction falls, since parts of ions, which were connected to the ion-exchange groups, are transferred from the sorbent to the external solution.

3 EXPERIMENTAL METHOD

Most of experiments were carried out with model solutions in a laboratory installation. The isotopes ^{137}Cs , $^{90}Sr + ^{90}Y$, $^{238}UO_2^{2+}$ were added to the model solution (in the amount $1.85 \cdot 10^6$ Bq/L, approximately). The following sorbents were used in different experiments:

- (i) The sorbent "Fenix-A" (nickel ferrocyanide, precipitated on the silica gel, the size of granules is 0,5–0,8 mm),
- (ii) Clinoptilolite (natural zeolite),
- (iii) Natural clay and bentonite,
- (iv) Chitin-chitosan sorbents,
- (v) Anion resins of a type EDE-10P (made in Russia, crushed, size particles $<100 \mu m$),
- (vi) Cation resins of a type KA-11 (made in Russia, size granules 0,6–0,8 mm),
- (vii) Precipitate of barium sulfate.

A laboratory installation for experimental studies of electrosorption was designed and assembled (Fig.6). The main element of the laboratory installation is a five-chamber electromembrane cell with the working area of the membrane 30 cm^2 . The chamber with the sorbent and the electrode chambers were separated from the nearest chambers containing the model solution by the ultrafiltration membranes of type UPM-P (the average size of pores is

$5 \cdot 10^{-8}$ m). The electrode chambers were separated from the chambers containing the model solution in order to avoid contact of gases formed on electrodes with the surface of the sorbent, as well as to avoid the influence of the electrode reactions products on pH of the model solution contacting the sorbent.

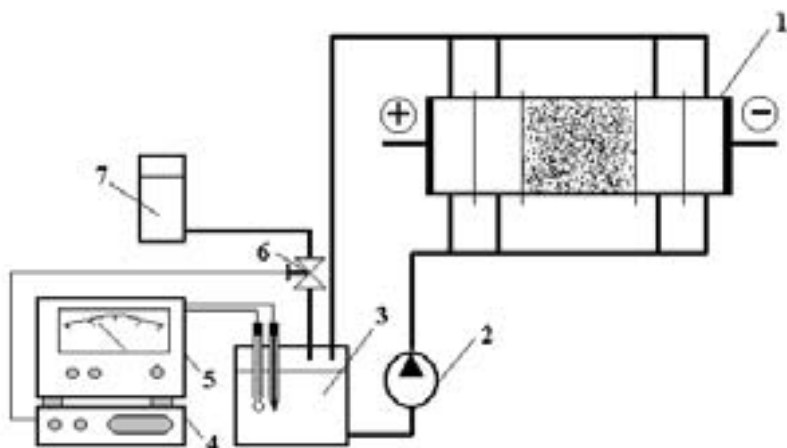


FIG.6. The principle scheme of the laboratory installation for electrosorption studies.
1 – electrosorption cell, 2 – peristaltic pump, 3 – vessel for the model solution, 4 – block of automatic titration, 5 – pH-meter, 6 – electromagnetic valve, 7 – vessel with nitric acid.

The model solution was circulated from the vessel through the flow-through chambers of the cell with the help of a peristaltic pump. The density of electrical current changed from 0 to 100 A/m^2 . A stabilized direct current power source of the type B5-47 was used. pH of the model solution was maintained at a given level by addition of nitric acid with the help of the block of automatic titration (the type BAT-15) and pH-meter (the type pH-673.M). In the experiments, pH of the model solution always increased.

Samples of the solutions were taken at the certain intervals of time. The ^{137}Cs contents was determined by gamma-spectrometry, contents of ^{90}Sr and ^{90}Y - by integral β -radiometric method (the ^{90}Sr and ^{90}Y contents were received from the calculations of the time dependence of the specific β -activity of the sample) and contents of ^{238}U - by an integral α -radiometric method.

On completion of the experiments with ^{137}Cs , the sorbent was removed from the cell, washed from solution remainders by distilled water and directed for the determination of ^{137}Cs concentration by the gamma-spectrometry.

4 RESULTS AND DISCUSSIONS

4.1. COMPARISON OF THE THEORY WITH THE EXPERIMENTS

The experimental testing of the calculation results was conducted on the model solution $0,02\text{M KNO}_3 + 0,0002\text{M CsNO}_3$ under different fixed pH values. The isotope ^{137}Cs was added to the model solution (in the amount $1,85 \cdot 10^6 \text{ Bq/L}$) and a sorbent "Fenix-A" was used. The main results of the experiments shown in Figs. 7–8 confirm the main theoretical dependencies (Figs. 2–3).

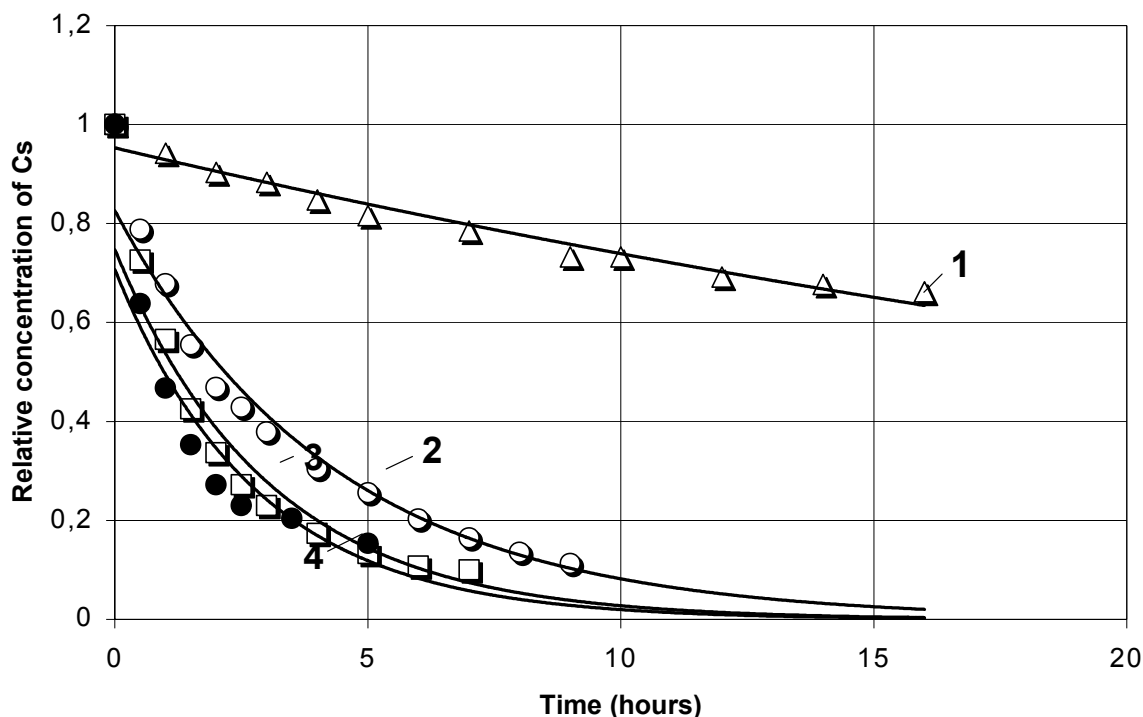


FIG.7. Dependence of the relative concentration of Cs^+ on time during electrosorption of the external solution $0,02\text{M KNO}_3 + 0,0002\text{M CsNO}_3$: 1– $I=0 \text{ A/m}^2$, 2– $I=25 \text{ A/m}^2$, 3– $I=50 \text{ A/m}^2$, 4 – $I=100 \text{ A/m}^2$).

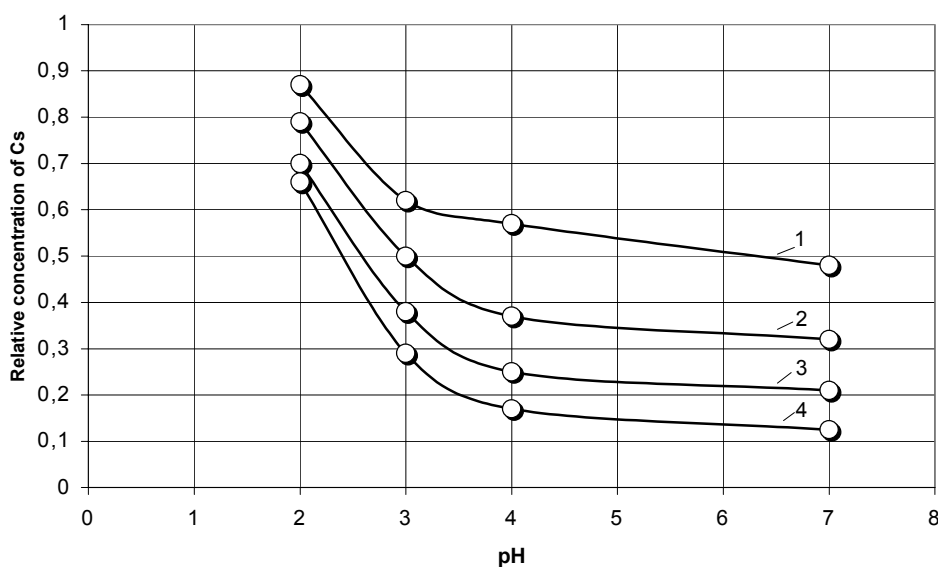


FIG.8. Dependence of the relative concentration of Cs^+ on pH during electrosorption of the external solution $0,02\text{M KNO}_3 + 0,0002\text{M CsNO}_3$: 1– $t=2 \text{ h}$, 2– 4 h , 3– 6 h , 4– 8 h .

4.2. DEPENDENCE OF THE ^{137}Cs ELECTROSORPTION KINETICS ON THE SORBENT TYPE

In the beginning, the experiments with the electrosorption of ^{137}Cs from the model solution $0.02\text{M KNO}_3 + 0.0002\text{M CsNO}_3$ were carried out with the ferrocyanide sorbent "Fenix-A" only. It was interesting to compare the treatment kinetics of the solution containing ^{137}Cs for other sorbents – clinoptilolite, bentonite and natural clay. The results of experiments (Fig.9) show that the treatment kinetics for the model solution depends significantly on the sorbent type.

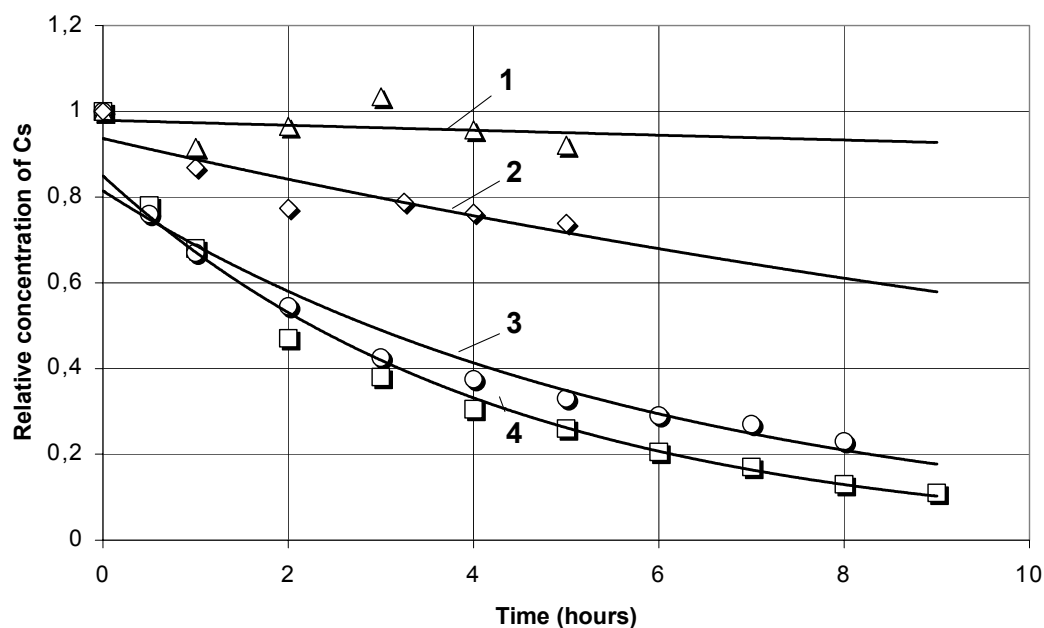


FIG.9. Dependence of the relative concentration of Cs^+ on time at electrosorption of the system $0,02M KNO_3 + 0,0002M CsNO_3$ (sorbents: 1-natural clay, 2-bentonite, 3-clinoptilolite, 4-Fenix-A, $I=25 A/m^2$).

4.3. INFLUENCE OF THE SIZE OF SORBENT PARTICLES ON THE ^{137}Cs ELECTROSORPTION KINETICS

It is known that the rate of sorption increases with the specific surface of the sorbent. At the reduction of particle sizes the specific surface grows. Therefore, the rate of sorption is greater for fine fractions of a sorbent in both the static and the dynamic regimes of sorption.

The results of experimental testing of the influence of the average size of the sorbent particles on the rate of electrosorption of ^{137}Cs on clinoptilolite have shown (Fig.10), that the electrosorption speed depends on the sorbent particles size insignificantly. This fact also confirms the main role of electromigration, the velocity of which insignificantly depends on the size-fraction distribution in the sorbent layer.

4.4. SORPTION AND ELECTROSORPTION OF ^{238}U ON THE CHITIN-CHITOSAN SORBENTS

As chitin-chitosan sorbents have an organic basis they can be easily incinerated after the end of treatment. Thus, the high volume reduction (>10) could be reached this way. However, chitin-chitosan sorbents have a fibrous structure. Their density is usually less than the density of water that creates huge problems in their use in traditional sorption devices. The electrosorption method is more reluctant to sorbent characteristics.

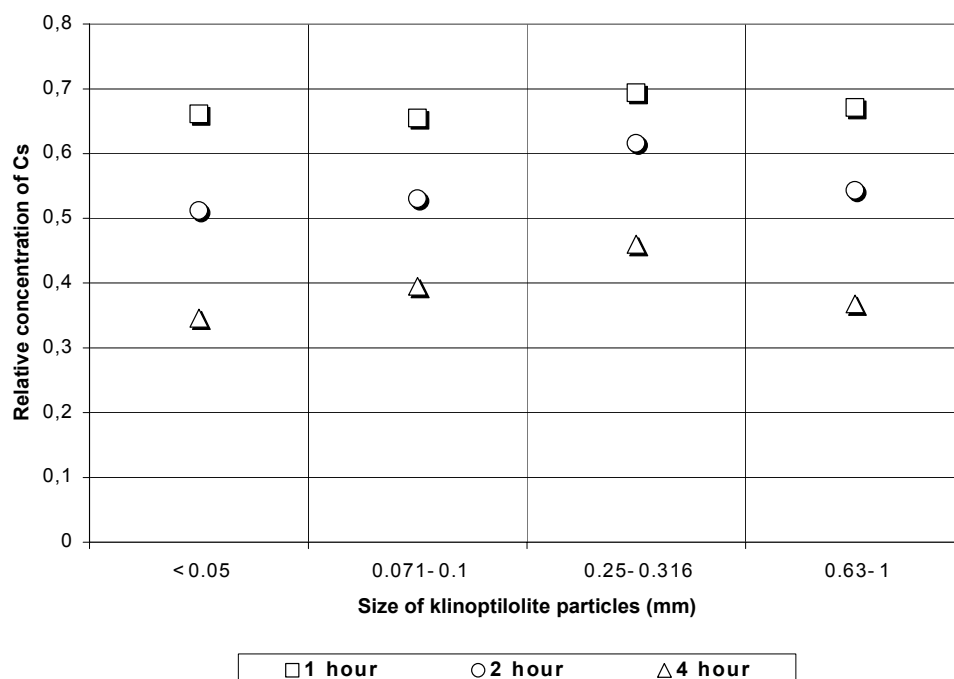


FIG.10. Dependence of ^{137}Cs electroadsorption rate on the size of clinoptilolite particles at different time of electroadsorption ($I=25 \text{ A/m}^2$)

A study on the use of chitin-chitosan sorbents in electroadsorption was carried out with the model solutions of $^{238}\text{UO}_2(\text{NO}_3)_2$. Three types of sorbents were tested: anion-exchange resins of a type EDE-10P (made in Russia, crushed, size particles $<100 \mu\text{m}$), granular chitin-chitosan sorbent (manufactured by the Institute of Bioorganic Chemistry of the Russian Academy of Sciences), crushed chitin-chitosan sorbent "Micoton" (manufactured by the Institute of Cell Biology and Genetic Engineering of the Ukrainian Academy of Sciences).

Two series of experiments – the study of the UO_2^{2+} sorption kinetics in the static regime and the study of UO_2^{2+} electroadsorption kinetics were carried out. All experiments were carried out with a model solution of $0.01\text{M KNO}_3 + \text{UO}_2(\text{NO}_3)_2$. The amount of uranium nitrate (used as isotope ^{238}U) added depended on the required concentration activity of the solution (in various experiments - from $1 \cdot 10^4 \text{ Bq/L}$ up to $2 \cdot 10^5 \text{ Bq/L}$ or from 1 g/L up to 30 g/L of uranium nitrate).

In the static regime of sorption the technique of experiments was the following. A sorbent under investigation (volume of the sorbent was 0.65 mL) was added to the model solution (100 mL) in a glass baker. The solution was mixed by a magnetic stirrer during the certain period of time, and then filtered through the paper filter of "a blue ribbon tape" and sent for radiometry.

The experimental results, Fig. 11, show that the crushed anion-exchange resins have the highest factor of accumulation of uranium ions and the highest kinetic characteristics of its extraction from the model solution. The crushed chitin-chitosan sorbent "Micoton" has the same kinetic characteristics, but the factor of accumulation is much smaller. The granulated chitin-chitosan sorbent has the worst characteristics of the extraction of uranium ions from the model solution.

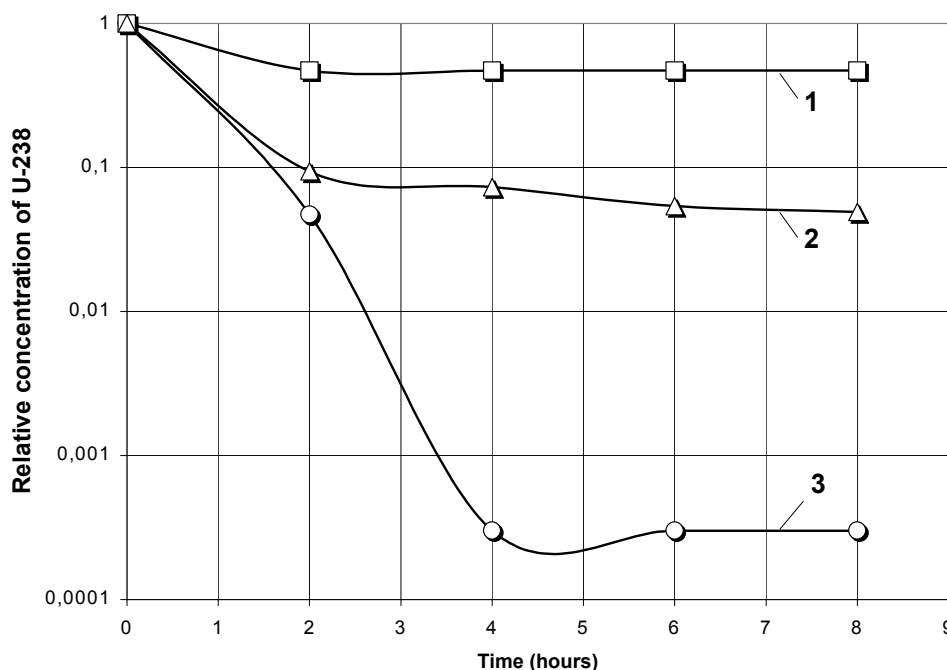


FIG. 11. Dependence of the relative concentration of ^{238}U on the sorption time (static regime, $0.01\text{M KNO}_3 + ^{238}\text{UO}_2(\text{NO}_3)_2$, 1 - granulated chitin-chitosan sorbent, 2 - chitin-chitosan sorbent "Micoton", 3 - anion-exchange resin).

The study of UO_2^{2+} electrosorption kinetics has shown that, in conditions of the laboratory five-chamber electrosorption cell (Fig. 6), the largest part of uranium ions is drop out on the cathode surface in the electro-precipitation process - presumably, as hydroxide, owing to increasing pH (up to 11 and more) of the solution near the cathode surface (consequence of electrolysis of water molecules). It is necessary to emphasize the necessity of the strict pH control of the solution under electrosorption treatment of ions (radionuclides), which may have a hydrolysis form.

However, despite of the suppression of UO_2^{2+} at electrosorption process, a high coefficient of the extraction of uranium ions from the solution was observed (Fig. 12).

Therefore, it is possible to speak about the potential opportunity of electrosorption for removal of radionuclides from contaminated water.

4.5. ELECTROSORPTION OF ^{90}Sr ON THE PRECIPITATED BaSO_4

It is known, that the precipitate of barium sulfate can selectively extract strontium ions from contaminated water containing the ions of calcium which is the nearest analogue of strontium. At the same time the precipitate of barium sulfate is effective only in a fine-powder form, as in a granular form the surface accessible for sorption is sharply reduced. However, there are significant difficulties in the subsequent separation of the fine-powder sorbent from the treated solution.

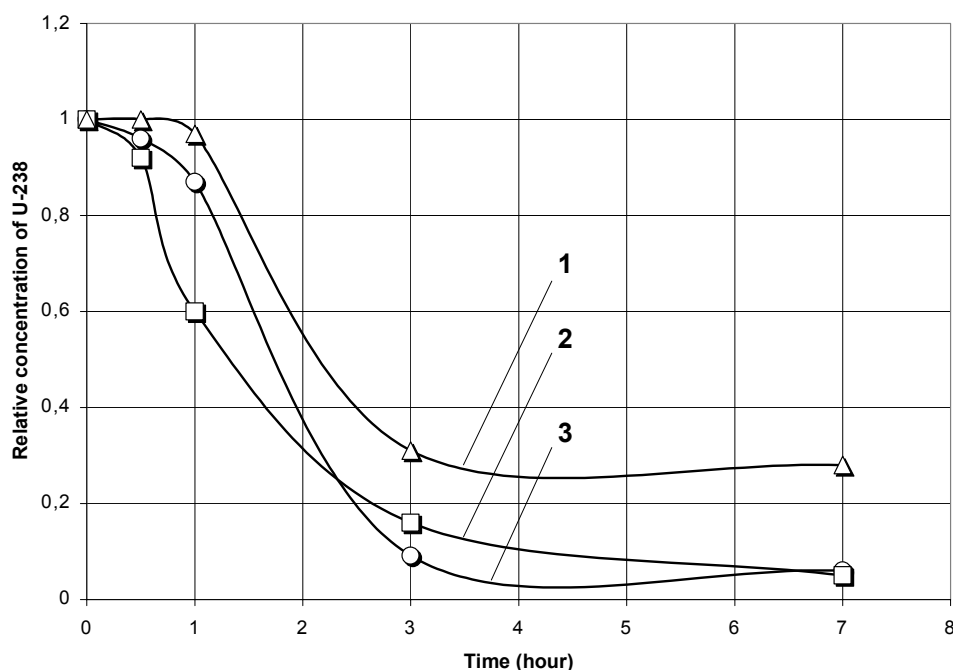


FIG.12. Dependence of the relative concentration of ^{238}U on the electroosorption time ($I=100 \text{ A/m}^2$, $0.01\text{M KNO}_3 + ^{238}\text{UO}_2(\text{NO}_3)_2$, 1 - pasteboard sorbent "Micoton", 2 - disperse sorbent "Micoton", 3 - anion-exchange resin).

Electroosorption has no such disadvantages, but it was not clear whether the strontium ions are fixed on the surface of barium sulfate as a result of electromigration. The results of experiments, which have been carried out with model solutions in the laboratory five-chamber cell, Fig.13, show that the selectivity of BaSO_4 to strontium ions is due to electroosorption.

It was found out that during electroosorption ^{90}Y is fixed on BaSO_4 much less than during normal sorption (without the direct electrical current). ^{90}Sr is less sensitive to passing the direct electrical current through the sorbent layer.

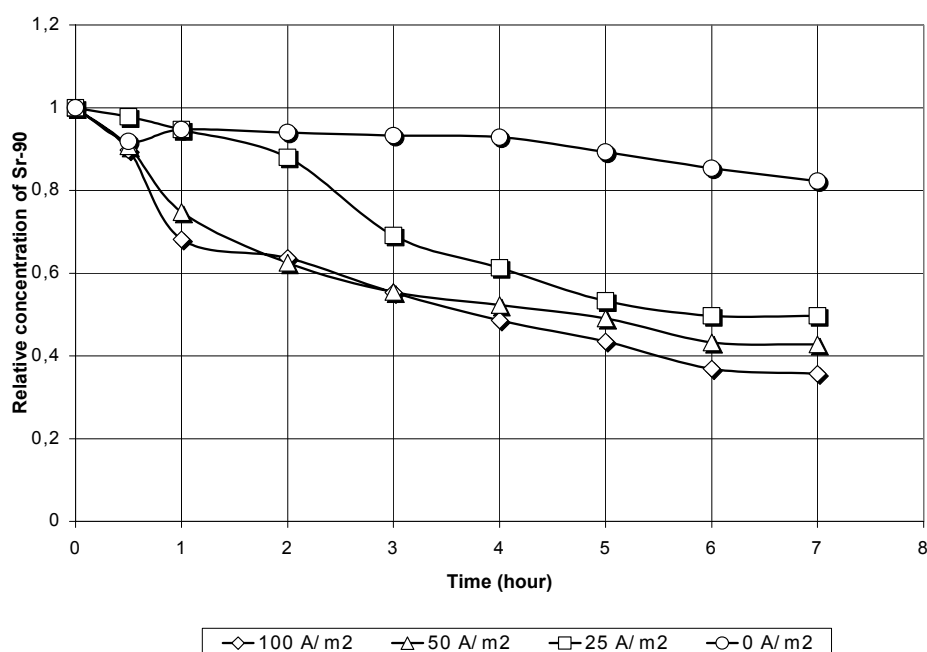


FIG. 13. Dependence of the relative concentration of ^{90}Sr on the electroosorption time (sorbent - BaSO_4 , $0.02\text{M KNO}_3 + 0.0002\text{M CsNO}_3 + ^{90}\text{Sr}$).

4.6. USING OF TRUMEM[®] CERMET MEMBRANES IN THE ELECTROSORPTION CELL

There is a trend in radioactive waste treatment to use thin porous (micro and ultrafiltration) inorganic membranes, which endure high radiation fields, temperatures, and are stable in aggressive media. The Russian company "Ultram International" has been developing TRUMEM[®] cermet membranes since 1991. After ten years of investigations, a broad spectrum of cermet membranes (from microfiltration up to nanofiltration ones) has been developed as well as composite reverse osmosis membranes in which an organic layer is put on a cermet base.

In our experiments, an attempt was made to combine selective sorbents and a cermet membrane in an electrosorption apparatus in order to treat intermediate and high level radioactive waste and also to increase the safety of the electromembrane apparatus.

As a first step, electrosorption of ⁹⁰Sr from a model solution with cation-exchange resins was carried out when one of electrodes (cathode) was a TRUMEM[®] membrane (Fig.14). The working area of the membrane was 60 cm². The results of experiment, Fig. 15, show that electrical current appreciably intensified the sorption process. The difference of potentials on the TRUMEM[®] membrane at the density of electrical current 100 A/m² does not exceed 1 V.

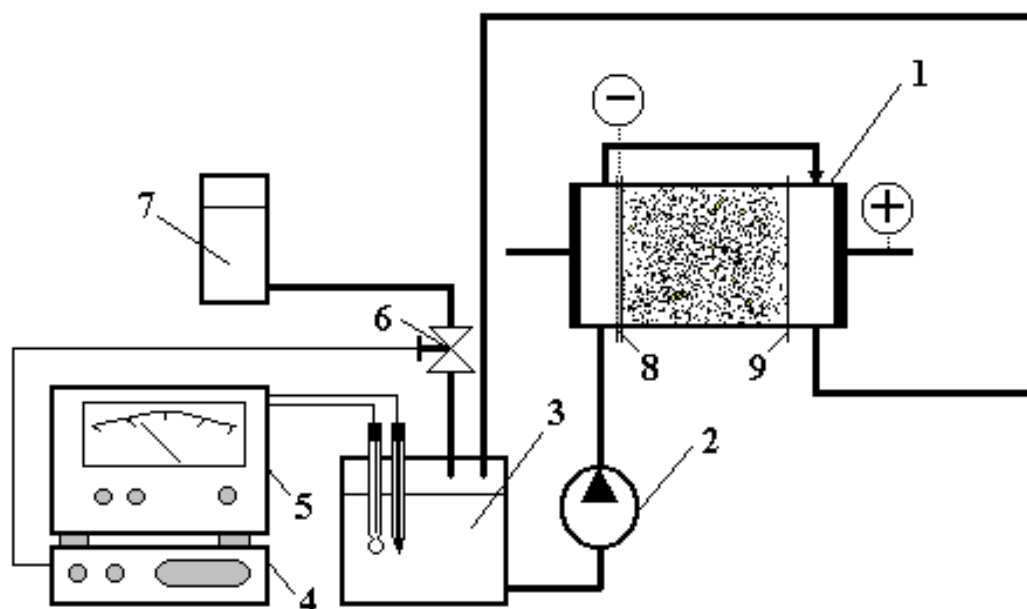


FIG.14. The laboratory installation for the study of the electrosorption with the TRUMEM[®] membrane: 1–electrosorption cell, 2–peristaltic pump, 3–vessel for the model solution, 4– the block automatic titration, 5–pH-meter, 6–electromagnetic valve, 7–vessel with the nitric acid, 8 - TRUMEM[®] membrane, 9 - filtration fabric.

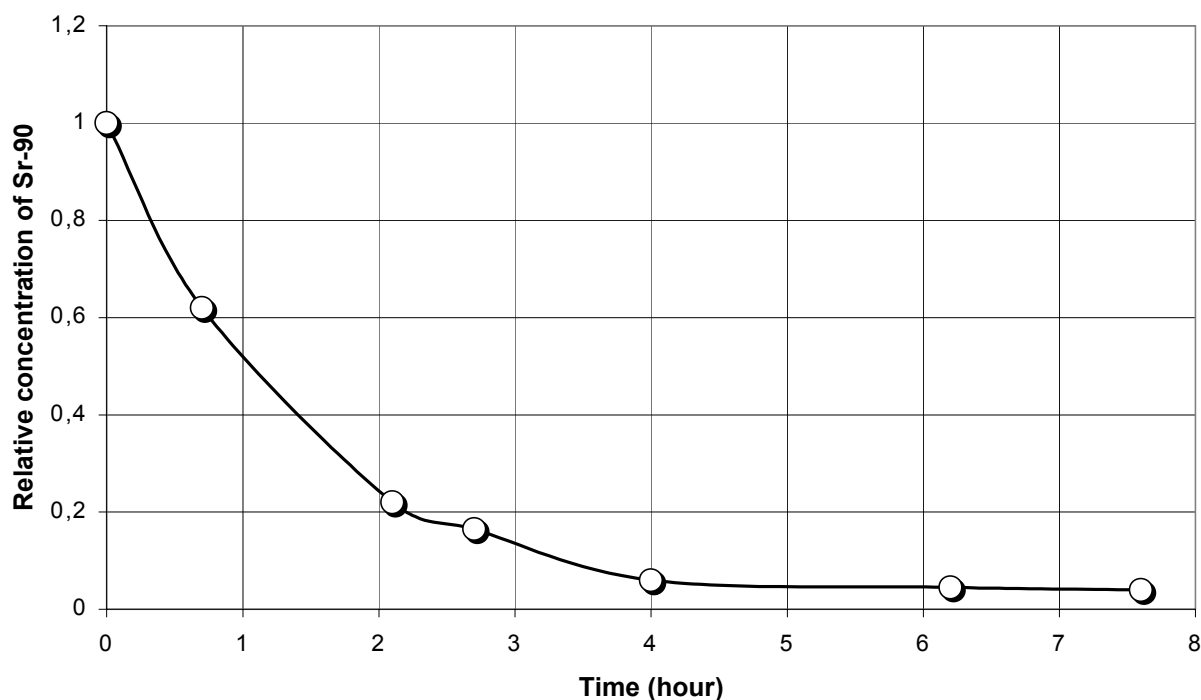


FIG.15. Dependence of the relative concentration of ^{90}Sr on the electrosorption time (sorbent - cation-exchange resins, filtration fabric and membrane TRUMEM[®], ground water + 0,0085M $\text{Ca}(\text{NO}_3)_2$ + ^{90}Sr).

5. PROSPECTS FOR THE PRACTICAL REALIZATION OF ELECTROSORPTION

5.1. GENERAL

The results of experimental and theoretical investigations show that electrosorption occupies an intermediate place between the dynamic and static variants of sorption (regarding the efficiency of the target ion extraction from the solution). Its features are: the possibility to regulate the speed of sorption by changing the density of electrical current; the absence of blocking of the sorbent surface with precipitates and colloids and the absence of high hydraulic resistance of the sorbent layer.

Electrosorption can be practically realized in a filter-press apparatus with interleaving sorbent chambers and chambers filled with a treated solution (Fig.16). Electrodes are placed on the edges of such a multichamber assembly, to which the difference of electrical potential is applied. In order to reduce the influence of polarization of the concentration on the surface of porous membranes, the treated solution must be passed through the chambers with the linear velocity greater than 0,1 m/s.

The design of such a device is close to the design of the electrodialyser with the dialysate chambers filled with ion-exchange materials, however in the case of the electrosorption apparatus the chambers filled with the sorbent are not running.

Different variants of such a device are possible. In one of them, loading of the fresh sorbent and unloading of the spent sorbent can be realized hydraulically. In another one, the sorption chambers can represent removable cassettes, which can be replaced by fresh cassettes or regenerated.

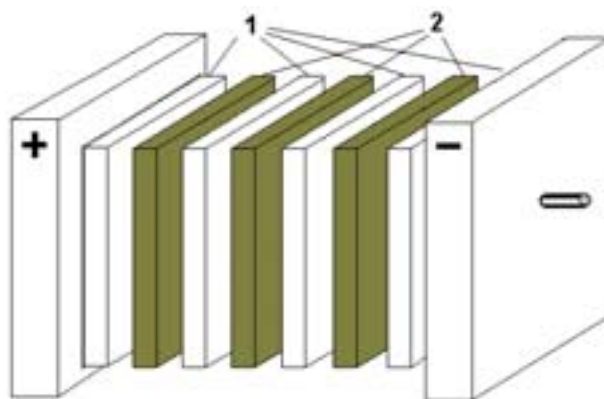


FIG.16. The filter-press multichamber device for non-contact electrosorption: 1-running chambers with the treating solution, 2-chambers with the sorbent.

5.2. TESTING OF A LABYRINTH ELECTROSORPTION APPARATUS

The design of the electrosorption device in many respects defines its efficiency. One of perspective variants of its design is the labyrinth device. The basic advantage of such design is that for one pass of the solution through the device it is possible to achieve a significant degree of extraction of the toxic impurity (radionuclide).

Testing of the labyrinth electrosorption device was carried out in the 7-chamber laboratory apparatus, Fig.17. The working area of the chamber was 30 cm². The chambers were filled with "Fenix-A" sorbent. Electrosorption of ¹³⁷Cs from the model solution of 0.02M KNO₃ + 0.0002M CsNO₃ + ¹³⁷Cs (approximately 1·10⁵ Bq/L) was studied. The solution flow rate through the chambers was 80 mL/min. The density of direct electric current was 50 A/m².

The results (Fig.18) show that the electrosorption device works steadily, but the degree of ¹³⁷Cs extraction did not exceed 20%. The extraction degree can be increased considerably by increasing the number of sorbent chambers (more than 100), to reduce the linear speed of the solution flow, Fig.19, and to increase the density of electrical current, Fig.20. The latest experiments were carried out with real LLRW.

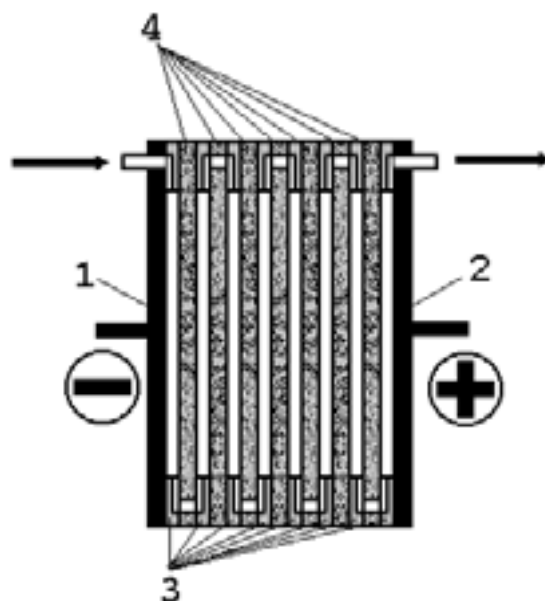


FIG.17. The labyrinth electrosorption apparatus: 1 - cathode, 2 - anode, 3 - running chambers, 4 - chambers with the sorbent.

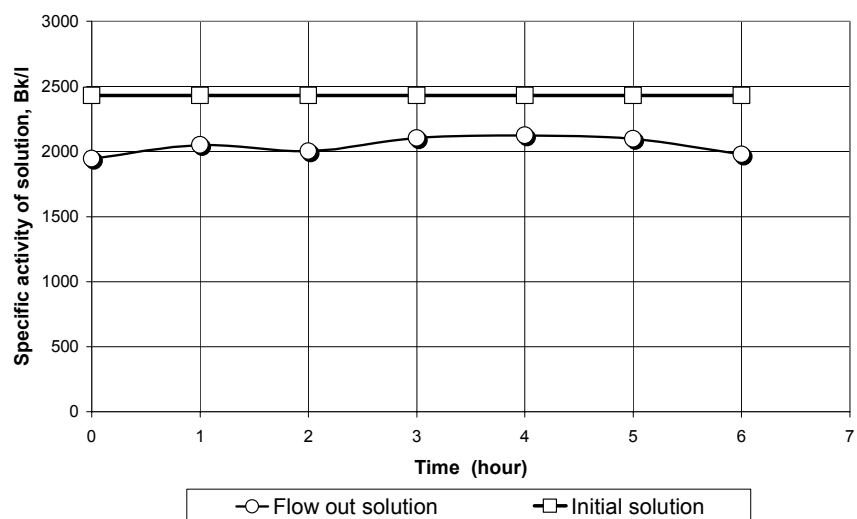


FIG. 18. Dependence of the specific activity of the initial and the flow-out solutions on the electrosorption time in the labyrinth electrosorption apparatus (sor bent Fenix-A; $0,02M KNO_3 + 0,0002M CsNO_3 + {}^{137}Cs$; $I=50 A/m^2$).

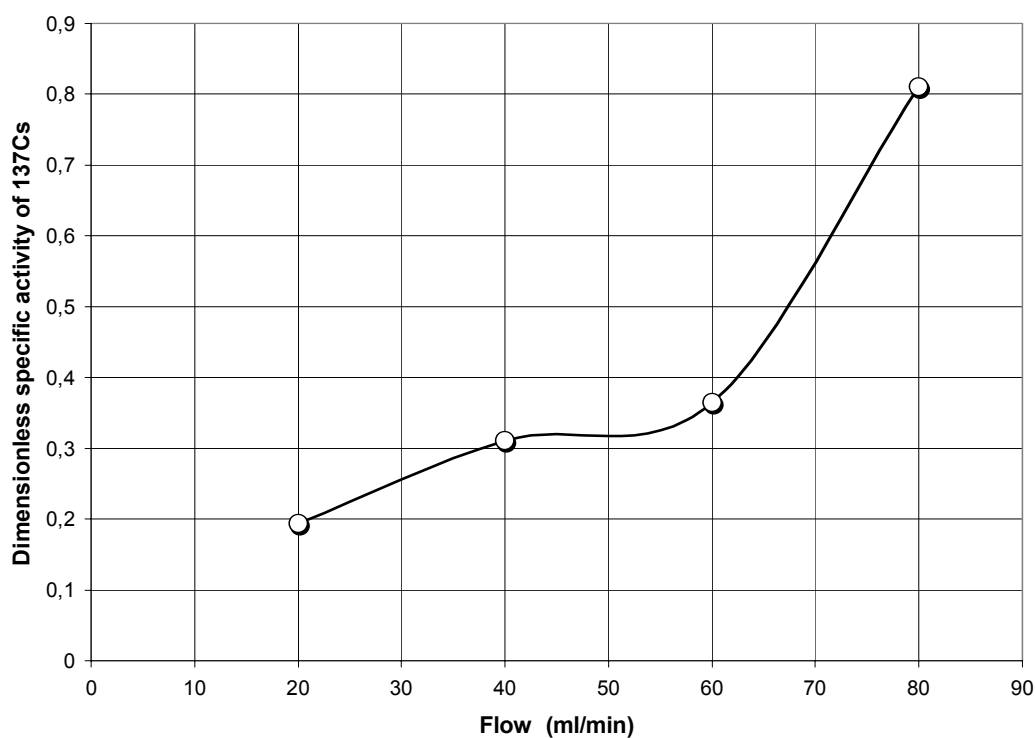


FIG.19. Dependence of the relative specific activity ${}^{137}Cs$ of the flow-out solution on the flow in the labyrinth electrosorption apparatus (sor bent Fenix-A, real LLRW, $I=150 A/m^2$).

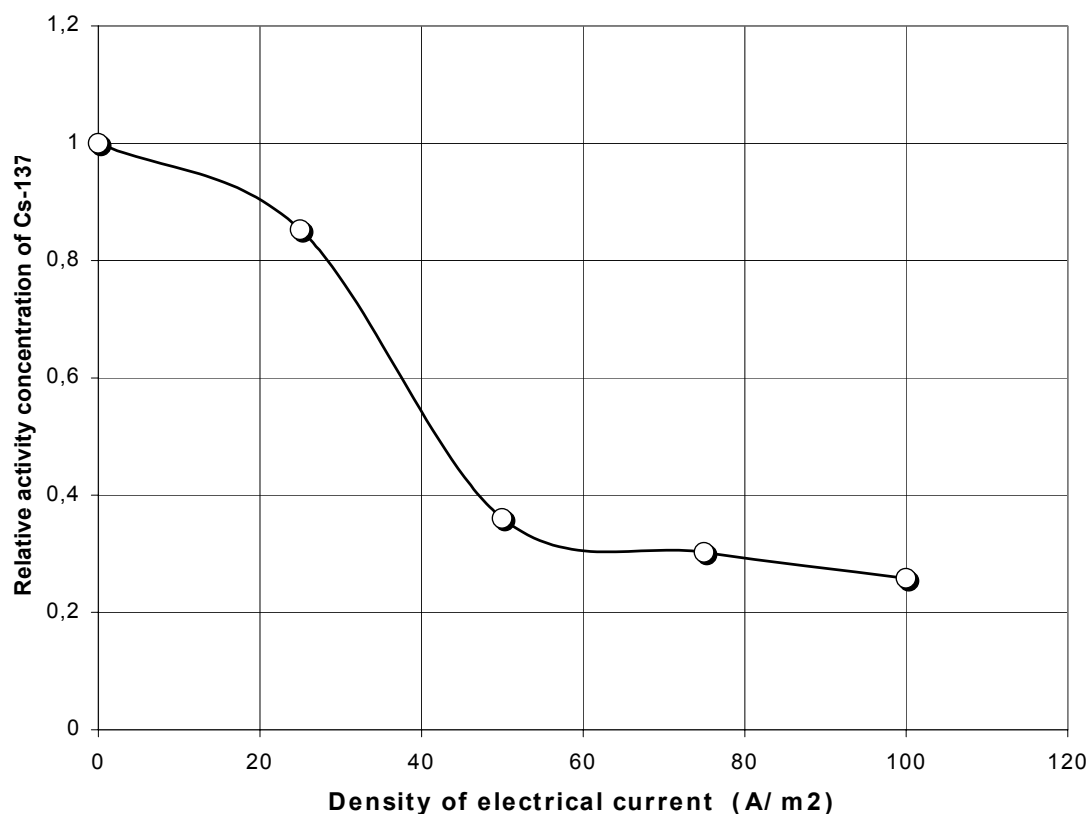


FIG.20. Dependence of the relative specific activity ^{137}Cs of the flow-out solution on the density of electrical current in the labyrinth electrosorption apparatus (sorbent Fenix-A, real LLRW, flow is 60 ml/min).

5.3. ESTIMATION OF THE EFFICIENCY OF ELECTROSORPTION IN COMPARISON WITH CONVENTIONAL SORPTION METHODS

The main indicators of the efficiency of the majority of technological processes are capacity of the process and power consumption. The capacity of the sorption processes is defined by such factors as the extent of the extraction of a target ion from the solution and the life time of a sorbent. The efficiency of removal of the given ion is characterized by the decontamination coefficient. The life time of the sorbent has a physical sense in the dynamic regime of sorption only and is characterized by the beginning of the reduction of the decontamination coefficient below a certain given value.

Regarding the change of the concentration of the extracted ion in the external solution (Fig.21), electrosorption is closer to the static regime of sorption. Our investigations have shown that electrosorption for a sufficiently long time allows to reach the same decontamination factor as for the sorption in the static regime, but at an initial period it has a lower extraction rate.

The power consumption for electrosorption is higher than for traditional regimes of sorption because:

- (i) in the static regime, power is consumed while mixing reagents and separating the spent sorbent. In each particular case, the power consumption depends on the method selected,

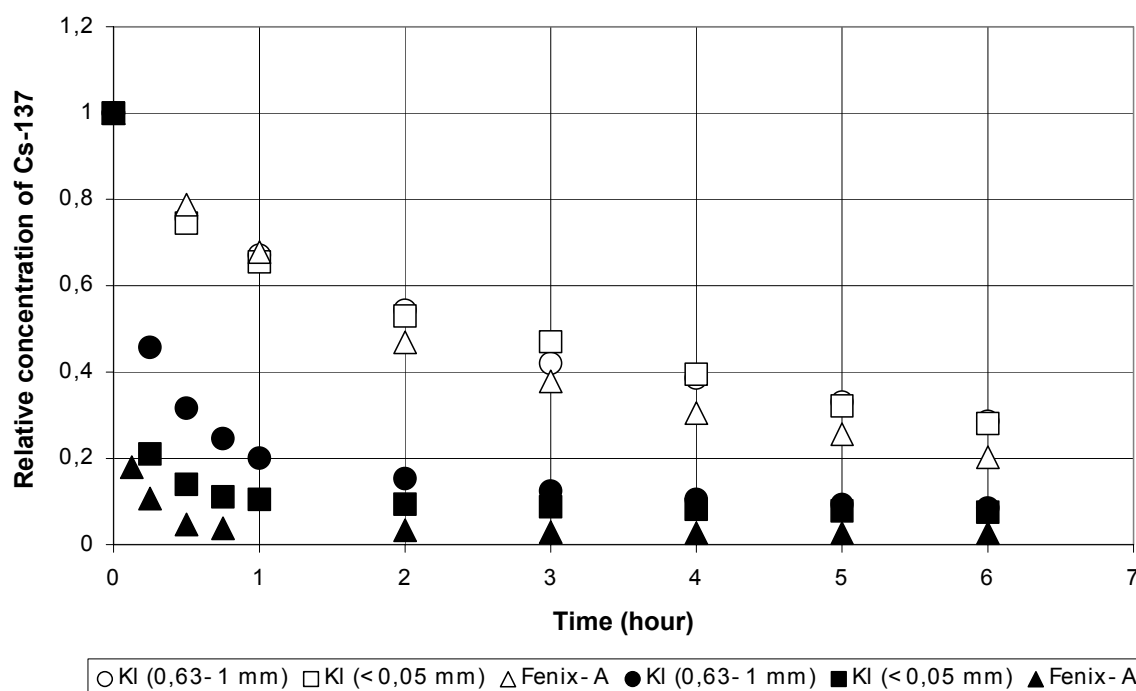


FIG. 21. Dependence of the relative concentration Cs^{+} on the time at static sorption (dark symbols) and electrosorption (light symbols) with the system $0.02M KNO_3 + 0.0002M CsNO_3$ (at each experiment the amount of sorbent was 7g and the volume of the treated solution 1L, KI - clinoptilolite).

- (ii) in the dynamic regime, the power consumption depends on the hydraulic resistance of the sorption column, which, in turn, depends on the size of the sorbent particles, turbidity and the concentration of colloidal particles in the treated solution, and the the solution flow rate in the sorbent layer.

Most of these factors have no impact on the power consumption at electrosorption and it is difficult to standardize the conditions for carrying out the comparative assessment. In addition, the power consumption at electrosorption depends very much on the design of the electrosorption devices.

6. CONCLUSION

The studies have shown that electrosorption (as a process, in which ions move from the solution to the sorbent layer by action of the electric field) allows to remove radionuclides from aqueous radioactive waste. Electrosorption allows to treat waste in one stage by using even powder and colloid sorbents (bentonite, crushed chitin-chitosan sorbent, precipitate of barium sulfate) but the rate of the radionuclide removal is lower than in the case of direct introduction of sorbents into the solution and intermixing. Electrosorption could be potentially applied for:

- application of non-standard sorbents, which are ineffective in traditional sorption technologies,
- for chemical and radiochemical analysis of water solutions (for example, as a concentrator of radionuclides),
- household filters not only for water cleaning, but also for the disinfecting water and sorption filter.

REFERENCES

- [1] INTERNATIONAL ATOMIC ENERGY AGENCY, Treatment of Low and Intermediate Level Liquid Radioactive Wastes, Technical Reports Series No. 236, IAEA, Vienna (1984).
- [2] KARLIN, Y., DAVLETHANOV, R., SOBOLEV, I., Cleanup of water from toxic ions by electrosorption method, Proc. of 3-th Int. Cong. "ECWATECH-98" Moscow, Russia, May 26–30, 1998, (1998) 406–407.
- [3] KARLIN, Y., DAVLETHANOV, R., Theoretical and practical aspects of electrosorption at ion-exchange systems, Russian Journal of Electrochemistry, **35** 4 (1999) 493–499.
- [4] RAUZEN, F.V., CULESHOV, N.F., SMOLKIN, I.M., TROFIMOV, D.I., DIAKOV, A.A., "The Results of Pilot Electrodialysis Plant Exploitation on Cleaning of Low level Liquid Radioactive Wastes", Peaceful uses of atomic energy, Preprint IAEA, **11** (1972) 387–398.
- [5] DEMKIN, V.I., TUBASHOV, Y.A., PANTELEEV, V.I., KARLIN, Y.V., Cleaning Low Mineral Water by Electrodialysis, Desalination, **64** (1987) 367–374.
- [6] FULE, L., ZHONGMEI, Z., GUOZHEN, L., et al., A Research into the Mechanism of Packed Bed Electrodialysis and it's Tentative Application for Treating Low level Radioactive Waste, Water Treatment (China), **1** №1 (1987) 58–67.

COMBINED METHODS FOR COMPLETE DECONTAMINATION OF LRW OF LOW AND INTERMEDIATE LEVEL OF ACTIVITY BY USING CHITIN CONTAINING FIBER MATERIAL «MYCOTON» AND ITS MODIFICATIONS

V.N. KOSYAKOV^a, I.E. VELESHKO^a, N.G. YAKOVLEV^a, L.F. GOROVY^b.

^aRRC “Kurchatov Institute”, Moscow, Russian Federation

^bInstitute of Cellular Biology and Genetic Engineering, Kiev, Ukraine

Abstract. A fibrous sorbent (Mycoton), containing chiton-chitosan, has been produced in a joint Ukrainian/Russian programme. The sorption of transuranium elements (U, Pu, An, Cm), long lived fission products (Sr, Cs, Ce, Eu) and some heavy metals (Pb, Hg, Cr, Cd, Bi) has been investigated. The influence of pH and salt concentration, adsorption kinetics and sorption capacity has been studied. Modification of the sorbent to provide ferromagnetic properties is being considered to provide a materials suitable for the decontamination of bottom sediments and slurries. Combination of sorption processes with precipitation and electrochemical degradation of complex ions was investigated.

1. INTRODUCTION

At the nuclear plants, entertainments and installations of Russia more then 400 millions m³ of LRW of low and intermedium level of activity (with the total activity about 200 millions Kuries) are accumulated by the time being. The main problem is complicated by the situation when the most part of such wastes is in entirely uncontrolled conditions (in open water reservoirs or in deep drillholes)

The base of long term radioactive contamination of such wastes consist of long-lived radionuclides including mostly such fission products as Cs-137, Sr-90, Zr-93, 95, Ru-106, Ce-144, Sm-151, Eu-154, transuranium isotopes (Np-237, Pu-238, 239, 240, Am-241, 243, Cm-244) and radioactive isotopes induced in construction materials as a result of their interaction with neutrons (Mn-54 and Co-60).

Many scientists dealing with LRW treatment are followed the concept, providing for the decontamination of the wastes up to the level, which allows their disposal into the environment with simultaneous concentrating radioactivity and following solidification of the concentrate obtained. Realization of such approach could allow in the future to eliminate entirely the harmful effect of LRW of low and intermediate level of activity to the environment. However, low efficiency of the existing methods for LRW decontamination practically can not provide required purification degree and concentrating factor without sufficient increasing of the treatment cost by using too complicated combinations of the methods.

During last 15 years the systematic studies directed to the search and development of new, more efficient techniques for LRW decontamination have been carried out in RRC “Kurchatov Institute” with application of a new, relatively cheap, natural, chitin containing sorbent of fiber structure named “Mycoton”. Some parts of the work was carried out in collaboration with several institutes in Russia and Ukraine. We understood quite well, that panacea does not exist, and required technology will represent a combination of various methods, which should provide not only maximal enlargement of the spectrum of radionuclides to be absorbed, but also to solve the problems associated with the states of radionuclides in real LRW and with the effect of chemical composition of the wastes. Newer the less we tried to minimize as much as possible the number of methods in the combination by using the most efficient ones and to unify the technological characteristics of the sorbents used. As a result we have succeeded to develop quite a promising combined absorption-flocculative method for decontamination of LRW of low and intermediate level of activity.

The method is based on the using only Mycoton and its various modifications [1,2,3] as sorbents and water soluble chitozan – as flocculent [4,5], with flocculation providing coprecipitation of the radionuclides existing in the wastes in a colloid form and can not be recovered by absorption technique. Mycoton and its modifications are produced in Kiev by ICBGE and water soluble chitozan – in Moscow by Institute of Organic Chemistry of Russian Academy of Sciences. Both (sorbent and flocculent) could be produced in industrial scales

Such an intercomplementary combination of two ashless natural polymers provides high degree of LRW purification from the large number of long lived radionuclides, including fission products, actinides and elements with induced radioactivity with the simultaneous compacting secondary wastes. Additional concentrating factor could be achieved by incineration of the sorbent and flocculent loaded with the radionuclides separated.

Special studies have been carried out in order to select and develop an efficient technique for destruction of strong complexing agents often presenting in LRW and preventing the decontamination process. Continuous electrochemical method operating in flow-through conditions is under development. Large development work is carried out in constructing a pilot installation providing the organization of a continuous counter-current absorption process for industrial decontamination of LRW by using proposed technology [6].

In spite of the most of studies having been carried out with modeling solutions, the results obtained allow to recommend the method for decontamination of LRW with various radionuclide and chemical composition. However, for real industrial application of proposed technology it is still much to do. The main thing is to develop specific technologies applicable for the wastes of certain chemical and radionuclide composition, which could require the development of some additional sorbent modifications, special equipment, etc in order to overcome some unforeseen difficulties and problems.

The goal of the report is to show what is succeeded to achieve as a result of the application of combined methods for decontamination of LRW of low and intermedium level of activity and what has to be done for industrial realization of the concept of complete decontamination of such wastes with the application of the proposed absorption-flocculative technology.

2. «MYCOTON», TECHNICAL AND ABSORPTION CHARACTERISTICS

Chitin containing sorbents

Fig. 1 shows the chemical structure of two rather widely spread natural polymers chitin and chitosan, which belong to the class of polysaccharides. The presence in their composition of amine, acetamide, carbinolic and carboxylic functional groups as well as of oxygen bonds determines the formation of very strong complexes with heavy metals and the complicated mechanism of their interaction.

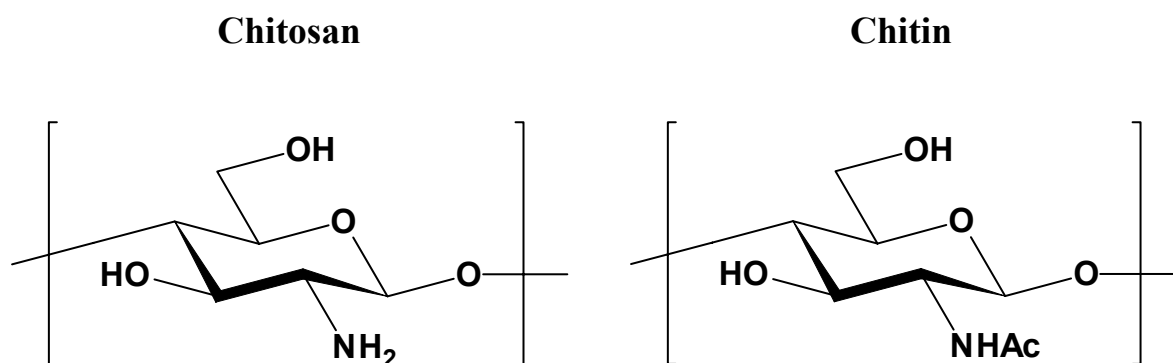


FIG. 1. Chemical structure of Chitin and Chitosan.

The application of chitin as an efficient sorbent of heavy metals is studied in many countries [7,8,9]. The annual production of chitin and its derivatives in USA, for example, achieves several thousands tons. However, in spite of abundance of the material and patents there is no any real industrial technology developed with the application of such sorbents. The reason is in the technological properties of the chitin, which is usually produced from the sea food production wastes (shells of lobsters, crabs, shrimps etc) and wastes of microbiological industry. In this case the product properties are hardly usable for its application as a sorbent. It represents a fine powder, quickly swelling in water media. In our work we have preferred to deal with the material obtained out of higher fungus of *Basidiomycet* class [1], has fiber structure and relatively high stability to the swelling. It was named "Mycoton".

Mycoton is a natural chitin-glucan-melanin complex (consist of about 70% of chitin, 25% of R-glucans and 5% of melanin), locating in cell walls. Content of the complex in some kinds of fungus exceeds 50% relative to the total weight of the dry fungi. The complex is destined by the nature itself to protect the living cell against penetration of any toxins, including heavy metals [10]. Being separated the complex possess higher sorbability towards heavy metals then purified chitin. Therefore, the Mycoton production is aimed at the separation of the natural complex, trying to preserve not only the composition, but also its fiber structure. Mycoton practically does not contain mineral admixtures (less then 1%) and is actually ashless, that provides additional compacting factor for secondary wastes due to incineration. These features ensure very valuable absorption and technological characteristics of Mycoton.

Mycoton represents cylindrical hollow fibers with 3 – 5 microns in diameter and 1 – 10 mm in length, that provides very large surface (up to 1000m² /g) and high hygroscopicity. The fibers are very strong and elastic, are resistant to the effect of strong acids, alkalines, organic solvents, ultraviolet and ionizing radiation, are biologically inert. The material does not lose these properties up to 150⁰C.

The fiber structure and large surface of Mycoton determine such important features as high kinetic characteristics of absorption process, ability to form paper like and non-woven materials of specified thickness and porosity, as well as to produce various composites and modifications, providing practically unlimited feasibilities to produce the materials with the specified absorption and technological properties.

The cultures of fungus have been found, which allows to grow them on the wastes of agriculture and woodworking industries. It makes the Mycoton production resources practically unlimited. At the present the pilot installation of the Institute of Cell Biology and Genetic Engineering in Ukraine is capable to produce 50 tons of Mycoton per year.

Mycoton absorption properties

Similar to other chitin containing materials, Mycoton possess high sorbability towards heavy metals, which are represented by many radionuclides containing in LRW (all the actinides and many fission products). In our sorbability investigations the main attention we paid to actinides (uranium, plutonium, americium, curium) as well as cesium, strontium, rare earth fission products and cobalt. The effect of pH, salt concentration and presence of various anions to Mycoton sorbability were studied for these elements.

One of the main characteristics of the material sorbability towards any element is the value of distribution coefficient, K_d , which is calculated as the relation of concentration or activity of the absorbing element in the sorbent, A/g, to those in the solution, A/ml at the equilibrium conditions. By other words: $K_d = (A_s \times V_l) / (A_l \times P_s)$ and expressed in term of mL/g.

Our investigation of the Mycoton sorbability have been started with the actinide isotopes [3, 11], which are alpha emitters and the most long lived radionuclides presenting

the highest radioecological danger. That time we were trying to apply Mycoton for sampling and preliminary concentrating actinides in alpha monitoring [12] of the contaminated Chernobyl areas.

Fig.2 shows the effect of the solution pH to the distribution coefficients of uranium, plutonium, americium and curium at their absorption by Mycoton. As it is seen from the results obtained, the maximal values of distribution coefficients more than 10^4) for all the actinides are in the pH range from 4 to 6 being rather high (more than 10^3) in the large range of pH. It has to note, that the charge and the structure of absorbing ions have not serious influence. In mineral acids solutions with the concentration higher than 1 mol/l the actinides practically do not absorbed and this effect could be apply for Mycoton regeneration.

Similar regularities are observed also with lanthanide (rare earth fission products) absorption, in particular cerium, promethium and europium. High values of distribution coefficients were observed also for many other long lived fission products, such as Zr, Nb, Mo, Ru, Pd and others. Sorbability of pure Mycoton towards strontium and cobalt is wicker. Usually at pH range from 3 to 8 the distribution coefficients of these elements are in the interval from 200 to 400. The distribution coefficients of cesium in similar systems are even ten times less. Trying to solve this problem we at first time met with the necessity to use some combined methods, however, how this problem was solved, it is the subject of the next chapter.

The second very important characteristics of absorption process efficiency is its kinetics. Even at the high distribution coefficients the real absorption efficiency will depend on the rate of absorption equilibrium settling, or on the contact time necessary to achieve the absorption equilibrium. It means that absorption kinetics determines the output of absorption apparatus used. Therefore, apart from distribution coefficients, we usually measured the kinetic characteristics of the absorption process studied, which allows as to calculate the dynamic regiment of absorption columns often used for testing the process with both modeling solutions and real LRW.

By using absorption processes much attention is usually paid to the value of exchange capacity. At the LRW treatment the exchange capacity plays not significant role since here we usually deal with very low radionuclide concentrations and the actual saturation of the sorbent dos not reach. Never the less, we have measured the values of Mycoton exchange capacity for europium, uranium and plutonium. Depending on the element and solution composition the value was in the range of 0.6 – 1.0 mg-equivalent/g.

Since the chitin containing sorbents do not interact with the cations of light metals (sodium, potassium, calcium and others) the presence of such metals should not have much influence to the absorption of heavy metals from such solutions. The assumption have been confirmed by the experimental results, which are shown in the Table 1. The increasing sodium nitrate concentration from 5g/L to 400 g/L effects not very much to the distribution coefficients of plutonium, americium and cesium. Exception is only strontium, but in reality this metal could be hardly related to the series of heavy metals. The presence of phosphate anion even increases distribution coefficients for some elements. And very harmful influence exert the presence of EDTA on the absorption of plutonium and americium.

3. MYCOTON MODIFICATIONS

The presence in Mycoton composition many functional groups and also possessing high specific surface of its fibers make the material a good basic sorbent, which could be easily modified in order to attach to the sorbent practically any preassigned absorption and technological characteristics. Two types of modifications could be apply with Mycoton: chemical modification, when functional groups are used for this purpose and composite one, when sorbability power of developed surface of Mycoton fibers is used.

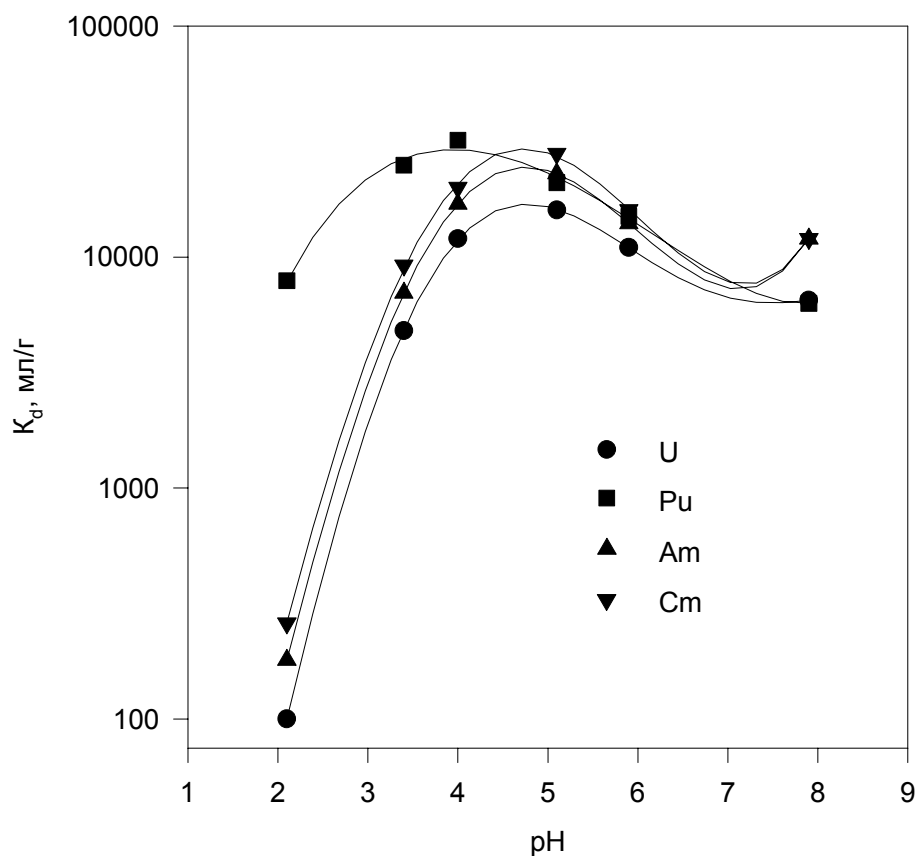


FIG. 2. The pH effect to the distribution coefficients of U(VI), Pu(IV), Am(III), Cm(III). (Acetate – phosphate buffer).

TABLE. 1. THE EFFECT OF SOME SALT ADDITIVES TO DISTRIBUTION COEFFICIENTS OF Cs, Sr, Pu AND Am BY MYCOTON ABSORPTION

Salt additive	Concentration of additive, g/L	Distribution coefficient, mL/g			
		Cs*	Sr	Pu	Am
NaNO ₃	5	15500	470	1100	3450
NaNO ₃	400	16000	2.0	780	1700
PO ₄ ³⁻	0.5	6240	580	3300	950
EDTA	0.1	4040	560	320	135

* Cesium Mycoton modification.

In this case a binding agent could be used to ensure strong retention of the modifier on the fiber surface. It is quite obvious, that the first way is much more expensive than the second one, especially in a pure kind, when the functional groups of Mycoton are used for direct binding with additional functional groups having specific absorption or technological properties. An intermediate modification mechanism is based on the application of some Mycoton groups to produce required compound directly on the fiber surface. The example of such technique is production of the modifications with advanced cesium and strontium sorbability, Mycoton-Cs and Mycoton-Sr. Even in case of pure composite modification the formation of required modifier directly on the fiber surface results in its stronger retention by Mycoton.

Cesium modification

Cesium – 137 is the most spread radionuclide, existing practically in all kinds of LRW. Therefore, it would be impossible to recommend Mycoton for LRW decontamination without cesium absorption. It was decided to use here a combination of absorption by chitin containing sorbent, possessing wide spectrum of radionuclide sorbability with well known selective inorganic ionexchanger, ferrocyanide of a divalent metal. Copper ferrocyanide have been selected from its toxicity and solubility point of view.

Fine grained compound of copper ferrocyanide was formed directly on the fiber surface as a result of reducing interaction between ferric ions and acetylamine and amine groups of Mycoton in the process of alkalification of the Mycoton, preliminary impregnated by corresponding solutions. As a result the very efficient cesium sorbent, Mycoton-Cs, have been prepared. It has not only high distribution coefficient (higher than 10^4) in large range of pH and salt concentration, but also very fast absorption kinetics (the equilibrium is reached for about 3 minutes, see Fig. 3).

Strontium modification

In order to increase Mycoton absorption efficiency towards strontium we tried to prepare modification with MnO_2 . The modification consists in impregnation of Mycoton with a solution of KMnO_4 in distilled water with the subsequent drying of the intermixture at temperature $\sim 100^\circ\text{C}$. The solution concentration is determined by the quantity of KMnO_4 , which is supposed to introduce to modified sorbent. However practice of operation has shown, that for meeting the safety requirement (the intermixture of Mycoton with potassium permanganate is explosive) at drying operation the concentration of KMnO_4 in solution for Mycoton impregnation should be not more than 2.5 g/L. It means, that in one cycle impregnation - drying it is possible to prepare modification containing approximately 1 % MnO_2 , and for more concentrated modification the multiple recurring of cycles is necessary. We prepared and tested a sample containing 2 % MnO_2 . It gave quite good results for low salt containing solutions (see Table 2). We are still studying the possibilities to prepare more advanced modification for efficient strontium absorption from high salinity solutions.

Ferromagnetic modification

As it was shown by the measurements in contaminated Chernobyl area, the main part of the basin radioactivity (more than 99%) accumulated in bottom sediments. By nowadays the bottom sediments decontamination remains a totally unsolved problem. From this point of view the application of a sorbent possessing ferromagnetic properties looks quite promising. So we have developed technique for preparation of such sorbent by composite modification of Mycoton [2].

Several ferromagnetic additives can be used here, but the cheapest and the most convenient one is magnetite, forming in the process of alkalification of the Mycoton

suspension, preliminary impregnated with the corresponding mixed solution of iron salts. After drying and milling the composite is ready for application. The content of ferromagnetic component can be varied from 5 to 60%. Such sorbent could be easily removed from the working media (slurry, bottom sediment or soil) by a magnetic separation technique. Double modification of Mycoton with copper ferrocyanide and magnetite (up to 40 weight %) have been realized and the samples obtained were successfully tested with real bottom sediments from Chernobyl cooling pond.

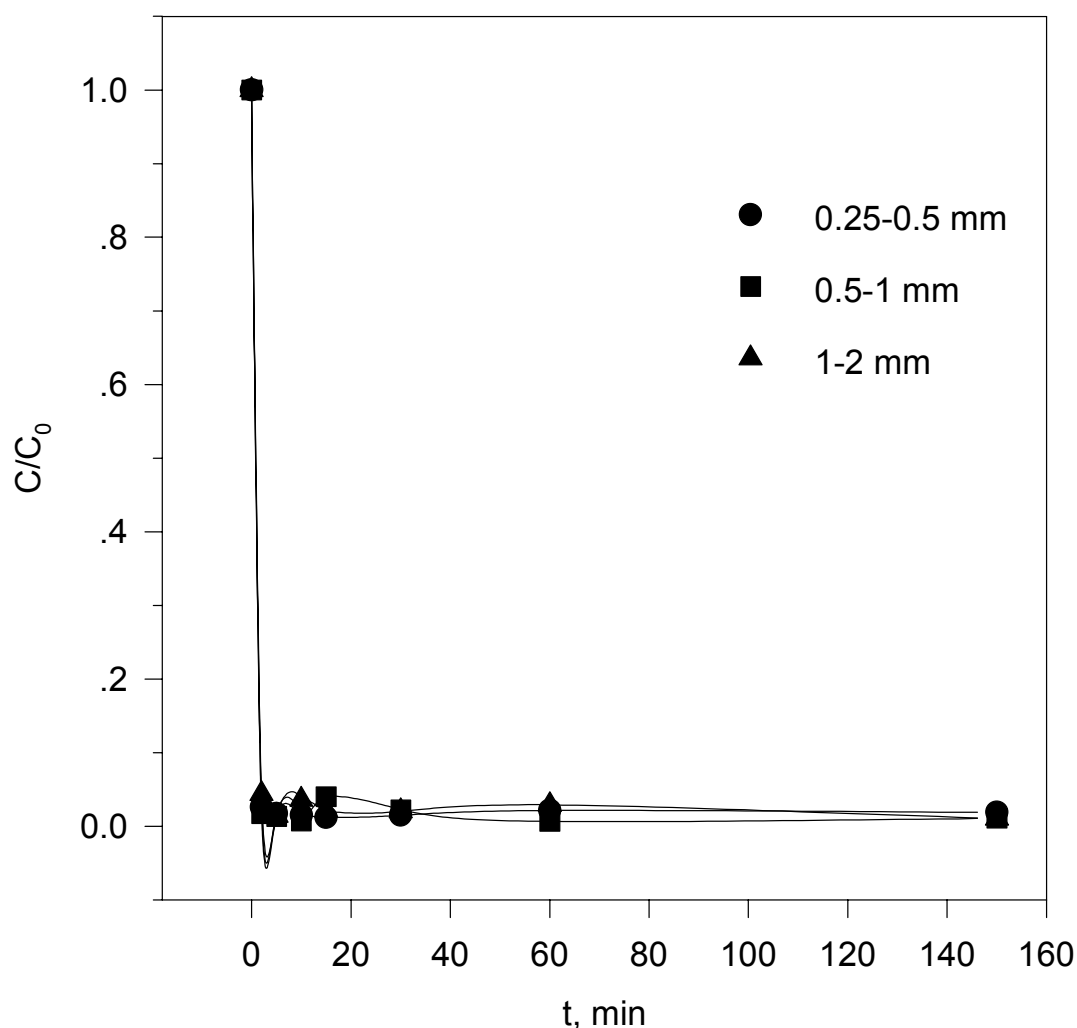


FIG. 3. Absorption kinetics of Cs by ground Mycoton-Cs from the solution containing 50 g/L NaNO_3 and $\text{pH} = 11$, depending on sorbent particles size. Solid:liquid=1:100

The distribution coefficients of such modification for Cs, Sr, Pu and Am are shown in Table II. It should be noted that Mycoton in all the modifications has practically preserved its basic absorption properties. In spite of no any binding agent was used in preparation of the modifications, we have not noticed any separation of the modifier from the material surface for two years underwater testing

TABLE II. DISTRIBUTION COEFFICIENTS FOR Pu, Am, Cs AND Sr IN DRINKING WATER AT THE ABSORPTION WITH MYCOTON AND ITS MODIFICATIONS

Sorbent*	Distribution coefficient			
	Pu-239	Am-241	Cs-137	Sr-90
Mycoton-Ch	970	6800	30	300
Mycoton-Cs1	600	2500	25000	350
Mycoton-Sr2	800	3500	45	1100
Mycoton-Cs1-M40	3800	6700	14000	400

Mycoton –Ch – pure Mycoton. Mycoton-Cs1 – modification with 1% of ferrocyanide. Mycoton-Sr2 – modification with 2% MnO₂. Mycoton-Cs1-M40 – double modification with 1% of ferrocyanide + 40% of magnetite.

The results obtained completely confirm our assumption on the feasibility to obtain with Mycoton the sorbents with assigned absorption and technological properties. Therefore we are planing to continue the work in this direction in drder to synthesize some composites with advanced absorption properties towards Sr, Ru, Co, Ra and others.

4. FLOCCULATIVE PRECIPITATION OF RADIONUCLIDES IN COLLOIDAL FORM

At long storage of real LRW some radionuclides are often in colloidal form. In this case neither ion-exchangers nor sorbents are capable to ensure the required purification factor. Especially often such colloidal solutions form cobalt and plutonium in alkali solutions [13, 14]. For solution of this problem another combination of methods have been applied, combination of the absorption technology with preliminary flocculative coprecipitation of the colloidal radionuclides with freshly precipitated chitosan. In comparison with inorganic flocculates chitosan precipitate have the following advantages:

- It forms a bulky precipitate with well developed surface, allowing to use smaller quantity of the flocculate.
- The presence of several functional groups in the chitosan structure provides to precipitate additional absorption properties.
- The chitosan is also an ashless material providing an efficient compacting due to incineration.

The application of chitosan for flocculative purification of waste water is described in [15]. We have studied the feasibility of application of several samples of the water soluble chitosan, synthesized in the Institute of Organic Chemistry of RAN [4]. The water chitosan solution was added to slightly acidified radionuclide solution and then precipitation was carried out by alkalification of the solution up to pH more then 8.5 The results obtained are shown in Table III. The difference in the flocculation efficiency between the samples is not significant. The most complete coprecipitation is observed for Mn, Pu and Co. The optimal consumption of chitosan is 1g/l.

TABLE III. COPRECIPITATION OF RADIONUCLIDES WITH CHITOSAN SAMPLES.
CHITOSAN CONCENTRATION IN INITIAL SOLUTION - 1 g/L

Chitosan*	Coprecipitation degree, %				
	Mn-54	Co-60	Sr-85	Cs-137	Pu-239
N1	95,7	86,8	33	3,0	95
N2	>99,5	80,8	27,2	3,4	95,8

* № 1 - high molecular weight ($M_w = 1,5-2,0 \cdot 10^6$), acetyl groups - 37%;
№ 2 – low molecular weight ($M_w = 5-10 \cdot 10^3$), acetyl groups – less then 10%.

It is quite obvious, that preliminary solution of the chitosan the waste treated would be the most efficient procedure, in this case an additional operation would be required for acidification of alkali wastes. Therefore the possibility to introduce the chitosan solution directly to alkali wastes have been studied. Concentrating chitosan solution (50 g/L) was slowly introduced while mixing into the radionuclide solution being at pH = 9.5. As it is seen from the Table IV, where the results of the both variants are compared, not significant reduction of the coprecipitation efficiency is observed in the second variant only in case of cobalt.

TABLE IV. COPRECIPITATION OF RADIONUCLIDES WITH CHITOSAN
DEPENDING ON TECHNIQUE OF ITS INTRODUCTION INTO THE SYSTEM

CHITOSAN CONSUMPTION - 1 g/L.

Variant	Introduction technique	Coprecipitation degree, %				
		Mn-54	Co-60	Sr-85	Cs-137	Pu-239
1	Chitosan dissolved in initial solution	99,3	88,7	57,3	18,7	95,6
2	Chitosan solution introduced in LRW (pH=9,5)	99,2	77,3	57,8	23,0	94,1

Therefore the water soluble chitosan could be considered as new efficient means [16] for flocculative decontamination of LRW. In a combination with Mycoton absorption technique it can give very promising results, because they both well complement one another.

5. EDTA DESTRUCTION

Experience in absorption of radionuclides from solutions of various chemical composition has shown, that the greatest effect to the values of their distribution coefficients render the presence in the solution strong complexing agents, such as ethylenediaminetetraacetate (EDTA) and their harmful effect could be avoided only by their

destruction. The EDTA in LRW, usually appeared as a result of decontamination operations and its content could amount up to 400 mg/L.

There are several well known methods of EDTA destruction in LRW [17]. Among them the greatest attention deserve application of hydrogen peroxide [18], ozone [19] and photochemical oxidizing on the heterogeneous catalytic agent, titanium dioxide [20]. From these methods only oxidizing by ozone allows to organize really continuous process, the remaining suppose batch processing that, naturally, is not their advantage. However even the oxidizing by ozone has a series of disadvantages, principal of them - low stability of this gas hardly reducing effectiveness of its application especially at considerable distance of the ozonizer from ozonized object. Therefore till now there is a necessity to prolong searches and developments of more effective methods of oxidizing destruction of EDTA. The methods permitting to organize continuous process would have an advantage here. In this work three methods for EDTA destruction in alkaline solutions with high salt content were investigated and feasibilities of their application were compared: oxidizing by means of hydrogen peroxide, oxidizing by means of lead dioxide and electrochemical oxidizing on platinum and carbon electrodes.. Solution containing 300 g/L NaNO_3 and 400 mg/l EDTA at pH=11 was taken as tested solution.

Oxidizing by hydrogen peroxide

The effect of the pH value of the tested solution on EDTA destruction kinetics was investigated at 80°C with Co(II) as catalyst. Hydrogen peroxide was added into reaction mixture by portions each 10 minutes, each portion having produced H_2O_2 concentration in solution equaled $2 \cdot 10^{-2}$ mol/L. The following pH values were tested: pH=3, pH=8 and pH=11. The results are presented in Fig. 4.

As it is seen from the results obtained, increasing the pH value of the solution resulted in strong increasing of initial rate and efficiency of EDTA destruction. So, at pH=11 in 10 minutes 75 % EDTA, and in 60 minutes - approximately 90 % EDTA was decomposed. The consumption of hydrogen peroxide amounts 5.8 g/L. These digits quite encourage and testify that hydrogen peroxide quite efficiently could be used for EDTA destruction in LRW with high salt content at pH=11 and above. However the necessity of adding the catalytic agent and the application of prolonged heating essentially complicate the organization of continuous process.

Oxidizing by lead dioxide

Lead dioxide is a strong oxidizing agent. It was utilized earlier by us for cerium and berkelium oxidation to tetravalent state in acidic solutions [21]. The advantage of this oxidizing agent is the possibility of its use in a flow-through column for organization of continuous process. Low solubility of lead dioxide could ensure rather small consumption of this reactant.

First experiments on EDTA oxidizing destruction by means of lead dioxide were carried out at the pH=11. In such conditions EDTA destruction was found to proceed very slowly. Increasing the temperature up to 90°C and adding into solution nitrate of divalent cobalt as catalyst did not result in appreciable increasing of efficiency of oxidation process.

The effect of the pH value of the tested solution on EDTA destruction kinetics was investigated at room temperature. Solutions with the following initial pH values were tested: pH=11; pH=8; pH=3; and pH=3 being kept constant in course of experiment by addition of 0.1 mol/L HNO_3 into the system. The results are plotted in Fig. 5.

As it is seen from the results obtained, decreasing the pH value of the tested solution resulted in increasing of EDTA destruction. The most effective process of EDTA oxidizing destruction occurred here at pH=3, especially in case, when this value was kept constant in

course of the experiment. In optimal conditions the degree of EDTA destruction reached up to 88% in 60 minutes of oxidation.

Thus, the appeal of simplicity of organization of continuous process with the use of lead dioxide as an oxidizing agent for EDTA destruction is canceled by necessity to acidify usually alkaline LRW to pH=3.

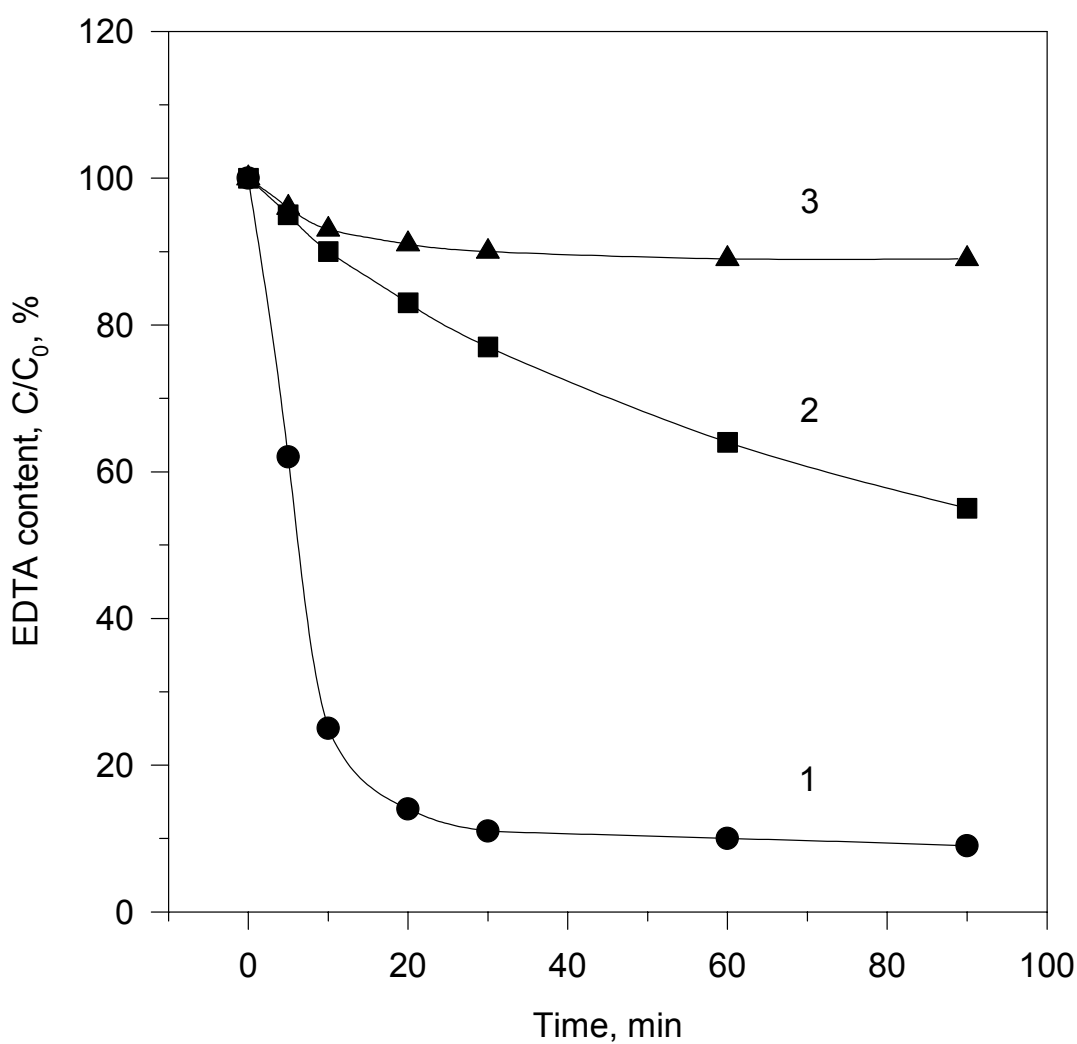


FIG. 4. Kinetics of EDTA destruction by hydrogen peroxide at 80 °C depending on the pH of the stock solution. Stock solution contained 2×10^{-4} mol/L Co(II).

1 - pH=11; 2 - pH=8; 3 - pH=3

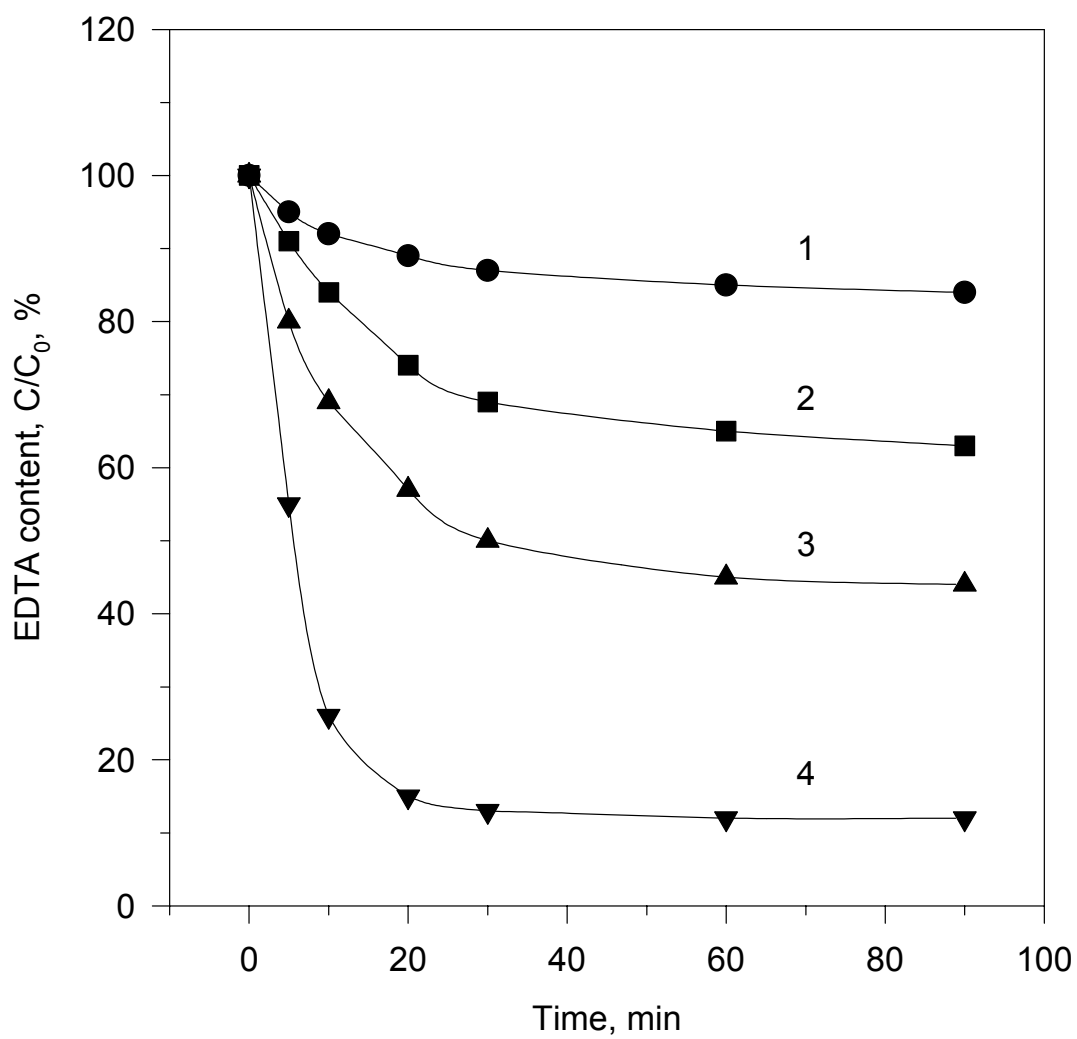


FIG. 5. Kinetics of EDTA destruction by lead dioxide (5 g/L PbO_2) depending on the pH of the stock solution

1 - pH=11; 2 - pH=8; 3 - pH=3; 4 - pH=3 (const)

Electrochemical oxidizing

There are several controversial works on EDTA electrochemical behavior [22, 23], and the data available in the literature are not enough to make a conclusion on real application of electrochemical oxidation to destroy EDTA in alkaline solutions with high salt content. In such solutions EDTA oxidation process was not investigated at all.

The work included investigations with platinum and glassy carbon anode as well as carbon fiber material (CFM). The effect of the working electrode potential to EDTA oxidation kinetics was investigated with all electrode materials in range from $E=1.1$ V (SCE) to $E=1.4$ V (SCE) and initial pH values from 8 to 12. The optimal value of the potential appeared to be 1.3 V (SCE) for all three electrodes. This potential value was used in all experiments on pH effect to the kinetics of EDTA destruction. The best results was obtained with CFM electrode. And they are shown in Fig. 6.

As it is seen from the results obtained, increasing the initial pH of the solution results in increasing of efficiency of EDTA anodic oxidation. The value $\text{pH}=11$ appeared to be an optimal one for electrolysis of EDTA containing solutions.

From the results obtained the following conclusions could be made. The application of CFM electrode ensures fast and quantitative anodic oxidation of EDTA in alkaline solutions with high salt content. Optimal conditions for electrolysis realization using CFM – electrode proved to be the following: electrode potential $E=1.3$ V (SCE), solution $\text{pH}=11$. In 30 minutes of electrolysis in such conditions the EDTA destruction degree is more than 98%. The current yield at this condition was about 37%.

The correctness of conclusion made was checked experimentally by measuring americium distribution coefficient in the solution containing EDTA before and after electrolysis. The data obtained are shown in Table V.

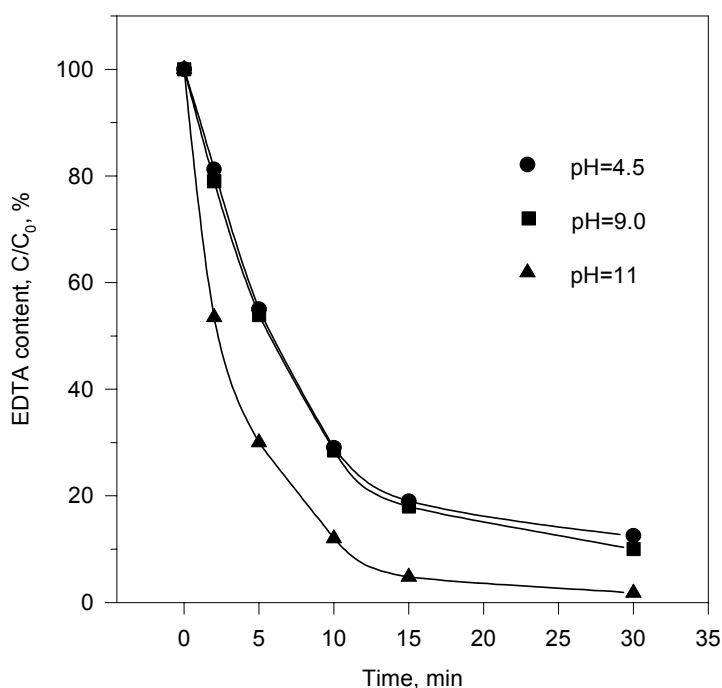


FIG. 6. Effect of the initial pH value of the stock solution to EDTA destruction kinetics by electrolysis on CFM electrode at $E=1.3$ V (SCE)

TABLE V. DISTRIBUTION COEFFICIENTS OF AM IN THE SYSTEM MYCOTON-Ch – SALT SOLUTION AT pH=7 BEFORE AND AFTER ELECTROLYSIS WITH CFM ELECTRODE AT E=1.3 V (SCE) FOR 45 MINUTES

Distribution coefficient of Am, mL/g		
Solution No.1	Solution No.2	Solution No.3
2450	50	2430

Solution No.1: 300 g/L NaNO₃;

Solution No.2: 300 g/L NaNO₃ + 400 mg/L EDTA;

Solution No.3: 300 g/L NaNO₃ + 400 mg/L EDTA after electrolysis.

As it is seen from Table V, the presence of 400 mg/l EDTA in sodium nitrate solution (Sol. No 2) reduces the value of distribution coefficient of americium $K_d(\text{Am})$ by about 50 times. After electrochemical destruction of EDTA the value of $K_d(\text{Am})$ in solution No.3 corresponds to that in solution No.1. This fact testifies two aspects: at first, that quantitative destruction of EDTA is observed, and, secondly, that products of EDTA destruction do not effect to americium distribution coefficient value.

Conclusion

The comparison of the efficiency of the investigated methods of EDTA destruction shows, that the most perspective one is the method of electrochemical oxidation of EDTA on CFM electrode. This electrode material is much less expensive then glassy carbon or noble metals and has very large specific surface, that makes it the most convenient material for further application in development of flow-through electrolyzer.

6. INDUSTRIAL APPLICATION

The testing experiments with real LRW have shown, that when the activity level is higher then 10⁵ Bk/l, the work with relatively large filtering columns was complicated due to accumulation of the radionuclides absorbed and radiolytic gas evolution in the bed volume. The problem could be solved by using larger size of sorbent granules or continuously mixing system. The charging and discharging operations are also time consuming in case of large columns and are not desirable at industrial scales. Therefor we have tried to consider two versions of organizing continuous counter - currant absorption process: by using pulsation column [24] with flat granules of sorbent and multistage cascade of centrifugal mixer – separators with ground sorbent.

As it is seen from the Fig. 7, the absorption kinetics depends very much on the size of the sorbent granules. So at the thickness of flat Mycoton granules 0.5 mm the complete equilibrium is settled for about 2.5 hours, while in case of fine ground sorbent it takes about 20 minutes. Moreover, the phase separation in pulsation columns is based on the natural gravitation sedimentation and takes additional time. In case of centrifugal mixer-separators fine ground Mycoton ensuring quick absorption kinetics could be used and the phase separation process is accelerated by the centrifugal force. Therefor, a centrifugal mixer-separator has been selected as absorption unit for organization of continuous counter current process. The design of such absorber has been developed and multistage installation constructed and tested in NIKIMT (Moscow) in cooperation with RWE NUKEM GmbH

(Germany). A demonstrating 5-stages installation with the output of 50 l/hour have been successfully tested recently. The installation is quite compact (it occupies about 1,5 m²) and its design could be applied in the development of mobile installations. The flow-sheet of the continuous multistage counter-current absorption process using centrifugal mixer-separators is shown in Fig. 8.

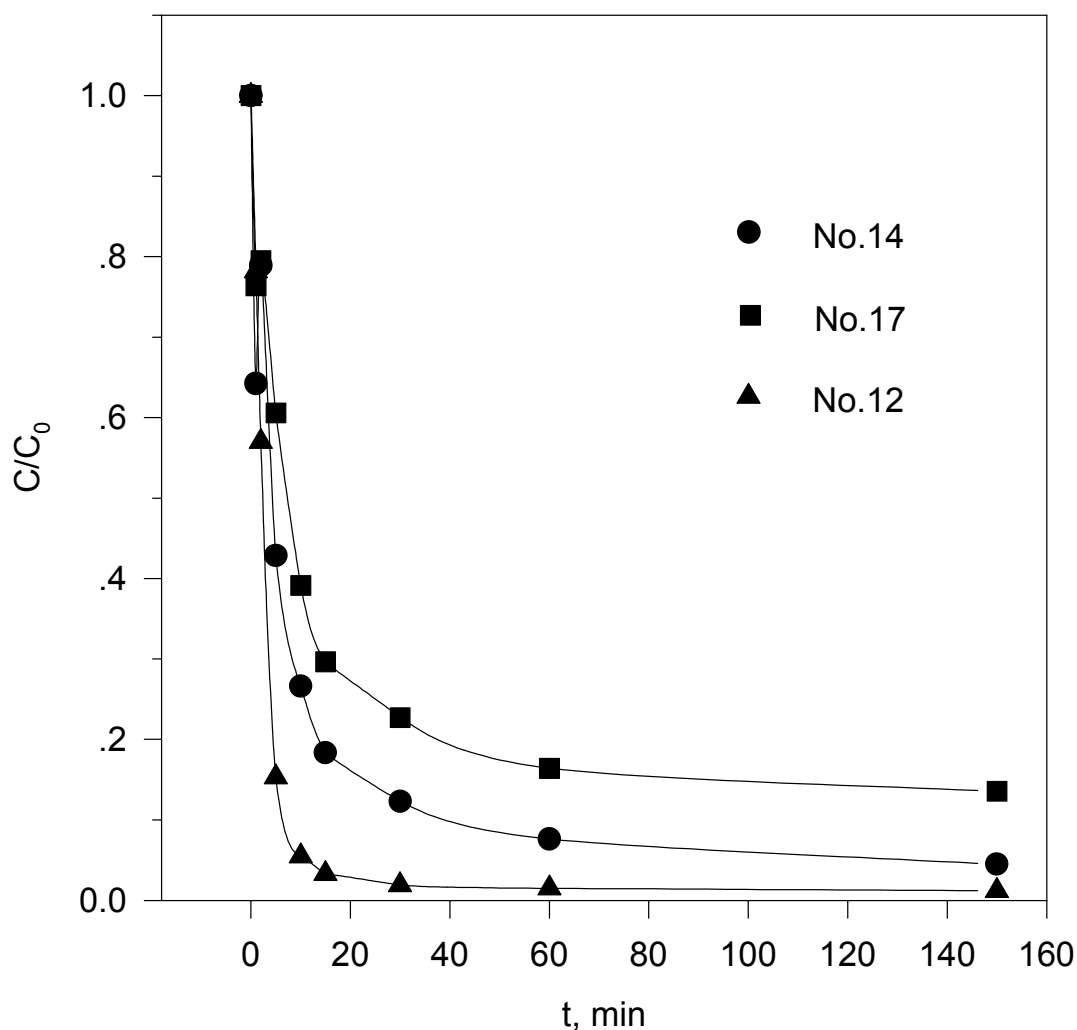


FIG. 7. The effect of granule size to absorption kinetics of Am by Mycoton-Ch.
Solid:liquid=1:100.

sample No.14, granule thickness - 0.50 mm, density 0.44 g/cm³;
sample No.17, granule thickness - 0.27 mm, density 0.42 g/cm³;
sample No.12, fine ground Mycoton with the particle size 0.25 – 0,5 mm.

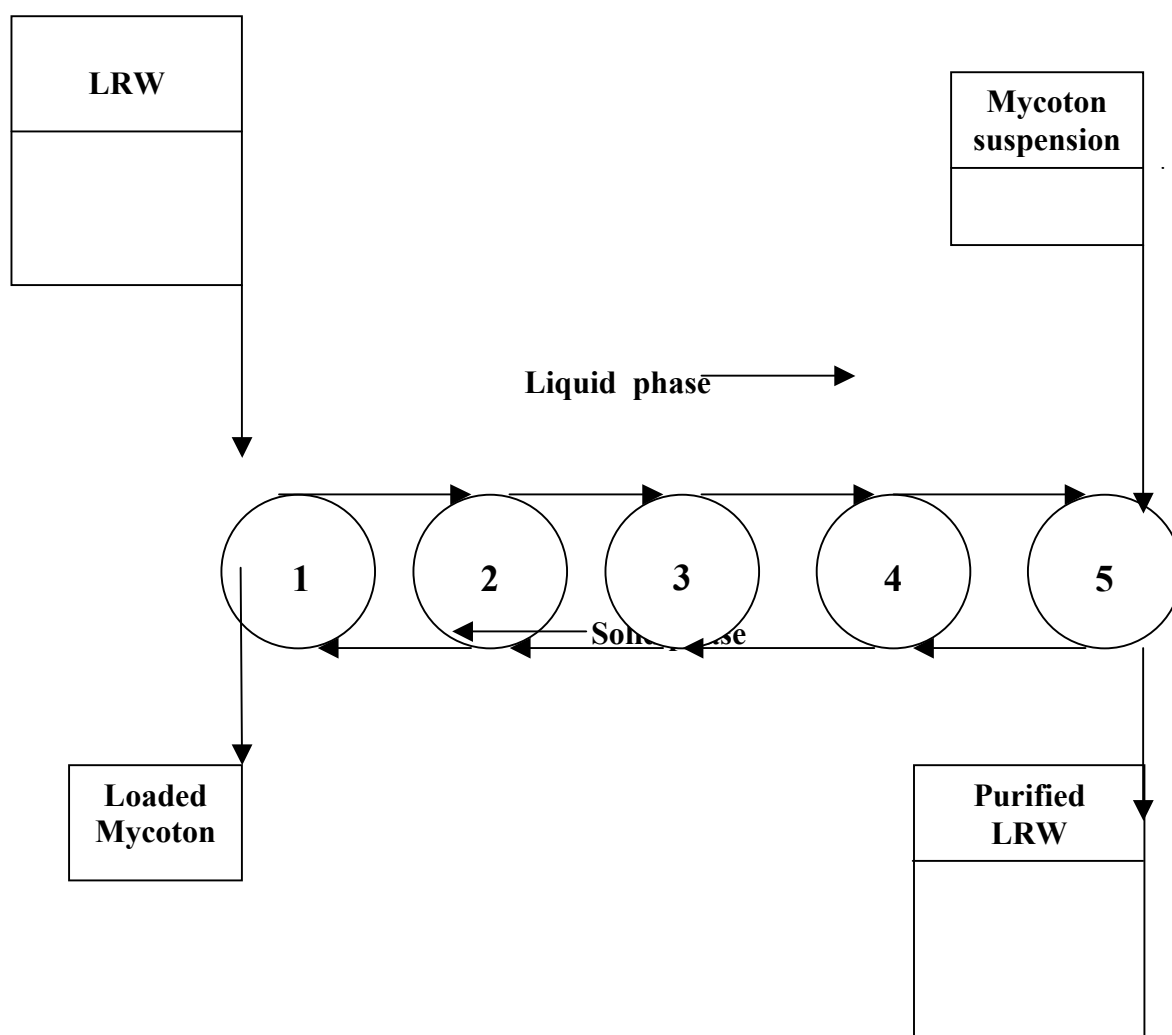


FIG. 8. The flow-sheet of continuous, multistage, counter-current absorption process with centrifugal sorbers.

REFERENCES

- [1] Gorovoj L.F. et al // USSR Invention certificate № 1575552, 1988.
- [2] Gorovoj L.F., Kosyakov V.N., // Russian Patent № 2073015, 1991.
- [3] V.N.Kosyakov, N.G.Yakovlev, L.F.Gorovoy – Application of Chitin-Chitozan Biosorbents for Environmental Decontamination and Radioactive Waste Management.- in book “Biosorbents for Waste Management and Site Restoration” p. 119 – 131, 1997 Kluwer Academic Publishers.
- [4] Chernetsky V.N., Nifantsev N.E. // Russian Patent № 2099351, 10.01.96.
- [5] Kosyakov V.N., Veleshko I.E., Chernetsky V.N., Nifantsev N.E. // Russian Patent // № 2110858, 07. 04. 97.
- [6] Gorovoj L.F., Kosyakov V.N., Kusnetsov G.I., Pushkov A.A., Shklyar L.I. // Russian Patent № 2165284, 18.05.99.
- [7] Muzzarelli R.A.A., Tanfani F., Scarpini G. // Biotechnol. Bioeng. 1980, 22, N4, p.885-896.

- [8] Muzzarelli R.A.A. – Natural Chelating Polymers. Oxford, Pergamon Press, 1973.
- [9] Muzzarelli R.A.A. – Chitin. Oxford, Pergamon Press, 1977.
- [10] Gorovoj L.F., Kosyakov V.N., // Russian J. Biopolymery i kletka. 1995, v. 12, № 4 p. 49-59.
- [11] Kosyakov V.N., Yakovlev N.G., Veleshko I.E. // Russ. J. Radiokhimiya, 1997, v. 39, № 6, p. 540-543.
- [12] Kosyakov V.N. // “Actinide Determination in Environment”, Proceedings of NATO Advanced Research Workshop “Monitoring of Natural and Man-Made Radionuclides and Heavy Metals in Environments”, 3 – 6 October 2000, Dubna, Russia.
- [13] “Techniques for Identifying Transuranic Speciation in Aquatic Environments.” IAEA, Vienna, 1981.
- [14] Vaidia M.F., Bulusa K.R. // J. Inst. Eng. (India) Environ. Eng. Div., 1984, v. 64, N 2, p. 43-47.
- [15] Dzunity T., Kiesy K // Japan Patent 63-17901, 1981 r.
- [16] Kosyakov V.N., Veleshko I.E., Yakovlev N.G., Nifantsev N.E., Chernetsky V.N., //Russ. J. Radiokhimiya 2001, in press.
- [17] Advances in technologies for the treatment of low and intermediate level radioactive wastes. Technical Rep. Series N 370. EAEA, Vienna 1994. P.69-76.
- [18] Holman D.J.. Process options for treatment of organic containing ILW by wet oxidation. // Rad.Waste Management 2 (Proc.Int.Conf.Brighton, 1989) BNES. P.41-44.
- [19] Savkin A.E., Sinyakin O.G. et al. //NPO ”Radon”. M., 1997. - 8 p. VINITI, №2553 – B97.
- [20] Christensen P.A. et al. Fundamental photocatalytic studies on immobilized films of TiO₂. // Trace Met. Environ. 1993. No.3. P.765-770.
- [21] Yakovlev N.G., Kosyakov V.N., Kazakova G.M. // J.Radioanal.Chem. 1982. Vol.75, No.1-2. P.7-16.
- [22] Kopeck’a. // Chem. Listy. 1956. V.50. P.1085.
- [23] Johnson J.W., Jiang H.W., et al. // J.Electrochem.Soc.: Electrochem.Sci.Tech. 1972. Vol.119, No.5. P.574-580.
- [24] Karpacheva S.M., Zakharov E.I. // “Theory and calculation of pulsing column reactors”, M. Atomizdat, 1990.

SORPTION-REAGENT METHODS IN LRW MANAGEMENT

V.A. AVRAMENKO^a, A.P. GOLIKOV^a, V.V. ZHELEZNOV^a, E.V. KAPLUN^a,
N.I. LYSENKO^b, D.V. MARININ^a, T.A. SOKOLNITSKAYA^a, K.A. KHOKHLOV^a,
A.A. YUKHKAM^a

^aInstitute of Chemistry of the Far East Department of the Russian Academy of Sciences,
Vladivostok, Russian Federation

^bFederal State Unitary Establishment “DalRAO”, Russian Federation

Abstract. The report summarizes the results of work performed in the Institute of Chemistry FEDRAS in the frames of the IAEA CRP “Combined Methods of Liquid Radioactive Waste Treatment”. The factors decreasing the efficiency of sorption technologies of low-level radioactive waste (LLRW) treatment were analyzed. It was shown that one of the main factors undermining the sorption technologies of LLRW processing propagation is a low selectivity of the applied sorbents in regard to strontium radionuclides. The basic principles of the sorption-reagent method of strontium removal from solutions with high hardness salts content and LLRW of complex chemical composition were generalized. The method is based on the sorbent reaction with anions present in the solution followed by the formation of a system with a high selectivity to strontium. Mechanisms of strontium removal and pros and contras of the sorption-reagent method were discussed. The results of decontamination of solutions of different composition and pilot plant-scale tests of the sorption-reagent method of LLRW decontamination from long-lived cesium and strontium radionuclides were presented. The most efficient industrial setups of the sorption-reagent method application in LLRW decontamination were considered.

1 INTRODUCTION

One of the main factors causing environmental problems from operation of nuclear power units is a large volume of low level (with the activity less than 10^5 Bq/L) liquid radioactive operational waste (LRW). Long-lived radionuclides contained in LRW are able to escape the waste more quickly than radionuclides contained in solidified or solid radioactive waste (SRW). Transformation of LRW into SRW for safe disposal is one of the most crucial issues in improving the protection of the environment in from nuclear activities. From the economic viewpoint, the use of such reliable waste solidification methods as vitrification and incorporation into ceramic matrices is quite advantageous since it also leads to high volume reduction.

Existing technologies for the treatment of large volumes of LRW are mainly concerned with the consecutive application of the following processes: mechanical filtration, coagulation and ion exchange on filters with combined functions. Since a major part of low-level LRW including primary coolant liquids, decontamination liquids and liquids from special sewages and laundries has a low salt content (usually within 1 g/L), the use of the above techniques enables to reduce the LRW volume from 100 up to 300. The solutions obtained after using this approach contain around 300 g/L of salts and have a specific activity around 10^6 Bq/L. Further cementation of these solutions results in the volume increase. In this case the cost of disposal of SRW may ten times higher than the cost of processing of LRW. That is why one of the main problems of radioactive waste management is reduction of the volume of LRW with high salt contents and improvement of the safety of SRW disposal [1].

The use of sorbents that are selective to long-lived radionuclides enables to a great extent solve many problems of LRW management. The selective application of sorbents in LRW management has a long history [2,3]. Different classes of selective sorbents were used to decontaminate LRW from radionuclides of cesium, strontium, cobalt and transuranium elements. Best selective sorbents provide decontamination of some LRW types more

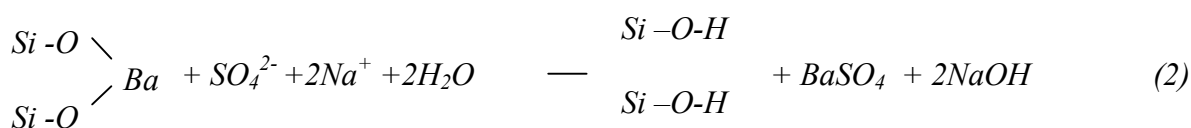
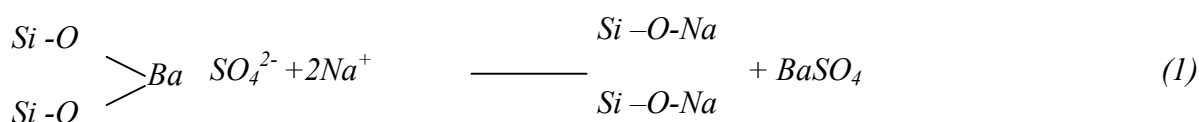
efficiently than ion-exchange resins (tens- and hundreds-fold) [4-8]. However, the sorbent selectivity to a great extent depends on the LRW chemical composition. The presence of admixtures in LRW reduces substantially the efficiency of the selective application of sorbents and, in some cases, even makes decontamination virtually impossible. If the removal of cesium from high-salinity solutions can be performed quite efficiently by using a number of sorbents [4,8], but is not a case for the removal of strontium from the solutions with high hardness salts contents. Indeed, strontium-calcium selectivity coefficients for most selective sorbents are around 1-10. Such a low selectivity does not provide good strontium removal from the solutions with a high hardness salts content. The same problems exist for the removal of cobalt from LRW.

Thus, the improvement of sorbent selectivity and operation stability in the solutions with a complex chemical composition is one of the main factors in using a sorption technology for LRW treatment.

The present study is concerned with the development of sorption-reagent methods for LRW treatment enabling to improve substantially the efficiency of sorption treatment technologies and application of selective sorbents and sorption-reagent materials in LRW treatment from the Russia Pacific Navy nuclear units.

2 HYDROXIDE SORPTION-REAGENT MATERIALS

Ion-exchange systems in which chemical precipitation reactions occur (Chemical Reaction Ion Exchange) have been thoroughly studied (see, for example, the review [9]). In general, the systems in which the processes of ion-exchange, non-exchange sorption, substance co-precipitation on the precipitate formed on the surface and/or in the porous medium and/or in the bulk solution take place could be called **sorption-reagent systems**, since attempts to separate all these processes (exchange, sorption and co-precipitation), as it will be shown later, fail at the present state of knowledge. An interesting example of a sorption-reagent system is barium amorphous silicate [10,11], which undergoes the following reactions in the sodium sulfate solution:

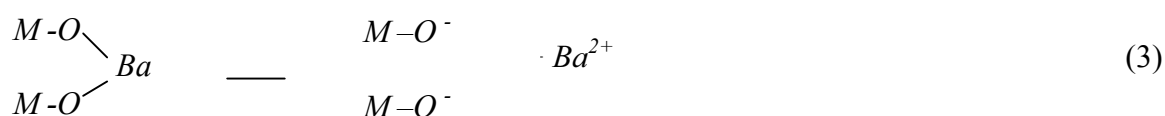


The existence of reaction (1) can be proved by the results of IR-spectroscopy and X-ray phase analysis of barium silicate before and after treatment with the sodium sulfate solution (Figs. 1, 2). After barium silicate contacts the sodium sulfate solution one can observe reflections corresponding to those of barium sulfate in the solid phase X-ray pictures. Absorption bands corresponding to barium sulfate are observed in the barium silicate IR-spectrum. The existence of reaction (2) is shown in Figs. 3, 4 presenting pH change after the sodium sulfate solution contacts barium silicate and the dependence of a number of exchangeable sodium ions in barium silicate after reaction with sulfate at different pH respectively.

It is clearly seen that pH changes significantly at the sulfate concentration from 0.1 up to 0.5 g/L. Similar hydrolysis of the amorphous silica matrix is much less in the presence of

rare earth metal ions (Fig.3, curves 2,3). The exchange capacity of the sorbent for sodium ions after contacting with the sodium sulfate solution decreases at the reduction of pH. In other words, the equilibrium of reaction (2) shifts to the right.

Information on the interaction of exchangeable barium ions with sulfate ions in solutions can be obtained by considering the results of sorbent decomposition by hydrochloric acid after sorbent titration by the sodium sulfate solution. In this case, it is suggested that treatment of expended sorbent by hydrochloric acid does not virtually lead to solving of the microdisperse barium silicate precipitates. Figure 5 shows the results of barium silicate sulfate titration. It can be seen that there are two forms of barium bound to a matrix having respective reaction constants ($1 \cdot 10^{-9}$ и $3 \cdot 10^{-9}$). The estimation of the constant was made without taking into account the saturation related to the microdisperse precipitate curvature [9,10] (see below) according to the equilibrium equation: $K = C_{Ba}^l / C_{Ba}^s = \Pi P_{BaSO_4} / C_{SO_4} \cdot C_{Ba}^s$.



Here indices *s* and *l* are related to the solid and liquid phase, respectively. A barium silicate reaction with the solution sulfate ions results in the substantial change of selectivity of strontium removal from the solutions containing calcium ions. In this case, aside from reactions (1) and (2), the exchange reactions (Na-Ca) and (Na-Sr) should be added as well as the reaction of co-precipitation of strontium on the barium sulfate precipitates formed on the reaction (1).

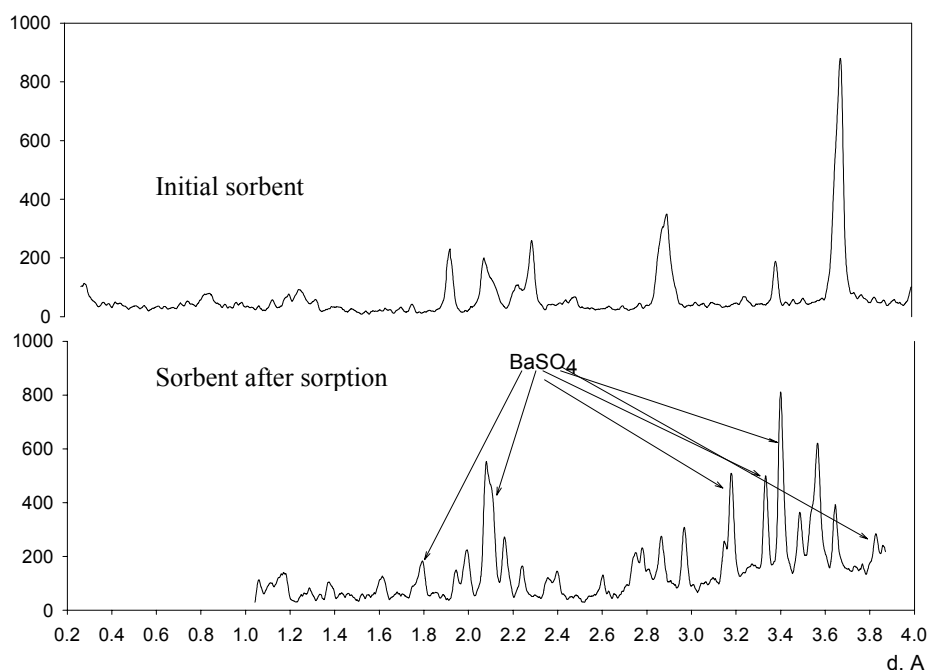


FIG. 1. The X-ray spectrum of the sorption-reagent material before and after sorption.

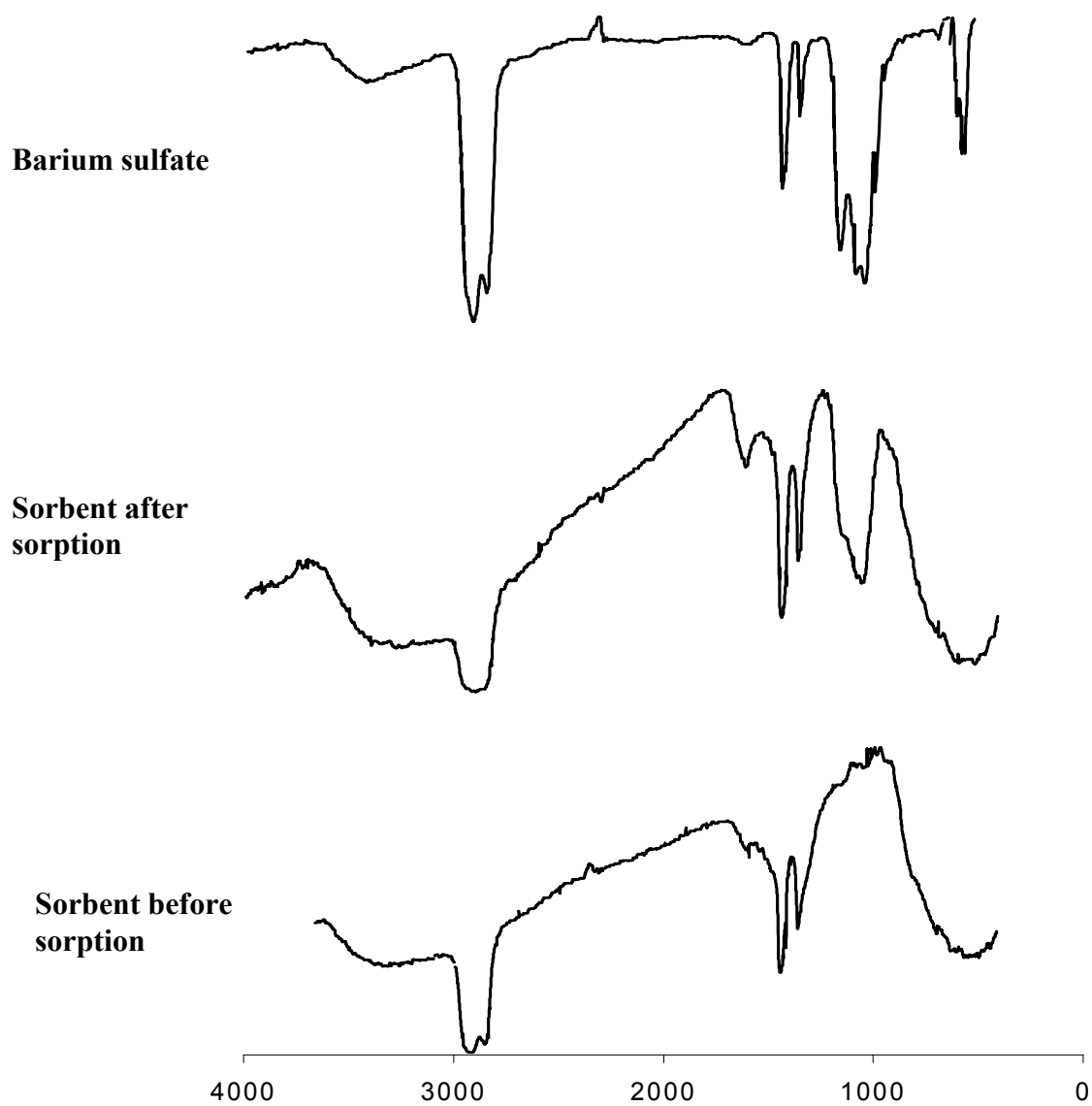


Fig.2. IR-spectra of the sorption-reagent material SSW before and after strontium sorption.

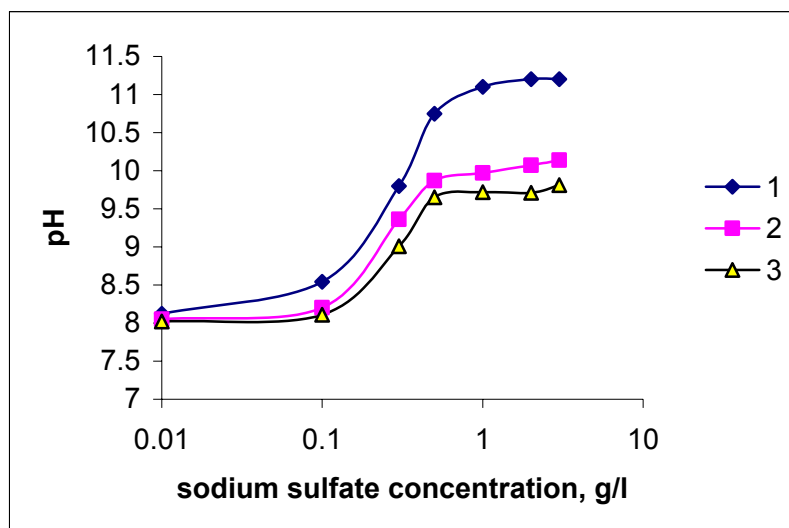


FIG. 3. pH change as a result of the contact of barium silicate with the solution of sodium sulfate and calcium chloride (calcium chloride concentration: 1-0 g/L; 2-0.5 g/L; 3-2 g/L).

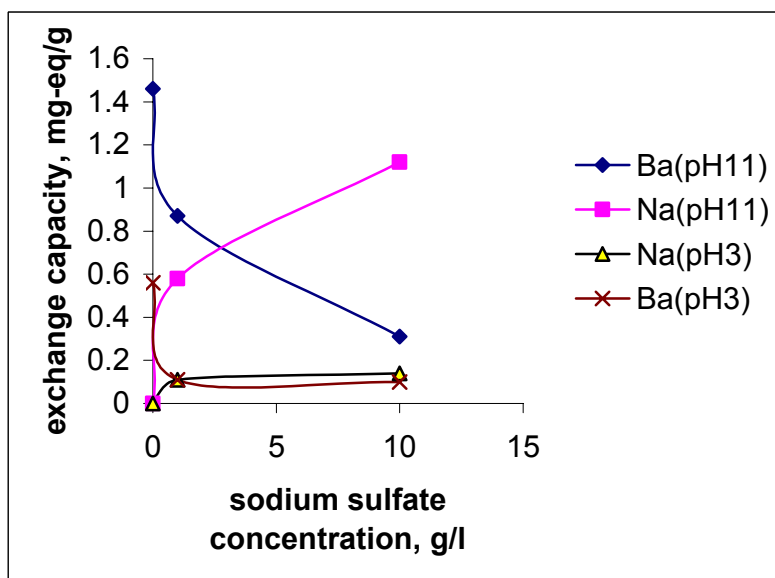


FIG. 4. Barium-sodium exchange in barium silicate during the contact with the sodium sulfate solution at different pH.



solid solutions of barium-strontium-calcium sulfate was rather extensively investigated in several studies [12,13] where it was shown that up to 10% of strontium in the mixed strontium-barium sulfate composition have significant deviations from ideal solution properties that results in the significant strontium concentration in the mixed sulfate.

As it can be seen from Fig.5, the reaction of barium ions exchange followed by barium sulfate formation is possible only at definite sodium sulfate concentrations determined by the dissociation constant of reaction (3). Here the sorption selectivity increases dramatically when the sulfate-ions concentration increases above a critical value (Fig.6).

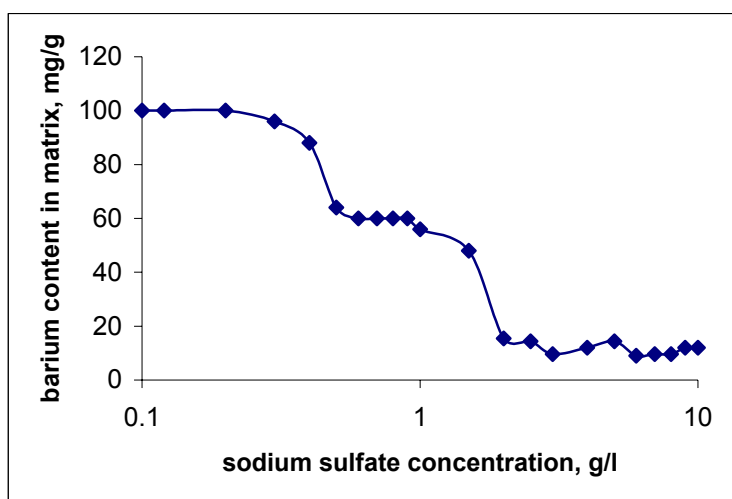


FIG. 5. Sulfate titration of the SRM sorbent.

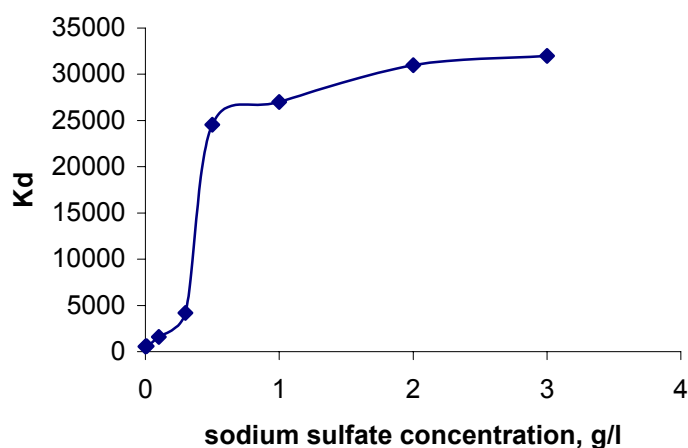


FIG. 6. The change of selectivity of strontium sorption from the calcium chloride solutions (0.5 g/L) depending on the sodium sulfate concentration.

It is also interesting to consider a problem of the barium sulfate precipitate location. It is known that the formation of the porous ion-exchangers precipitate is possible on the internal pore surface, in the pore central part, on the external sorbent particle surface, and in a bulk solution. The conditions of the precipitate formation in one of the above area are determined by the solution saturation extent, interfacial tension of precipitate nuclei at the nucleus-solution interface and the matrix surface-nucleus and internal pore surface curvature [14,15]. For conventional strongly bound ion-exchange resins, by taking into account the approximate values of interfacial tension for barium sulfate (150 erg/cm^2 [15, p.304]), it can be suggested that the formation of the barium sulfate precipitate is possible either on the ion-exchanger surface or in the bulk solution [14]. At the same time, for the porous amorphous barium silicate, where the pore size, according to water vapor adsorption data, is 40-80 nm, the precipitate formation is possible in the sorbent pore central part. The principal difference of strontium sorption on barium silicate and ion-exchanger KU-2x8 in the barium form can be seen in Fig. 7. Nevertheless, to attribute the high selectivity of the sorption-reagent system – barium silicate – exclusively to formation of barium sulfate highly dispersed precipitate in the sorbent pores followed by the formation of solid solutions of mixed barium-strontium sulfates is impossible due to results of sorbent with sorbed strontium decomposition by different methods: 1) hydrochloric acid treatment and 2) melting with calcium carbonate and further solving in hydrochloric acid. In the latter case, both strontium ions sorbed on the sorbent matrix and that co-precipitated in reaction (6) go into solution. Table I (will be added later) presents the results of the treatment of a number of test samples of barium silicate and the strontium distribution coefficients on these samples. It is seen that samples of the highest selectivity have largest contributions of a sorption part.

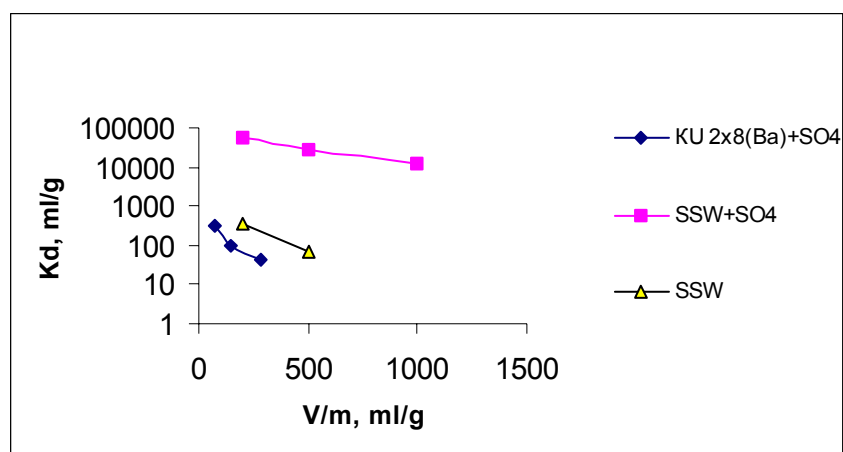


FIG. 7. Dependence of the distribution coefficient on V/m ratio for different sorption-reagent systems.

In a view of a multiple character of reactions, the sorption behavior of cations in such sorption-reagent systems differs substantially from conventional sorption and ion exchange. The difference is the most pronounced at the application of sorbent/sorption-reagent material in dynamic conditions.

Figure 8 shows the dependence of the strontium sorption dynamics from the sulfate solutions at different sorbent layer thickness. It is evident that the value of the retention volume does not increase proportionally with the sorbent layer thickness. The sorbent dynamic capacity decreases with the increase of the sorbent layer thickness. The difference between the capacities of the sorbent/sorption-reagent materials for strontium increases with the reduction of the calcium contents in the solution.

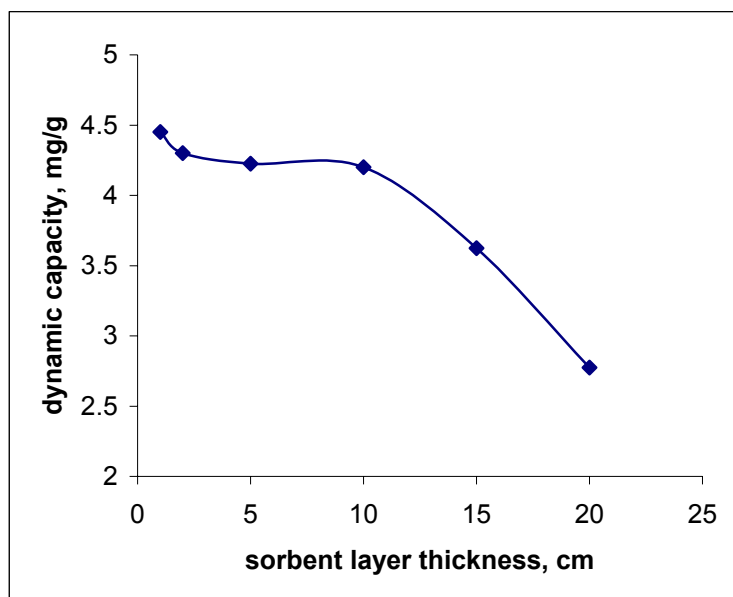


FIG. 8. Dependence of the sorption material dynamic capacity on the layer thickness.

2.1 MATHEMATICAL SIMULATION OF THE PROCESSES IN THE SORPTION-REAGENT MATERIALS

The above observations can be explained by considering the motion of several concentration fronts along a column filled by a sorption-reagent material:

- The front of the reagent (sulfate ion) spent on the formation of insoluble precipitate;
- The front of the flow of barium sulfate formed in the sorbent matrix;
- The fronts of the flow of exchangeable sodium, calcium, strontium, and barium;
- The front of hydrolysis of the sorbent matrix;
- The front of pH.

A mathematical simulation of the sorption dynamics in such a sorption-reagent system has been performed. The simulated system is a sorption column (L_s -length, d -diameter) filled with a granulated silicate sorbent (d_s -the average granule diameter, ϵ -a volume part occupied by the sorbent). The buffer volume with length L_{buf} (without sorbent) is located in the lower part of the column. Initially, a part of sorbent surface groups (in $-\text{Si}-\text{OH}$ form) is modified by barium ions (in $-\text{Si}-\text{OBa}-\text{OH}$ form) – concentration C_{mat} , mg/g.

In the moment $\tau=0$ a solution containing ions of rare earth elements (with the concentration C_{Me}), sodium sulfate (with the concentration C_{SO4}) and, possibly, HCl (with the concentration C_a) or NaOH (with the concentration C_b) starts to enter the column with the volume rate v (mL/min). During the numerical simulation, the system is divided into two phases: a) a mobile phase – the solution washing the sorbent granules and b) a stationary phase – the solution located in pore space of sorbent granules.

For all ions of the mobile phase (except for H^+ and OH^-), on every time step the transfer equations containing the following terms should be solved:

- convection transfer ($v\partial C_{Me}/\partial x$) – the solution motion through the column;
- transfer due to longitudinal diffusion ($D\partial^2 C_{Me}/\partial x^2$, where D – the coefficient of longitudinal diffusion);

- mass exchange with the stationary phase ($K_m S/V/(1-\epsilon)(C_{Me} - C_{Me}^s)$, where K_m - the coefficient of mass transfer, C_{Me}^s – the ion concentration in the stationary phase).

Therefore, one can obtain the following equation of mass transfer:

$$\frac{\partial[A]_L}{\partial x} + (1-\epsilon)\frac{\partial[A]_L}{\partial \tau} - (1-\epsilon)\left(\frac{K_m S}{V(1-\epsilon)}([A]_s - [A]_L)\right) = D \frac{\partial^2[A]_L}{\partial x^2}, \quad (7)$$

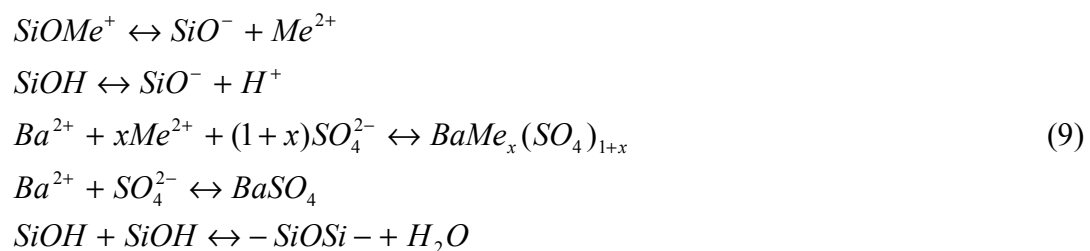
where $[A]_L$, $[A]_s$ – the concentrations of transferred ions per volume of the mobile and stationary phase, respectively; S – the interface area; V – the column volume; D – the coefficient of longitudinal diffusion; K_m – the coefficient of mass transfer between phases. By expressing S through the average sorbent granule diameter, Eq. 7 can be rewritten as:

$$\frac{\partial[A]_L}{\partial x} + (1-\epsilon)\frac{\partial[A]_L}{\partial \tau} - \lambda([A]_s - [A]_L) = D \frac{\partial^2[A]_L}{\partial x^2}, \quad (8)$$

where: $\lambda = \frac{6\epsilon K_m}{d_s}$

When solving the mass transfer equation, the concentration change along the column is taken into account for its active part only. In the column buffer volume, the concentration does not depend on the x coordinate. As could be seen from the above equation, an external diffusion model for kinetics of exchange between stationary and mobile phases has been adopted. In the case of an unknown limiting stage (internal or external diffusion) of a process under study, one should consider a general case – a mixed-diffusion model of exchange kinetics. However, the use of such a model requires solving transfer equations in each time layer in each point of special network that consumes unreasonably much computer time. If absolute values of external and internal diffusion coefficients and concentration distribution of diffusing ions in sorbent granules are not important for a specific study, the processes of external and internal diffusion could be united into one “averaged” mass transfer process with a some effective coefficient of mass transfer (K_m) and averaged (over sorbent granule) concentrations in the stationary phase. To simplify the interpretation of simulation results, equal averaged coefficients of longitudinal diffusion and mass transfer for all ions under consideration were assumed. An immediate achievement of local acid-base equilibrium from the electroneutrality condition for every phase (this enables to calculate the concentrations of H^+ and OH^- ions) was also assumed. Thus, according to the model, no chemical or exchange reaction of transferred ions occur in the mobile phase.

The following equilibria were taken into account for the stationary phase:



The above processes are described by the following equations:

Association-dissociation of rare earth metal ions with active centers in a silicate matrix:

$$\frac{\partial [SiOMe]}{\partial \tau} = K_{Me}^a [SiO][Me]_S - K_{Me}^i [SiOMe] , \quad (10)$$

Hydrolysis and ageing of a matrix:

$$\frac{\partial [SiOH]}{\partial \tau} = K_H^a [SiO][H]_S - K_H^i [SiOH] - K^o [SiOH]^2 \quad (11)$$

Formation of mixed sulfates:

$$\frac{\partial [BaMeSO_4]}{\partial \tau} = K_{Me}^s [Ba][Me]_S^x [SO_4]_S^{1+x} - K_{Me}^s PP_{Me} 1(BaMeSO_4) \quad (12)$$

Formation of barium sulfate:

$$\frac{\partial [BaSO_4]}{\partial \tau} = K_{Ba}^s [Ba][SO_4]_S - K_{Ba}^s PP_{Ba} 1(BaSO_4) \quad (13)$$

Formation of active centers:

$$\frac{\partial [SiO]}{\partial \tau} = K_H^i [SiOH] + \sum_{Me} K_{Me}^i [SiOMe] - K_H^a [SiO][H]_S \quad (14)$$

Rare earth metal ions (except barium) balance:

$$\begin{aligned} \frac{\partial [Me]_S}{\partial \tau} = & -\frac{\lambda}{\varepsilon} ([Me]_S - [Me]_L) + K_{Me}^i [SiOMe] - K_{Me}^a [SiO][Me]_S - \\ & xK_{Me}^s [Ba][Me]_S^x [SO_4]_S^{1+x} + xK_{Me}^s PP_{Me} 1(BaMeSO_4) \end{aligned} \quad (15)$$

Barium ion balance:

$$\begin{aligned} \frac{\partial [Ba]_S}{\partial \tau} = & K_{Ba}^i [SiOBa] - K_{Ba}^a [SiO][Ba]_S - \\ & \sum_{Me \neq Ba} xK_{Me}^s [Ba][Me]_S^x [SO_4]_S^{1+x} + \sum_{Me \neq Ba} xK_{Me}^s PP_{Me} 1(BaMeSO_4) - \\ & K_{Ba}^s [Ba][SO_4]_S + K_{Ba}^s PP_{Ba} 1(BaSO_4) \end{aligned} \quad (16)$$

Sulfate ion balance:

$$\begin{aligned} \frac{\partial [SO_4]_S}{\partial \tau} = & -\frac{\lambda}{\varepsilon} ([SO_4]_S - [SO_4]_L) - \\ & \sum_{Me \neq Ba} (x+1)K_{Me}^s [Ba][Me]_S^x [SO_4]_S^{1+x} + \sum_{Me \neq Ba} (x+1)K_{Me}^s PP_{Me} 1(BaMeSO_4) - \\ & K_{Ba}^s [Ba][SO_4]_S + K_{Ba}^s PP_{Ba} 1(BaSO_4) \end{aligned} \quad (17)$$

Sodium and chlorine ion balance:

$$\frac{\partial [AK]_s}{\partial \tau} = -\frac{\lambda}{\varepsilon} ([AK]_s - [AK]_L) \quad (18)$$

where Me=Ca, Mg, Sr, Ba; x – the stoichiometric coefficient in mixed sulfate ($\text{BaMe}_x(\text{SO}_4)_{1+x}$); AK=Na, Cl; K_{Me}^i – the dissociation rate constant of rare earth metal (Me) bound to silicate matrix; K_{Me}^a – the association rate constant of rare earth metal (Me) with active center of silicate matrix; K_{Me}^s – the association rate constant of mixed sulfate of rare earth metal (Me) (or barium sulfate); IP_{Me} – the solubility product of mixed sulfate of rare earth metal (Me) (or barium sulfate); K^o – the matrix ageing rate constant; $1([C])$ – function equal 1 if the concentration C is zero or positive and equal 0 if it is negative (the introduction of this function is necessary, since due to the application of an explicit way for solving kinetic equations in the static phase the ion the concentrations may become too large in the case of too long time step that makes finding the solution impossible).

As it was mentioned above, the concentration of hydrogen and hydroxyl ions in both phases was calculated on the basis of suggestion on the momentary local establishment of these ions equilibrium concentrations. In this case their concentrations in the mobile phase can be determined from the equation:

$$\begin{aligned} [H]_L &= \frac{2K_w}{\Delta + \sqrt{\Delta^2 + 4K_w}} \\ [OH]_L &= K_w / [H]_L, \\ \text{where } \Delta &= 2 \sum_{\text{Me}} [Me]_L + [Na]_L - [Cl]_L - 2[SO_4]_L \end{aligned} \quad (19)$$

In the static phase:

$$\begin{aligned} [H]_s &= \frac{2K_w}{\Delta + \sqrt{\Delta^2 + 4K_w}} \\ [OH]_s &= K_w / [H]_s, \\ \text{where } \Delta &= \sum_{\text{Me}} ([SiOMe] + 2[Me]_s) + [Na]_s - [Cl]_s - 2[SO_4]_s - [SiO] \end{aligned} \quad (20)$$

It was assumed in the process of simulation that barium ions emerging in the static phase at the matrix dissociation did not achieve the mobile phase, since they interacted with sulfate ions forming either mixed sulfates or barium sulfate.

The numerical solution of the transfer equation was performed according to an implicit scheme. In view of this, all ion concentrations appearing in terms with derivatives on coordinate and in exchange term should be written for a time layer to be found. If to substitute here the expressions for $[Me]_s$, a system of non-linear equations in partial derivatives would not possible to solve by a succession method. That is why an iteration method was chosen to solve this system of equations. At the first iteration of every time layer, concentration $[Me]_s$ was assigned with the value equal to that in a previous time layer; then transfer equations were solved successively; the obtained $[Me]_L$ values were substituted into kinetic equations and corrected values of $[Me]_s$ were calculated explicitly from them and current $[Me]_s$ values. The obtained values were again substituted into transfer equations and the next iteration was performed. It was found out that the iteration process results in the virtually constant

concentration values within 10-15 iterations in every time layer. If during the iteration process some of the concentration values became negative, the time step was reduced two-fold and calculations were repeated.

The simulation results are shown in Figs. 9,10 where the curves of different concentration front motions determining sorption processes and reaction as well as output component curves are presented. It can be seen from Fig.11 that the sorbent dynamic capacity decreases with the increase of the sorbent layer length. This effect depends immediately on the sorbent matrix hydrolysis rate constant.

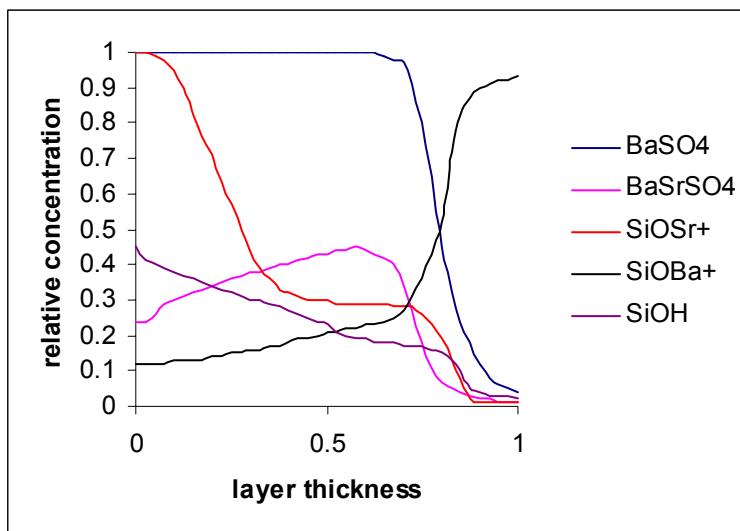


FIG. 9. Contents of the forms in the sorbent layer.

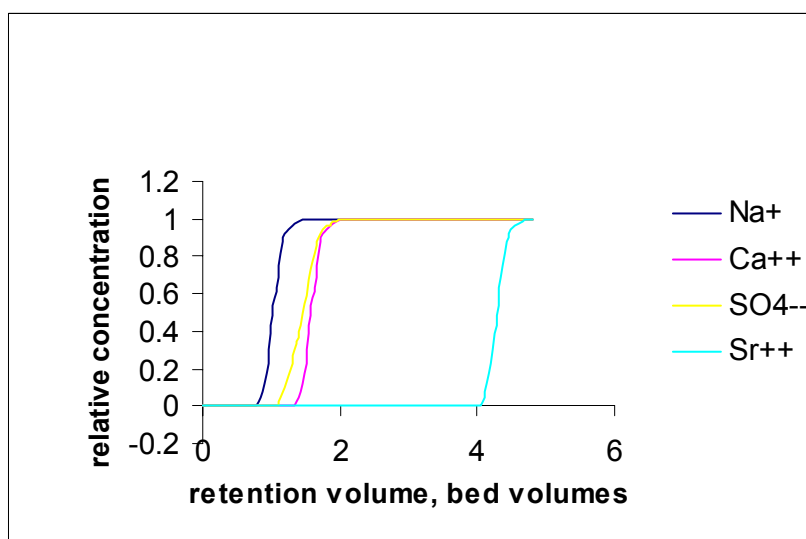


FIG. 10. Simulation of the output curve.

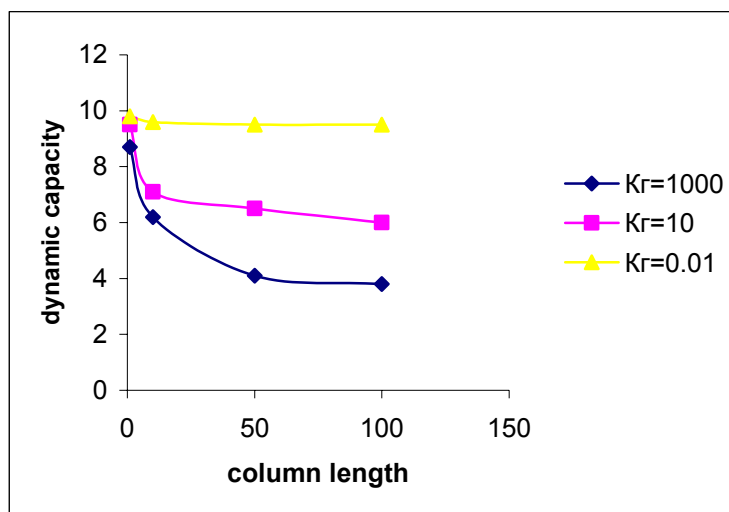


FIG. 11. Simulation of the dynamic capacity dependence on the column length at different matrix hydrolysis constants.

2.2 MANGANESE DIOXIDE SORPTION-REAGENT MATERIALS

In [16,17], a system of sodium permanganate-activated carbon was suggested as an efficient radionuclide sorption system. The efficient removal of strontium from the solutions of easily oxidated organic complexing agents on manganese sorbents assume the possibility of the removal of strontium by a sorbent-reagent. Indeed, at organics oxidation by sodium permanganate in a neutral medium, hydrated manganese dioxide and various non-stoichiometric manganites of rare earth metals are formed [18,19] which themselves are good sorbents for rare earth elements including strontium. And potassium permanganate in neutral a medium is rather efficiently adsorbed by carbon with the formation of hydrated manganese dioxide. Fig. 12 shows the removal of strontium from the sodium humate solutions in such sorption-reagent systems.

It is evident that the efficient removal of strontium by the sorption-reagent method would depend on many parameters: the permanganate concentration in the solution; the nature of a sorbent used for obtaining hydrated manganese dioxide; medium pH of organic complexing agents oxidation; a linear flow rate of the sorption-reagent implementation in dynamic conditions. Figs. 12-15 show the influence of these factors on the efficiency of the sorption-reagent method of strontium removal with using humic substances as complexing agents.

As it could be seen from the above figures, the sorption-reagent method with using potassium permanganate as reagent and thin-layer manganese (IV) hydroxides put on activated carbon fibers as sorbents can be rather efficiently applied for the removal of strontium from the large amounts of hard-to-oxidate complexing agents such as humic and fulvic acids. The decontamination factors corresponding to the given linear flow rate remain virtually constant along 100-300 bed volumes decontaminated depending on the hardness salts content in the solution. The use of pure carbon surfaces (in our case carbon fiber Aktilen) as a matrix reacting with potassium permanganate provides far less efficiency of strontium removal as compared to a carbon matrix with pretreatment by potassium permanganate in a strong acid medium (sorbent FFM) – see Fig. 13. Indeed, it was found out in preliminary experiments that the rate of carbon-graphite materials reaction with sodium permanganate in neutral media increases dramatically at carbon matrix oxidation.

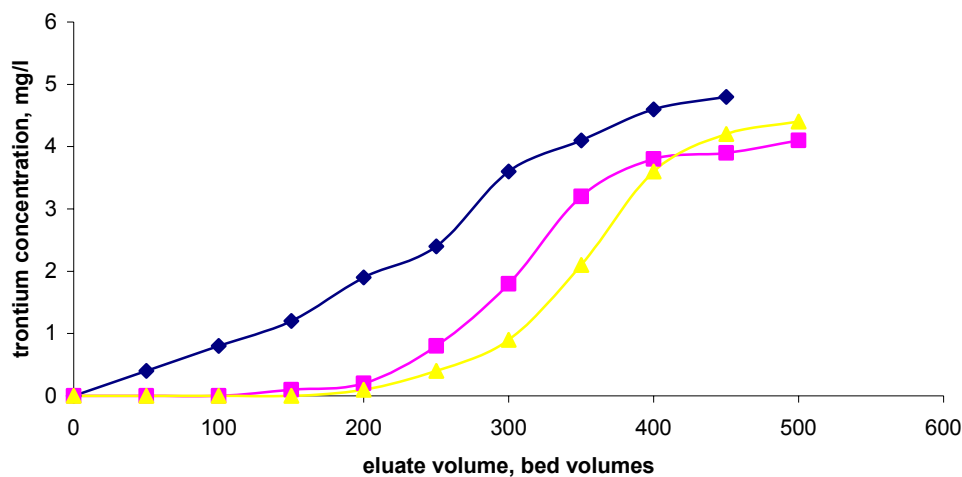


FIG. 12. Sorption of strontium from the sodium humate solutions on FMM at different concentrations of potassium permanganate.

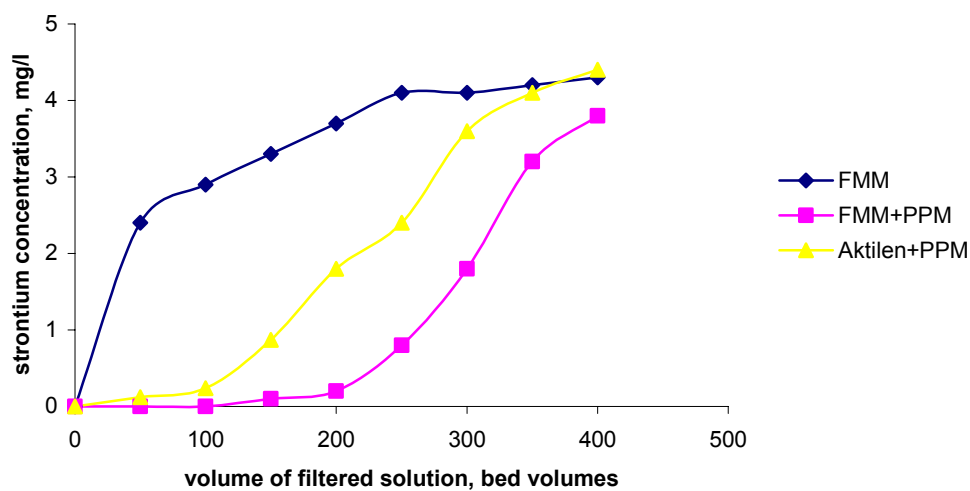


FIG. 13. Sorption of strontium from the sodium humate solutions.

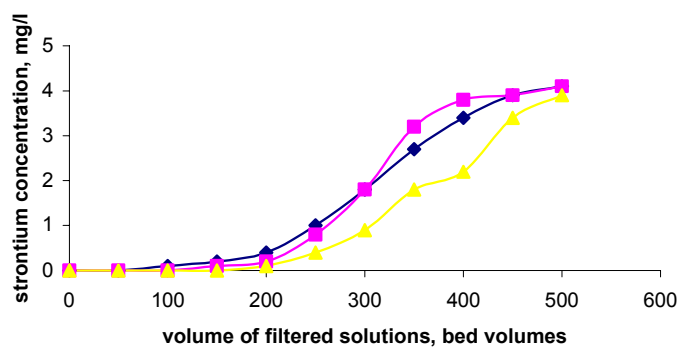


FIG. 14. Sorption of strontium from the sodium humate solutions on FMM at potassium permanganate concentration 0.03% and different pH.

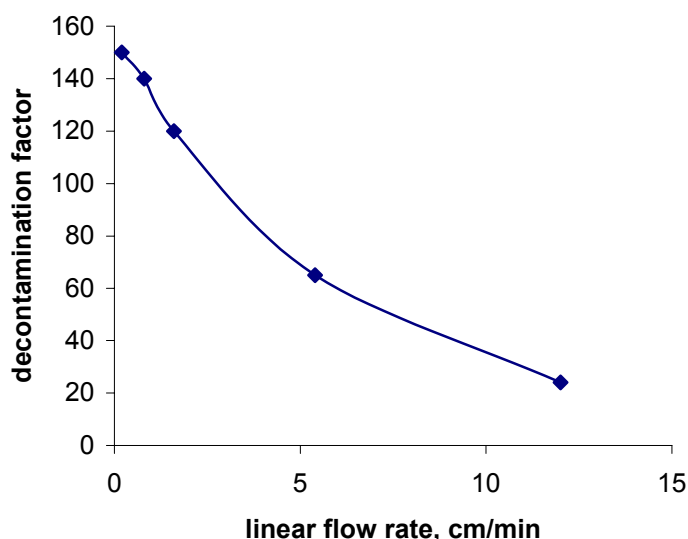


FIG. 15. Dependence of the decontamination factor for strontium on the flow rate in the sodium humate solutions.

Beside the sorption radionuclide removal, the use of permanganate sorption-reagent method of treatment is possible for the removal of radionuclides in colloid form from LRW. The example of this is flow-based co-precipitation of colloid iron hydroxide in the sorption-reagent system sodium permanganate-carbon fiber. The efficiency of this co-precipitation is shown in Fig.16.

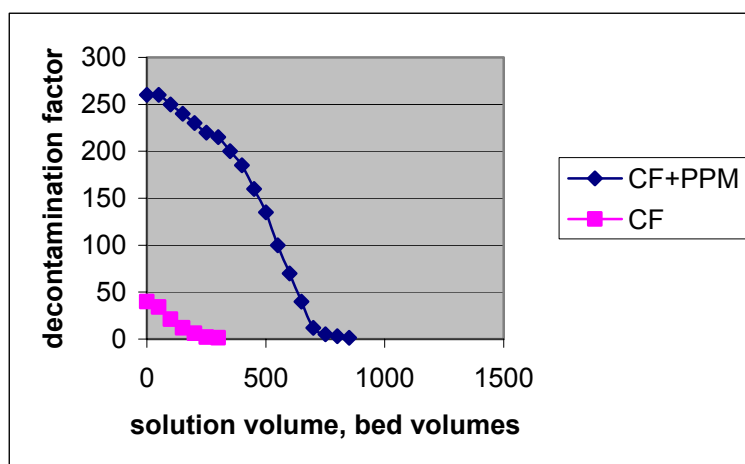


FIG. 16. Treatment with the use of colloid iron hydroxide.

However, this variant of the sorption-reagent method of the removal of strontium ions and radionuclides has some limitations arising from the increase of column hydrodynamic resistance emerging, possibly, both as a result carbon fiber oxidation destruction and due to accumulation of thin-dispersed hydrated manganese dioxide precipitate not only on carbon fiber surface but also inside the column. This fact to some extent reduces method's applicability in the cases when low strontium decontamination factors but high LRW/SRW volume ratios are required in a treatment process.

As a practical implementation of this treatment approach, let us consider treatment of LRW from the primary coolant of a nuclear submarine to be dismantled. Treatment was performed at a pilot-plant installation shown in Fig.17. The sorption-reagent treatment system containing the sodium permanganate-carbon fiber material was used as a system for additional treatment of intermediate level LRW (the activity 10^{-4} Ci/L). In this installation, the decontamination factor of $2 \cdot 10^6$ was obtained for the treatment of the reactor primary coolant water from cesium, strontium and cobalt at the LRW flow rate of 2.5 filter volume/hour.

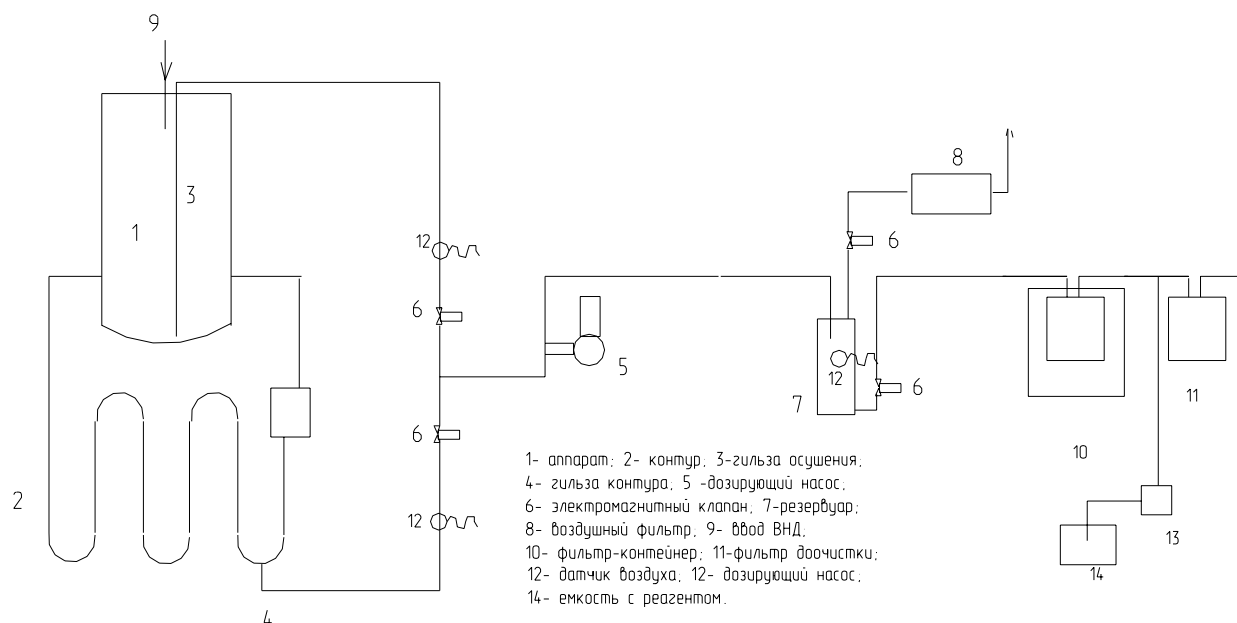


FIG. 17. A pilot plant for the treatment of the primary coolant. 1- apparatus, 2 – countour, 3 –drying unit, 4 –countour unit, 5 –dosing pump, 6 –electromagnetic pump, 7 reservoir, 8 –air folter inlet, 10 –folter container, 11 –additional decontamination folter, 12 –air gauge, 13 – dosing pump, 14 –reagent container.

3 FERROCYANIDE SORBENTS

Application of ferrocyanide sorbents enabled to solve many problems of LRW treatment technologies related to the removal of cesium. Nevertheless, the application of ferrocyanide sorbents has a number of limitations owing to the fact that generally used composite ferrocyanide sorbents have rather low hydrolytic and mechanical stability, since ferrocyanides of transition metals have very small crystals.

Figure 18 shows the change of distribution coefficients of some ferrocyanide sorbents in the process of treatment of some inactive solutions. It is seen that the reduction of selectivity is rather significant for some types of ferrocyanide sorbents. Besides, as shown in Fig.19, the ferrocyanide content in the solution is substantial. Such a destruction of composite ferrocyanide sorbents not only reduce the extent of removal of cesium from LRW but also may require additional water treatment until the level of residual activity regulated by the normative documents. This requires new approaches to the application of ferrocyanide sorbents, especially in the treatment of intermediate level LRW until activity level appropriate for discharge into environment.

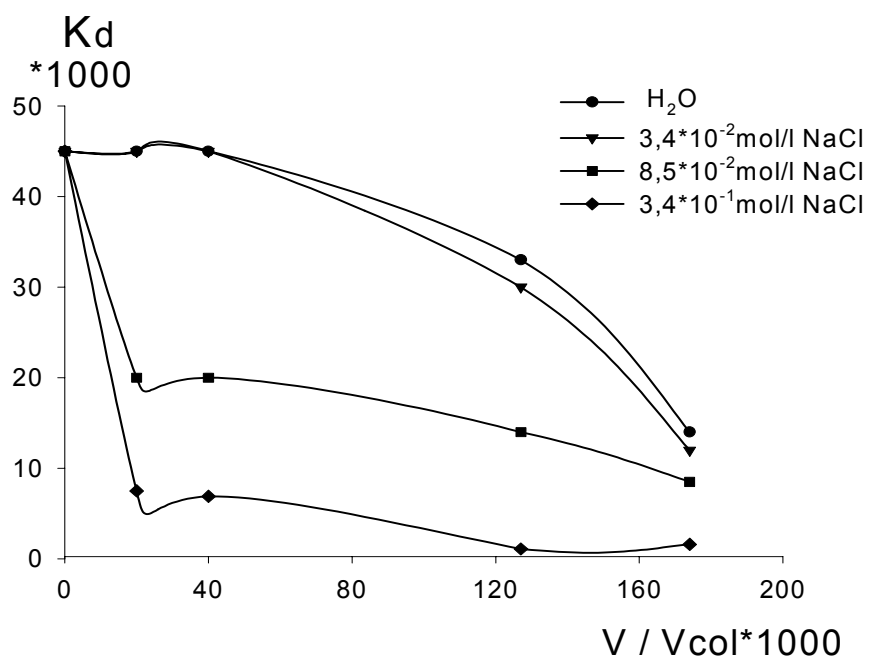


FIG. 18. Dependence of the cesium distribution coefficient on the treated volume and eluate salinity for the sorbent FF (carbon fiber treated by iron ferrocyanide).

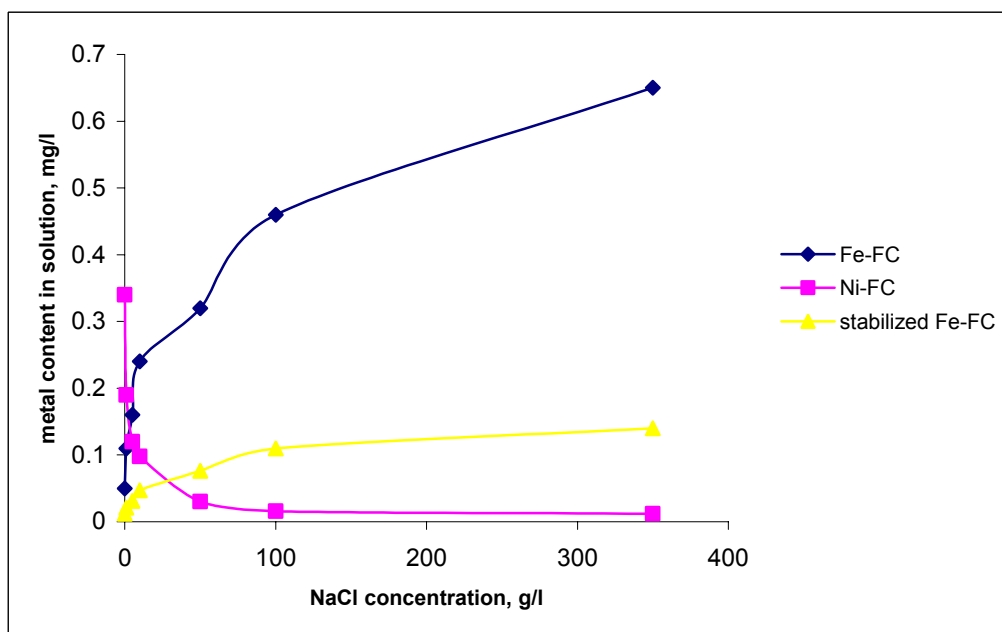


FIG. 19. Instability of ferrocyanide sorption materials.

Interesting results were also obtained in application of polyelectrolytes stabilizing radiocolloids at electrochemical deactivation of metallic radioactive waste.

All the above considerations confirm that detailed studies of radiocolloids stability/instability would enable to make a significant advance in technical applications concerned with LRW management, deactivation of solid surfaces and soils.

4 CONCLUSIONS

- One of the main factors hampering the development of sorption technologies in LRW management is an insufficient selectivity of available sorbents in regard to strontium radionuclides.
- Development of the sorption-reagent method, in which, during the interaction with the solution to be decontaminated, the reactions of ion exchange and microdisperse precipitates formation in sorbent porous structure take place, enables to increase substantially (in many times) the sorbent selectivity to strontium radionuclides.
- Mechanism of strontium sorption in a number of developed sorption-reagent materials was studied by means of different chemical and physico-chemical methods and peculiarities of the sorption-reagent process were considered.
- Sorption-reagent inorganic ion-exchange materials interacting with sulfate-, carbonate-, oxalate-, sulfide-, and permanganate-ions were studied. Insoluble compounds formed as a result of this interaction increase tens- and hundreds-fold the sorption selectivity of different radionuclides – strontium, cobalt, mercury, iron, and manganese as compared to conventional ion-exchange systems.
- Mathematical model for concentration front motions in the sorption process was developed. It appears to describe basic experimentally observed features of the process.
- The problem of radiocolloid stability/instability in LRW management was discussed. It was shown that detailed studies of this problem are promising in view of development of generally accepted technologies such as CITROX process.
- Pilot-plant tests of sorption-reagent materials in sorption technology of LRW management were performed and prospects of these materials application for decontamination of LRW of complex chemical composition were shown.
- The most efficient technological setups of the sorption-reagent method use in LRW decontamination were considered and prospects of its application in combination with membrane technologies were demonstrated.
- About **1500 cubic meters** of various LRW from research facilities and nuclear power objects were decontaminated. It was shown that application of the sorption-reagent approach provides a proper flexibility at solutions of different LRW management problems.
- **Examples** of systems that can be successfully treated with using sorption-reagent materials:
 - *seawater;*
 - *high-salinity solutions;*
 - *solutions with colloids and complexants (CITROX waste etc.)*
 - *medium-activity waste.*

REFERENCES

- [1] POLYAKOV, A. S., Radioactive waste management: state, problems, research. Russian Chemical Journal, 1996, v.49, N6, p.26-35. [In Russian].
- [2] HONIKOVICH, A. A., Radioactively polluted water decontamination. Moscow: Atomizdat, 1974, 312pp. [In Russian].
- [3] KUZNETZOV, YU. V., SHEBETKOVSKY, V.N., TRUSOV, A.G., Basics of water decontamination from radioactive admixtures. Moscow; Atomizdat, 1974, 360pp. [In Russian].
- [4] ILYUTIN, V.V., GELIS, V.M., PENZIN, R.A., Characterization of sorption-selective properties of inorganic sorbents and ion-exchange resins in regard to cesium and strontium. Russ. J. of Radiochemistry, 1993, N3, p.76-81. [In Russian].
- [5] HAAS, P.A., A Review of Information on Ferrocyanide Solids for Removal of Cesium from Solution. Separation Sci and Tech.1993, v.28, N17&18, p.2479-2506.
- [6] SERGIENKO, V.I., AVRAMENKO, V.A., GLUSHCHENKO, V. Yu., Sorption technology of LRW treatment. J.Ecotechnology Res., 1995, v.1, N2, p.152.
- [7] LEHTO, J., HARJULA, R., Selective Separation of Radionuclides from Nuclear Waste Solutions with Inorganic Ion Exchangers. Radiochem. Acta, 1999, v.86, pp.65-70.
- [8] SAVKIN, A.E., DMITRIEV, S.A., et. al. Russ. J. of Radiochemistry, 1999, v.41, N2, p.172-176. [In Russian].
- [9] JANAUER, G.E., GIBBONS, R.E., BERNIER, W.E., In: "Ion exchange and Solvent Extr. vol.9", N.Y.: Basel, 1985, p. 53-173.
- [10] AVRAMENKO, V.A., GLUSHCHENKO, V.Yu., ZHELEZNOV, V.V., MARININ, V., SERGIENKO, V.I., CHERVONETSKY, D.V., Sorption technology of high-salinity liquid radioactive waste management. In: Proc. Intern. Symp. on Radiation Safety Management '99, Taejon, Korea, Nov.1999, p.271-276.
- [11] AVRAMENKO, V.A., et.al. Method of strontium removal from high-salinity solutions. Russian patent application N....
- [12] LIESER, K.H., HILD, W., Naturwissenschaften, 1959, B.46, S.599-600.
- [13] PRIETO, M., FERNANDES-GONZALEZ, A., PUTNIS, A., FERNANDES-DIAZ, L., Geoquimica et Cosmoquimica Acta, 1997, v.61, N16, p. 3383-3397.
- [14] HAMIZOV, R.Kh., MYASOEDOV, B.F., TIKHONOV, N.A., RUDENKO, B.A., Bulletin of Russian Acad. Sci., 1997, v.356, N2, p.216-220. [In Russian].
- [15] ADAMSON, A., Physical chemistry of surfaces. Moscow: Mir, 1979, 568pp. [In Russian].
- [16] MARTON, G., SZANYA, T., HANAK, L., SIMON, G., HIDEK, J., MAKAI, J., SCHUNK, J., Purification of nuclear power plant decontamination solutions by preparative scale reactive adsorption. Chemical Engineering Science, 1996, v.51, N11, p.2655-2660.
- [17] AVRAMENKO, V.A., et.al. Selective MSP decontamination from strontium ions. Scientific Report, Vladivostok, Russia, 1998. [In Russian].
- [18] RODE, E.Ya., Oxygen compounds of manganese. Moscow: AN SSSR, 1952, 398pp. [In Russian].
- [19] BRATSKAYA, S.Yu., Integral description of acid-base equilibria in polyelectrolyte solutions and heterophase systems. Thesis: Vladivostok, Russia, 1998. [In Russian].

SORPTION-CATALYTIC TREATMENT OF LIQUID RADIOACTIVE WASTE BASED ON TITANIUM DIOXIDE SORBENTS

P. MANORIK, M. PHEDORENKO, T. MAKOVSKAYA, V. LYTVIN, S. DEMESHKO
L.V. Pysarzhevsky Institute of Physical Chemistry,
National Academy of Sciences, Ukraine

Abstract. Methods were elaborated for synthesis of a few types of materials: I. Dispersed porous TiO_2 materials containing 3d-metals (V, Mo) including materials with hydrophobized surface; II. Dispersed porous TiO_2 materials with big pores size (by means of template synthesis with DB18C6 (L2) and DB24C8 (L3) and DB30C10 (L1); III. Dispersed porous TiO_2 materials containing some tetraazamacrocyclic ligand (L4); IV. Dispersed porous TiO_2 / SiO_2 materials. Different types of materials, which were obtained, were tested in different sorption and catalytic processes of liquid radioactive waste processing.

1 INTRODUCTION

The treatment of liquid radioactive waste containing organic impurities represents a problem taking into account large volumes of this waste, its potential hazard and a complex of technical issues.

The application of TiO_2 materials for sorption-catalytic liquid waste treatment has good prospects owing to their unique properties. Such materials may be used as catalysts in different catalytic oxidation processes [1-6] and as sorbents [7-10]. Such materials have also photocatalytic properties under ultraviolet irradiation [11-14].

The application of different modified ligands, metal oxides and photosensibilizing components for the formation of materials with a high porous structure may lead to the creation of new materials suitable for the sorption-catalytic treatment of radioactive water solutions, containing organic impurities, in combination with other methods (e.g. reagent methods, magnetic separation etc.).

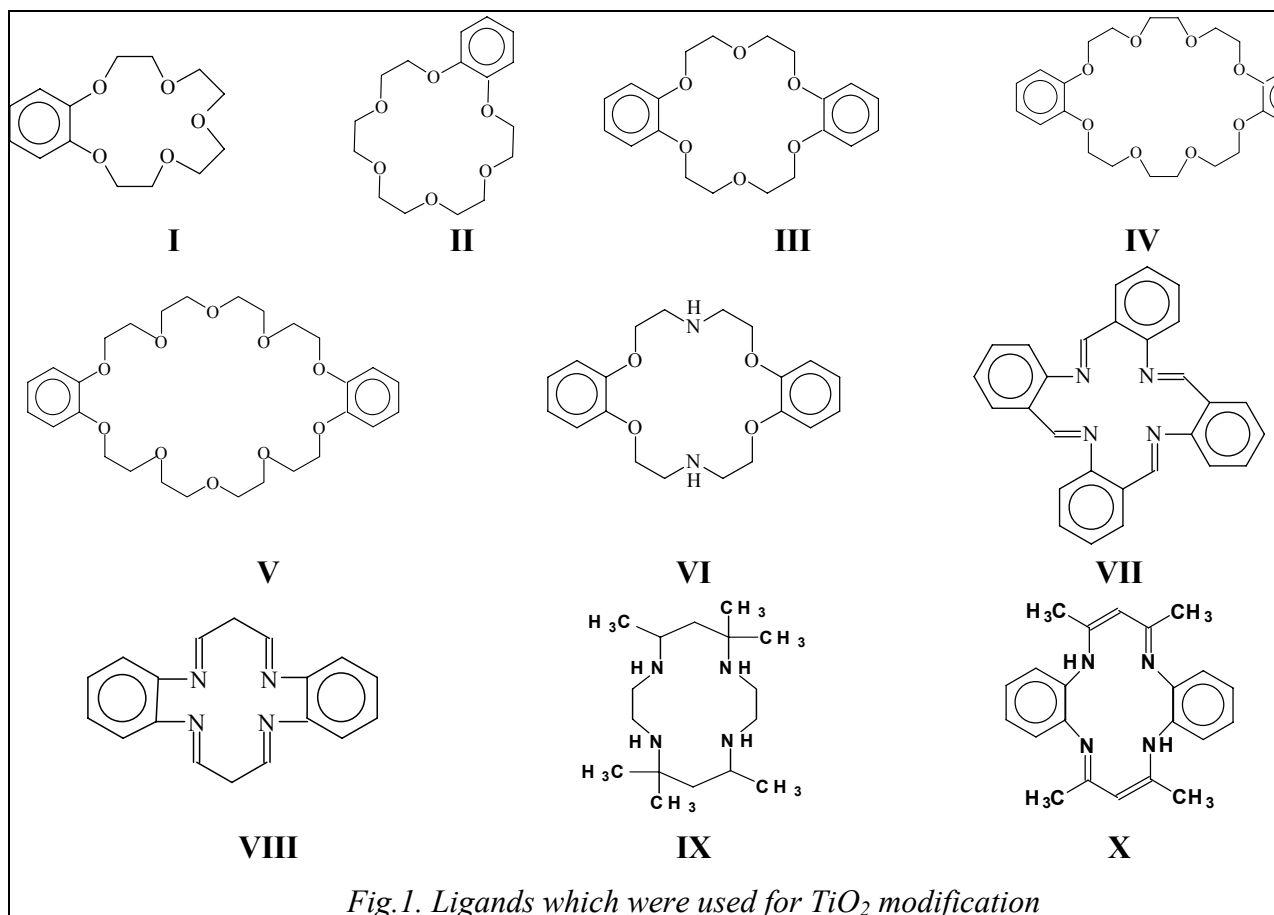
Studies in the following directions have been carried out:

- (a) Synthesis of new TiO_2 (L), TiO_2 / SiO_2 (L) materials (L=crown-ethers or macrocyclic ligands) by means of sol-gel synthesis, their characterization with regard to the sorption capacity towards Cs, Sr, Ru, Co, and Cr.
- (b) Synthesis of mesoporous TiO_2 , SiO_2 , $\text{TiO}_2/\text{SiO}_2$ materials by means of sol-gel template synthesis (as templates crown-ethers or macrocyclic ligands were used, which can form stacking-adducts), their regulated hydrophobization, and the investigation of sorption capacity towards organic impurities.
- (c) Synthesis of new TiO_2 (X), TiO_2 / SiO_2 (X) materials (X=transition metals oxides and their mixtures) by means of the sol-gel method and the investigation of their sorption-catalytic properties.
- (d) Synthesis of dispersed porous TiO_2 materials containing nanoparticles of semiconductors (oxides and sulfides of Zn, Cd, Pb) and also other TiO_2 materials and the investigation of their photocatalytic properties
- (e) Development and optimization of a combined technology for sorption-catalytic treatment (in combination with reagent and magnetic separation methods) of liquid radioactive waste, containing organic impurities.

2 PREPARATION OF MODIFIED TiO₂, SiO₂ AND TiO₂/SiO₂

Methods for the synthesis of the following new materials have been elaborated:

- Dispersed porous TiO₂, SiO₂ crown-ethers (*L* I-*L* VI in Fig. 1);
- Dispersed porous TiO₂ containing some tetraazamacrocyclic ligands (*L* VII-*L* X in Fig. 1);
- Dispersed porous SiO₂ with the large pore size (by means of template synthesis with DB18C6 (*L* III), DB24C8 (*L* IV), DB30C10 (*L* V) – Fig. 1;
- Dispersed porous TiO₂ containing 3d-metal (Fe, Mn, Cr, V, Mo) oxides including materials with the ophobized surface and semiconductors (oxides, sulphides of Zn, Cd, Pb);
- Dispersed porous TiO₂/SiO₂ materials.



Various methods have been used for obtaining materials on the basis of titanium oxide for the sorption-catalytic treatment of liquid radioactive waste containing organic impurities. The first group of methods was used for obtaining of TiO₂ (*L*) materials (types I and type II with some modifications).

2.1 MODIFIED POROUS TiO₂ (*L*, *L*=I-VI) MATERIALS

The common synthesis procedure for TiO₂ (*L*) was as follows: 20 mL of tetraisobutoxytitanium (Ti(*i*-buto)₄) with 20-40 mL of isopropanol solution of *L*, 2-6 mL of water and 2 mL of acidic catalyst were mixed, and studiously stirred during 10-20 minutes. After a day the gel precipitate obtained was separated by decantation and dried during 6 hours under vacuum at 75 °C in a special glass.

2.2 MODIFIED POROUS SiO₂ AND TiO₂ MATERIALS WITH THE LARGE PORE SIZE

The synthesised samples of TiO₂ and SiO₂ were used as reagents for new synthesis. The synthesis was stopped only after obtaining a negative result (spectrophotometric determination of crown-ether in UV-region) of crown-ether presence in alcohol after sample treatment. The samples were dried during 4 hours under vacuum at 75°C. By this way the samples of TiO₂ and SiO₂ (50 % of hydrophobization) were obtained.

These samples were also used for the surface regulated hydrophobization procedure. The surface hydrophobization procedure was carried out by treating of initial samples with toluene solution of hexamethyl disilozane, which form chemical bonds with surface atoms and as a result hydrophobize the surface of material. The sample of the of about 5 g was placed in the Erlenmeyer vessel and 30 mL of toluene solution of hexamethyl disilozane was added. The vessel was closed and shaking during 7 hours at 20°C and after this the sample was filtered and dried at a room temperature. In order to obtaine the different level of hydrophobization (50% and 100%) different quantities of hexamethyl disilozane were used, which were dissolved in toluene: 2,4 g (for 50 %) of hydrophobized surface and 4,5 g (for 100 %) of hydrophobized surface.

2.3 DISPERSED POROUS TiO₂ MATERIALS CONTAINING 3-d METALS

The porous dispersed TiO₂ containing 3-d metals was synthesised in the following way: to 20 mL of Ti(i-buto)₄ 20 mL of isopropanol, the needed quantity of the metal salt dissolved in 2-3 mL of distilled water, and 2 mL of acidic catalyst were added. The solution was studiously stirred during 5 minutes. After that the gel formed was washed in distilled water and dried during 6 hours under vacuum at 75°C.

2.4 DISPERSED POROUS TiO₂ MATERIALS CONTAINING 3d-METAL OXIDES

New TiO₂ materials containing d-metal oxides were synthesised by means of introduction of the metastable coordination compounds on the stage of the gel formation followed by thermal treatment (at 50-200°C). The ratio of metal/metal oxide was varied by using of inert atmosphere at temperature treatment procedure.

The general procedure was as follows: to 20 mL of Ti(i-buto)₄ 20 mL of isopropanol, 2-4 mL of coordination compound (0,1-1 g) solution in distilled water, and 2 mL of acidic catalyst were added. The solution was studiously stirred during 5 minutes. Then the gel formed was broken and washed in distilled water. After that during 1-2 hours it was heated at temperature, which was selected on the basis of the thermogravimetric data analysis. This procedure was carried out at both atmosphere and inert conditions. Then the gel obtained was washed in distilled water and dried during 6 hours under vacuum at 75 °C.

2.5 DISPERSED POROUS SiO₂ MATERIALS CONTAINING 3d-METAL OXIDES

The common synthesis procedure for SiO₂(M) materials was as follows: to acidic solution (in H₂SO₄) of chromium chloride, the solution of sodium silicate was added under permanent stirring up to receiving of pH6,5-7. The gel obtained was placed in a glass for crystallization and left for 24 hours. Then it was cutted in pieces of 0,5-1 cm, many times was washed in distilled water up to the negative reaction (with BaCl₂ solution). The washed gel was dried at 100-120°C during 12-24 hours.

2.6 DISPERSED POROUS TiO₂/SiO₂ MATERIALS

The common synthesis procedure for TiO₂/SiO₂ materials was as follows: to the mixture of Ti(i-buto)₄ and Si(Eto)₄ 20 mL of isopropanol were added. The solution was

studiously stirred during 5 minutes. After that 20 mL of $\text{Ti}(\text{i-buto})_4$ were mixed with 20 mL of isopropanol solution of B18C6 ($1,77 \cdot 10^{-5}$ M) and 2 mL of water and 2 mL of acidic catalyst, and studiously stirred during 15 minutes. After that 3,2 – 4 mL of 4 N HCl (pH was 2,5-4) were added and the solution was stirred. The gel formed was broken and washed in distilled water (up to negative probe on Cl⁻) and dried during 6 hours under vacuum at 75 °C in a special glass.

2.7 SOME CHEMICAL PECULIARITIES OF THE SYNTHESIZED MATERIALS AND THEIR TEXTURE CHARACTERISTICS

For some samples dynamic chemisorption was studied. It was found out that for all the samples containing crown ethers the chemisorption of Cs and Sr occurred during 30 minutes. The chemisorption of Co^{2+} , Cr^{2+} (inert atmosphere), Ru^{4+} occurred during 15, 20 minutes and two days, respectively. From these data the time for static chemisorption was determined.

The chemisorption of Sr was examined by mixing of 0,5 g of sorbent with 25 mL of the $\text{Sr}(\text{NO}_3)_2$ solution (80 mg/L) during 2 hours under stirring. Then the solutions after centrifugation and filtration were analyzed for the Sr concentration by the atomic-adsorption technique.

The chemisorption of Sr was also studied using a solution of ^{85}Sr (500 mL, pH 1,7 (HNO_3)); the activity of the solution was 132,5 Bq/mL. These results were in good accordance with data of atomic-adsorption determination.

3 STUDIES OF THE STRUCTURE, COMPOSITION AND REACTIVITY OF 3d-METALS COMPLEXES WITH THE HYPOPHOSPHITE ABILITY

In 3d-metals complexes an electroconduction process is provided by thermal excitation. As a result a metallic phase is formed. The mechanism of thermal decomposition of hypophosphites of nickel (II), cobalt (II), zinc (II) studied and also known data for hypophosphite of copper(II) [15-17] allow to conclude that a ligand will affect the concentration of active hypophosphite ions and the amount of free protons in the crystalline lattice. The change of the molecular design of co-ordination sphere of a metal and the change of the reaction conditions can influence the temperature of decomposition, speed of reaction, composition and properties of products of decomposition.

Hypophosphites of 3d-metals are obtained from the water solution containing a metal salt (or metals salts), sodium hypophosphite and glycerol. Recipency methods of obtaining of hypophosphite of copper [18] were used. 7-10 g of a metal salt (or metal salt mixture) were dissolved in 50 mL of water, then 7.3 mL of glycerol and 6.9 g of $\text{NaH}_2\text{PO}_2 \cdot \text{H}_2\text{O}$ were added under permanent stirring. Crystals of suitable hypophosphites fall out after keeping the solution during 2-7 days at 0-2°C.

Ammoniac complexes were obtained by dissolution of the obtained hypophosphites in surplus (8 to aliquot) of ammonia solution. For the sedimentation of these complexes acetone was used as a suitable precipitant.

A chemical analysis of the synthesized complexes was made for the metal [19] contents, hypophosphite - ion iodometrically [20], nitrogen and hydrogen (CHN-analyzer) and water crystallizing. The results of chemical analysis are given in Table I.

The IR-spectra of the complexes were made on IR-20 (Karl Zeiss Jena) spectrophotometer in pills from KBr. The IR-spectra of the ammoniac complexes contain all typical for the absorption stripe hypophosphite - ion, which well jump with calculated oscillation frequencies senses for model clean of hypophosphite with equated bonds P-O (C_{2v} symmetry) [21], and also stretching ($3600\text{-}3100\text{ cm}^{-1}$), deformational ($1630\text{-}1600\text{ cm}^{-1}$) and rocking ($980\text{-}960\text{ cm}^{-1}$) oscillations of NH_3 - group.

The thermogravimetric explorations were conducted on derivatograph Q-1500D. The substance was triturated in a mortar and admixed with Al_2O_3 , changing components ratio from 1:1 up to 1:9. The heating rate of sample was 0,6 and 2,5 K/min. The radiophase analysis was conducted on setting DRON-3M with copper K_{α} - radiance.

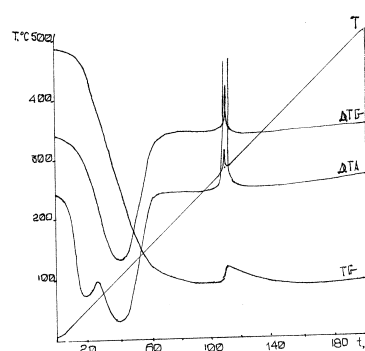
The thermogravimetric exploration of crystallohydrate of nickel hypophosphite has shown, that the reaction of a thermal decomposition starts with process of dehydration at the temperature of 70°C and descends to maximal speed at 110-120°C (Fig. 2a).

TABLE I. RESULTS OF THE ELEMENT ANALYSIS OF THE SYNTHESIZING COMPOUNDS

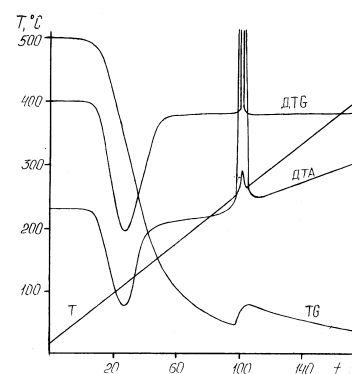
№	Compound	Mm	M		H		N		H_2PO_2^-		H_2O	
			obt	calc	obt	calc	obt	calc	obt	calc	obt	calc
1	$\text{Cu}(\text{H}_2\text{PO}_2)_2$	193.52	32.61	32.84	1.97	2.08			67.05	67.18	18.51	18.60
2	$\text{Ni}(\text{H}_2\text{PO}_2)_2 \cdot 6\text{H}_2\text{O}$	296.76	19.85	19.78	5.36	5.43			43.74	43.81	36.49	36.39
3	$\text{Co}(\text{H}_2\text{PO}_2)_2 \cdot 6\text{H}_2\text{O}$	297.00	20.01	19.84	5.32	5.43			43.56	43.77	36.45	36.36
4	$\text{Zn}(\text{H}_2\text{PO}_2)_2 \cdot 6\text{H}_2\text{O}$	303.46	21.66	21.548	5.36	5.31			42.69	42.84	35.41	35.59
5	$\text{NiCo}(\text{H}_2\text{PO}_2)_4 \cdot 12\text{H}_2\text{O}^*$	593.76	19.76**	19.81	5.38	5.43			43.67	43.79	36.49	36.38
6	$\text{CuCo}(\text{H}_2\text{PO}_2)_4 \cdot 8\text{H}_2\text{O}$	526.56	23.25**	23.26	4.69	4.59			49.58	49.38	27.15	27.35
7	$\text{CuNi}(\text{H}_2\text{PO}_2)_4 \cdot 8\text{H}_2\text{O}$	526.32	23.38**	23.23	4.74	4.60			49.61	49.40	27.19	27.36
8	$\text{CuZn}(\text{H}_2\text{PO}_2)_4 \cdot 8\text{H}_2\text{O}$	533.01	24.27**	24.19	4.32	4.54			48.59	48.78	27.17	27.02
9	$\text{Cu}(\text{NH}_3)_4(\text{H}_2\text{PO}_2)_2^*$	261.65	24.35	24.29	6.07	6.16	21.69	21.41	49.54	49.69		
10	$\text{Ni}(\text{NH}_3)_6(\text{H}_2\text{PO}_2)_2^*$	290.85	19.99	20.18	7.43	7.62	28.67	28.89	44.61	44.70		
11	$\text{Co}(\text{NH}_3)_6(\text{H}_2\text{PO}_2)_2^*$	291.09	20.16	20.25	7.52	7.62	28.77	28.87	44.69	44.66		
12	$\text{Zn}(\text{NH}_3)_4(\text{H}_2\text{PO}_2)_2$	263.49	24.69	24.82	6.05	6.12	21.05	21.26	49.21	49.34		
13	$\text{NiCo}(\text{NH}_3)_{12}(\text{H}_2\text{PO}_2)_4^*$	581.95	20.21**	20.39	7.79	7.62	28.92	28.88	44.43	44.68		
14	$\text{CuCo}(\text{NH}_3)_{10}(\text{H}_2\text{PO}_2)_4$	552.74	22.16**	22.13	7.05	6.93	25.52	25.34	47.20	47.04		
15	$\text{CuNi}(\text{NH}_3)_{10}(\text{H}_2\text{PO}_2)_4$	552.50	22.12**	22.06	7.01	6.93	25.47	25.35	47.15	47.06		
16	$\text{CuZn}(\text{NH}_3)_8(\text{H}_2\text{PO}_2)_4$	525.13	24.55**	24.77	6.08	6.14	21.29	21.34	49.70	49.51		

* First compounds synthesized

** Sum quantity



a



b

Fig. 2. Thermograms of nickel (a) and cobalt (b) hypophosphite crystallohydrates; shot 0,5 g + 0,5 g Al_2O_3 , $T=500$ oC, $v=2,5$ o/min, $TG=500$ μV , $DTA=100$ μV , $DTG=500$ μ .

The results show that 5 molecules of water are lost. The process of dehydration at 180-220°C is completed. The radiophase analysis of nickel hypophosphite after dehydration testifies that the process of loss of water by crystallohydrate is tracked by shattering of a crystal lattice (product becomes X-ray amorphous). Purely thermal decomposition of anhydrous hypophosphite is tracked by the strong exothermic effect that results in self-heating of the sample and rough excretion of light-end products of the reaction. Therefore, it is concluded that the temperatures of the start of dehydration process and of thermal decomposition depend on the mixture ratio and do not depend on the heating rate variations from 0,6 up to 2,5 K/min) (Table II).

The temperature of the beginning of nickel hypophosphite thermal decomposition is in the range of 210-270°C (depending on the amount of the substance). The previous partial dehydration of the complex (Table II) results in the essential decrease of temperature. The observable features of process are related to miscellaneous conditions owing to the variations of density of nickel hypophosphite in the sample.

TABLE II. TEMPERATURE CHARACTERISTICS OF THERMAL DECOMPOSITION REACTION OF NICKEL HYPOPHOSPHITE

№	Hypophosphite nickel content in mixture with Al ₂ O ₃ , mass %	Crystallisation water quantity, mole	Heat rate, °C/min	Temperature of the beginning of dehydration process, °C	Temperature of the beginning of thermal decomposition reaction, °C
1	50	6	0.6	70	270
2	50	6	2.5	70	270
3	25	6	0.6	60	240
4	10	6	2.5	50	230
5	50	2	0.6	50	220
6	50	1	0.6	40	210
7	50	0.5	0.6	30	210

During thermal decomposition there is a minor augmentation of a mass of the sample (Fig. 2), that is related to the oxydation of products of the decomposition by oxygen in the air. By using optical microscopy it was detected that the decomposition wears brightly expressed topochemical nature: appearance in a crystal of dark fields - nucleuses, which one then are spreaded to all crystal.

At the dissolution of a product of a thermolysis in water the unsolvable solid deposit is formed, X-ray phase assaying of it has shown which one formation of nickel, its oxide and phosphide. The obtained filter liquor gives highly acid a reaction and contains a phosphate - ion. In a IR-spectrum of a product of decomposition of hypophosphite the bands are not detected, which one answer characteristic oscillations of P-H bond in a hypophosphite - ion. Proceeding from obtained data and with allowance for items of information on decomposition of an hypophosphoric acid [22], the chemical reaction of a thermal decomposition of nickel hypophosphite can be given by the following equation:



The experimental data testify the possibility of using of nickel hypophosphite as an activator of the surface not only for conductors but also for dielectrics. As a result of the thermal decomposition nickel will be formed, which accelerates the chemical Ni reduction. The products of its thermolysis catalyze process of chemical plating of a surface of dielectric, and ensure the high adhesion of a plating to ceramics. The temperature of thermal decomposition of blended nickel - cobalt is peer 210°C, that is it is lower, than the

decomposition point of the clean nickel hypophosphites (240°C) and cobalt (270°C) hypophosphite.

Thus, the availability of two miscellaneous cations even with close radiuses ($r_{Ni^{2+}} = 0,82 \text{ \AA}$, $r_{Co^{2+}} = 0,78 \text{ \AA}$) in a cationic sublattice of a crystal results in reducing of to lowering of temperature of reaction of a thermal decomposition.

As a result of a thermolysis of heteronuclear nickel - cobalt hypophosphite the highly dispersive mixture of metals, their oxides and phosphides will be formed. Thus, the synthesis of such blended compounds allows not only to influence temperature of a thermolysis of hypophosphite, but also opens out possibility of using of such aspect of heteronuclear compounds for obtaining composites with interesting magnetic and mechanical characteristics.

At a thermal decomposition of ammoniac complexes of hypophosphites ammonia after cleavage of bond with an ion of metal bounds free positive protons, complicates their migration and due to this retards propagation of nucleuses of a metal phase. In result after providing of access of cation of metal to the fissile shape of a hypophosphite - ion the reaction is hereinafter inhibited at the expense of binding by molecules of ammonia of positive protons, which one are reclaimed after breaking-up of intermediate products of reaction. This process descends down to full removal of ammonia from volume of a crystal.

Thus, the obtained experimental data testify that the introduction in coordination sphere of metal of ammonia, which one is proton acceptor ligand, results in lowering of temperature of reaction of a thermal decomposition and variations of composition of reaction products.

The synthesis of heteronuclear hypophosphites of metals, and also mixed-ligand complexes on their base resolves to receive with usage of a reaction of a thermal decomposition of these compounds highly dispersive compositions, which one contain miscellaneous metals, their oxides and phosphides. The composition of these compositions can be varied in the broad boundaries by design of coordination sphere.

Proceeding from obtained results it is possible to consider that the synthesized and investigated coordination compounds of 3d-metals with hypophosphite can be utilised for TiO_2 , SiO_2 materials obtaining, which containie metal oxides. The indicated coordination compounds are soluble in organic solvents, first of all in alcohols, which is necessary for their application for pointd materials obtaining.

TABLE III. SAMPLES GIVING SURFACE AREA, PORE SIZE AND CHEMISORPTION PARAMETERS TOWARD Sr^{2+}

Sample TiO_2 (L)	S, m^2/g	V_s , cm^3/g	d, nm	L, maintainance, $\times 10^{-4}$, M	Statical chem. sorp.capacity towards. Sr^{2+} (mg/g)
L=DB24C8	510	0,34	2,8	0,17	2
L=DB24C8	507	0,33	2,7	1,7	18
L=DB24C8	505	0,32	2,6	3,8	41
L=DB24C8	501	0,31	2,5	6,27	59
L=DB24C8	496	0,30	2,4	8,93	81
L=DB24C8	492	0,29	2,3	9,8	86
L= DB24C8	488	0,27	2,2	43	88
L=DB30C10	530	0,35	2,9	1,75	20
L= DB30C10	527	0,34	2,8	3,75	42
L= DB30C10	525	0,33	2,7	5,21	55
L= DB30C10	521	0,32		8,57	72
L= DB30C10	516	0,31	2,5	17,5	90
L= DB30C10	507	0,29	2,4	43	92
L=DB-2aza- O_4	507	0,34	2,7	0,13	1

L=DB-2aza-O ₄	505	0,32	2,5	1,3	14
L=DB-2aza-O ₄	500	0,31	2,6	3,8	33
L=DB-2aza-O ₄	496	0,30	2,5	6,4	54
L=DB-2aza-O ₄	494	0,29	2,3	9,0	72
L=DB-2aza-O ₄	489	0,27	2,2	9,6	76
L=DB18C6	506	0,34	2,7	0,17	2
L=DB18C6	503	0,32	2,5	1,69	17
L=DB18C6	498	0,31	2,6	3,8	39
L=DB18C6	495	0,30	2,5	6,3	59
L=DB18C6	492	0,29	2,3	9,0	79
L=DB18C6	487	0,27	2,2	9,5	84
L=DB18C6	480	0,25	2,1	43	85
SiO ₂ (DB18C6)	100	1,42	57	3,07	27
SiO ₂ (DB18C6)	75	1,53	82	3,707	32,5

These data shows that samples of TiO₂, containing DB24C8 and DB18-2aza-O₄ crown ethers, have higher sorption capacity toward Sr comparing with corresponding analogous using SiO₂ materials and TiO₂ materials with DB18C6. This may be connected with higher quantity of modifying ligand in titanium oxide samples and higher ability of TiO₂ materials to nonselective uptaking of such metal ions as Sr²⁺ and also better correspondence of DB24C6 hole size for Sr²⁺. Chemisorption capacity of titanium oxide samples is greater despite of the porous texture characteristics for these samples comparing with corresponding SiO₂ samples are less favourable (see table 3). But it is important that the introduction of different crown ethers in the reaction mixture on the stage of TiO₂ gel formation leads to changes of received materials texture characteristics (see table 3).

On comparing of results obtained for samples 5, 6, 3 (table 3) shows that in fact the increase of pores sizes leads to increase of macrocyclic ligand maintainance in the received materials. But from comparing the data for these samples it is clear that ligand, for example DB24C8 concentration increasing is changed nonlinear with increasing of pores sizes. In our opinion it is connected with the saturation of TiO₂ matrix by DB24C8 and self-association of DB24C8 as also DB18C6. As result on the surface are present “active” and “non-active” crown-ether molecules. The maintainance of “active” DB18C6 was measured using statical chemisorption capacity toward Sr²⁺.

This phenomenon is very interesting from the point of view of receiving mesoporous dispersed porous materials of TiO₂ and attempts were made for synthesis of such materials. We tried to use the presence of sorptive “active” and “non-active” crown-ether molecules on the TiO₂ matrix surface, which are connected with self association of macrocyclic molecules (stacking-adducts formation), in order to receive principally new mesopores dispersed porous TiO₂ (as also SiO₂) materials.

Taking into account that crown ether should be kept away by heating of such samples in alcohol, the received porous materials may have mesopores of predetermined size. As a result of verification of synthetic procedure conditions, a few materials were obtained which are able to form the stable space-oriented stacking adducts in concentrations higher than 1·10⁻³ mol/L. As a result materials were obtained containing in their pores (channels) template space-ordered linkages of such stacking-adducts as shown in Fig. 3.

The peculiarity of structure of some titanogel (Fig. 3) according to X-ray phase analysis data, shows the presence of repetitiveness. Reflexes in the region of small angles support this. These structures look like corresponding structures, which appear in the presence of surfactants as templates during synthesis of mesoporous molecular sieves.

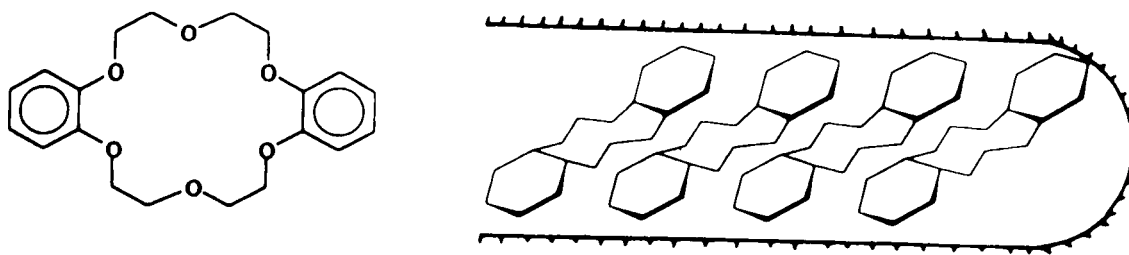


Fig. 3. Stacking adducts of DB18C6 as template for obtaining pores (channels) with determined size

The role of templates during titanium gel synthesis from $\text{Ti}(\text{i-Buto})_4$ may be the products of condensation, which are formed as a result of organic ether hydrolysis. The attempts of such meso structure stabilisation on the stage of titanogel synthesis (with surfactants as templates) were unsuccessful. After some time it destroyed completely and accompanied with anatase crystallisation. When crown ethers used as templates, the stable mesophases containing crown-ethers with $S=480\text{-}530 \text{ m}^2/\text{g}$ were obtained (Table IV). The characteristics of such materials is the combination of nanopericodic and anatase crystal structures (Fig.4) both in freshly precipitated samples and “old” samples even after 10 months. After evaluation of template, materials were obtained with $S=515\text{-}550 \text{ m}^2/\text{g}$ (Table V).

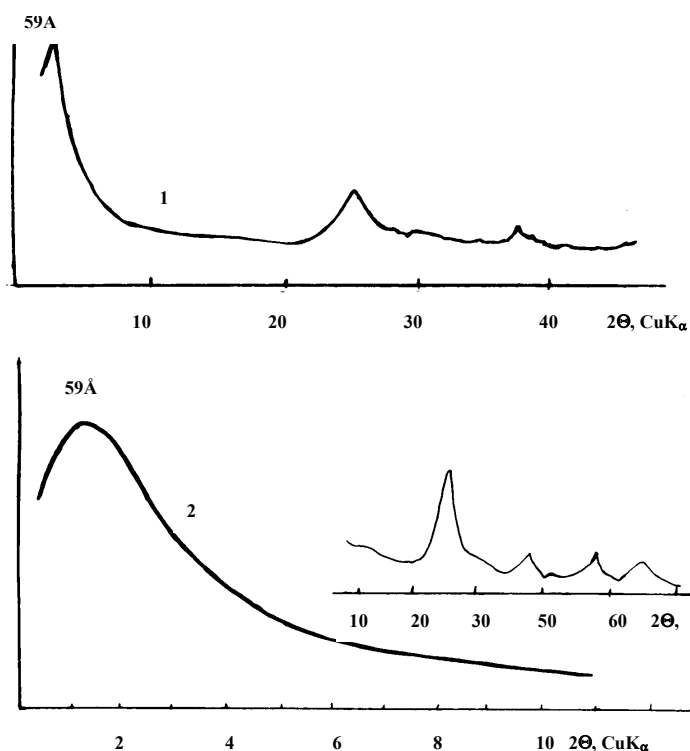


Fig. 4. Diffractograms of the initial (1) and stored during 10 months titanium gel, which was obtained by sol-gel template synthesis procedure (DB18C6 was used as template)

TABLE IV. PORES AND SURFACE CHARACTERISTICS AND STATICAL CHEMISORPTION CAPACITY OF TiO₂ SAMPLES WITH DB18C6, DB24C8, DB30C10

Sample TiO ₂ (L)/ SiO ₂	S, m ² /g	V _s , cm ³ /g	d, nm	L maintenance, x10 ⁻⁴ , M	Statical chemisorbtion capacity tow. Sr ²⁺ , mg/g
L=DB18C6	506	0,34	2,7	0,17	2
L=DB18C6	503	0,32	2,5	1,69	17
L=DB18C6	498	0,31	2,6	3,8	39
L=DB18C6	495	0,30	2,5	6,3	59
L=DB18C6	492	0,29	2,3	9,0	79
L=DB18C6	487	0,27	2,2	9,5	84
L=DB18C6	480	0,25	2,1	43	85
L=DB24C8	492	0,29	2,2	98	86
L= DB24C8	488	0,27	2,2	43	88
L=DB30C10	530	0,35	2,9	1,75	20
L= DB30C10	527	0,34	2,8	3,75	42
L= DB30C10	525	0,33	2,7	5,21	55
L= DB30C10	521	0,32	2,6	8,57	72
L= DB30C10	516	0,31	2,5	17,5	90
L= DB30C10	507	0,29	2,4	43	92

After the next treatment of such materials by ethanol under heating such templates viz;crown ethers stacking adducts, were removed and mesoporous dispersed materials with regulated pores diameter were obtained both for TiO₂ and for SiO₂. Pores and surface characteristics for these samples for TiO₂ were determined (Table V).

TABLE V. PORES AND SURFACE CHARACTERISTICS FOR TiO₂ SAMPLES OBTAINED BY TEMPLATE SYNTHESIS (CROWN ETHERS STACKING ADDUCTS AS TEMPLATES) WITH THE NEXT EVALUATION OF TEMPLATE WITH ORGANIC SOLVENT UNDER HEATING

Sample*	N of initial sample (and template maintenance, x10 ⁴ , M	S, medium/g	V _s , cm ³ /g	d, nm
TiO ₂ (DB30C10)	5.5.5 (17.5)	551	0,52	3,2
TiO ₂ (DB30C10)	5.5.6 (43)	559	0,54	3,4
TiO ₂ (DB18C6)	30.1 (43)	515	0,39	2,8
TiO ₂ (DB24C8)	31.1 (43)	535	0,42	3,0

* Here are pointed ligands, which were used for obtaining of initial samples.

Such mesoporous materials have good texture parameters. The quality of such materials may be regulated by means of varying the conditions of obtaining all the ratios of water/organic solvent and also considering the nature of the organic solvent. It's also interesting to use some coordination compounds, which have big size and also are capable for intermolecular stacking adduct formation , have low sublimation temperatures for such mesoporous materials with pore size greater than 3 nm. Such mesoporous materials were then partially treated with hexametyldisilozane, which form chemical bonds with the surface atoms and result in hydrophobization of the surface. This allowed to obtaine dispersed porous SiO₂ and TiO₂ samples with different degree of hydrophobicity. These may have high affinity to many of organic molecules (substrates), which are present in water, and may be selectivity toward such substrates. The presence of metal oxides in such materials also provide high sorption catalytic properties.

From these first results it was clear that pore diameter may be regulated by corresponding ligand. It is also interesting to use some co-ordination compounds, which have

big size and also are able for intermolecular stacking adduct formation and have low sublimation temperatures especially for mesoporous materials with pore size greater than 3 nm. These samples appeared effective sorbents for cesium and strontium ions (Table III.)

The data listed in Table III, samples containing teraazamacrocycles (VI, VII, Fig.1) are good sorbents for Co, Cr and Ru. The best among them are samples, which contains a greater amount of TAAB. It is interesting that sorption ability of Co, Cr and Ru does not relate linearly with the amount of TAAB in the samples. It is interesting (Table VI) that crown-ether (DB18-2aza-O₄) is good sorbent not only for Sr and Cs but also for cobalt.

The samples 12, 13 have good chemisorption characteristics (even higher than TiO₂ samples with DB18C6 and for corresponding SiO₂ materials) for Co, Cr, Ru decontamination. The selectivity of decontamination is quite high which is regulated by different pH values under which chemisorption was carried out.

TABLE VI. SURFACE AREA, PORE SIZE AND CHEMISORPTION PARAMETERS TOWARDS Co²⁺, Ru⁴⁺

Sample TiO ₂ (L)	S, m ² /g	V _s , cm ³ /g	d, nm	L maintainance, x10 ⁻⁴ , M	Statical chemisorption capacity tow. M, mg/g	
					Co ²⁺	Ru ⁴⁺
L=TAAB	530	0,37	3,0	0,13	1	1,9
L=TAAB	526	0,35	2,9	1,35	8,2	14,6
L=TAAB	514	0,34	2,8	4,02	24,2	42,2
L=TAAB	510	0,33	2,7	6,65	42	68,1
L=TAAB	506	0,32	2,6	7,51	45	75,2
L=TAAB	499	0,31	2,5	9,4	55	91,1
L=DB-2aza-O ₄	507	0,34	2,7	0,13	0,6	*
L=DB-2aza-O ₄	505	0,32	2,5	1,3	5,2	
L=DB-2aza-O ₄	500	0,31	2,6	3,8	20,1	
L=DB-2aza-O ₄	496	0,30	2,5	6,4	38,4	
L=DB-2aza-O ₄	494	0,29	2,3	9,0	49,7	
L=DB-2aza-O ₄	489	0,27	2,2	9,6	52,1	

* Not determined yet

Adsorption characteristics for TiO₂ dispersed porous materials containing metal oxides, some of which are listed in Table VII. It is quite surprising that these characteristics are quite close in their characterisation for corresponding samples before hydrophobisation.

TABLE VII. ADSORPTION CHARACTERISTICS FOR TiO₂ SAMPLES, CONTAINING 3d-METAL OXIDES WITH HYDROPHOBIZED SURFACE

Sample	Metal oxide content, mass %	S, m ² /g	Pores volume, cm ³ /g
Ti/Cr	30	365	0,19
Ti/Fe	20	459	0,35
Ti/Mn	20	481	0,38
Ti/(Fe+Mn)	16+16	471	0,45

The substitutal differences in characteristics of samples with different proportions of Vanadium and molybdenum oxides (Table VIII) points to the different structure of these oxides, which were formed in TiO₂ matrix pores. This is supported by IR-spectroscopy data.

TABLE VIII. ADSORPTION CHARACTERISTICS FOR TiO₂ SAMPLES, CONTAINING METAL OXIDES WITH HYDROPHOBISIZED AND NON-HYDROPHOBISIZED SURFACE

Sample	Metal oxide* content, %	S, m ² /g	V _s , cm ³ /g	d, nm
TiO ₂ (V)	2	434	0,30	2,8
TiO ₂ (V)	10	421	0,28	3,3
TiO ₂ (V)	15	403	0,24	3,5
TiO ₂ (V)	20	387	0,19	3,8
TiO ₂ (V)	25	394	0,21	4,1
TiO ₂ (Mo)	2	505	0,37	4,4
TiO ₂ (Mo)	10	495	0,33	3,9
TiO ₂ (Mo)	15	489	0,30	3,6
TiO ₂ (Mo)	20	476	0,27	3,3
TiO ₂ (Mo)	25	381	0,18	3,0
TiO ₂ (V+ Mo)	2 (1+1)	475	0,25	3,4
TiO ₂ (V+ Mo)	10(5+5)	460	0,24	3,7
TiO ₂ (V+ Mo)	15 (7,5+7,5)	445	0,23	3,8
TiO ₂ (V+ Mo)	20 (10+10)	420	0,22	4,0
TiO ₂ (V+ Mo)	25 (12,5+12,5)	390	0,20	4,2

* V₂O₅ or MoO₃, or V₂O₅ + MoO₃

There were synthesised titanium gel containing different quantities of metal oxides of different nature. X-ray phase analyses data shows (Fig. 5), that freshly precipitated samples containing 2 mol % of Cr₂O₃ and MnO₂ are practically amorphous. For the stability of sorbents containing V₂O₅ or Cr₂O₃ there are the peaks supporting the beginning of anathase crystallization (the intersquare distances d of the main anathase peaks are 3,52, 2,37, 1,88, 1,70 Å). The mainly strong reflexes, which may be attributed to anathase crystallization, are present in the case of MoO₃ containing sample.

It is well known that TiO₂ has great ability toward crystalliation, and even in respectively soft conditions of synthesis titanium gel contain quite high (20 % and more) quantities of anathase. Such high ability of TiO₂ toward crystallisation limits the possibilities for verification of titanium gel adsorption structure characteristics and also for the possibilities of binary (multicomponent) systems containing TiO₂ with wide diapazone of properties. In such cases influence of small quantities of chromium and manganese oxides have protecting influence on anathase crystallisation viz; theses inhibit anathase crystallization.

Such mesoporous materials and corresponding samples of titanium gel containing V₂O₅ and MoO₃ and also SiO₂/TiO₂ materials were portionally treated with hexametyldisilozane which form chemical bonds with surface atoms and thus hydrophobize the surface. This way one can obtain dispersed porous TiO₂ and SiO₂/TiO₂ and TiO₂ (MO_x) materials, which may have high affinity to many of the organic molecules (substrates), that are present in the water and may be selectivity toward such substrates. The presence of metal oxides in these materials can also provide high sorption catalytic properties.

4 CATALYTIC PROPERTIES OF SiO₂, TiO₂, SiO₂/TiO₂ MATERIALS IN OXIDATION PROCESSES OF ORGANIC SUBSTRATES

Over the years, many type of catalysts have been synthesized. These are SiO₂ (M_nO_m), TiO₂, SiO₂/TiO₂ synthetic zeolites etc. The important features of these catalysts are:

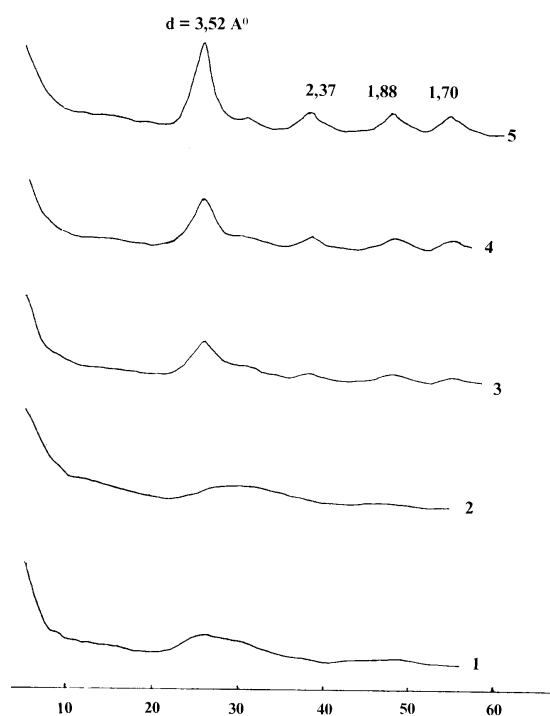


Fig. 5. Diffractogrammes of titania gels containing 2 mass % of metal oxide: 1- Cr_2O_3 , 2- MnO_2 , 3- V_2O_5 , 4- Fe_2O_3 , 5 - MoO_3 .

- (a) They are active in a variety of oxidative destruction processes with hydrogen peroxide such as hydroxylation of phenol to a mixture of hydroquinone and catechol, the oxidation of ethylene to ethylene oxide, the hydroxylation of alkanes and the ammonoxidation of cyclohexanone.
- (b) There is little non-productive hydrogen peroxide decomposition.
- (c) The catalyst is stable under reaction conditions and easy to recycle.

Unfortunately, the synthesis of the zeolite catalysts is quite difficult, requiring specialized expertise, equipment and use of proprietary knowledge. Also, the small pores of the zeolite limit access of the catalytic site by large organic substrates.

The introduction of oxygen containing functional groups in alkanes proceeds with low selectivities over most homogeneous and heterogeneous catalysts. The catalysts used in alkane oxidation are ineffective for alkanes [27, 28]. Many transition metal complexes on the other hand, are very effective in C-C bond cleavage leading to complete oxidation to respective acids. Oxyfunctionalization with high selectivities was reported from natural and synthetic metalloporphyrin systems [29, 30]. The use of zeolite and molecular sieve based catalysts in oxidation reactions is assuming a lot of importance in recent times. Titanium silicates exhibiting a pentasil structure (both TS-1 and TS-2), particularly, have been found to catalyse the oxidation of a variety of organic substrates with an aqueous solution of H_2O_2 and are found to be very selective in the oxidation of alkanes [31-33].

Vanadium silicate molecular sieves with vanadium in framework positions have also been synthesized [34]. These are found to be active in the hydroxylation (benzene to phenol, phenol to hydroquinone and catechol) and simultaneous oxidation and hydroxylation viz; toluene to benzyl alcohol, benzaldehyde and cresols aniline to nitrobenzene, azoxybenzene and hydroxy aniline reactions [34]. It was found that the addition of water to the initial solution results in decreasing of both the specific surface area and pore volume.

The disadvantage of hydrothermal synthesis of SiO₂/TiO₂ materials (Si:Ti=5:1), using different amines as templates takes long time (2-30 days) and over narrow pH intervals (10,2±0,2) [25] and also with small pores diameter (about 8 Å).

The disadvantage of SiO₂/TiO₂ materials (Si:Ti=30:1) with the sol-gel method (Ti and Si alkoxides sol-gel with cogel formation) [26] followed by impregnation of dried cogel samples with tetrapropylammonium hydroxide and calcination is that only about 3% of titanium is introduced into the matrix. But such procedure permits to obtain titanium silicalite-which is a molecular sieve with MFI structure and has Ti atoms inserted in the framework [26].

A new layered hydrous titanium dioxide H_xTi_{2-x/4}O₄H₂O, was prepared [35] by calcining a mixture of TiO₂ and CsCO₃ at 1073 K for 20 hours obtaining of Cs_xTi_{2-x/4}. Decontamination capacity of this material toward Cs was only 20 mg/g.

Silica pillaring procedure for the preparation of silica-pillared layered tetratitanate by a novel pillaring procedure [36] were also synthesized. It entails first intercalating layered tetratitanate with n-hexylamine and then treating the n-hexylamine-intercalated tetratitanate with an aqueous solution of NH₂(CH₂)₃Si(OEt)₃, and finally calcining the solid product in air to remove the interlayer organics. The resultant silica-pillared layered tetratitanate is porous, and has a high surface area of 184,5 mg/g and shows thermal stability at temperatures >550⁰C.

Calcination in air leads to the decomposition of interlayer organics, and silica-like clusters are formed in situ within the layers which act as pillars to prop up the tetratitanate layers, eg, a silica-pillared layered tetratitanate is obtained. This has an interlayer distance of 13,4 Å (2Θ=6,6⁰) and retains thermal stability to >550⁰C. The interlayer spacing of 13,4 Å collapses upon heating to 650⁰C. Elemental analysis results show that the SiO₂ content in this silica-pillared material is 87,2 wt % [36]. The pore-size distribution analysis results show that both micro- and meso-pores are present, with an average pore diameter of 30,8 Å. n-Hexylamine intercalated tetratitanate decompose at the same outgassing conditions (350⁰C, 0,26 Pa, 4 h). The surface area of the starting material (K₂Ti₄O₉) is very low (3,3 m²/g). By comparison, the silica-pillared layered tetratitanate has a much higher surface area of 184,5 m²/g, indicative of an appreciable intracrystal surface area suitable for molecular adsorption and shape-selective catalysis [36].

The most interesting is oxidantive destruction by hydrogen peroxide, which can handle enormous amounts of waste such as commonly used oxidants dichromate, permanganate or manganese dioxide. H₂O₂ owing to its availability, low cost and environmentally safe by products (H₂O and O₂) is the oxidant of choice. Among of the most important tasks is the catalytic activation of H₂O₂. Such materials are of great interest.

In order to get the desirable properties of catalyst it should have large pores of up to 100 Å by a simple synthetic procedure. Amorphous metallosilicalite xerogels MO_x-SiO₂, (Ti^{IV}, V^V Mo^{VI}, W^{VI} and Se^{IV}) synthesized by the sol-gel method [37] were used as catalysts in the oxidation with hydrogen peroxide [24]. Silicalite xerogels are easily synthesized by the acid- or base-catalysed combined hydrolysis, and condensation reaction of silicon tetraalkoxides.



In order to prepare the required metallosilicalites [31], mixtures of silicon and metal alkoxides are used. The typical procedure for the preparation of the MO_x-SiO₂ xerogels is as follows. Silicon tetraethoxide (57 mmol) was dissolved in absolute ethanol (17 mL) and water (114 mmol) added as a 0.15 mol/L HCl solution. The solution was heated to 60⁰C for 1.5 h and then cooled to room temperature followed by addition with stirring of 3 mmol of the metal isopropoxide or ethoxide. The mixture formed a gel almost immediately and was then

left in an open beaker allowing slow evaporation of the solvent; within 12-24 hrs, a brittle 5% $\text{MO}_x\text{-SiO}_2$ xerogel was formed.

In the presence of hydrogen peroxide the metal oxides under consideration are known to form inorganic peracids which may oxidize organic substrates by a heterolytic or homolytic mechanism [38].

As it was shown in Ref. [38], H_2O_2 reacts with rutile TiO_2 powder forming not only surface O_2^- anions but also two newly identified surface $\text{S}=1$ triplet radical anion pairs composed of two interacting $\text{O}^-\cdots\text{O}^-$ centres, which are very important for oxidative and catalytic properties of TiO_2 containing materials.

5 CATALYTIC ACTIVITY OF THE SORBENTS FOR SIMULATED WASTE

Simple model compounds including alkenes, alcohols and phenol were reacted to test the catalytic activity of the metallocitanate gels. In a typical reaction, substrate (1.0 mmol) and 30% hydrogen peroxide (1.0 mmol) were reacted in ButOH (0.5 mL) in the presence of 5% $\text{MO}_x\text{-TiO}_2$ (5 mg) at 60 °C in a sealed 3 mL vial. The results of some reactions are summarized in Table IX. The specific substrates were chosen to represent various possible oxidation reactions. Thus, for alkenes, one may distinguish between epoxidation, allylic oxidation and carbon-carbon bond cleavage reaction pathways. Although reaction conditions were not optimized the results show interesting trends. Thus, the $\text{TiO}_2\text{-SiO}_2$ compound (Table IX) is the poorest catalyst having almost no activity for epoxidation of cyclooctene and hydroxylation of phenol, and only slight activity for carbon-carbon bond cleavage in styrene, allylic oxidation in cyclohexene and oxidation of 1-phenylethanol to acetophenone. Samples of $\text{SiO}_2/\text{TiO}_2$ materials with different texture parameters are listed in Table X.

$\text{V}_2\text{O}_5\text{-TiO}_2$, $\text{MoO}_3\text{-TiO}_2$ gels (Table IX, XI) are the preferred catalysts, all three having high catalytic activity, in general $\text{V}_2\text{O}_5\text{-TiO}_2 > \text{MoO}_3\text{-TiO}_2$. Activated alkenes such as cyclooctene are efficiently epoxidised to cyclooctene oxide. Cyclohexene are very susceptible to allylic oxidation and yielded mostly cyclohexen-2-ol and cyclohexen-2-one in *ca.* 1:1 ratio. The more nucleophilic styrene shows high activity for carbon-carbon bond cleavage, with formation of both benzaldehyde as primary product and benzoic acid. No styrene oxide was observed. 1-Phenylethanol is efficiently oxidised to acetophenone. Phenol was hydroxylated to a significant extent only with $\text{V}_2\text{O}_5\text{-TiO}_2$ as catalyst. Surprisingly, only hydroquinone and catechol were formed with no formation of benzoquinone or tars.

Several preliminary experiments were conducted to test the integrity of the heterogeneous catalyst, the effect of different solvents on the reaction and the yield based on hydrogen peroxide. First, it was demonstrated that we have a truly heterogeneous catalyst, *i.e.* the metal oxides are not leached into solution. A reaction mixture as described above without the organic substrate was stirred and heated at 60°C for two hours and then filtered. Cyclooctene was added to the filtrate and the mixture heated overnight. No cyclooctene oxide was observed by the gas liquid chromatography analysis. On the other hand, the filtered catalyst in a new reaction mixture showed the usual activity. Other solvents could be used in the catalytic oxidation. Thus, methanol gave somewhat inferior results, whereas acetonitrile was generally as effective as ButOH. Acetonitrile, however, caused considerable leaching of V_2O_5 , MoO_3 so that in this solvent the catalyst is not heterogeneous but is composed of soluble metal oxides [37, 38]. Finally, the decomposition of hydrogen peroxide was investigated in the presence of cyclooctene as substrate by the iodide-thiosulfate titration method. After 18 h 15%, 25% and 35% of the original hydrogen peroxide had been used for $\text{TiO}_2\text{-SiO}_2$, $\text{V}_2\text{O}_5\text{-TiO}_2$, $\text{MoO}_3\text{-TiO}_2$ gels, respectively, indicating relatively slow non-productive dioxygen formation and fair utilisation of hydrogen peroxide.

TABLE IX. OXIDATION OF ALKENES CATALYZED BY METALLOTITANATE XEROGELS^A

Substrate	Product ^c	SiO ₂ -TiO ₂ ^b (12.2)		TiO ₂ -V ₂ O ₅ ^f (11.7.3, 11.5.5)		TiO ₂ -MoO ₃ ^k (11.6.4)	
		Yield ^d	Turnover ^c	Yield ^d	Turnover ^c	Yield ^d	Turnover ^c
Cyclooctene	Cyclooctene oxide	Trace	-	88.57	291	18.9	109
Styrene	Benzaldehyde	3.6	12	21.15	143	19.3	222
	Benzoic acid	-	-	12.1	117	2.2	35
Cyclohexene	Cyclohexene oxide	Trace	-	1.6	5	Trace	—
	Cyclohexen-2-ol	0.2	0.6	23.3	78	2.9	18
	Cyclohexen-2-one	0.5	1.5	11.5.0	87	3.3.3	25
Phenol	Hydroquinone	-	-	11.4.4	52	<1	—
	Catechol	-	-	7.9	27	<1	—
1-Phenylethanol	Acetophenone	2.4	8	89.8	299	16.9	96

^a Reaction conditions: 1 mmol substrate, 1 mmol 30% hydrogen peroxide, 5 mg catalyst, 1 ml ButOH; 60 °C, 20 h.

^b Ratio TiO₂: substrate 1:320.

^c The reaction mixture was analyzed by GLC with reference standards using an SPB-5 25 m 0.25 u capillary column. All possible products except adipic acid (in the cyclohexene oxidation; not found) can be analysed by this method. The absence of adipic acid was confirmed by methylation of the reaction mixture with diazomethane and analysis of the resulting dimethyl adipate by GLC.

^d (mol product/mol substrate) x 100. ^e mol H₂O₂ required/mol catalyst. ^f Ratio V₂O₅ : substrate 1:330.

^g Ratio MoO₃: substrate 1:572.

TABLE X. THE ADSORPTION-STRUCTURAL CHARACTERISTICS* OF THE SYNTHESISED SAMPLES

Sample	S, m ² /g	V _s , cm ³ /g	d, nm
TiO ₂ / SiO ₂ (85 % / 15 %) ^x	461	0.20	1.7
TiO ₂ / SiO ₂ (85 % / 15 %) ^{xx}	476	0.23	1.9
TiO ₂ / SiO ₂ (72 % / 28 %) ^x	397	0.17	1.7
TiO ₂ / SiO ₂ (72 % / 28 %) ^{xx}	437	0.19	1.7

* Samples were dried at 30 °C (^x) and 90 °C (^{xx})

Vanadium titanate can oxidize unactivated alkanes under mild conditions with aqueous hydrogen peroxide. Unlike titanium silicates, vanadium analogues are able to oxidize the primary carbon atoms of alkanes to corresponding alcohols and aldehydes.

The catalytic reactions were carried out in a stirred autoclave of 300 mL capacity at a temperature of 373 K under autogeneous pressure. Typically 0.1 g of the catalyst (sample 11.5.5, which contains 25 % of V₂O₅), 2.53 g of 26% aqueous H₂O₂; (alkane-H₂O₂ = 3 moles) and 5 g of alkane were mixed in 25 mL of acetonitrile (solvent) and the reaction was carried out for 8 h. After the completion of the reaction, 25 mL of acetone was added to the products. The products were then separated from the catalyst and analyzed by gas chromatography using a capillary (crosslinked methylsilicone gum) column and flame ionization detector.

The results of the oxidation of linear saturated hydrocarbons, viz., n-hexane, n-heptane, and n-octane and cyclohexane are summarised in Table VIII. The major products of the reaction are corresponding alcohols, aldehydes and ketones. Small quantities of other products with more than one functional group (elaboratg. Dihydroxyalkanes) and lactones were also detected. In addition, a higher aldehyde and ketones to alcohol ratio in the product distribution (Table IX) indicates a greater oxidation ability of vanadium titanates compared to titanium silicates in this reaction.

The oxidation turnover (Table VIII) of n-hexane and n-heptane is found to be over 1000 and that of n-octane and cyclohexane is only marginally lower. On titanium silicates, similar activity and slightly higher H₂O₂ selectivity have been reported [32, 33].

Investigation of the extent of oxidation with time revealed that the ratio of aldehyde (ketones) to alcohol increased with time. This suggests that the aldehydes and ketones are secondary products from respective primary and secondary alcohols. After 8 h. the product distribution levelled off to the values given in Table XII.

A test reaction with silicalite-2 or vanadium impregnated silicalite-2 as catalysts resulted in 3 to 4% n-hexane conversion with less than 2% selectivity to desired products.

TABLE XII. THE PRODUCTS OF OXIDATION OF TOLUENE OVER VANADIUM TITANATE CATALYST (25 % V₂O₅)^A

Benzyl alcohol	Benz-aldehyde	Obtain Cresol	π Cresol	Others	Conversion (wt.%)	H ₂ O ₂ ^b selectivity
7.7	52.2	19.7	17.1	3.7	11.7	49.5

^a Reaction conditions: catalyst=0.1 g; toluene =1 g; t=353 K; alkane:H₂O₂ (mole ratio)=3; solvent=acetonitrile; reaction duration=12 h.

^b H₂O₂ utilized in the formation of benzyl alcohol, benzaldehyde and cresol

TABLE XI. OXIDATION OF ALKANES OVER VANADIUM TITANATE CATALYST (25 % V₂O₅)^a

Substrate	Turnover ^b	H ₂ O ₂ selectivity ^c	Product distribution (wt.%) ^d									Product selectivity ^f
			1-ol	2-ol	3-ol	4-ol	1-al	2-one	3-one	4-one	Others ^e	
n-Hexane	1198	57.1	3.8	9.3	8.1	-	7.1	11.5.5	24.8	-	21.4	79.5
n-Heptane	1030	50.1	3.0	6.8	5.8	2.1	3.3.2	25.1	21.7	7.0	24.2	75.8
n-Octane	821	43.4	3.3.8	5.7	3.3.7	3.7	3.3	21.8	17.8	7.7.6	24.2	75.6
Cyclohexane	706	8.8.7			33.3 ^g				60.7 ^h		6.0	94.0

(a) Reaction conditions: catalyst=0.1 g (Ti:V=78); alkane=5 g; t=373 K; alkane:H₂O₂ (mole ratio)=3; solvent=acetonitrile; reaction duration=8 h.

(b) Moles of alkane converted per mole of vanadium.

(c) H₂O₂ utilized for monofunctional product formation.

(d) 1-ol=alcoh-1-ol; 2-ol=alcoh-2-ol; 3-ol=alcoh-3-ol; 4-ol=alcoh-4-ol; 1-al=1-aldehyde; 2-one=ket-2-one; 3-one=ket-3-one and 4-one=ket-4-one of corresponding alkanes.

(e) Mostly oxygenates with more than one functional group and lactones.

(f) (Alcohols, aldehyde and ketones/alkane reacted)x100/

(g) Cyclohexanol.

(h) Cyclohexanone

The studies of the combined technology for the treatment of liquid radioactive waste containing organic impurities, and its optimization gives the possibility to propose few

schemes for the removal of radionuclides and organic impurities from this waste. Such scheme includes some main stages indicated in Fig. 5.

The low level liquid radioactive waste containing Cs, Sr, Ru, Co, Cr, and organic impurities will be treated with non-expensive ferrous chloride and sodium hydroxide. As a result colloid particles of ferrous hydroxide with high surface area and sorption ability will form. The reaction mixture - can then be made to react with these ferrous hydroxide, after intensive agitation and can be separated by magnetic filtration. The particles of colloidal $\text{Fe}(\text{OH})_3$, will provide strong interaction throughout the solution a good sorbent for radionuclides. The precipitate, which is formed, after filtration and separation will be immobilized.

The liquid waste, which contains small amounts of radionuclides and organic impurities, after such a treatment will be sorbed on ($\text{TiO}_2(\text{L})$, $\text{SiO}_2(\text{L})$). After sorption oxidative decomposition with hydrogen peroxide will be attempted. After evaluation of oxidation products new mesoporous TiO_2 materials will be used for decontamination of organic impurities. After this the leaching of sorbents will be carried out. This scheme was tested on the pilot scale and provided good results.

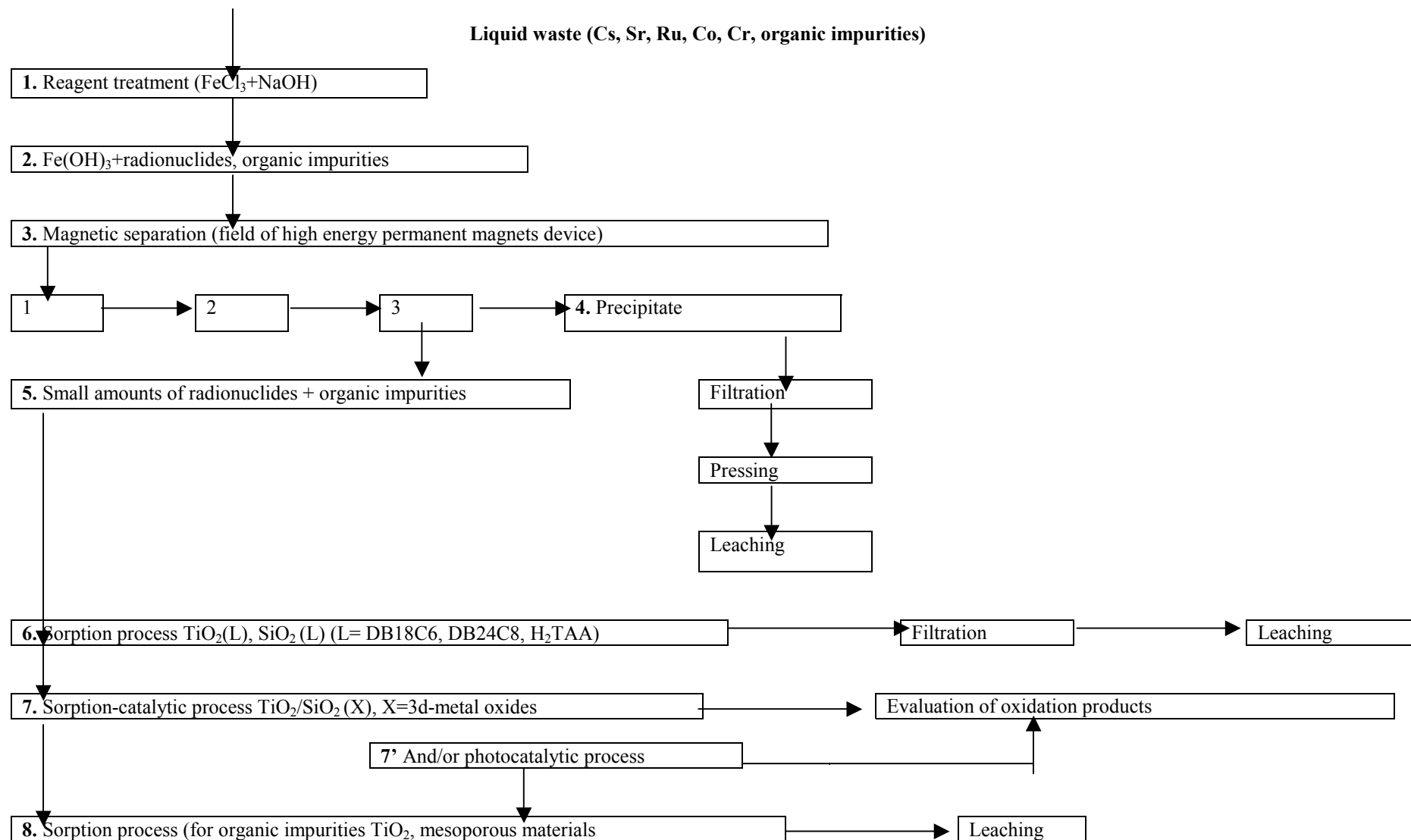


FIG. 5. Scheme of removal of radionuclides and organic impurities on the finish stages of liquid wastes treatment

REFERENCES

- [1] HUMS ERICH; SIEMENS AG.- No P3701984.8; Prioritet 23.01-87; Publ. 04.08.88.
- [2] MATSUDA, S., KATO, A. , Appl.Catal., 1983, **8**, 149.
- [3] HADJIVANOV, K.I., KISSURSKI, D.G., Chem.Soc.Rev., 1996, **25**, 61.
- [4] MEHROTRA, R.C., SINGH A., Chem. Soc.Rev., 1996, **25**, 1.
- [5] HOU W., YAU Q., FU X., J.Chem.Soc., Chem.Comm., 1994, **4**, 1371.
- [6] WANG F.-L., YU, L.LEE.M.S, J.Chem.Soc., Chem.Comm., 1994, **7**, 811.
- [7] ZANG L., C.- LIUY., X.-, REN M., J.Chem.Soc., Chem.Comm., 1994, **16**, 1865.
- [8] HADFELDT, A., GRÄTZEL, M., Chem.Rev., 1995, **95**, 49.
- [9] SASAKI T., Y., KOMATSU..FUJIKI Y, J.Chem.Soc., Chem.Comm., 1994, **12**, 817.
- [10] SATO S., OSIMATSU S., TAKAHASHI R. ET AL, J.Chem.Soc., Chem.Comm., 1997, **21**, 2219.
- [11] LU G., GAO H., SUO J., LI S., J.Chem.Soc., Chem.Comm., 1994, **21**, 2423.
- [12] MILLS A., WORSLEY D., DAVIES R.H., J.Chem.Soc., Chem.Comm., 1994, **23**, 2677.
- [13] HOFFMANN M.R., MARTIN S.T., CHOI W., BEHNEMANN D.W., Chem.Rev., 1995, **95**, 69.
- [14] DILLYRT R., BAHNEMANN D., EPA Newsletter, 1994, **52**, 33.
- [15] В.В.СВИРИДОВ, Т.Н.ВОРОБЬЕВА, Т.В.ГАЕВСКАЯ, Л.И.СТЕПАНОВА, Химическое осаждение металлов из водных растворов, Минск: Университетское, 1987, 270 с.
- [16] ЛОМОВСКИЙ О.И., МИХАЙЛОВ Ю.И., БРОСАЛИН А.В. Получение и некоторые свойства гипофосфита меди, Изв. СО АН СССР, Серия хим. Наук, 1978, **2**, №4, 47-50.
- [17] ЛОМОВСКИЙ О.И., БОЛДЫРЕВ В.В. Беспалладиевая металлизация в технологии печатных плат, Журн.прикладной химии, 1989, **62**, №11, 2444-2455.
- [18] KASZUWARA W., LEONOWICZ M. Long-term corrosion tests on Nd-Fe-B sintered magnets. Materials Letters 1999, **40**, 18-22.
- [19] ШВАРЦЕНБАХ Г., ФЛАШКА Г. Комплексонометрическое титрование, Химия, 1970, 360 с.
- [20] ГОРБУНОВА К.М., НИКИФОРОВА А.А. Физико-химические основы процесса химического никелирования, Из-во АН СССР, 1980, 207с.
- [21] МАЯНЦ Л.С., SAILORS Е.И. Спектры и строение солей фосфорных кислот. Гипофосфиты, Изв. АН СССР, Серия неорг. Матер., 1965, **1**, №4.-546-553.
- [22] ВАН ВЕЗЕР. ФОСФОР И ЕГО СОЕДИНЕНИЯ, М.: ИЛ, 1962, 687 с.
- [23] МАКОВСКАЯ V., MANORIK T., P. et al, Influence of template synthesis conditions on TiO₂ gels structure formation, in press
- [24] NEUMANN R., CHAVA M., LEVIN M.. J.Chem.Soc.Che.Comm., 1993, N 22, p.1685-1687.
- [25] VALTCHEV V.P., J.Chem.Soc.Che.Comm., 1994, N 3, p.261-262.
- [26] UQUINE M.A., OVEJERO G., R.VAN GRIEKEN ET AL, J.Chem.Soc.Che.Comm., 1994, N 1, p.27-11.7.
- [27] SHELDON R. A. AND . KOCHI I. K.. Metal-Catalysed Oxidations of
- [28] Organic Compounds. Academic Press. New York. 1981.
- [29] LYONS J. E.. Appl. Ind. Catal., 1981, 3, 131.
- [30] MEUNIER B.. Bull. Soc. Chim. Fr., 1986, 578.
- [31] HCRRON N. AND TOLMAN C.A. J.Am.Chem.Soc., 1987, 109, 2837.

- [32] TATSMUL T., NAKAMURA M., NEGISHI S. AND TOMINAGA H.. J.Chem.Soc.Che.Comm., 1990, 476.
- [33] HUYBRECHTS D. R. C., BRUYCKER L. D. AND P. JACOBS A.. Nature, 1990, 345, 240.
- [34] REDDY J.S., SIVASANKERS. AND RATNASAMY P.. J.Mol.Catal., 1991, 70, 335.
- [35] RAO P.R., RAMASWAMY A.V., J.Chem.Soc.Che.Comm., 1992, N 17, p.1245-1246.
- [36] SASAKI T., KOMATSU YU., FUJIKY. i, J.Chem.Soc.Che.Comm., 1991, N 12, p.817-818.
- [37] HOU W., YAU Q., FU X., J.Chem.Soc.Che.Comm., 1994, N 11, p.1371-1372.
- [38] LIVAGE J, HENRY M. AND SANCHEZ C., Prog. Solid Slate Chem., 1988, **18**, 259.

LIST OF PARTICIPANTS

Belarus

Y. Davydov
Belarus Academy of Sciences,
Institute of Radioecological Problems
Radiochemistry Laboratory,
Sosny, 220109 Minsk
Fax: 0375 0172 46 70 55
Email: davydov@doktor.belpak.minsk.by

Belgium

A. Bruggeman
SCK/CEN,
Departement BR2,
Boeretang 200,
B-2400 Mol
Fax: 0032 1432 15 29
Email: abruggem@sckcen.be

Bulgaria

I. Stefanova
Bulgarian Academy of Sciences,
Institute for Nuclear Research
and Nuclear Energy, Department of
Radiochemistry and Radioecology,
Tsarigradsko chaussee 72,
1784 Sofia
Fax: 00359 297 53619
Email: irast@inrne.acad.bg

China

Xiguang Su
China Institute of Atomic Energy,
Department of Radiochemistry,
PO Box 275 (93),
Beijing 102413
Fax: 0861 069 357008
Email: eceg@iris.ciae.ac.cn

Czech Republic

J. John
Czech Technical University of Prague,
Faculty of Nuclear Science and
Physical Engineering,
Department of Nuclear Chemistry,
Brehova 7, 115 19 Prague 1
Fax: 004 202 232 0861
Email: JOHN@br.fjfi.cvut.cz

Hungary

T. Szanya
Department of Radiochemistry,
University of Veszprém,
8201 Veszprem
Fax: 0036 88 400 613
Email: szanya@almos.vein.hu

India

P.K. Wattal
Bhabha Atomic Research Centre,
Process Engineering and Systems Division,
Trombay, Mumbai 400 085
Fax: 0091 22 550 5151 or 551 9613
Email: wattal@magnum.barc.ernet.in

Korea, Republic of

Yo-Yeon Yang
Nuclear Environment Technology Inst.,
PO Box 149, Yuseong, Daejeon, 305-600
Fax: +82 42 870 0214
Email: hyyang@khnp.co.kr

Malaysia

S.H. Hakimi
Malaysian Institute for Nuclear
Technology Research,
Bangi, 43000 Kajang,
Selangor Darul Ehsan
Fax: 6 03 825 8262
Email: shakimi@mint.gov.my

Russian Federation

Y. Karlin
Scientific and Industrial Association
Radon,
Applied Research Centre,
7th Rostovsky per. 2/14,
Moscow 119121
Fax: 007 095 248 1941
Email: karlinyr@tsinet.ru

V. Kosyakov
Russian Research Center,
Kurchatov Institute,
Department of Nuclear Physics
and Radiochemistry,
Kurchatov Square 1,
Moscow 123182
Fax: 007 095 882 5804
Email: olgas@libfl.ru

V. Avramenko
Russian Academy of Sciences,
Institute of Chemistry, Far East Department
Laboratory of Sorption Processes,
159, Prosp. 100 Let Vladivostoku,
Vladivostok 690022
Fax: 4232 261025
Email: SMTP: chemist@ext.dvgu.ru

D. Marinine
Institute of Chemistry, Far East Dept.,
Russian Academy of Sciences,
159, Prosp. 100-letya Vladivostoku
Vladivostok 690022
Fax: 007 4232 313 583
Email: dmarinin@ich.dvo.ru

Ukraine

P. Manorik
Ukrainian Academy of Sciences,
L.V. Pisarzhevsky Institute of
Physical Chemistry,
Prospect Nauki 31,
252039 Kiev
Fax: 0038 044 265 6216
Email: manorik@ipcnas.kiev.ua